Assessment of Direct Methods in Power System Transient Stability Analysis for On-line Applications

by

Armando Llamas

Dissertation submitted to the Faculty of the
Virginia Polytechnic Institute and State University
in partial fulfillment of the requirements for the degree of

DOCTOR OF PHILOSOPHY

in

Electrical Engineering

APPROVED:

Dr. Jaime De La Ree

Dr. A. G. Phadke

Dr. Lamine Mili

Dr. W. T. Baumann

Dr. Lee Johnson

Blacksburg, Virginia

12/1/92

Abstract

The advent of synchronized phasor measurements allows the problem of real time prediction of instability and control to be considered. The use of direct methods for these on-line applications is assessed.

The classical representation of a power system allows the use of two reference frames: Center of angle and one machine as reference. Formulae allowing transition between the two reference frames are derived. It is shown that the transient energy in both formulations is the same, and that line resistances do not dampen system oscillations.

Examples illustrating the mathematical characterization of the region of attraction, exit-point, closest u.e.p. and controlling u.e.p. methods are presented.

Half-dimensional systems (reduced-order systems) are discussed. The general expression for the gradient system which accounts for transfer conductances is derived without making use of the infinite bus assumption. Examples illustrating the following items are presented: a) Effect of the linear ray approximation on the potential energy (inability to accurately locate the u.e.p.'s); b) Comparison of Kakimoto's and Athay's approach for PEBS crossing detection; c) BCU method and; d) One-parameter transversality condition.

It is illustrated that if the assumption of the one-parameter transversality condition is not satisfied, the PEBS and BCU methods may give incorrect results for multi-swing stability. A procedure to determine if the u.e.p. found by the BCU method lies on the stability boundary of the original system is given. This procedure improves the BCU method for off-line applications when there is time for a hybrid approach (direct and conventional), but it does not improve it for on-line applications due to the following: a) It is time consuming and b) If it finds that the u.e.p. does not belong to the stability boundary it provides no information concerning the stability/instability of the system.

Acknowledgements

I would like to thank the following people and companies with their aid in and support for my dissertation Transient Stability Analysis by Direct Methods.

Dr. Jaime De La Ree

Dr. A. G. Phadke

Dr. L. Mili

Dr. W. T. Bauman

Dr. Lee Johnson

Dr. M. A. Pai

Dr. J. S. Thorp

Dr. Dave Gharpure

Dr. Ali H. Nayfeh

The New York Power Authority

My family

Contents

List of Figures

Chapter 1

Introduction

Our interest in direct methods for transient stability analysis stems from the problem of real-time prediction of instability and control. It has become possible to contemplate such tasks because of the newly developed technique of synchronized phasor measurements and their use in adaptive out-of-step relaying and other real-time control functions.

We began by considering the TEF (transient energy function) method as a likely candidate for these applications. Phasors can track system behavior, and through them, a prediction about the outcome of an evolving swing could be made. We wanted to investigate if the TEF method, or the PEBS (potential energy surface) method, or the BCU (boundary of stability region based controlling unstable equilibrium point) method, offer a practical technique for instability prediction.

Since we are interested in assessing the use of direct methods for on-line stability prediction, where computing time is an important factor, the classical model of a power system will be used throughout this dissertation.

1.1 Chapter outline

1. **Introduction.** The next section of this chapter is the statement of the problem where power system transient stability is defined from the point of view of both conventional and direct methods. The last sections describe the scope of this dissertation and the related bibliography.

2. **Transient energy method for the one-machine infinite bus system.** The second chapter provides the background information needed to undertake a study of transient stability analysis, and as such, the reader familiar with the subject may skip it. The basics principles of Newton's second law and Faraday's law are discussed within the context of rotating machines, allowing the derivation of the swing equation. Equilibrium points, as related to electric power system transients, are discussed. Two methods of determining stability for the one-machine infinite-bus case are presented: the equal area criteria and the transient energy method. These methods are shown to be equivalent.

3. **Transient energy function for multi-machine systems.** The third chapter extends the notion of transient energy to the multi-machine case. Classical modeling of electric power systems is presented and is used throughout the paper. The use of this model allows the reduction of any power system to its internal nodes. Two formulations for the state equations of the power system are then presented: Center of Angle (COA) and one machine reference frame. These formulations provide two means of determining the transient energy function. The formulae to go from one reference frame to the other are found. It is shown that both of these reference frames result in the same transient energy function. The reduction to internal nodes may yield an admittance matrix with non-negligible transfer conductances. This in turn causes the transient energy to be path-dependent or non-integrable. To circumvent this problem, the projection of the post-fault trajectory onto the angle subspace is assumed to be linear allowing the use of the linear ray approximation. The effect of line resistances on system damping is discussed.

4. **Fundamentals of direct methods.** In this chapter, the exit point, the closest u.e.p., and the controlling u.e.p. methods are presented. The notion of a region of attraction is mathematically described and several step-by-step procedures which help characterize such a region are delineated. It is concluded that the controlling u.e.p. method is superior to the other two methods, but that finding the controlling u.e.p. is difficult especially for large systems.

5. **PEBS and BCU methods.** The last chapter investigates two methods of transient stability assessment: the Potential Energy Boundary Surface (PEBS) method and the

Boundary of stability based Controlling U.e.p. (BCU) method. Both of these methods require a lower dimensional system which is described. It is shown that the BCU method, although superior to all other current methods, may fail if insufficient damping is present.

6. **Conclusions.** The most important results of this dissertation are briefly stated.

1.2 Problem statement

1.2.1 Power system transient stability analysis

The following definitions taken from [42] define power system transient stability..

1. *Power System*: A network of one or more electrical generating units, loads, and/or power transmission lines.

2. *Operating Quantities of a Power System*: Physical quantities, which can be measured or calculated, that can be used to describe the operating conditions of a power system. Operating quantities include rms values or corresponding *phasors*.

3. *Steady-State Operating Condition of a Power System*: An operating condition of a power system in which all of the operating quantities that characterize it can be considered to be constant for the purpose of analysis.

4. *Synchronous Operation*

   (a) *Synchronous Operation of a Machine*: A machine is in synchronous operation with a network or another machine to which it is connected if its average electrical speed (product of its rotor angular velocity and the number of pole pairs) is equal to the angular frequency of the ac network voltage or to the electrical speed of the other machine.

   (b) *Synchronous Operation of a Power System*: A power system is in synchronous operation if all its connected synchronous machines are in synchronous operation with the ac network and with each other.

5. *Asynchronous Operation*

(a) *Asynchronous Operation of a Machine*: A machine is in asynchronous operation with a network or another machine to which it is connected if it is not in synchronous operation.

(b) *Asynchronous Operation of a Power System*: A power system is in asynchronous operation if one or more of its connected synchronous machines are in asynchronous operation.

6. *Hunting of a Machine*: A machine is hunting if any of its operating quantities experience sustained oscillations.

7. *Disturbance in a Power System*: A disturbance in a power system is a sudden change or a sequence of changes in one or more of the parameters of the system, or in or more of the operating quantities.

   (a) *Small Disturbance in a Power System*: A small disturbance is a disturbance for which the equations that describe the dynamics of the power system may be linearized for the purpose of analysis.

   (b) *Large Disturbance in a Power System*: A large disturbance is a disturbance for which the equations that describe the dynamics of the power system cannot be linearized.

8. *Steady-State Stability of a Power System*: A power system is steady-state stable for a particular steady-state operating condition if, following any small disturbance, it reaches a steady-state operating condition which is identical or close to the pre-disturbance operating condition. This is also known as *Small Disturbance Stability of a Power System.*

9. *Transient Stability of a Power System*: A power system is transiently stable for a particular steady-state operating condition and for a particular disturbance if, following that disturbance, it reaches an acceptable steady-state operating condition.

10. *Power System Stability Limits*

    (a) *Steady-State Stability Limit*: The steady-state stability limit is a steady-state operating condition for which the power system is steady-state stable but for which

an arbitrarily small change in any of the operating quantities in an unfavorable direction causes the power system to lose stability. This is also known as the *Small Disturbance Stability Limit.*

(b) *Transient Stability Limit*: The transient stability limit for a particular disturbance is the steady-state operating condition for which the power system is transiently but for which an arbitrarily small change in any of the operating quantities in an unfavorable direction causes the power system to lose stability for that disturbance.

11. *Critical Clearing Time*: If a particular disturbance includes the initiation and isolation of fault on a power system, the critical clearing time is the maximum time between the initiation and the isolation such that the power system is transiently stable.

We are interested in transient stability and not in steady-state stability. However, the definitions related to steady-state stability were kept to make the rest of the definitions easier to understand. The following paragraph taken from [66], answers to our question.

What is transient stability analysis? Power system stability may be defined as that property of the system which enables the synchronous machines of the system to respond to a disturbance from a normal operating condition so as to return to a condition where the operation is again normal. Transient stability analysis is aimed at determining if the system will remain in synchronism following *major* disturbances such as transmission system faults, sudden load changes, loss of generating units, or line switching.

1.2.2 Conventional or step-by-step transient stability analysis

In conventional transient stability analysis the state equations are numerically integrated (step-by-step integration). Assuming that the disturbance includes the initiation and isolation of a fault on a power system, conventional analysis proceeds as follows. The initial system state is obtained from the pre-fault system. This is the starting point used for the integration of the fault-on dynamic equations. After the fault is cleared, the post-fault dynamic equations are used in the numerical integration. These simulations yield the fault-on and post-fault trajectories. The angles relative to a reference machine may be plotted versus time and if these angles are bounded, the system is stable, otherwise it is unstable. This is illustrated in

Fig. 1-1. This figure corresponds to a three-machine power system. The reference machine is machine 3. Notice that for this particular disturbance, the critical clearing time is some value between 0.1950 and 0.1955 seconds. Multiple runs were required to obtain these bounds on the critical clearing time. This trial and error approach is a major disadvantage of the conventional method.

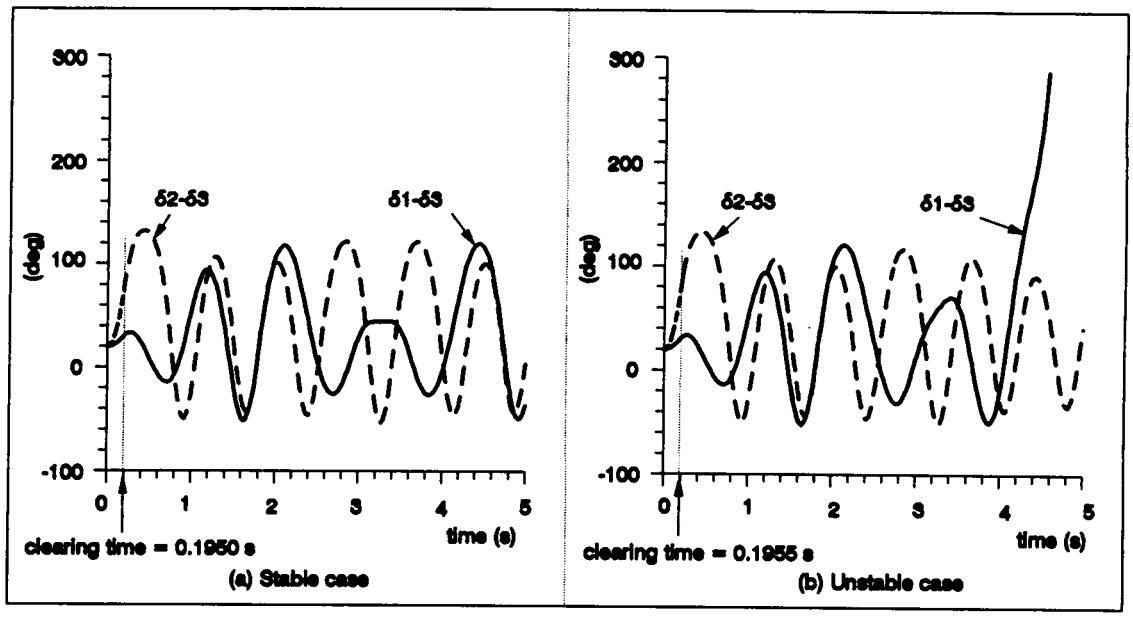

Figure 1-1: Conventional transient stability analysis

1.2.3 Transient stability analysis by direct methods

A direct method for transient stability analysis was defined in [41] as *"a method to determine stability without explicitly solving the differential equations"*. In [10] it was defined as *"a method to determine the stability of a post-fault system based on energy functions without explicitly integrating differential equations describing the post-fault system."*

The following paragraph, taken from [1], gives an excellent description of direct methods in transient stability analysis: "The transient energy method offers the opportunity of assessing the transient stability of power systems *more directly and effectively than the conventional approach based on simulation.* For example, it allows critical clearing times to be calculated directly from a *single* solution. More fundamentally and, in terms of potential applications,

more significantly it also provides *a quantitative measure of how stable or unstable a particular case may be.*"

Direct methods have one disadvantage when compared to conventional methods - the models used in direct methods are less detailed, e.g. turbine governors, voltages regulators, and static VAR compensators are not considered.

A definition of transient stability analysis more suitable for direct methods is as follows [95]. "The stable equilibrium point of a nonlinear dynamic system is surrounded by a stability region, or region of attraction. Whether a given initial state is within this region is a fundamental question underlying many engineering problems such as the monitoring of electric power system stability."

1.3 Scope of this dissertation

In this dissertation we are interested in power system transient stability analysis by direct methods and we will concentrate on a simplified model called the *classical model.* All of the books on power system transient stability by direct methods begin their study with the classical model [56], [55], [25]. As mentioned, before, because we are interested in assessing the use of direct methods for on-line stability prediction where computing time is an important factor, this model will also be used throughout this dissertation. More advanced analysis using direct methods must consider a more detailed model of the power system. For information on structure preserving methods see [7], [38], [37], [79], [82], [83], [86], [55] and [25]. For information on energy function methods with detailed models see [68], [69], [26], [55] and [25].

1.4 About the bibliography

The bibliography presented at the end of this dissertation contains more than ninety items and has been sorted in alphabetical order by author's last name. Some additional items, not referenced in the paper, are included so that the bibliography can serve as a complete list of sources on the subject of transient stability analysis by direct methods.

The core of this dissertation comes from the following references:

- Books on direct methods: [56], [55] and [25].

- Survey papers: [33], [41], [64], [78] and [83].
  - Mathematical characterization of the region of attraction: [20] and [95].
- Closest unstable equilibrium point, potential energy boundary surface, controlling unstable equilibrium point, and boundary of stability based controlling unstable equilibrium point methods: [1], [2], [9], [10], [11], [13], [17], [43] and [46].

Chapter 2

Transient Energy Method for the One-machine Infinite-bus System

2.1 Background

2.1.1 Notation

We will begin by describing the notation used in deriving the swing equation. Quantities in bold face are phasors; $\mathbf{E} = Ee^{j\delta}$ means that the phasor $\mathbf{E}$ has a magnitude E and a phase angle δ.

A variable with no subscript is an electrical quantity in a synchronously rotating frame. A variable with the subscript "a" only, is an electrical quantity in a stationary frame. A variable name with the subscript "m" only is a mechanical quantity in a synchronously rotating frame. A variable with both subscripts "m" and "a" is a mechanical quantity in a stationary frame. The subscript "s" indicates synchronous frequency. Fig. 2-1 illustrates examples of these electrical and mechanical quantities.

f_s Synchronous frequency, $f_s = 60$ Hz

ω_s Synchronous angular velocity, rad/s, $\omega_s = 2 \cdot \pi \cdot f_s = 120 \cdot \pi$ rad/s

ω_{ms} Mechanical synchronous angular velocity, mec-rad/s. $\omega_{ms} = \frac{2}{P}\omega_s$, where P is the number of poles

ω_{ma} Mechanical angular velocity in a stationary frame, mec-rad/s

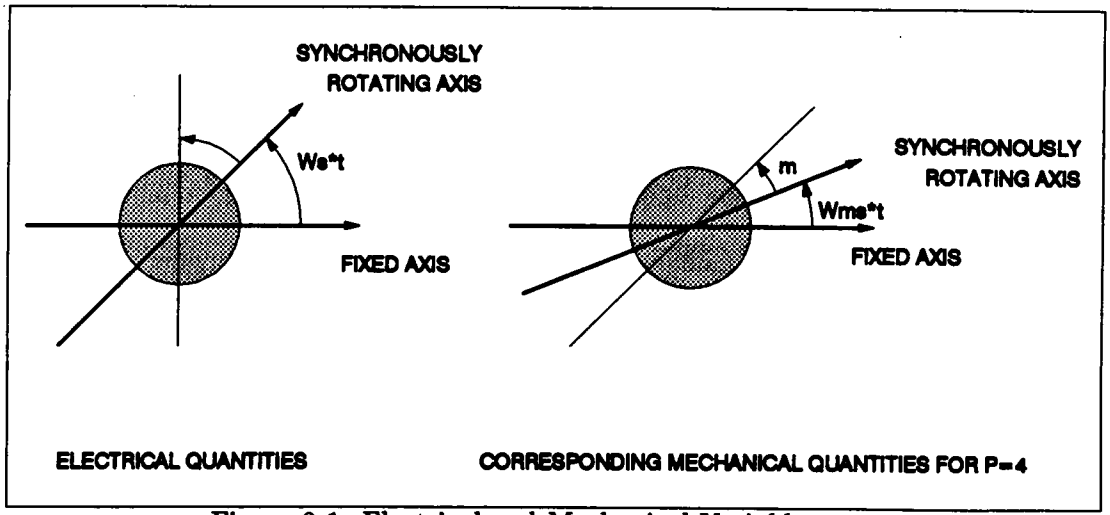

Figure 2-1: Electrical and Mechanical Variables

ω_m Mechanical angular velocity in a synchronously rotating frame. $\omega_m = \omega_{ma} - \omega_{ms}$.

ω_a Electrical angular velocity with respect to a stationary axis, rad/s

ω Electrical angular velocity with respect to a synchronously rotating axis. $\omega = \omega_a - \omega_s$.

θ_a, δ_a Electrical angles in a stationary frame, rad

θ_{ma}, δ_{ma} Mechanical angles in a stationary frame, mec-rad. $\theta_{ma} = \frac{2}{P}\theta_a$, where P is the number of poles

θ, δ Electrical angles in a synchronously rotating frame. $\delta = \delta_a - \omega_s t$

2.1.2 Faraday's law

In Fig 2-2, the angle θ is the rotor angle in a synchronously rotating frame in rad/s. The flux linkage due to the field is then $\lambda_f = \lambda_f e^{j\theta}$. The active convention of Faraday's law states that $e_f = -\frac{d\lambda_f}{dt}$, where its phasor form is $\mathbf{E_f} = -j \cdot \omega_s \cdot \lambda_f$. The phasor form of Faraday's law can be obtained from $e_f = -\frac{d\lambda_f}{dt}$ in the same way that the $E - I$ relationship in an inductor is determined. If $\mathbf{E_f} = E_f e^{j\delta}$, then $\delta = \theta - \pi/2$.

2.1.3 Newton's second law

This law, $f = m \cdot a$, takes the form $\tau = J \cdot \alpha_{ma}$ for angular motion.

J is the moment of inertia in kg m.

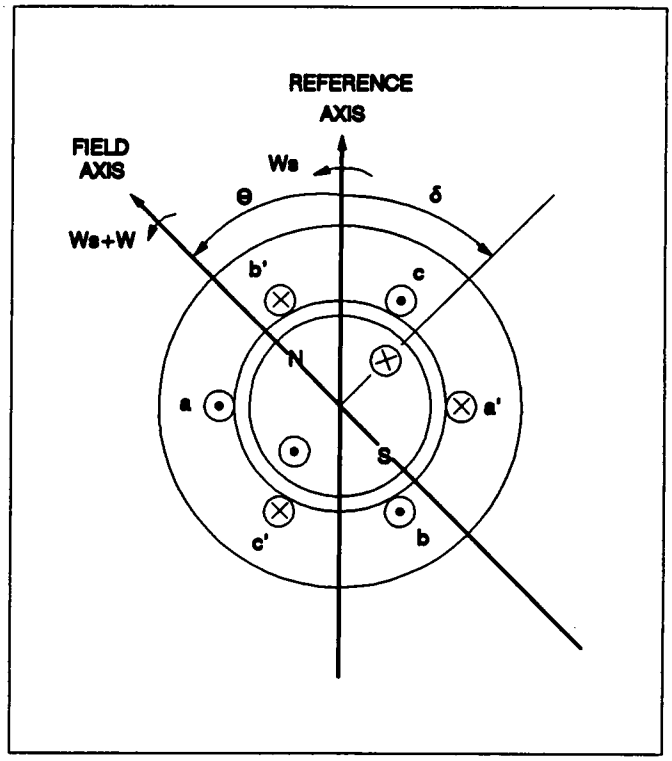

Figure 2-2: Elementary Synchronous Machine

τ is the resulting torque in N m.

α_{ma} is the angular acceleration in mec-rad/s^2.

Fig. 2-3 shows a solid cylinder of radius r and the formula for obtaining its moment of inertia. The rotational kinetic energy for a solid cylinder rotating about the shown axis is given by the equation

$$\frac{1}{2} \cdot J \cdot \omega_{ma}^2$$

2.1.4 The swing equation

Let us apply Newton's second law with the resulting torque equal to $\tau_m - \tau_e$. From Fig. 2-4 we get the equation

$$\tau_m - \tau_e = (Jp + J_g) \cdot \alpha, \mathrm{N} \cdot \mathrm{m}$$

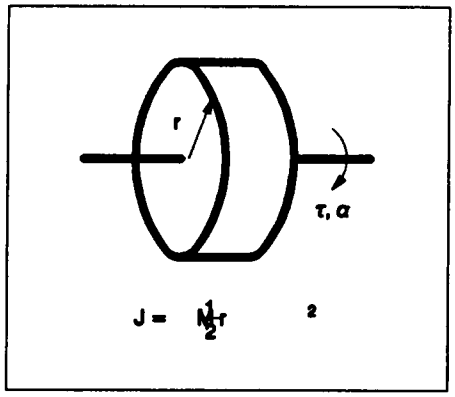

Figure 2-3: Moment of Inertia of a Solid Cylinder with Radius r

or

$$J \cdot \alpha_{ma} = \tau_m - \tau_e \tag{2.1}$$

τ_m is the torque due to the prime mover inN·m

τ_e is the torque due to the generator in N·m, and is opposite to τ_m

α_{ma} is the angular acceleration in mec-rad/s^2, this is a mechanical quantity in a stationary reference frame.

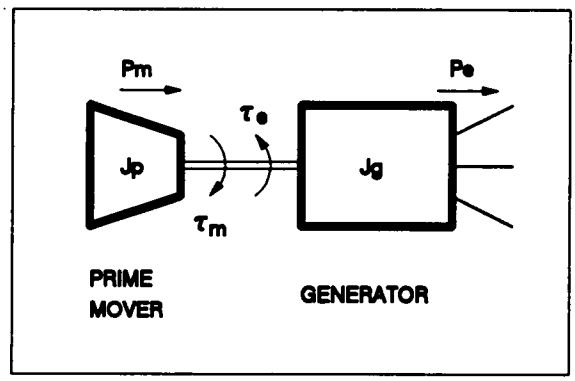

Figure 2-4: Generator and Prime Mover

By multiplying both sides of Eq. 2.1 by ω_{ma}, the units change from Newton meters to watts.

$$J \cdot \omega_{ma} \cdot \alpha_{ma} = P_m - P_e, \text{ W} \tag{2.2}$$

ω_{ma} is the angular velocity in mec-rad/s

P_m is the mechanical power in W

Pe is the electrical power in W

Per unit (pu) electrical quantities are more convenient. Replace the mechanical quantities by their electrical equivalents and divide both sides of Eq. 2.2 by the complex power base, S_{base}. The following equations illustrate the relationships between the electrical and mechanical quantities. The angular acceleration is the first derivative of the angular velocity and the second derivative of the angle. The variable P is the number poles and δ is the phase angle of the induced voltage.

$$\theta_{ma} = \frac{2}{P}\theta_a = \frac{2}{P}(\theta + \omega_s \cdot t)$$

$$\omega_{ma} = \frac{2}{P}\omega_a = \frac{2}{P}\left(\frac{d\theta}{dt} + \omega_s\right)$$

$$\alpha_{ma} = \frac{2}{P}\frac{d^2\theta}{dt^2} = \frac{2}{P}\frac{d^2\delta}{dt^2}$$

By substituting these equations into Eq. 2.2 and dividing each side by S_{base}, we get the following equation:

$$\left(\frac{2}{P}\right)^2 \cdot \frac{J \cdot \omega_a}{S_{base}} \cdot \frac{d^2\delta}{dt^2} = P_m - P_e, \text{ pu} \tag{2.3}$$

Now let us define the following function of ω_a :

$$M(\omega_a) = \left(\frac{2}{P}\right)^2 \cdot \frac{J \cdot \omega_a}{S_{base}}, \frac{\text{pu} \cdot \text{s}^2}{\text{rad}}$$

By substituting $M(\omega_a)$ in Eq. 2.3 we get Eq. 2.4.

$$M(\omega_a) \cdot \frac{d^2\delta}{d\,t^2} = P_m - P_e, \text{ pu} \tag{2.4}$$

If ω_a and ω_s are nearly equal, M may be defined as Eq. 2.5,

$$M = \left(\frac{2}{P}\right)^2 \cdot \frac{J \cdot \omega_s}{S_{base}}, \frac{\text{pu} \cdot \text{s}^2}{\text{rad}} \tag{2.5}$$

Eq. 2.4 can be written as the swing equation, Eq. 2.6.

$$M\frac{d^2\delta}{dt^2} \cong P_m - P_e, \text{ pu} \tag{2.6}$$

2.1.5 Electric power and the Power-angle Curve

Let us assume that the synchronous machine is connected to an infinite bus through a lossless line as shown in Fig 2-5. The power transferred from the synchronous machine to the infinite bus is given by

$$P_e = P_{max} \sin(\delta)$$
$$P_{max} = \frac{E \cdot V_\infty}{X}, \text{ pu}$$

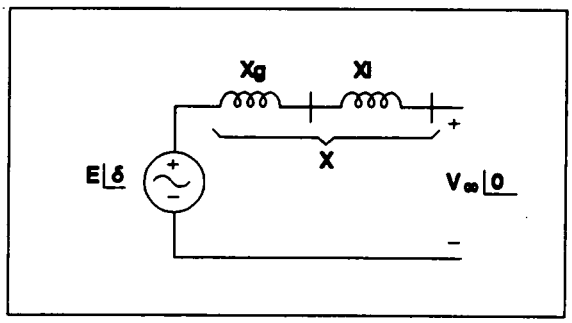

Figure 2-5: One Machine Infinite Bus System

The plot of P_e vs. δ is known as the power-angle curve, see Fig 2-6. Also shown in Fig 2-6 is the mechanical power P_m and the equilibrium points δs and δu.

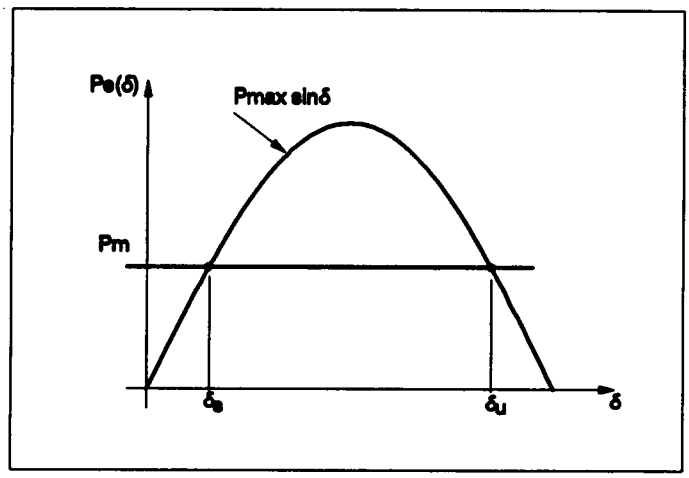

Figure 2-6: Power Angle Curve

2.1.6 Stable and unstable equilibrium points

The equilibrium points are obtained by making the left-hand side of Eq. 2.6 equal to zero.

$$0 = P_m - P_e, \text{ pu}$$

$$0 = P_m - P_{max}\sin(\delta)$$

$$\delta = sin^{-1}\left(\frac{P_m}{P_{max}}\right)$$

The equilibrium point δ_s is a stable one (s.e.p.), whereas δ_u is unstable (u.e.p.). We have two ways to determine whether or not an equilibrium point is stable.

In one method, the system has to be linearized, then the roots of the linearized system are evaluated at that equilibrium point. If the roots are on the left-hand side of the complex plane then the equilibrium point is stable, otherwise it is unstable. For a small system, the second method is simpler, let us assume that $\delta = \delta_s + \Delta\delta$ and $\omega = 0$, $(\delta_s + \Delta\delta, 0)$. The acceleration $\alpha = [P_m - P_e(\delta)]/M$ is negative, then ω and, hence, δ will decrease with time. Therefore, the system torque will move the system towards δ_s, see Fig 2-7.

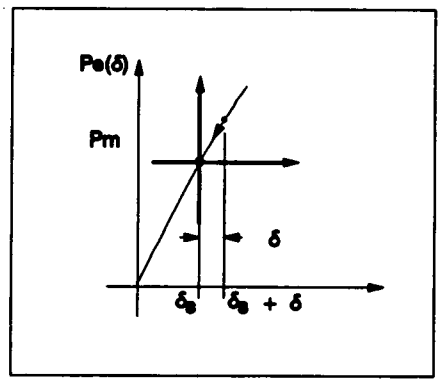

Figure 2-7: Stable Equilibrium Points

Following the same analysis it can be proven that δ_u is unstable. Any displacement of the system from that equilibrium point, no matter how small the displacement is, will move the system away from it.

2.2 Equal-area criterion

Fig 2-8 a) shows one machine connected to an infinite bus through two parallel lossless lines. At pre-fault P_{max} is given by

$$P_{\max}^{(1)} = \frac{E \cdot V\infty}{X_g + X_l}, \text{ pu}$$

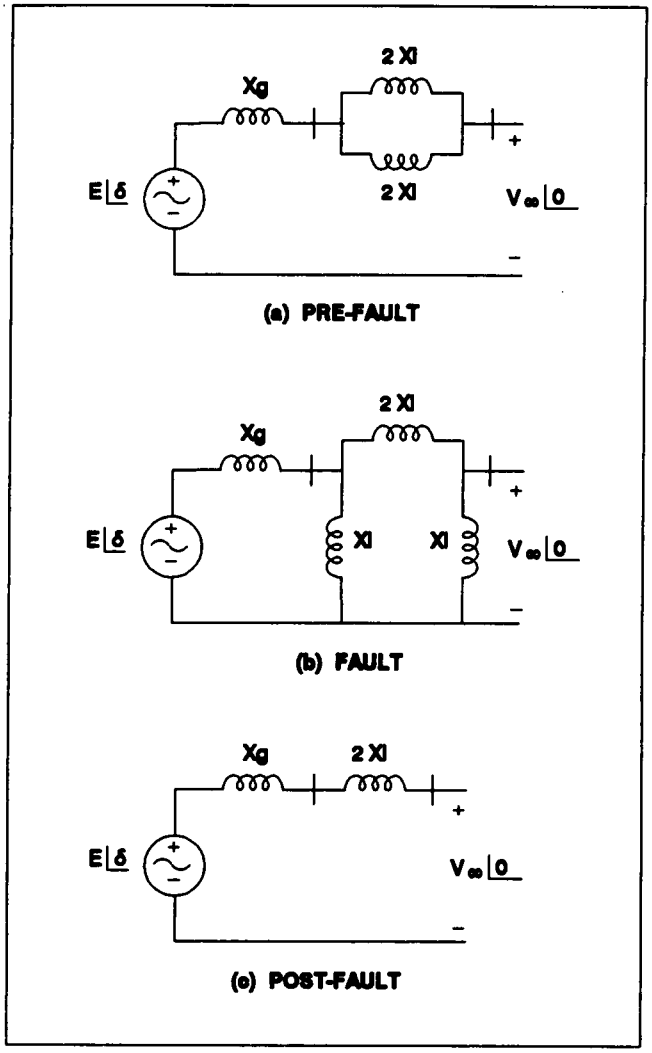

Figure 2-8: Fault in the Middle of One Line

$X_g + X_l$ is the reactance connecting the two machines. The fault is a solid three-phase short circuit in the middle of one of the lines as shown in Fig 2-8 b). P_{max} during the fault can be obtained using the $\Delta - Y$ conversion formulas to eliminate the node without injection and it is

given by the equation

$$P_{\max}^{(2)} = \frac{E \cdot V\infty}{3\,X_g + 2\,X_l},\ \text{pu}$$

From Fig. 2-8 c), the post-fault P_{max} is given by the equation

$$P_{\max}^{(3)} = \frac{E \cdot V\infty}{X_g + 2X_l},\ \text{pu}$$

Fig. 2-9 shows the corresponding three power-angle curves. Now, let us make some remarks about the points on these three curves.

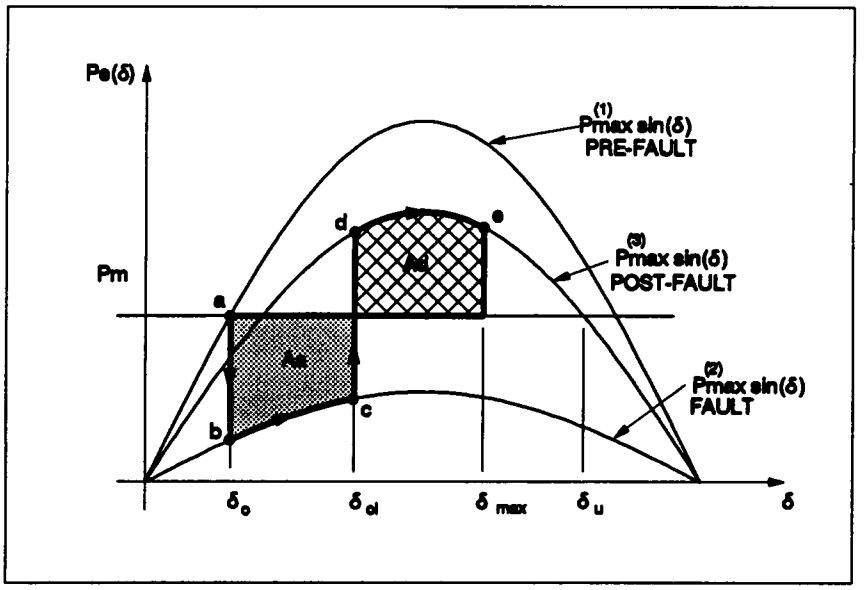

Figure 2-9: Equal Area Criterion

- Pre-fault:
  - Point a. The system is in equilibrium, $\frac{d\omega}{dt} = P_m - P_e(\delta) = 0$, $\omega = 0$, and $\delta = \delta_o$.
- Fault:
  - Point b. δ and ω can not change suddenly. Therefore, $\omega = 0$ and $\delta = \delta_o$. We have accelerating power, since the acceleration is given by the equation

$$\alpha = \frac{d\omega}{dt} = \frac{P_m - P_{max}^{(2)} \sin(\delta_o)}{M} > 0$$

- Point c. At this point the breakers in the faulted line open and the system has moved to $(\delta_{cl}, \omega_{cl})$. The acceleration is given by the equation

$$\alpha = \frac{d\omega}{dt} = \frac{P_m - P_{max}^{(2)} \sin(\delta_{cl})}{M} > 0$$

- Post-Fault:

  - Point d. The state is still the same $(\delta_{cl}, \omega_{cl})$ but now the acceleration is negative, hence decelerating power.

$$\alpha = \frac{d\omega}{dt} = \frac{P_m - P_{max}^{(3)} \sin(\delta_{cl})}{M} < 0$$

  - Point e. Now the system decelerates and reaches this point where the state is $(\delta_{max}, 0)$. The speed will continue decreasing and will be negative. The decelerating power is still present.

The equal-area criterion establishes that δ_{max} is such that the decelerating area is equal to the accelerating area, i.e. $A_d = A_a$. In order to prove this let us start with Eq. 2.6.

$$M\frac{d^2\delta}{dt^2} = P_m - P_e, \text{ pu}$$

After multiplying both sides by $\omega = d\delta/dt$ we get the equation

$$M\omega\frac{d\omega}{dt} = [P_m - P_e(\delta)]\frac{d\delta}{dt}, \ \frac{\text{MW rad}}{\text{MVA s}}$$

The $dt's$ cancel, yielding the equation

$$M\omega d\omega = [P_m - P_e(\delta)] \cdot d\delta, \ \frac{\text{MW rad}}{\text{MVA}}$$

Now let us integrate this differential equation from δ_o to δ_{max} to obtain the equation

$$\int_{\omega(\delta_0)}^{\omega(\delta_{max})} M\omega\, d\omega = \int_{\delta_0}^{\delta_{max}} [P_m - P_e(\delta)]\, d\delta, \ \frac{\text{MW rad}}{\text{MVA}}$$

Noting that $\omega(\delta_{max}) = \omega(\delta_o) = 0$ we get the equation

$$0 = \int_{\delta_0}^{\delta_{max}} [P_m - P_e(\delta)]\, d\delta, \ \frac{\text{MW rad}}{\text{MVA}}$$

The above integral has to be evaluated in two parts due to $P_e(\delta)$ being one function from δ_o to δ_{cl} and another from δ_{cl} to δ_{max}.

$$\int_{\delta_0}^{\delta_{cl}} [P_m - P^{(2)}_{max} \sin(\delta)]\, d\delta + \int_{\delta_{cl}}^{\delta_{max}} \left[P_m - P^{(3)}_{max} \sin(\delta)\right]\, d\delta = 0$$

$$\int_{\delta_0}^{\delta_{cl}} [P_m - P^{(2)}_{max} \sin(\delta)]\, d\delta = \int_{\delta_{cl}}^{\delta_{max}} [P^{(3)}_{max} \sin(\delta) - P_m]\, d\delta$$

Note that the left-hand side of the above equation corresponds to the accelerating area A_a and the right-hand side corresponds to the decelerating area A_d.

$$A_a = A_d$$

Although ω is zero at point e, the system will keep moving until it reaches point g. Remarks about points e, f and g in Fig. 2-10 follow.

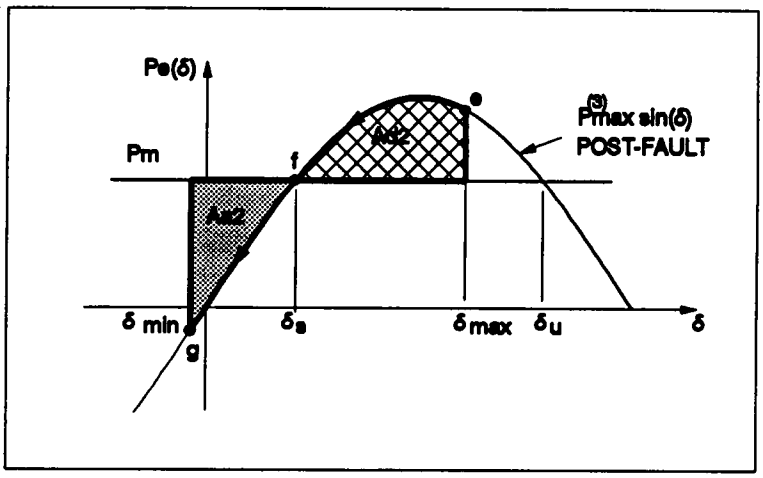

Figure 2-10: Post Fault Accelerating and Decelerating Areas

- Point e. $(\delta_{max}, 0)$. The speed is zero; but there is decelerating power.

$$\alpha = \frac{d\omega}{dt} = \frac{P_m - P_{max}^{(3)} \sin(\delta_{cl})}{M} < 0$$

The transient kinetic energy is zero, the transient potential energy is maximum.

- Point f. This is the s.e.p.; therefore, there is no acceleration.

$$\alpha = \frac{d\omega}{dt} = \frac{P_m - P_{max}^{(3)} \sin(\delta_s)}{M} = 0$$

The angular velocity is a minimum,$-\omega_{max}$, the transient kinetic energy is maximum, and the transient potential energy is zero. Since the speed is not zero, the system will continue moving towards point g.

- Point g. At this point, $(\delta_{min}, 0)$, the angular velocity is zero and the angle is minimum. The system will not remain here due to the accelerating power.

$$\alpha = \frac{d\omega}{dt} = \frac{P_m - P_{max}^{(3)} \sin(\delta min)}{M} > 0$$

The transient kinetic energy is zero, the transient potential energy is maximum, the angle δ_{min} is such that the equal-area criterion is satisfied, $A_{d2} = A_{a2}$.

According to our model, the system will oscillate between points e and g forever, this is because our model does not include any damping.

2.3 Transient energy

Fig 2-11 is similar to Fig 2-10 but the arrows indicate motion from point g to e. At point g the system has zero speed, and as the system moves towards δ_s it gains speed, hence, kinetic energy. We stated previously that the expression for the kinetic energy was the equation

$$Wke_{ma} = \frac{1}{2} J \omega_{ma}^2, \text{ J}$$

Notice the subscripts "m"and"a" in Wke_{ma}, they indicate that this energy is mechanical

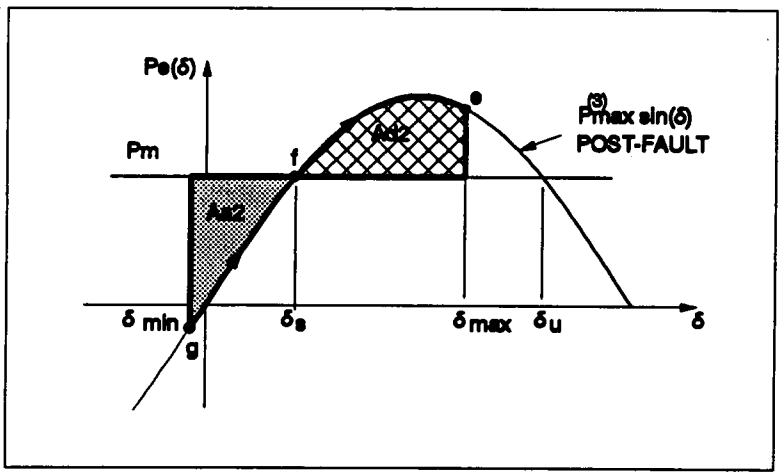

Figure 2-11: Post Fault Accelerating and Decelerating Areas

and it is a function of the speed in a stationary reference frame. Let us define kinetic energy of speed deviation as Eq. 2.7.

$$Wke_m = \frac{1}{2}J\omega_m^2 = \frac{1}{2}J\left(\frac{2}{P}\right)^2\omega^2, \text{ J} \tag{2.7}$$

The kinetic energy of deviation speed is zero at synchronous speed as shown in Fig 2-12.

Notice that this kinetic energy has the same units as the mechanical one. Also notice that it is not a linearization of the mechanical kinetic energy. A question may arise now, *does* A_{a2} *in Fig 2-11 represent this kinetic energy of deviation;* the answer is *no.* In order to prove this we will again make use of Eq. 2.6.

$$M\frac{d\omega}{dt} = [P_m - P_e(\delta)], \frac{\text{MW}}{\text{MVA}}$$

We will multiply this equation by $\omega = d\delta/dt$, and cancel dt on both sides to get the equation

$$M\omega d\omega = [P_m - P_e(\delta)]\, d\delta, \frac{\text{MW rad}}{\text{MVA}}$$

We now multiply and divide the left-hand side of the above differential equation by 2 in order

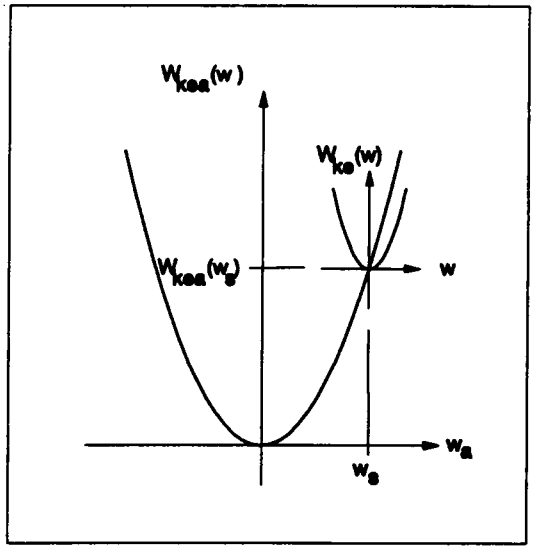

Figure 2-12: Kinetic Energy

to complete the differential $d(\omega^2)$.

$$\frac{M}{2} 2\omega d\omega = [P_m - P_e(\delta)]\, d\delta, \frac{\text{MW rad}}{\text{MVA}}$$

$$\frac{M}{2} d(\omega^2) = [P_m - P_e(\delta)]\, d\delta, \frac{\text{MW rad}}{\text{MVA}}$$

We must then integrate the above differential from δ_{min} to δ.

$$\frac{M}{2} \int_{\omega(\delta_{\min})}^{\omega(\delta)} d(\omega^2) = \int_{\delta_{\min}}^{\delta} [P_m - P_e(\delta)]\, d\delta, \frac{\text{MW rad}}{\text{MVA}}$$

Since $\omega(\delta_{min}) = 0$ we get the equation

$$\frac{M}{2}\omega^2 = \int_{\delta_{\min}}^{\delta} [P_m - P_e(\delta)] \cdot d\delta, \frac{\text{MW rad}}{\text{MVA}}$$

If we make the upper limit equal to δ_s we will get the accelerating area A_{a2} depicted in Fig. 2-11.

$$\frac{M}{2}(\omega(\delta_s))^2 = \int_{\delta_{\min}}^{\delta_s} [P_m - P_e(\delta)]\, d\delta, \frac{\text{MW rad}}{\text{MVA}}$$

$$A_{a2} = \int_{\delta_{\min}}^{\delta_s} [P_m - P_e(\delta)]\, d\delta, \frac{\text{MW rad}}{\text{MVA}}$$

We can see that A_{a2} is not equal to the kinetic energy of speed deviation; it is equal to a similar expression which has M in it instead of $J\left(\frac{2}{P}\right)^2$.

The *transient kinetic energy* is defined in Eq. 2.8.

$$V_{ke} = \frac{1}{2}M\omega^2, \frac{\text{MW rad}}{\text{MVA}} \tag{2.8}$$

Replacing M by Eq. 2.5 we get the equation

$$V_{ke} = \frac{1}{2}J\left(\frac{2}{P}\right)^2 \frac{\omega_s}{S_{base}}\omega^2, \frac{\text{MW rad}}{\text{MVA}}$$

From Eq. 2.7,

$$Wke_m = \frac{1}{2}J\left(\frac{2}{P}\right)^2 \omega^2, \text{J}$$

From the last two equations the following equation is obtained.

$$V_{ke} = \frac{\omega_s}{S_{base}}Wke_m, \frac{\text{MW rad}}{\text{MVA}}$$

At point f in Fig. 2-11, the kinetic energy is at a maximum because $\omega = \omega_{max}$. As the system moves from f to e the transient kinetic energy V_{ke} deceases until it gets to zero exactly at point e. At this point the transient kinetic energy has been converted to transient potential energy, $V_{pe}(\delta)$. This occurs because the system has no losses. As in the case of mechanical potential energy, the transient potential energy, V_{pe}, is a function of displacement. The maximum potential energy is equal to the decelerating area A_{d2}. As in the case of total mechanical energy, the total transient energy is the sum of the potential and kinetic energies.

$$V(\delta,\omega) = V_{pe}(\delta) + V_{ke}(\omega), \frac{\text{MW rad}}{\text{MVA}}$$

Since there are no losses, $dV/dt = 0$.

$$0 = \dot{V}_{pe} + \dot{V}_{ke}, \frac{\text{MW rad}}{\text{MVA s}}$$

From Eq. 2.8 we can find that $\dot{V}_{ke} = M\omega\dot{\omega}$. Substituting this result in the above equation,

yields the equation

$$\dot{V}_{pe} = -M\omega\dot{\omega}$$

According to the chain rule,

$$\frac{dV_{pe}}{dt} = \frac{dV_{pe}(\delta)}{d\delta}\frac{d\delta}{dt}$$

Therefore,

$$\frac{dV_{pe}(\delta)}{d\delta}\frac{d\delta}{dt} = -M\omega\dot{\omega}$$

We can cancel $d\delta/dt$ on the left-hand side with ω on the right hand-side to get the equation

$$\frac{dV_{pe}(\delta)}{d\delta} = -M\dot{\omega}$$

After multiplying both sides by $d\delta$,we get the following equation:

$$dV_{pe}(\delta) = -M\dot{\omega}d\delta$$

$M\dot{\omega}$ is the left hand-side of the swing equation and after substituting by the right-hand side, we get the following equation:

$$dV_{pe}(\delta) = -\left(P_m - P_e(\delta)\right)\, d\delta$$

We can integrate this differential equation from δ_s to δ.

$$\int_{V_{pe}(\delta_s)}^{V_{pe}(\delta)} dV_{pe} = -\int_{\delta_s}^{\delta} \left(P_m - P_e(\delta)\right)\, d\delta$$

Since $V_{pe}(\delta_s) = 0$,

$$V_{pe}(\delta) = -\int_{\delta_s}^{\delta} \left(P_m - P_e(\delta)\right)\, d\delta, \frac{\text{MW rad}}{\text{MVA}} \tag{2.9}$$

2.4 A few remarks about the transient energy

When a disturbance occurs, the system gains transient energy. Even if no fault occurs, the system gains transient energy. In a change of topology, like the opening of a line, there is no fault, but the system gains transient potential energy because the stable equilibrium point,

s.e.p., changes. Fig. 2-13 explains these ideas. Before the disturbance, the system has zero transient energy. The disturbance will inject transient energy into the system. When the disturbance disappears we have a system which has gained transient energy. The issue now is whether or not the system is stable after a disturbance.

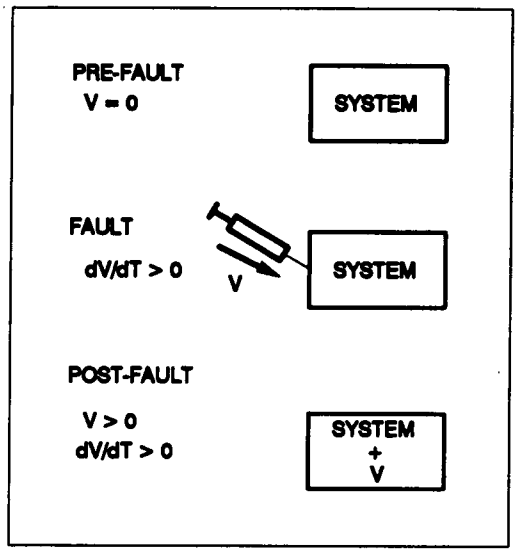

Figure 2-13: Injection of Transient Energy

2.5 The equal-area stability criterion and the transient energy method

The equal-area criterion establishes that $A_a = A_d$ when the system is stable. Referring to Fig 2-14 a), the accelerating and decelerating areas are given by Eq. 2.10 and Eq. 2.11.

$$A_a = \int_{\delta_0}^{\delta_{cl}} \left[P_m - P_{\max}^{(2)} \sin(\delta) \right] d\delta \tag{2.10}$$

$$A_d = \int_{\delta_{cl}}^{\delta_{\max}} \left[P_{\max}^{(3)} \sin(\delta) - P_m \right] d\delta \tag{2.11}$$

A different way of stating the *equal-area stability criterion* is using the inequality $A_a < A_{dmax}$. These areas are shown in Fig 2-14 b). A_{dmax} is obtained by replacing δ_{max} by δ_u in

Eq. 2.11, yielding the following equation:

$$A_{dmax} = \int_{\delta_{cl}}^{\delta u} \left[P_{max}^{(3)} \sin(\delta) - P_m \right] d\delta$$

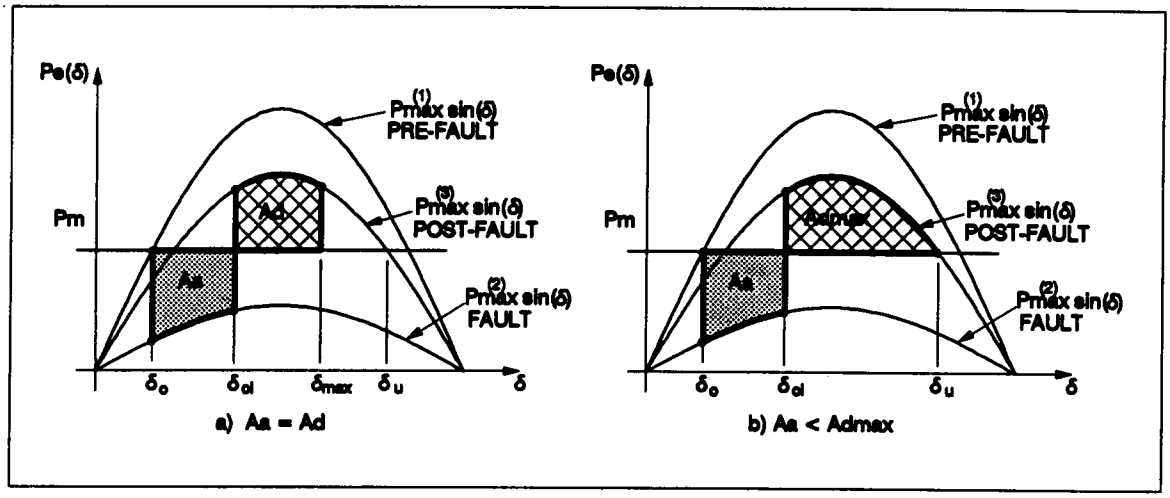

Figure 2-14: Equal Area Stability Criterion

The inequality $A_a < A_{dmax}$ simply establishes that following a disturbance, the system is transiently stable if the accelerating area is less than the maximum decelerating area.

The case for which $\delta_{max} = \delta_u$, and $A_a = A_{dmax}$, is critically stable (Fig 2-15). The system will reach the state $(\delta_u, 0)$ as time tends to infinity. This theoretical situation will never happen in reality, because any disturbance, no matter how small, will move the system either towards δ_s or towards instability as shown in Fig 2-15.

The equal-area criterion of stability and the transient energy method are the same.

Fig 2-16 shows the accelerating area, A_a, the decelerating area, A_d, and an area labeled as A_c. The equal-area stability criterion is mathematically stated by Eq. 2.12.

$$A_a < A_{dmax} \tag{2.12}$$

We can add area A_c to both sides of this inequality to get Eq. 2.13.

$$A_a + A_c < A_c + A_{dmax} \tag{2.13}$$

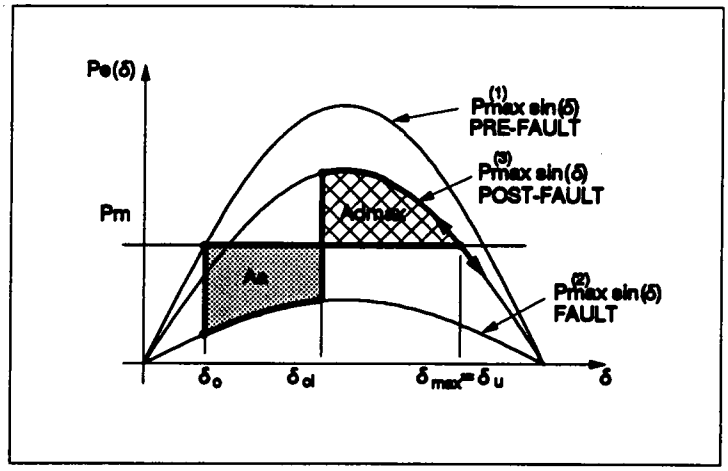

Figure 2-15: Critically Stable Case

A_a is given by the equation

$$A_a = \frac{1}{2} M \omega_{cl}^2 = V_{ke}(\omega_{cl}), \frac{\text{MW rad}}{\text{MVA}}$$

The accelerating area equals the transient kinetic energy injected into the system by the disturbance.

A_c is given by the equation

$$A_c = \int_{\delta_s}^{\delta_{cl}} \left\{ - \left[P_m - P_{\max}^{(3)} \sin(\delta) \right] \right\} d\delta$$

By comparing this equation to Eq. 2.9, we can see that A_c *is the transient potential energy at clearing time*, i.e. $A_c = V_{pe}(\delta_{cl}), \frac{\text{MW rad}}{\text{MVA}}$.

Now, we must find out what $(A_c + A_{dmax})$ represents. $A_c + A_{dmax}$ is given by the equation

$$A_c + A_{dmax} = \int_{\delta_s}^{\delta_u} \left\{ - \left[P_m - P_{\max}^{(3)} \sin(\delta) \right] \right\} d\delta$$

$A_c + A_{dmax}$ *is the transient potential energy at* δ_u. $A_c + A_{dmax} = V_{pe}(\delta_u)$

We have just obtained the following results: $A_a = V_{ke}(\omega_{cl})$, $A_c = V_{pe}(\delta_{cl})$, and $A_c +$

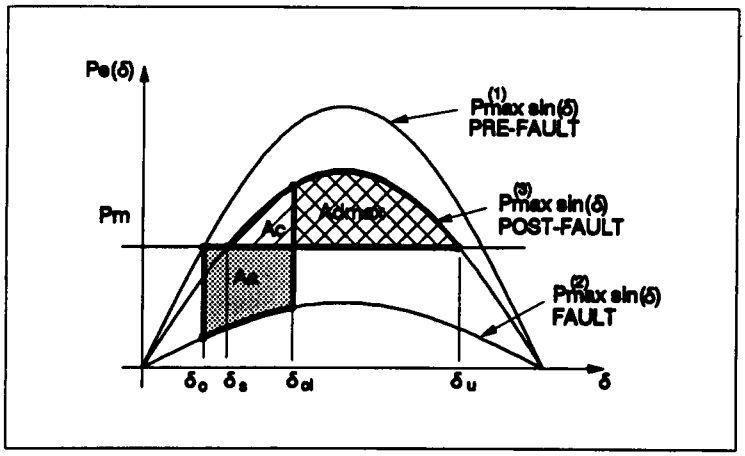

Figure 2-16: Modified Equal Area Criterion

$A_{dmax} = V_{pe}(\delta_u)$. After substituting them in inequality 2.13 we get the equation

$$V_{ke}(\omega_{cl}) + V_{pe}(\delta_{cl}) < V_{pe}(\delta_u), \frac{\text{MW rad}}{\text{MVA}}$$

This inequality is the mathematical way of stating the *transient energy method.* The above inequality must hold not only at clearing time, but also during the post-fault.

$$V_{ke}(\omega) + V_{pe}(\delta) < V_{pe}(\delta_u) \tag{2.14}$$

$$\frac{M}{2}\omega^2 - P_m(\delta - \delta_s) - P_{\max}^{(3)}(\cos\delta - \cos\delta_s) < -P_m(\delta_u - \delta_s) - P_{\max}^{(3)}(\cos\delta_u - \cos\delta_s)$$

Following a disturbance the system is transiently stable if the total transient energy is less than the potential energy evaluated at the u.e.p.

2.6 Phase plane trajectories

We will find the trajectories corresponding to the pre-fault, fault and post-fault intervals.

- Pre-fault

- The equilibrium point at prefault is given by

$$\delta_o = sin^{-1}\left(\frac{P_m}{P_{\max}^{(1)}}\right), \text{ rad}; \omega = 0, rad/s$$

The trajectory during pre-fault is the point $(\delta_o, 0)$.

- Fault

  - The motion during the fault starts at $(\delta_o, 0)$, since these quantities cannot change instantaneously. The model during the fault is represented by the following equations.

$$\frac{d\delta}{dt} = \omega, \frac{\text{rad}}{\text{s}}$$

$$M\frac{d\omega}{dt} = P_m - P_{\max}^{(2)}\sin(\delta), \frac{\text{MW}}{\text{MVA}}$$

The accelerating area A_a equals the transient kinetic energy.

$$A_a = \frac{1}{2}M\omega^2$$

$$A_a = \int_{\delta_0}^{\delta_{cl}} \left[P_m - P_{\max}^{(2)}\sin(\delta)\right] d\delta$$

$$\omega = \sqrt{\frac{2}{M}\int_{\delta_0}^{\delta_{cl}} \left[P_m - P_{\max}^{(2)}\sin(\delta)\right] d\delta}, \frac{\text{rad}}{s}$$

The positive radical was taken because we know that the system is accelerating during the fault.

- Post-fault

  - After the fault is cleared the model is represented by the following equations:

$$\frac{d\delta}{dt} = \omega, \frac{\text{rad}}{\text{s}}$$

$$M\frac{d\omega}{dt} = P_m - P_{\max}^{(3)}\sin(\delta), \frac{\text{MW}}{\text{MVA}}$$

- Since the idealized model provides no damping, $V(\delta,\omega)$ is constant and equal to $V(\delta_{sl},\omega_{cl})$ after the fault, i.e.

$$\frac{1}{2}M\omega^2 + V_{pe}(\delta) = V(\delta_{cl},\omega_{cl}), \text{ or}$$

$$\omega = \pm\sqrt{\frac{2}{M}\left\{V(\delta_{cl},\omega_{cl}) + P_m(\delta-\delta_s) + P_{\max}^{(3)}[\cos(\delta)-\cos(\delta_s)]\right\}}, \frac{\text{rad}}{\text{s}}.$$

This equation gives the trajectory after the disturbance.

Fig 2-17 a) shows the potential energy vs. δ according to Eq. 2.9. The parameters of the system used to obtain this plot are the following:

$P_{\max}^{postfault} = 1.5$ pu,

$P_m = 1.0$ pu,

$M = 0.025\ \frac{\text{MW s}^2}{\text{MVA rad}}$.

Using these parameters we get that

$V_{pe}(\delta_u) = 0.554$ and

$V_{pe}(\delta_u - 2\cdot\pi) = 6.837$.

Fig 2-17 a) also illustrates the following results:

$$A_c = V_{pe}(\delta_{cl})$$

$$A_a = V_{ke}(\omega_{cl})$$

$$A_c + A_{dmax} = V_{pe}(\delta_u)$$

Fig 2-17 b) shows the pre-fault stable equilibrium point, δ_o; the faulted trajectory, which initiates at $(\delta_o, 0)$ and ends at $(\delta_{cl}, \omega_{cl})$; the post-fault trajectory (constant V); and the contour map for the transient energy, this contour map has increments of $V_{pe}(\delta_u)/5$, i.e. the inner-most contour represents a level of $V_{pe}(\delta_u)/5$, the second contour represents twice as much. The solid contour represents the post-fault trajectory corresponding to the critically stable case, the state

tends to $(\delta_u, 0)$ as time tends to ∞. A small amount of energy less than this critical energy makes the system stable. Whereas a small amount of energy more than this critical energy makes the system unstable, i.e. if the fault is cleared when the total energy is less than $V_{pe}(\delta_u)$ then the system is stable, otherwise is unstable

From Fig 2-17 c) we gain a better understanding of the way the areas relate to transient energy.

Fig 2-18 is the 3-D plot of the transient energy vs. δ and ω. From this figure we can see why this plot is sometimes called the energy well. This plot has stacked contour lines with a contour interval of 0.5 $\frac{\text{MW rad}}{\text{MVA}}$.

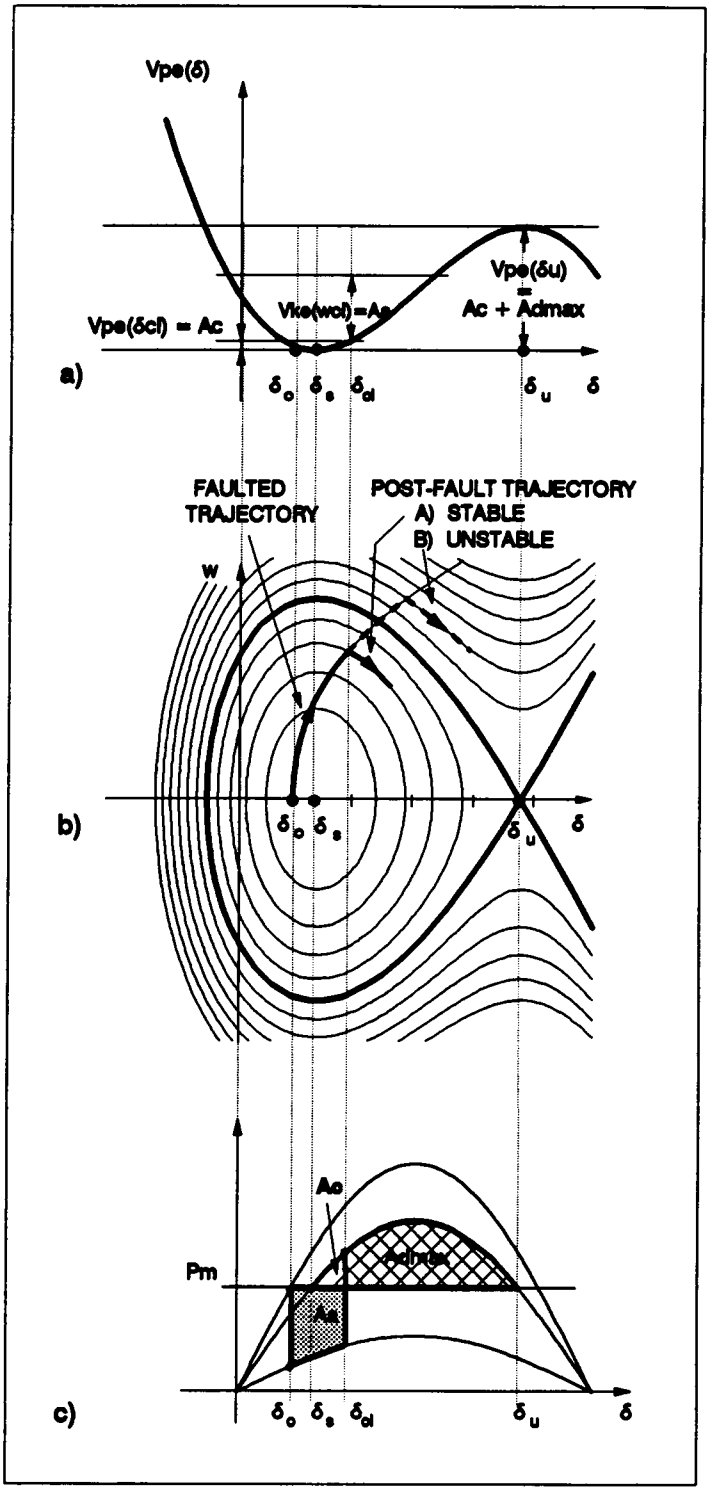

Figure 2-17: Transient Energy Method

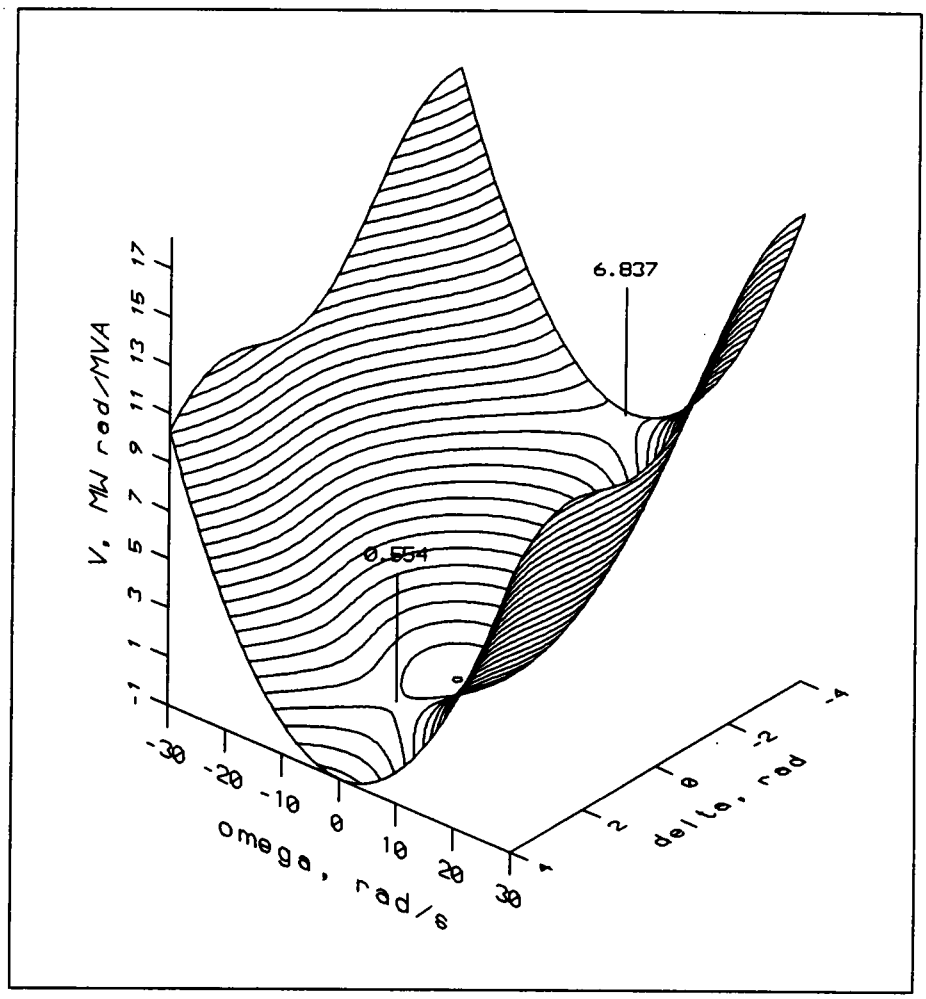

Figure 2-18: Transient Energy Function

Chapter 3

Transient Energy Function for Multi-machine Systems

3.1 Power system representation

The synchronous machines are represented as a constant voltage source behind the direct-axis transient reactance, X'_d. The loads are modeled as constant admittance, and the input power from the prime mover, P_m, is assumed constant. These parameters constitute the classical representation of a power system.

3.2 Reduction to internal nodes

In order to get an expression for the electrical power at the internal nodes of the machines, it is convenient to reduce the system to the internal nodes. The steps to accomplish this reduction are the following [56]:

1. Use the prefault load-flow, $Y_L = (P_{load} - jQ_{load})/V^2$,to obtain the admittance value of the loads. These values are included in the diagonal of the admittance matrix, Y_{bus}. $Y^{new}_{bus}(i,i) = Y_{bus}(i,i) + Y_l(i)$ (see Fig. 3-1 and Fig. 3-2).

2. Update $\underline{Y}^{new}_{bus}$ to include the transient reactances. Create the $\underline{Y}_{12}$, $\underline{Y}_{21}$, and $\underline{Y}_{22}$ matrices. These three matrices are part of the extended matrix, $\underline{Y}_{ext}$, which includes all of the

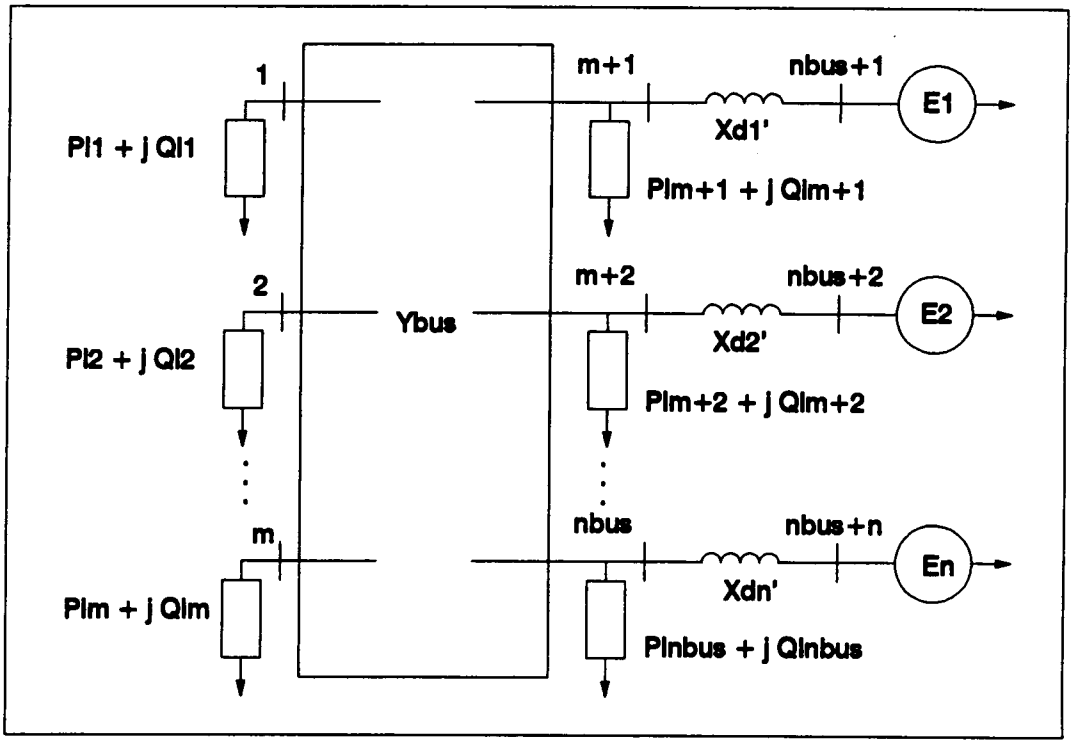

Figure 3-1: Original System

original buses plus the internal nodes (see Fig. 3-3). The partition of $\underline{\mathbf{Y}}_{ext}$ is the following matrix:

$$\underline{\mathbf{Y}}_{ext} = \begin{bmatrix} \underline{\mathbf{Y}}_{bus}^{new} & \underline{\mathbf{Y}}_{12} \\ \underline{\mathbf{Y}}_{21} & \underline{\mathbf{Y}}_{22} \end{bmatrix}$$

If n is the number of buses with generation and $nbus$ is the number of buses in the system, then

$\underline{\mathbf{Y}}_{bus}^{new}$ is of order $(nbus \times nbus)$

$\underline{\mathbf{Y}}_{12}$ is of order $(nbus \times n)$

$\underline{\mathbf{Y}}_{21}$ is of order $(n \times nbus)$

$\underline{\mathbf{Y}}_{22}$ is of order $(n \times n)$

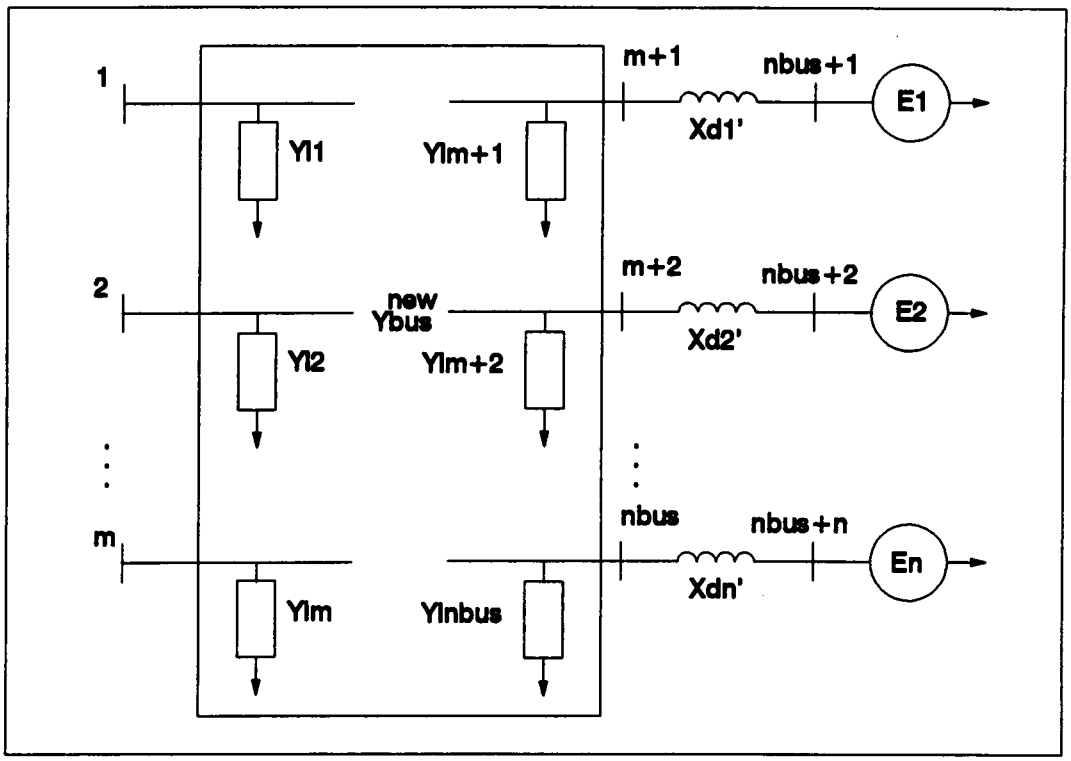

Figure 3-2: Loads Modelled as constant Admittances

3. Notice from Fig. 3-4 that for the extended system the following system of equations holds:

$$\begin{bmatrix} \underline{0} \\ \underline{I}_{int} \end{bmatrix} = \begin{bmatrix} \underline{Y}_{bus}^{new} & \underline{Y}_{12} \\ \underline{Y}_{21} & \underline{Y}_{22} \end{bmatrix} \begin{bmatrix} \underline{V} \\ \underline{E} \end{bmatrix}$$

The following equation eliminates all external nodes.

$$\underline{Y}_{red} = \underline{Y}_{22} - \underline{Y}_{21} [\underline{Y}_{bus}^{new}]^{-1} \underline{Y}_{12}$$

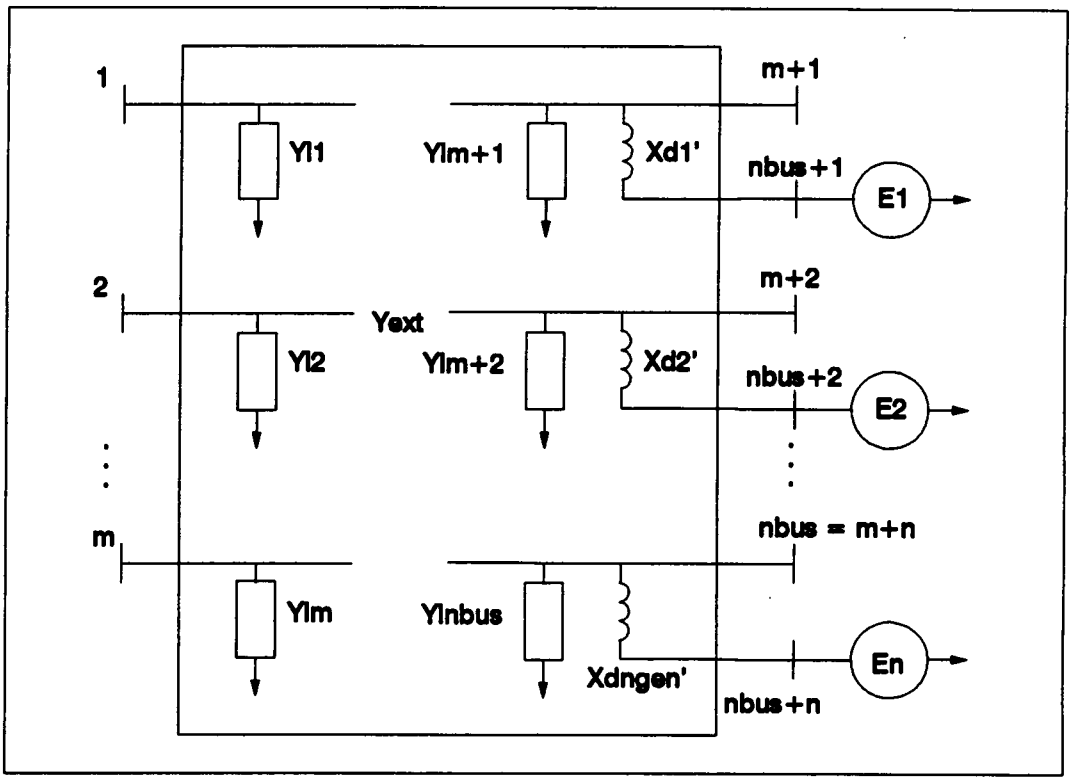

Figure 3-3: Extended System

3.3 Electrical power

Now we will find an expression for the electrical power at the internal node i [56]. The complex power at node i is given by the equation

$$P_{gi} + jQ_{gi} = \mathbf{E_i I_i^*}, \text{ pu} \tag{3.1}$$

The current injection, $\mathbf{I_i}$, is given by Eq. 3.2

$$\mathbf{I_i} = \sum_{k=1}^{n} [(G_{ik} + jB_{ik})\,\mathbf{E_k}] \tag{3.2}$$

$G_{ik} + jB_{ik}$ is the element i, k of the reduced admittance matrix. After substituting Eq. 3.2 into

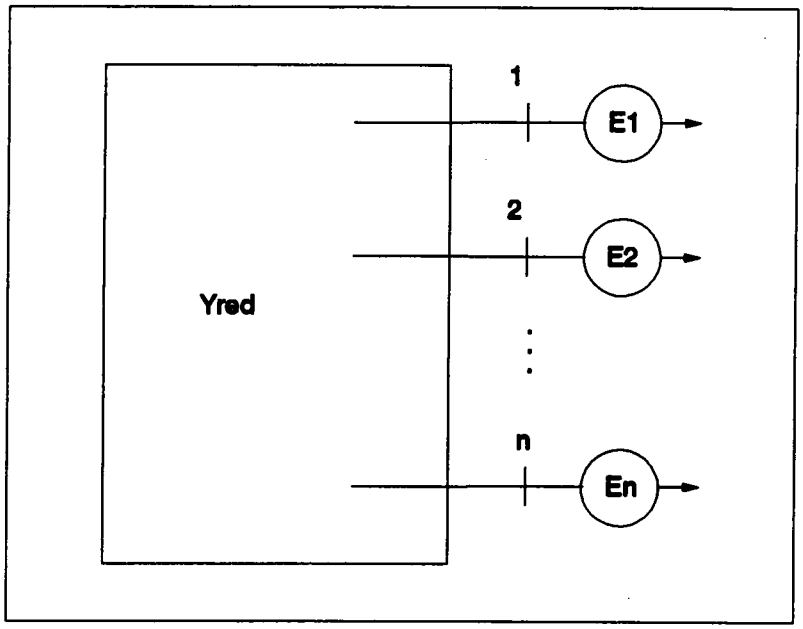

Figure 3-4: System Reduced to Internal Nodes

Eq. 3.1 we get

$$P_{gi} + jQ_{gi} = \sum_{k=1}^{n} \left[(G_{ik} - jB_{ik}) E_i E_k e^{j(\delta_i - \delta_k)} \right]$$

The imaginary term is ignored to yield

$$P_{gi} = \sum_{k=1}^{n} [B_{ik} E_i E_k \sin(\delta_i - \delta_k) + G_{ik} E_i E_k \cos(\delta_i - \delta_k)]$$

or

$$P_{gi} = G_{ii} E_i^2 + \sum_{k=1, \neq i}^{n} [B_{ik} E_i E_k \sin(\delta_i - \delta_k) + G_{ik} E_i E_k \cos(\delta_i - \delta_k)]$$

Let us define the following terms:

$$C_{ik} = B_{ik} E_i E_k$$

$$D_{ik} = G_{ik} E_i E_k$$

$$P_{ei} = \sum_{k=1, \neq i}^{n} [C_{ik} \sin(\delta_i - \delta_k) + D_{ik} \cos(\delta_i - \delta_k)]$$

Eq. 3.3 results.

$$P_{gi} = G_{ii} \; E_i^2 + P_{ei} \tag{3.3}$$

3.4 Differential equations

The swing equation (Eq. 2.6) for machine i results in the following equation:

$$M_i \frac{d^2\delta_i}{dt^2} = P_{mi} - P_{gi}, \text{ pu}$$

After substituting Eq. 3.3 into the above equation we get

$$M_i \frac{d^2\delta_i}{dt^2} = P_{mi} - G_{ii}\, E_i^2 - P_{ei}, \text{ pu}$$

If we define $P_i = P_{mi} - G_{ii}E_i^2$, the swing equation results in Eq.3.4.

$$M_i \frac{d^2\delta_i}{dt^2} = P_i - P_{ei}, \text{ pu}, i = 1, \cdots, n \tag{3.4}$$

3.5 Number of state variables

From Eq. 3.4 we have n second-order differential equations. For the state equation, we need the following $2n$ first-order differential equations:

$$\begin{aligned} \frac{d\delta_i}{dt} &= \omega_i, \text{ rad/s}; \\ \frac{d\omega_i}{dt} &= \frac{P_i - P_{ei}}{M_i}, \text{ rad/s}^2, \text{ for } i = 1, \cdots, n \end{aligned} \tag{3.5}$$

In the right-hand side of the swing equation (Eq. 3.4), angle differences are used instead of the angles with respect to a synchronously rotating axis, i.e. we need $\delta_i - \delta_k$ instead of only δ_i. This reasoning suggests that the number of state variables is $2(n-1)$ instead of $2n$. In order to assess the transient stability of a power system, we must consider relative angles instead of the actual angles in a synchronously rotating frame (Eq. 3.5). As explained in reference [56] there are two choices:

- Angles-with-respect-to-a-reference machine formulation
- Center of angle formulation

both choices lead to $2 \cdot (n-1)$ state variables. Eq. 3.5 is not the state equation.

$$nstate = 2(n-1)$$

3.6 One-machine reference frame

In this formulation, the machine with the largest inertia is usually chosen as the reference. *We will designate the last machine as reference*. From Eq. 3.5, the first-order differential equation of the reference machine is

$$\begin{aligned} \frac{d\delta_n}{dt} &= \omega_n, \text{ rad/s} \\ \frac{d\omega_n}{dt} &= \frac{P_n - P_{en}}{Mn}, \text{ rad/s}^2 \end{aligned}$$

After subtracting the above equation from Eq. 3.5 we get the *state equation* with machine-n as the reference formulation (Eq. 3.6).

$$\begin{aligned} \frac{d\delta_{in}}{dt} &= \omega_{in}, \text{ rad/s} \\ \frac{d\omega_{in}}{dt} &= \frac{P_i - P_{ei}}{M_i} - \frac{P_n - P_{en}}{M_n}, \text{ rad/s}^2 \text{ (for } i = 1, \cdots, n-1) \end{aligned} \tag{3.6}$$

where

$\delta_{in} = \delta_i - \delta_n,$

$\omega_{in} = \omega_i - \omega_n,$

$P_i = P_{mi} - G_{ii}\ E^2$

$P_{ei} = \sum_{j=1,\neq i}^{n-1} [C_{ij} \sin(\delta_{in} - \delta_{jn}) + D_{ij} \cos(\delta_{in} - \delta_{jn})] + C_{in} \sin \delta_{in} + D_{in} \cos \delta_{in}$

$P_{en} = \sum_{j=1}^{n-1} [C_{nj} \sin(-\delta_{jn}) + D_{nj} \cos(-\delta_{jn})]$

$C_{ij} = B_{ij} E_i E_j$

$D_{ij} = G_{ij}\ E_i\ E_j$

$G_{ij} + j\ B_{ij}$ is the element ij of the reduced admittance matrix.

If we define the *angle subspace* as

$$\underline{\delta} = \begin{bmatrix} \delta_{1n} \\ \delta_{2n} \\ \vdots \\ \delta_{(n-1)n} \end{bmatrix}$$

and the *angular velocity subspace* as

$$\underline{\omega} = \begin{bmatrix} \omega_{1n} \\ \omega_{2n} \\ \vdots \\ \omega_{(n-1)n} \end{bmatrix}$$

then the *state vector* is the following vector:

$$\underline{x} = \begin{bmatrix} \underline{\delta} \\ \underline{\omega} \end{bmatrix}$$

3.7 Center of angle reference frame

This formulation uses the inertia-weighed average of the n angles as reference [73]. The center of angle is defined as Eq. 3.7

$$\delta_o = \frac{1}{M_t} \sum_{i=1}^{n} M_i \delta_i; \; M_t = \sum_{i=1}^{n} M_i \tag{3.7}$$

The angles with respect to the center angle are

$$\tilde{\delta}_i = \delta_i - \delta_o$$

The same is taken into account for the angular velocities.

$$\dot{\delta}_0 = \omega_0$$

$$\omega_0 = \frac{1}{M_t}\sum_{i=1}^{n} M_i\omega_i$$

The first derivatives of the angles in center of angle, COA, are

$$\tilde{\omega}_i = \omega_i - \omega_o$$

To obtain the dynamics of the COA, multiply Eq. 3.7 by M_t to get Eq. 3.8.

$$M_t \cdot \delta_o = \sum_{i=1}^{n} M_i \cdot \delta_i \tag{3.8}$$

After taking the second derivative we obtain $M_t \cdot \ddot{\delta}_o = \sum_{i=1}^{n} M_i \cdot \ddot{\delta}_i$. Notice that the right-hand side of this equation is the sum of all n swing equations.

$$\begin{aligned} M_t \cdot \ddot{\delta}_o &= \sum_{i=1}^{n} P_i - \sum_{i=1}^{n} P_{ei} \\ &= \sum_{i=1}^{n} P_i - 2\sum_{i=1}^{n-1}\sum_{j=i+1}^{n} D_{ij}\cos\tilde{\delta}_{ij} \end{aligned}$$

If we define the power of the center of the COA as

$$P_{coa} = \sum_{i=1}^{n} P_i - 2\sum_{i=1}^{n-1}\sum_{j=i+1}^{n} D_{ij}\cos\tilde{\delta}_{ij}$$

then the dynamics of the COA are given by Eq. 3.9.

$$\begin{aligned} \dot{\delta}_0 &= \omega_0 \\ \dot{\omega}_0 &= \frac{1}{M_t} P_{coa} \end{aligned} \tag{3.9}$$

According to Eq. 3.4, P_{coa} is also equal to the mechanical input power minus the electrical output power, i.e. $P_{coa} = \sum_{i=1}^{n} P_{mi} - \sum_{i=1}^{n} P_{gi}$.

Now we can subtract Eq. 3.9 from Eq. 3.5 to get

$$\begin{aligned} \frac{d\tilde{\delta}_i}{dt} &= \tilde{\omega}_i, \text{ rad/s} \\ \frac{d\tilde{\omega}_i}{dt} &= \frac{P_i - P_{ei}}{M_i} - \frac{P_{coa}}{M_t}, \text{ rad/s}^2 \text{ for } i = 1, 2, \cdots, n \end{aligned} \tag{3.10}$$

Notice that we still have $2 \cdot n$ equations, but we will show that only $2 \cdot (n-1)$ are required. We

can rewrite Eq. 3.8 as

$$\sum_{i=1}^{n} M_i \tilde{\delta}_i = 0 \tag{3.11}$$

By taking the first and second derivatives we get

$$\begin{aligned} \textstyle\sum_{i=1}^{n} M_i \tilde{\omega}_i &= 0 \\ \textstyle\sum_{i=1}^{n} M_i \frac{d\tilde{\omega}_i}{dt} &= 0 \end{aligned} \tag{3.12}$$

From the last equation we can conclude that any pair of the $2n$ equations in Eq. 3.10 can be expressed as a linear combination of the rest. We will arbitrarily choose the pair corresponding to $i = n$ in order to get the *state equation in COA* (Eq. 3.13).

$$\begin{aligned} \tfrac{d\tilde{\delta}_i}{dt} &= \tilde{\omega}_i, \text{ rad/s;} \\ \tfrac{d\tilde{\omega}_i}{dt} &= \tfrac{P_i - P_{ei}}{M_i} - \tfrac{P_{coa}}{M_t}, \text{ rad/s}^2 \text{ (for } i = 1, 2, \cdots, n-1) \end{aligned} \tag{3.13}$$

where

$$P_i = P_{mi} - G_{ii}\, E_i^2$$

$$P_{ei} = \textstyle\sum_{j=1,\neq i}^{n-1} \left\{ C_{ij} \sin(\tilde{\delta}_i - \tilde{\delta}_j) + D_{ij} \cos(\tilde{\delta}_i - \tilde{\delta}_j) \right\} + C_{in} \sin(\tilde{\delta}_i - \tilde{\delta}_n) + D_{in} \cos(\tilde{\delta}_i - \tilde{\delta}_n)$$

$$C_{ij} = B_{ij} E_i E_j$$

$$D_{ij} = G_{ij} E_i E$$

$G_{ij} + j\, B_{ij}$ is the element ij of the reduced admittance matrix.

$$P_{coa} = \textstyle\sum_{i=1}^{n} P_i - 2 \sum_{i=1}^{n-2} \sum_{j=i+1}^{n-1} D_{ij} \cos(\tilde{\delta}_i - \tilde{\delta}_j) - \sum_{i=1}^{n-1} D_{in} \cos(\tilde{\delta}_i - \tilde{\delta}_n)$$

From Eq. 3.11 and Eq. 3.12, $\tilde{\delta}_n$ and $\tilde{\omega}_n$ are given by the following equations:

$$\begin{aligned} \tilde{\delta}_n &= -\tfrac{1}{M_n} \textstyle\sum_{i=1}^{n-1} M_i \tilde{\delta}_i \\ \tilde{\omega}_n &= -\tfrac{1}{M_n} \textstyle\sum_{i=1}^{n-1} M_i \tilde{\omega}_i \end{aligned} \tag{3.14}$$

Notice that although $\tilde{\delta}_n$ appears in Eq. 3.13, it is given as a function of the angle subspace in Eq. 3.14.

Now, if we define the *angle subspace* as

$$\tilde{\underline{\delta}} = \begin{bmatrix} \tilde{\delta}_1 \\ \tilde{\delta}_2 \\ \vdots \\ \tilde{\delta}_{n-1} \end{bmatrix}$$

and the *angular velocity subspace* as

$$\tilde{\underline{\omega}} = \begin{bmatrix} \tilde{\omega}_1 \\ \tilde{\omega}_2 \\ \vdots \\ \tilde{\omega}_{n-1} \end{bmatrix}$$

the *state vector* results in the following equation:

$$\tilde{\underline{x}} = \begin{bmatrix} \tilde{\underline{\delta}} \\ \tilde{\underline{\omega}} \end{bmatrix}$$

3.8 Step-by-step transient stability analysis

At prefault, $t = 0$. Before the fault the system is in equilibrium, i.e. the initial angular velocity subspace is zero, $\tilde{\underline{\omega}}^o = 0$; and the initial angle subspace, $\tilde{\underline{\delta}}^o$, is obtained from the following load-flow solution:

- $E_i e^{j\delta_i} = \mathbf{V_t} + jX'_d \frac{(P_g + jQ_g)^*}{\mathbf{V_t^*}}$
- $P_g + jQ_g$ is the complex power supplied by machine i,
- V_t is the phasor voltage at the terminals of machine i, and
- X'_d is the transient reactance of machine i.

During the fault, $0 < t \leq tcl$. The state equation is given by Eq. 3.13 if the reference is the COA or Eq. 3.6 if the reference is an arbitrary machine. We then integrate this equation

numerically. For instance, Runge-Kutta fourth order can be used. P_i^f, C_{ik}^f and D_{ik}^f are obtained considering the fault.

During postfault, $tcl < t \leq t_f$. The state equation is again integrated numerically. But P_i, C_{ik} and D_{ik} are not the same as those of the fault-on period since these do not include the fault, and generally a line opens in order to clear the fault.

3.9 The transient energy in the center of angle formulation

The following steps obtain the transient energy function in COA formulation for multimachine-systems [57].

1. Obtain the swing equation in COA formulation. Eq. 3.4 is the swing equation for machine i.

$$M_i \cdot \frac{d^2\delta_i}{dt^2} = P_i - P_{ei}, \quad \text{for } i = 1, ..., n$$

Eq. 3.9 represents the dynamics of the center of angle.

$$\frac{d^2\delta_0}{dt^2} = P_{coa}/M_t, \text{ rad/s}^2$$

To get the *swing equation in COA formulation* (Eq. 3.15), we have to multiply the last equation by M_i and subtract the result from the swing equation (Eq. 3.4).

$$M_i \frac{d^2\tilde{\delta}_i}{dt^2} = P_i - P_{ei} - \frac{M_i}{M_t} P_{coa}, \text{ for } i = 1, \cdots n$$

or

$$M_i \frac{d^2\tilde{\delta}_i}{dt^2} - P_i + P_{ei} + \frac{M_i}{M_t} P_{coa} = 0 \qquad (3.15)$$

$$i = 1, 2, \cdots, n$$

where

$$P_i = P_{mi} - G_{ii}\, E_i^2$$

$$P_{ei} = \sum_{j=1, \neq i}^{n} \left[C_{ij} \sin \tilde{\delta}_{ij} + D_{ij} \cos \tilde{\delta}_{ij} \right]$$

$$C_{ij} = B_{ij} E_i E_j$$

$D_{ij} = G_{ij} E_i E_j$

$G_{ij} + j\, B_{ij}$ is the element ij of the reduced admittance matrix.

$P_{coa} = \sum_{i=1}^{n} P_i - 2 \sum_{i=1}^{n-1} \sum_{j=i+1}^{n} D_{ij} \cos \tilde{\delta}_{ij}$

$M_t = \sum_{i=1}^{n} M_i$

2. Multiply Eq. 3.15 by $\frac{d\tilde{\delta}_i}{dt}$.

$$M_i \frac{d\tilde{\delta}_i}{dt} \frac{d^2\tilde{\delta}_i}{dt^2} - P_i \frac{d\tilde{\delta}_i}{dt} + P_{ei} \frac{d\tilde{\delta}_i}{dt} + \frac{M_i}{M_t} P_{coa} \frac{d\tilde{\delta}_i}{dt} = 0$$

$$i = 1, 2, \cdots, n$$

3. Add all n previous equations.

$$\sum_{i=1}^{n} M_i \tilde{\omega}_i \frac{d\tilde{\omega}_i}{dt} - \sum_{i=1}^{n} P_i \frac{d\tilde{\delta}_i}{dt} + \underline{\sum_{i=1}^{n} \sum_{j=1, \neq i}^{n} [C_{ij} \sin \tilde{\delta}_{ij} + D_{ij} \cos \tilde{\delta}_{ij}] \frac{d\tilde{\delta}_i}{dt}} + \underline{\sum_{i=1}^{n} \frac{P_{coa}}{M_t} M_i \frac{d\tilde{\delta}_i}{dt}} = 0 \tag{3.16}$$

Let us do some algebra on the underlined terms.

–

$$\sum_{i=1}^{n} \sum_{j=1, \neq i}^{n} C_{ij} \sin \tilde{\delta}_{ij} \frac{d\tilde{\delta}_i}{dt} = \sum_{i=1}^{n-1} \sum_{j=i+1}^{n} C_{ij} \sin(\tilde{\delta}_i - \tilde{\delta}_j) \frac{d}{dt}(\tilde{\delta}_i - \tilde{\delta}_j)$$

$$\sum_{i=1}^{n} \sum_{j=1, \neq i}^{n} D_{ij} \cos \tilde{\delta}_{ij} \frac{d\tilde{\delta}_i}{dt} = \sum_{i=1}^{n-1} \sum_{j=i+1}^{n} D_{ij} \cos(\tilde{\delta}_i - \tilde{\delta}_j) \frac{d}{dt}(\tilde{\delta}_i + \tilde{\delta}_j)$$

If $C_{ij} = C_{ji}$ and $D_{ij} = D_{ji}$,

–

$$\sum_{i=1}^{n} \frac{P_{coa}}{M_t} M_i \frac{d\tilde{\delta}_i}{dt} = \frac{P_{coa}}{M_t} \sum_{i=1}^{n} M_i \frac{d\tilde{\delta}_i}{dt}$$

From Eq. 3.12 $\sum_{i=1}^{n} M_i \frac{d\tilde{\delta}_i}{dt} = 0$; therefore, $\frac{P_{coa}}{M_t} \sum_{i=1}^{n} M_i \frac{d\tilde{\delta}_i}{dt} = 0$. Substituting these results into Eq. 3.16 we get Eq. 3.17.

$$\begin{aligned} 0 \;=\; & \sum_{i=1}^{n} M_i \tilde{\omega}_i \frac{d\tilde{\omega}_i}{dt} - \sum_{i=1}^{n} P_i \frac{d\tilde{\delta}_i}{dt} \\ + \; & \sum_{i=1}^{n} \sum_{j=i+1}^{n} \left\{ C_{ij} \sin \tilde{\delta}_{ij} \frac{d(\tilde{\delta}_i - \tilde{\delta}_j)}{dt} + D_{ij} \cos \tilde{\delta}_{ij} \frac{d(\tilde{\delta}_i + \tilde{\delta}_j)}{dt} \right\} \end{aligned} \tag{3.17}$$

4. As mentioned in the previous chapter, in the absence of damping, the transient energy remains constant, i.e. $\frac{dV}{dt} = 0$. During the disturbance, transient energy is injected to the system. After the disturbance (postfault), the transient energy $V(\tilde{\underline{\delta}}, \tilde{\underline{\omega}})$ remains constant. The last equation is $-\frac{dV}{dt}$.To obtain $V(\tilde{\underline{\delta}}, \tilde{\underline{\omega}})$ we must integrate from t to t_s;

$$V(\tilde{\underline{\delta}}, \tilde{\underline{\omega}}) = \int_t^{t_s} \left(\frac{dV}{dt}\right) dt$$

or

$$V(\tilde{\underline{\delta}}, \tilde{\underline{\omega}}) = \int_{t_s}^{t} \left(-\frac{dV}{dt}\right) dt \tag{3.18}$$

where $t \geq t_{cl}$ and t_s is the time when the stable equilibrium point, *s.e.p.*, is reached. Notice that this is a mathematical trick. Because of the absence of damping, the s.e.p. is never reached. After substituting Eq. 3.17 we get

$$\begin{aligned} V(\tilde{\underline{\delta}}, \tilde{\underline{\omega}}) &= \int_{t_s}^{t} \sum_{i=1}^{n} M_i \tilde{\omega}_i \frac{d\tilde{\omega}_i}{dt} - \sum_{i=1}^{n} P_i \frac{d\tilde{\delta}_i}{dt} \\ &+ \sum_{i=1}^{n-1} \sum_{j=i+1}^{n} \left[C_{ij} \sin \tilde{\delta}_{ij} \frac{d}{dt}\tilde{\delta}_{ij} + D_{ij} \cos(\tilde{\delta}_i - \tilde{\delta}_j) \frac{d}{dt}(\tilde{\delta}_i + \tilde{\delta}_j) \right] dt \end{aligned}$$

or

$$\begin{aligned} V(\tilde{\underline{\delta}}, \tilde{\underline{\omega}}) &= \int_{\tilde{\omega}_i(t_s)}^{\tilde{\omega}_i(t)} \left[\sum_{i=1}^{n} M_i \tilde{\omega}_i\right] d\tilde{\omega}_i - \int_{\tilde{\delta}_i(t_s)}^{\tilde{\delta}_i(t)} \left[\sum_{i=1}^{n} P_i\right] d\tilde{\delta}_i \\ &+ \int_{\tilde{\delta}_{ij}(t_s)}^{\tilde{\delta}_{ij}(t)} \left[\sum_{i=1}^{n-1} \sum_{j=i+1}^{n} C_{ij} \sin \tilde{\delta}_{ij}\right] d\tilde{\delta}_{ij} \\ &+ \int_{\tilde{\delta}_i(t_s)+\tilde{\delta}_j(t_s)}^{\tilde{\delta}_i(t)+\tilde{\delta}_j(t)} \left[\sum_{i=1}^{n-1} \sum_{j=i+1}^{n} D_{ij} \cos(\tilde{\delta}_i - \tilde{\delta}_j)\right] d(\tilde{\delta}_i + \tilde{\delta}_j) \end{aligned}$$

If $\tilde{\omega}_i(t_s) = 0$, $\tilde{\omega}_i(t) = \tilde{\omega}_i$, $\tilde{\delta}_i(t_s) = \tilde{\delta}_i^s$ and $\tilde{\delta}_i(t) = \tilde{\delta}_i$, then

$$\begin{aligned} V(\tilde{\underline{\delta}}, \tilde{\underline{\omega}}) &= \sum_{i=1}^{n} \left[M_i \int_0^{\tilde{\omega}_i} \tilde{\omega}_i \, d\tilde{\omega}_i\right] - \sum_{i=1}^{n} \left[\int_{\tilde{\delta}_i^s}^{\tilde{\delta}_i} P_i \, d\tilde{\delta}_i\right] \\ &+ \sum_{i=1}^{n-1} \sum_{j=i+1}^{n} \left[\int_{\tilde{\delta}_{ij}^s}^{\tilde{\delta}_{ij}} C_{ij} \sin \tilde{\delta}_{ij} \, d\tilde{\delta}_{ij}\right] \\ &+ \sum_{i=1}^{n-1} \sum_{j=i+1}^{n} \left[\int_{\tilde{\delta}_i^s+\tilde{\delta}_j^s}^{\tilde{\delta}_i+\tilde{\delta}_j} D_{ij} \cos(\tilde{\delta}_i - \tilde{\delta}_j) \, d(\tilde{\delta}_i + \tilde{\delta}_j)\right] \end{aligned}$$

After integrating we get the *transient energy in COA formulation*:

$$\begin{aligned} V\left(\tilde{\underline{\delta}},\tilde{\underline{\omega}}\right) &= \sum_{i=1}^{n-1}\frac{M_i}{2}\tilde{\omega}_i^2+\frac{M_n}{2}\tilde{\omega}_n^2-\sum_{i=1}^{n-1}P_i\left(\tilde{\delta}_i-\tilde{\delta}_i^s\right)\\ &- P_n\left(\tilde{\delta}_n-\tilde{\delta}_n^s\right)-\sum_{i=1}^{n-2}\sum_{j=i+1}^{n-1}C_{ij}\left(\cos\tilde{\delta}_{ij}-\cos\tilde{\delta}_{ij}^s\right)\\ &- \sum_{i=1}^{n-1}C_{in}\left(\cos\tilde{\delta}_{in}-\cos\tilde{\delta}_{in}^s\right)\\ &+ \sum_{i=1}^{n-2}\sum_{j=i+1}^{n-1}\left[\int_{\tilde{\delta}_i^s+\tilde{\delta}_j^s}^{\tilde{\delta}_i+\tilde{\delta}_j}D_{ij}\cos(\tilde{\delta}_i-\tilde{\delta}_j)\,d(\tilde{\delta}_i+\tilde{\delta}_j)\right]\\ &- \sum_{i=1}^{n-1}\left[\int_{\tilde{\delta}_i^s+\tilde{\delta}_n^s}^{\tilde{\delta}_i+\tilde{\delta}_n}D_{in}\cos(\tilde{\delta}_i-\tilde{\delta}_n)\,d(\tilde{\delta}_i+\tilde{\delta}_n)\right] \end{aligned}$$

Although $\tilde{\omega}_n$ and $\tilde{\delta}_n$ appear in the above equation they are expressed as functions of $\tilde{\underline{\omega}}$ and $\tilde{\underline{\delta}}$ (Eq. 3.14). The notation, $V(\tilde{\delta},\tilde{\omega})$, is therefore correct. For simplicity we will use Eq. 3.19.

$$\begin{aligned} V\left(\tilde{\underline{\delta}},\tilde{\underline{\omega}}\right) &= \sum_{i=1}^{n}\frac{M_i}{2}\tilde{\omega}_i^2-\sum_{i=1}^{n}P_i\left(\tilde{\delta}_i-\tilde{\delta}_i^s\right)\\ &- \sum_{i=1}^{n-1}\sum_{j=i+1}^{n}C_{ij}\left(\cos\tilde{\delta}_{ij}-\cos\tilde{\delta}_{ij}^s\right)\\ &+ \sum_{i=1}^{n-1}\sum_{j=i+1}^{n}\left[\int_{\tilde{\delta}_i^s+\tilde{\delta}_j^s}^{\tilde{\delta}_i+\tilde{\delta}_j}D_{ij}\cos(\tilde{\delta}_i-\tilde{\delta}_j)\,d(\tilde{\delta}_i+\tilde{\delta}_j)\right] \end{aligned} \tag{3.19}$$

Now, let us discuss each of the terms in Eq. 3.19.

- The first term in Eq. 3.19 is the transient kinetic energy: $V_{ke}(\tilde{\underline{\omega}}) = \frac{1}{2}\sum_{i=1}^{n}M_i\tilde{\omega}_i^2$, $\frac{\text{MW rad}}{\text{MVA}}$.

The remainder is the transient potential energy, which, as proposed in reference [56], may be decomposed in the following two terms:

- $V_p(\tilde{\underline{\delta}}) = -\sum_{i=1}^{n}P_i\left(\tilde{\delta}_i-\tilde{\delta}_i^s\right)-\sum_{i=1}^{n-1}{}_j\sum_{j=i+1}^{n}C_{ij}(\cos\tilde{\delta}_{ij}-\cos\tilde{\delta}_{ij}^s)$, $\frac{\text{MW rad}}{\text{MVA}}$
- $V_d(\tilde{\underline{\delta}}) = \sum_{i=1}^{n-1}\sum_{j=i+1}^{n}\int_{\tilde{\delta}_i^s+\tilde{\delta}_j^s}^{\tilde{\delta}_i+\tilde{\delta}_j}D_{ij}\cos(\tilde{\delta}_i-\tilde{\delta}_j)\,d(\tilde{\delta}_i+\tilde{\delta}_j)$, $\frac{\text{MW rad}}{\text{MVA}}$. This term is path dependent, i.e. the term is integrable only if the path from $\tilde{\underline{\delta}}(t)$ to $\tilde{\underline{\delta}}(t_s)$ is known or if $n = 2$. This problem may be overcome by using the linear ray approximation proposed originally in reference [80].

3.10 Ray approximation in center of angle formulation

The trajectory from $\tilde{\underline{\xi}}$ to $\tilde{\underline{\xi}}^s$ can be approximated by a linear trajectory, [1]. Let us define I_{ij} as

$$I_{ij} = \int_{\tilde{\delta}_i^s + \tilde{\delta}_j^s}^{\tilde{\delta}_i + \tilde{\delta}_j} \cos(\tilde{\delta}_i - \tilde{\delta}_j)\, d(\tilde{\delta}_i + \tilde{\delta}_j), \frac{\text{MW rad}}{\text{MVA}} \tag{3.20}$$

The following equation results.

$$V_d(\tilde{\underline{\xi}}) = \sum_{i=1}^{n-1} \sum_{j=i+1}^{n} D_{ij}\, I_{ij}$$

Now, let us find an expression for I_{ij} using the ray approximation. Fig 3-5 shows the ray from $(\tilde{\delta}_j, \tilde{\delta}_i)$ to $(\tilde{\delta}_j^s, \tilde{\delta}_i^s)$; $\tilde{\delta}_i$ as a function of $\tilde{\delta}_j$ is given by the following equation:

$$\tilde{\delta}_i = \tilde{\delta}_i^s + \alpha(\tilde{\delta}_j - \tilde{\delta}_j^s)$$

where the slope is given by α.

$$\alpha = \frac{\tilde{\delta}_i - \tilde{\delta}_i^s}{\tilde{\delta}_j - \tilde{\delta}_j^s} \tag{3.21}$$

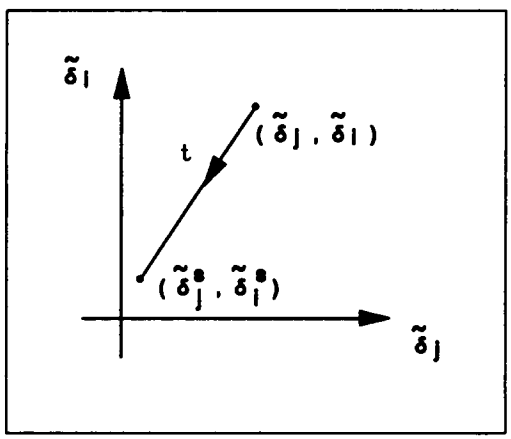

Figure 3-5: Ray Approximation

By subtracting $\tilde{\delta}_j$ from both sides we get Eq. 3.22.

$$\tilde{\delta}_i - \tilde{\delta}_j = \tilde{\delta}_i^s - \alpha\tilde{\delta}_j^s + (\alpha - 1)\tilde{\delta}_j \tag{3.22}$$

By adding $\tilde{\delta}_j$ to both sides we get Eq. 3.23.

$$\tilde{\delta}_i + \tilde{\delta}_j = \tilde{\delta}_i^s - \alpha\tilde{\delta}_j^s + (\alpha + 1)\tilde{\delta}_j \tag{3.23}$$

After substituting Eq. 3.22 and Eq. 3.23 into Eq. 3.20 we get

$$I_{ij} = \int_{\tilde{\delta}_j^s}^{\tilde{\delta}_j} \cos\left[\tilde{\delta}_i^s - \alpha\tilde{\delta}_j^s + (\alpha - 1)\tilde{\delta}_j\right] (\alpha - 1)\, d\tilde{\delta}_j$$

If we integrate we get

$$I_{ij} = \frac{\alpha + 1}{\alpha - 1}\left\{\sin\left[(\alpha - 1)\,\tilde{\delta}_j + \tilde{\delta}_i^s - \alpha\tilde{\delta}_j^s\right] - \sin\left[(\alpha - 1)\,\tilde{\delta}_j^s + \tilde{\delta}_i^s - \alpha\tilde{\delta}_j^s\right]\right\}$$

From Eq. 3.21 the following new expression for I_{ij} :

$$I_{ij} = \frac{\tilde{\delta}_i - \tilde{\delta}_i^s + \tilde{\delta}_j - \tilde{\delta}_j^s}{\tilde{\delta}_i - \tilde{\delta}_i^s - \tilde{\delta}_j + \tilde{\delta}_j^s}\left[\sin\left(\tilde{\delta}_i - \tilde{\delta}_j\right) - \sin\left(\tilde{\delta}_i^s - \tilde{\delta}_j^s\right)\right]$$

The *transient energy function in COA using the ray approximation* is given by

$$V^{ray}\left(\underline{\tilde{\delta}}, \underline{\tilde{\omega}}\right) = V_k\left(\underline{\tilde{\omega}}\right) + V_{p1}\left(\underline{\tilde{\delta}}\right) + V_{p2}\left(\underline{\tilde{\delta}}\right) + V_d^{ray}\left(\underline{\tilde{\delta}}\right) \tag{3.24}$$

where

$$V_k\left(\underline{\tilde{\omega}}\right) = \tfrac{1}{2}\textstyle\sum_{i=1}^{n-1} M_i\tilde{\omega}_i^2 + \tfrac{1}{2}M_n\tilde{\omega}_n^2$$

$$V_{p1}\left(\underline{\tilde{\delta}}\right) = -\textstyle\sum_{i=1}^{n-1}\left[P_i\left(\tilde{\delta}_i - \tilde{\delta}_i^s\right)\right] - P_n\left(\tilde{\delta}_n - \tilde{\delta}_n^s\right)$$

$$V_{p2}\left(\underline{\tilde{\delta}}\right) = -\textstyle\sum_{i=1}^{n-2}\sum_{j=i+1}^{n-1}\left[C_{ij}\left(\cos\tilde{\delta}_{ij} - \cos\tilde{\delta}_{ij}^s\right)\right] - \sum_{i=1}^{n-1} C_{in}\left[\cos\left(\tilde{\delta}_i - \tilde{\delta}_n\right) - \cos\left(\tilde{\delta}_i^s - \tilde{\delta}_n^s\right)\right]$$

$$V_d^{ray}\left(\underline{\tilde{\delta}}\right) = \textstyle\sum_{i=1}^{n-2}\sum_{j=i+1}^{n-1}\left\{D_{ij}\frac{\tilde{\delta}_i - \tilde{\delta}_i^s + \tilde{\delta}_j - \tilde{\delta}_j^s}{\tilde{\delta}_i - \tilde{\delta}_i^s - \tilde{\delta}_j + \tilde{\delta}_j^s}\left[\sin\left(\tilde{\delta}_i - \tilde{\delta}_j\right) - \sin\left(\tilde{\delta}_i^s - \tilde{\delta}_j^s\right)\right]\right\}$$
$$+ \textstyle\sum_{i=1}^{n-1}\left\{D_{in}\frac{\tilde{\delta}_i - \tilde{\delta}_i^s + \tilde{\delta}_n - \tilde{\delta}_n^s}{\tilde{\delta}_i - \tilde{\delta}_i^s - \tilde{\delta}_n + \tilde{\delta}_n^s}\left[\sin\left(\tilde{\delta}_i - \tilde{\delta}_n\right) - \sin\left(\tilde{\delta}_i^s - \tilde{\delta}_n^s\right)\right]\right\}$$

According to Eq. 3.14

$$\tilde{\delta}_n\left(\underline{\tilde{\delta}}\right) = -\frac{1}{M_n}\sum_{i=1}^{n-1} M_i\tilde{\delta}_i$$

and

$$\tilde{\omega}_n\left(\underline{\tilde{\omega}}\right) = -\frac{1}{M_n}\sum_{i=1}^{n-1} M_i\tilde{\omega}_i$$

There is no mathematical justification for using the ray approximation. Many attempts have also been made to include the transfer conductances in the transient energy; this has not been accomplished either. An attempt was also made to use the fault-on trajectory as an approximation to the post-fault trajectory, but since $\tilde{\underline{\delta}}^0$ and $\tilde{\underline{\delta}}^s$ (Fig. 2-6) are not equal, this approximation is worse than the ray approximation [1]. There are two options: a) to neglect $V_d(\tilde{\delta})$ or *b*) to use $V_d^{ray}(\tilde{\underline{\delta}})$. The ray approximation seems to be the most accurate choice.

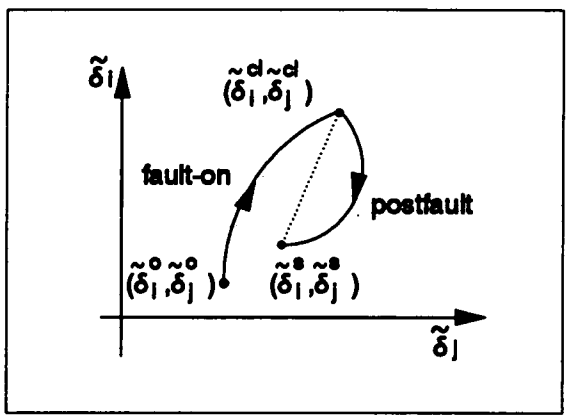

Figure 3-6: Fault on and Post Fault Trajectories

3.11 The transient energy in one-machine reference frame

The *transient energy function with machine n as reference* is given by the following equation:

$$V\left(\underline{\delta},\underline{\omega}\right) = V_k\left(\underline{\omega}\right) + V_{p1}\left(\underline{\delta}\right) + V_{p2}\left(\underline{\delta}\right) + V_d\left(\underline{\delta}\right) \tag{3.25}$$

where

$$V_k(\underline{\omega}) = \sum_{i=1}^{n-2}\sum_{j=i+1}^{n-1}\frac{M_iM_j}{2M_t}(\omega_{in}-\omega_{jn})^2 + \sum_{i=1}^{n-1}\frac{M_iM_n}{2M_t}\omega_{in}^2$$

$$\begin{aligned}V_{p1}(\underline{\delta}) = & -\sum_{i=1}^{n-2}\sum_{j=i+1}^{n-1}\frac{M_jP_i-M_iP_j}{M_t}\left(\delta_{in}-\delta_{jn}-\delta_{in}^s+\delta_{jn}^s\right)\\ & -\sum_{i=1}^{n-1}\frac{M_nP_i-M_iP_n}{M_t}\left(\delta_{in}-\delta_{in}^s\right)\end{aligned}$$

$$\begin{aligned}V_{p2}(\underline{\delta}) = & -\sum_{i=1}^{n-2}\sum_{j=i+1}^{n-1}C_{ij}\left[\cos\left(\delta_{in}-\delta_{jn}\right)-\cos\left(\delta_{in}^s-\delta_{jn}^s\right)\right]\\ & -\sum_{i=1}^{n-1}C_{in}\left[cos\delta_{in}-cos\delta_{in}^s\right]\end{aligned}$$

$$V_d(\underline{\delta}) = \sum_{i=1}^{n-2}\sum_{j=i+1}^{n-1}D_{ij}I_{ij} + \sum_{i=1}^{n-1}D_{in}I_{in}$$

$$I_{ij} = \int_{\delta_{in}^s+\delta_{jn}^s+2\tilde{\delta}_n^s}^{\delta_{in}+\delta_{jn}+2\tilde{\delta}_n}\cos\left(\delta_{in}-\delta_{jn}\right)d\left(\delta_{in}+\delta_{jn}+2\tilde{\delta}_n\right)$$

$$I_{in} = \int_{\delta_{in}^s+2\tilde{\delta}_n^s}^{\delta_{in}+2\tilde{\delta}_n}\cos\delta_{in}\,d\left(\delta_{in}+2\tilde{\delta}_n\right)$$

$$\tilde{\delta}_n(\underline{\delta}) = -\frac{1}{M_t}\sum_{i=1}^{n-1}M_i\delta_{in}$$

The proof for this energy function can be found in Appendix A. The transient energy function with machine n as reference cannot be evaluated. The ray approximation must be used.

3.12 Center of angle formulation compared to one-machine reference frame formulation

The state vectors in these formulations are the following:

$$\tilde{\underline{x}} = \begin{bmatrix}\tilde{\underline{\delta}}\\ \tilde{\underline{\omega}}\end{bmatrix} = \begin{bmatrix}\tilde{\delta}_1\\ \tilde{\delta}_2\\ \vdots\\ \tilde{\delta}_{n-1}\\ \tilde{\omega}_1\\ \tilde{\omega}_2\\ \vdots\\ \tilde{\omega}_{n-1}\end{bmatrix};\quad \underline{x} = \begin{bmatrix}\underline{\delta}\\ \underline{\omega}\end{bmatrix} = \begin{bmatrix}\delta_{1n}\\ \delta_{2n}\\ \vdots\\ \delta_{(n-1)n}\\ \omega_{1n}\\ \omega_{2n}\\ \vdots\\ \omega_{(n-1)n}\end{bmatrix}$$

The first question is how they relate to each other, i.e. how to go from one representation to the other . We will consider the angle subspace only since the relations are the same for the

angular velocity subspace.

1. *From machine n as reference to COA.* According to Eq. A.5,

$$\tilde{\delta}_n = -\frac{1}{M_t}\sum_{i=1}^{n-1} M_i \delta_{in}$$

By definition

$$\tilde{\delta}_i = \delta_i - \delta_0$$

or

$$\tilde{\delta}_i = \delta_i - \delta n - (\delta_o - \delta_n) = \delta_{in} + \tilde{\delta}_n$$

By summarizing, we get Eq. 3.26

$$\begin{aligned} \tilde{\delta}_n\,(\underline{\delta}) &= -\tfrac{1}{M_t}\textstyle\sum_{i=1}^{n-1} M_i \delta_{in} \\ \tilde{\delta}_i\,(\underline{\delta}) &= \delta_{in} + \tilde{\delta}_n, \text{ for } i = 1, \cdots, n-1 \end{aligned} \tag{3.26}$$

2. *From COA to machine n as reference.* From Eq. 3.14

$$\tilde{\delta}_n\left(\underline{\tilde{\delta}}\right) = -\frac{1}{M_n}\sum_{i=1}^{n-1} M_i \tilde{\delta}_i$$

From the second row of Eq. 3.26

$$\delta_{in}\left(\underline{\tilde{\delta}}\right) = \tilde{\delta}_i - \tilde{\delta}_n, \text{ for } i = 1, \cdots, n-1$$

summarizing

$$\begin{aligned} \tilde{\delta}_n\left(\underline{\tilde{\delta}}\right) &= -\tfrac{1}{M_n}\textstyle\sum_{i=1}^{n-1} M_i \tilde{\delta}_i \\ \delta_{in}\left(\underline{\tilde{\delta}}\right) &= \tilde{\delta}_i - \tilde{\delta}_n, \text{ for } i = 1, \cdots, n-1 \end{aligned} \tag{3.27}$$

The second question is how $V(\underline{\tilde{\delta}}, \underline{\tilde{\omega}})$ and $V(\underline{\delta}, \underline{\omega})$ relate to each other.

- Kinetic energy

$$V_k(\underline{\tilde{\omega}}) = V_k(\underline{\omega})$$

- Path independent potential energy

$$V_p(\tilde{\underline{\delta}}) = V_p(\underline{\delta})$$

- Path dependent potential energy

$$V_d(\tilde{\underline{\delta}}) = V_d(\underline{\delta})$$

According to these results, the transient energy is the same for each formulation.

$$V(\tilde{\underline{\delta}}, \tilde{\underline{\omega}}) = V(\underline{\delta}, \underline{\omega})$$

The proof for these results can be found in Appendix B.

3.13 Ray approximation in one-machine reference frame

We have shown that $V_d(\underline{\delta}) = V_d\left(\tilde{\underline{\delta}}\right)$; this equality must hold after the ray approximation is used, i.e.

$$V_d^{ray}(\underline{\delta}) = V_d^{ray}\left(\tilde{\underline{\delta}}\right)$$

From Eq. 3.19,

$$V_d^{ray}\left(\tilde{\underline{\delta}}\right) =$$

$$\sum_{i=1}^{n-1}\sum_{j=i+1}^{n} D_{ij}\frac{\tilde{\delta}_i + \tilde{\delta}_j - \left(\tilde{\delta}_i^s + \tilde{\delta}_j^s\right)}{\tilde{\delta}_i - \tilde{\delta}_j - \left(\tilde{\delta}_i^s - \tilde{\delta}_j^s\right)}\left[\sin\left(\tilde{\delta}_i - \tilde{\delta}_j\right) - \sin\left(\tilde{\delta}_i^s - \tilde{\delta}_j^s\right)\right]$$

According to Eq. 3.27, however, $\tilde{\delta}_i = \delta_{in} + \tilde{\delta}_n$, $i = 1, \cdots, n-1$.

$$V_d^{ray}(\underline{\delta}) =$$

$$\sum_{i=1}^{n-2}\sum_{j=i+1}^{n-1} D_{ij}\frac{\delta_{in} + \delta_{jn} + 2\tilde{\delta}_n - \left(\delta_{in}^s + \delta_{jn}^s + 2\tilde{\delta}_n^s\right)}{\delta_{in} - \delta_{jn} - \left(\delta_{in}^s - \delta_{jn}^s\right)}\left[\sin\left(\delta_{in} - \delta_{jn}\right) - \sin\left(\delta_{in}^s - \delta_{jn}^s\right)\right] +$$

$$\sum_{i=1}^{n-1} D_{in} \frac{\delta_{in} + 2\tilde{\delta}_n - \left(\delta_{in}^s + 2\tilde{\delta}_n^s\right)}{\delta_{in} - \delta_{in}^s} \left(\sin \delta_{in} - \sin \delta_{in}^s\right])$$

In conclusion, the *transient energy function with machine-n-as-reference and using the ray approximation* is given by:

$$V^{ray}(\underline{\delta}, \underline{\omega}) = V_k(\underline{\omega}) + V_{p1}(\underline{\delta}) + V_{p2}(\underline{\delta}) + V_d^{ray}(\underline{\delta}) \tag{3.28}$$

where

$$V_k(\underline{\omega}) = \sum_{i=1}^{n-2} \sum_{j=i+1}^{n-1} \frac{M_i M_j}{2M_t} (\omega_{in} - \omega_{jn})^2 + \sum_{i=1}^{n-1} \frac{M_i M_n}{2M_t} \omega_{in}^2$$

$$V_{p1}(\delta) =$$

$$-\sum_{i=1}^{n-2} \sum_{j=i+1}^{n-1} \frac{M_j P_i - M_i P_j}{M_t} \left[\delta_{in} - \delta_{jn} - \left(\delta_{in}^s - \delta_{jn}^s\right)\right] - \sum_{i=1}^{n-1} \frac{M_n P_i - M_i P_n}{M_t} \left(\delta_{in} - \delta_{in}^s\right)$$

$$V_{p2}(\underline{\delta}) = -\sum_{i=1}^{n-2} \sum_{j=i+1}^{n-1} C_{ij} \left[\cos\left(\delta_{in} - \delta_{jn}\right) - \cos\left(\delta_{in}^s - \delta_{jn}^s\right)\right] - \sum_{i=1}^{n-1} C_{in} \left(cos\delta_{in} - cos\delta_{in}^s\right)$$

$$V_d^{ray}(\underline{\delta}) =$$

$$+\sum_{i=1}^{n-2} \sum_{j=i+1}^{n-1} D_{ij} \frac{\delta_{in} + \delta_{jn} + 2\tilde{\delta}_n - \left(\delta_{in}^s + \delta_{jn}^s + 2\tilde{\delta}_n^s\right)}{\delta_{in} - \delta_{jn} - \left(\delta_{in}^s - \delta_{jn}^s\right)} \left[\sin\left(\delta_{in} - \delta_{jn}\right) - \sin\left(\delta_{in} - \delta_{jn}\right)\right]$$

$$+\sum_{i=1}^{n-1} D_{in} \frac{\delta_{in} + 2\tilde{\delta}_n - \left(\delta_{in}^s + 2\tilde{\delta}_n^s\right)}{\delta_{in} - \delta_{in}^s} \left(\sin \delta_{in} - \sin \delta_{in}^s\right)$$

$$\tilde{\delta}_n(\underline{\delta}) = -\frac{1}{M_t} \sum_{i=1}^{n-1} M_i \delta_{in}$$

Notice that although $\tilde{\delta}_n$ is in COA, the last equation gives this quantity as a function of the angle subspace in the machine-*n*-as-reference formulation.

3.14 Transient energy function and the ray approximation for two-machine systems

As mentioned before, the ray approximation is not required for $n = 2$. The energy function in this case is obtained from Eq. 3.19.

$$\begin{aligned} V\left(\tilde{\delta}_1, \tilde{\omega}_1\right) &= \tfrac{M_1}{2}\tilde{\omega}_1^2 + \tfrac{M_2}{2}\tilde{\omega}_2^2 - P_1\left(\tilde{\delta}_1 - \tilde{\delta}_1^s\right) - P_1\left(\tilde{\delta}_2 - \tilde{\delta}_2^s\right) \\ &\quad -C_{12}\left(\cos(\tilde{\delta}_1 - \tilde{\delta}_2) - \cos(\tilde{\delta}_1^s - \tilde{\delta}_2^s)\right) \\ &\quad +D_{12}\left[\int_{\tilde{\delta}_1^s+\tilde{\delta}_2^s}^{\tilde{\delta}_1+\tilde{\delta}_2} \cos(\tilde{\delta}_1 - \tilde{\delta}_2)\, d(\tilde{\delta}_1 + \tilde{\delta}_2)\right] \end{aligned}$$

According to Eq. 3.14

$$\tilde{\delta}_2 = -\frac{M_1}{M_2}\tilde{\delta}_1 \text{ and } \tilde{\omega}_2 = -\frac{M_1}{M_2}\tilde{\omega}_1$$

$$\tilde{\delta}_1 - \tilde{\delta}_2 = \frac{M_1 + M_2}{M_2}\tilde{\delta}_1 \text{ and } \tilde{\delta}_1 + \tilde{\delta}_2 = \frac{-M_1 + M_2}{M_2}\tilde{\delta}_1$$

Substituting with these equations, the transient energy function for a two-machine system in COA formulation is obtained.

$$\begin{aligned} V\left(\tilde{\delta}_1, \tilde{\omega}_1\right) &= \tfrac{M_1}{2}\left(1 + \tfrac{M_1}{M_2}\right)\tilde{\omega}_1^2 - \left(P_1 - \tfrac{M_1}{M_2}P_2\right)\left(\tilde{\delta}_1 - \tilde{\delta}_1^s\right) \\ &\quad -C_{12}\left\{\cos\left[\left(1 + \tfrac{M_1}{M_2}\right)\tilde{\delta}_1\right] - \cos\left[\left(1 + \tfrac{M_1}{M_2}\right)\tilde{\delta}_1^s\right]\right\} \\ &\quad +D_{12}\tfrac{-M_1+M_2}{M_1+M_2}\left\{\sin\left[\left(1 + \tfrac{M_1}{M_2}\right)\tilde{\delta}_1\right] - \sin\left[\left(1 + \tfrac{M_1}{M_2}\right)\tilde{\delta}_1^s\right]\right\} \end{aligned} \tag{3.29}$$

Notice that the ray approximation was not used. It can be easily shown in this case the ray approximation of the energy function results in the above equation (Eq. 3.24 results in Eq. 3.29 if n=2).

The energy function in one machine as reference formulation is obtained from Eq. 3.25.

$$\begin{aligned} V\left(\delta_{12}, \omega_{12}\right) &= \tfrac{M_1 M_2}{2M_t}\omega_{12}^2 - \tfrac{M_2 P_1 - M_1 P_2}{M_t}\left(\delta_{12} - \delta_{12}^s\right) \\ &\quad -C_{12}\left[\cos\left(\delta_{12}\right) - \cos\left(\delta_{12}^s\right)\right] \\ &\quad +D_{12}\int_{\delta_{12}^s+2\tilde{\delta}_2^s}^{\delta_{12}+2\tilde{\delta}_2} \cos\left(\delta_{12}\right) d\left(\delta_{12} + 2\tilde{\delta}_2\right) \end{aligned} \tag{3.30}$$

Also from Eq. 3.25 the following results.

$$\tilde{\delta}_2 = -\frac{M_1 \delta_{12}}{M_1 + M_2}$$

$$\delta_{12} + 2\tilde{\delta}_2 = \frac{-M_1 + M_2}{M_1 + M_2}\delta_{12}$$

Substituting this result into Eq. 3.30 yields the energy function for a two-machine system with machine-n-as-reference formulation

$$\begin{aligned} V(\delta_{12}, \omega_{12}) \;=\; & \tfrac{M_1 M_2}{2M_t}\omega_{12}^2 - \tfrac{M_2 P_1 - M_1 P_2}{M_t}(\delta_{12} - \delta_{12}^s) \\ & -C_{12}\left[\cos(\delta_{12}) - \cos(\delta_{12}^s)\right] \\ & +D_{12}\tfrac{-M_1+M_2}{M_1+M_2}\left[\sin(\delta_{12}) - \sin(\delta_{12}^s)\right] \end{aligned} \tag{3.31}$$

To repeat, the ray approximation was not used and it can be easily shown that substituting $n = 2$ in the ray approximation of the energy function results in the above equation (Eq. 3.28 results in Eq. 3.31 if n=2).

We have seen that $V^{ray}(state) = V(state)$ if $n = 2$. Which means that in a two-machine system, even if ray approximation formulas are used, the transient energy obtained is exact. Furthermore, if a multimachine system swings as a two-machine system, the ray approximation is very accurate [80].

3.15 Three machine example

The system shown in Fig. 3-7 has three buses, all of them with generation [2].

The arrows pointing to the generators indicate the active power supplied by each machine. C and D result in the following matrices:

i	j	C_{ij}	D_{ij}
1	2	1.1957	0.1874
1	3	2.6726	0.6728
2	3	6.7053	1.2869

Notice that the transfer conductances are not negligible since the ratio of $\frac{D_{ij}}{C_{ij}}$ is not negligible.

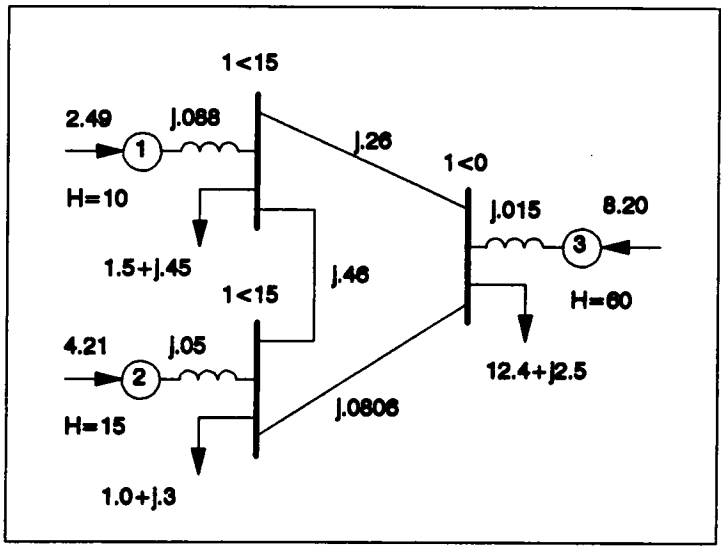

Figure 3-7: Athay's 3 - Machine System

The angles at the *s.e.p.*, the powers, P_i, and the voltages, E_i, are shown in the following table:

i	δ_i^s	δ_{in}^s	$\tilde{\delta}_i^s$	P_i	E_i
1	26.7167	20.0092	14.1671	1.73905	1.07363
2	26.4731	19.7656	13.9235	3.66147	1.05729
3	6.7075		−5.8421	−1.33908	1.05299

Fig. 3-8a) shows the potential energy (COA formulation) as given by Eq.3.19. This figure closely resembles the one shown in reference [2]. Fig. 3-8 b) shows the potential energy (machine-n-as-reference formulation) as given by Eq. 3.28.

By substituting the proper values into Eq. 3.27, we get the following results:

$$\delta_{13} = \frac{70\tilde{\delta}_1 + 15\tilde{\delta}_2}{60}$$
$$\delta_{23} = \frac{10\tilde{\delta}_1 + 75\tilde{\delta}_2}{60}$$

These equations can verify that $V_{pe}(\underline{\delta}) = V_{pe}\left(\tilde{\underline{\delta}}\right)$. For instance, if $\tilde{\delta}_1 = \tilde{\delta}_2 = 200°$ then $\delta_{13} = \delta_{23} = 258.33°$ and $V_{pe}(\tilde{\delta}_1, \tilde{\delta}_2) = V_{pe}(\delta_{13}, \delta_{23}) = -12.5 \frac{\text{MW rad}}{\text{MVA}}$. If $\tilde{\delta}_1 = \tilde{\delta}_2 = -100°$ then $\delta_{13} = \delta_{23} = -141.67°$ and $V_{pe}(\tilde{\delta}_1, \tilde{\delta}_2) = V_{pe}(\delta_{13}, \delta_{23}) = 26.5 \frac{\text{MW rad}}{\text{MVA}}$. It can also be seen that the energy level at the lowest saddle is almost 4, where the top of the hill is slightly more than 8.

The values of V_{pe} in the grid files used to create these surfaces matched up to six digits.

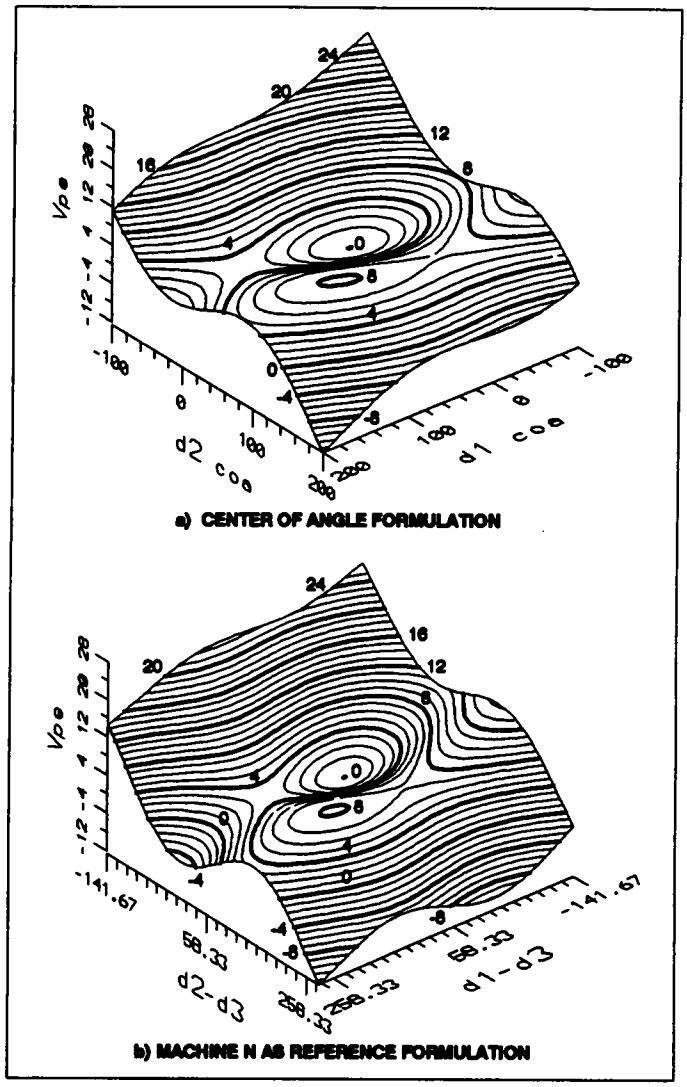

Figure 3-8: Potential Energy Surface, 3 - Machine System

Fig. 3-9 shows the variation of the state variables in COA for a self-clearing three-phase fault on bus 1; the fault clears in 0.1 seconds.

The same results were obtained using the machine–n – as-reference formulation for the dynamics and converting the state variables to COA. With this figure we can verify that due

to the absence of damping, the *s.e.p.*

$$\underline{\tilde{x}}^s = \begin{bmatrix} \tilde{\delta}_1^s \\ \tilde{\delta}_2^s \\ 0 \\ 0 \end{bmatrix}$$

is never reached. Instead our model will oscillate forever.

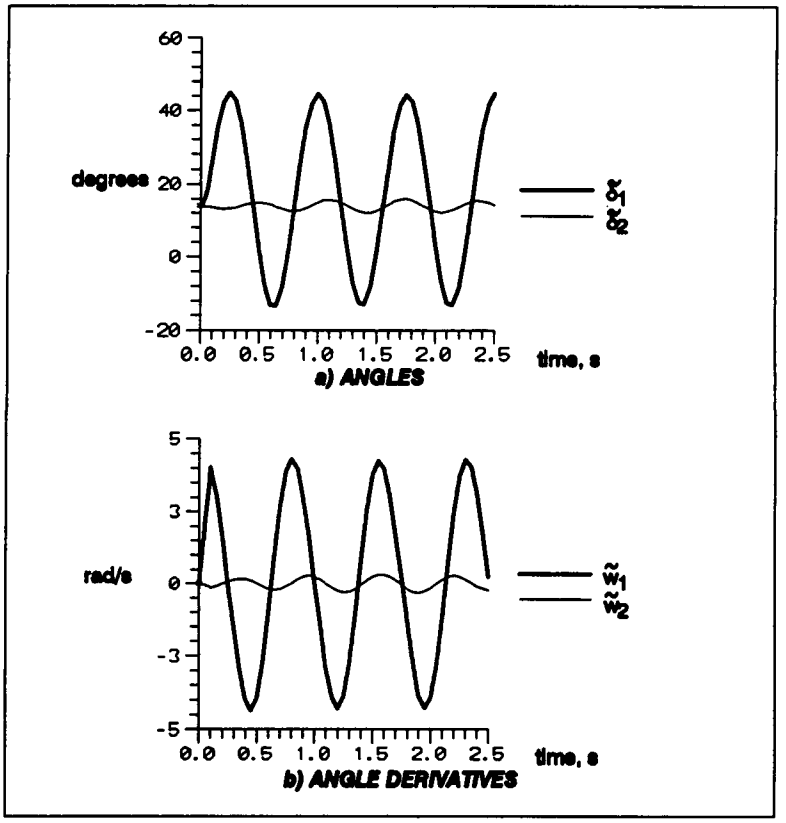

Figure 3-9: State Variable vs. Time, Self Clearing Fault on bus 1, tcl=.1s

Fig. 3-10a) shows the corresponding plots of kinetic, potential, and total energies versus time, as given by Eq. 3.19. Since the *s.e.p.* and the pre-fault state are the same, there is no sudden change in potential energy at $t = 0$. As mentioned in the preceding chapter, the fault injects energy into the system. Once the fault is cleared, $t > t_{cl} = 0.1\ s$, the total energy remains constant. Fig. 3-10b) shows the potential energy, the ray approximation of its path-dependent

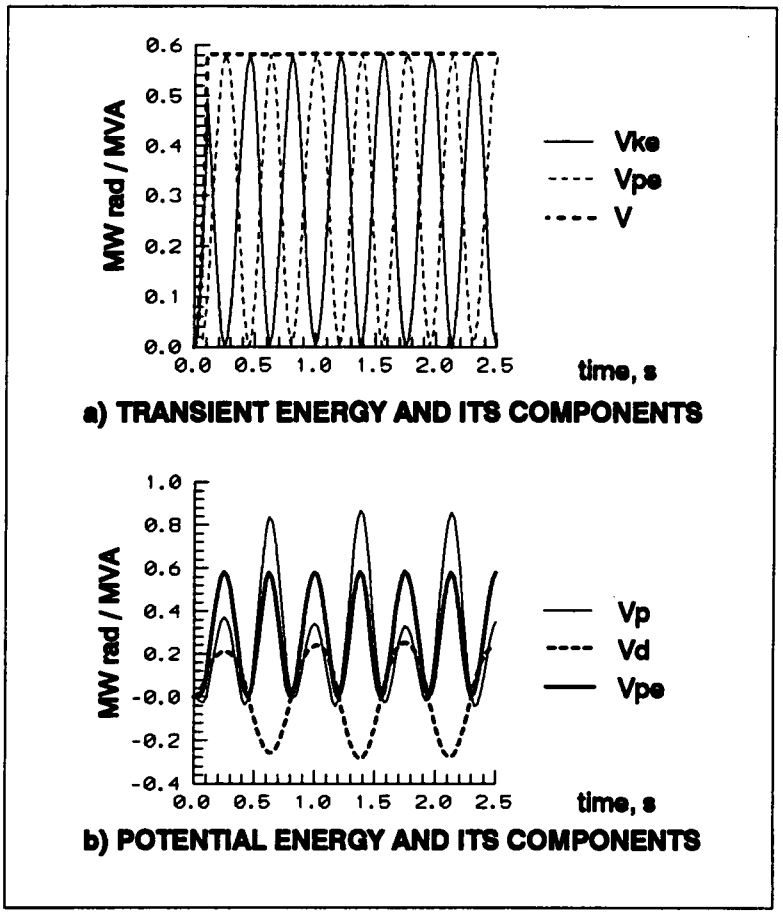

Figure 3-10: Transient Energy vs. Time, Self Clearing Fault on bus1, tcl=.1s

component, and its path-independent component.

V_d^{ray} results from the transfer conductances of the reduced admittance matrix, which in turn result from the resistance of the lines and the loads modeled as fixed impedances. This energy has nothing to do with the integral of the i^2R losses. This energy is "real" energy in MW hr, whereas the transient energy is a "conceptual" energy in $\frac{\text{MW rad}}{\text{MVA}}$. We saw in the previous chapter that the transient kinetic energy is zero at synchronous speed. The kinetic energy is not actually zero at synchronous speed. Similarly, we know that the energy due to ohmic losses is always dissipated; it increases or remains constant ($i^2R\ is \geq 0$), but it never decreases. We see from Fig. 3-10b) that V_d^{ray} decreases and even goes below zero. We can see that the diminishing of V_d occurs even without the ray approximation. V_d is not integrable because it is path dependent. We would have to know the path until the *s.e.p.* is reached, which

we know does not occur, since the total energy is constant once the fault is cleared, V_d = (Some constant) $- V_{ke} - V_p$. From the shapes of V_{ke} and V_p in Fig. 3-10 we see that V_d has to decrease. *The resistance of the lines does not dampen the swing.*

With a swing in angle comes a swing in power; power comes and goes from one generator to another while these swings in power increase the losses in the resistance of the lines. What happens with this increase in the losses and why does this not dampen the swings of the angles?.

In order to answer to these questions, let us make use of Eq. 3.9:

$$\frac{d\delta_o}{dt} = \omega_0, \text{ rad/s}$$
$$\frac{d\omega_o}{dt} = \frac{1}{M_t} \cdot P_{coa}(\tilde{\delta}), \text{ rad/s}^2$$

where

$$P_{coa}(\underline{\delta}) = \sum_{i=1}^{n} P_i - 2\sum_{i=1}^{n-2}\sum_{j=1+1}^{n-1} D_{ij}\cos\tilde{\delta}_{ij} - 2\sum_{i=1}^{n-1} D_{in}\cos\tilde{\delta}_{in}$$

After inspecting the above equality we can say that the following equation holds.

$$P_{coa} = P_m - \left(P_{load}^{red} + P_{loss}^{red}\right)$$

P_m is the sum of all input mechanical powers. P_{load}^{red} is the sum of all real power loads of the reduced system. P_{loss}^{red} is the sum of the losses in the transfer conductances of the reduced system. The sum of the loads and the losses in the transfer conductances of the reduced system equals sum of the constant-impedance power loads plus the losses in the lines of the original system, *i.e.*

$$P_{coa} = P_m - (P_{load} + P_{loss}) = P_m - P_{gen}$$

The rate of change of the angular velocity of the center of angle also given by

$$\frac{d\omega_o}{dt} = \frac{1}{M_t} \cdot [P_m - (P_{load} + P_{loss})]$$

Now we can see that the increase in losses in the lines will affect the dynamics of the center of angle. The increase in the losses in the lines, however, does not dampen the oscillation of each machine with respect to this inertia-weighed average of the angles. In the following example, we will illustrate these ideas.

3.16 Three machine system with line resistance

The system shown in Fig. 3-11 is based on Athay's three-machine system with resistance added in the lines. $R/X = 0.20$ for all the lines, which is unusually large in order to exhibit large losses in the lines. The slack bus is bus three; notice that this machine supplied power to compensate the increase in the losses in the system. P_g at bus three went from 8.20 to 8.418.

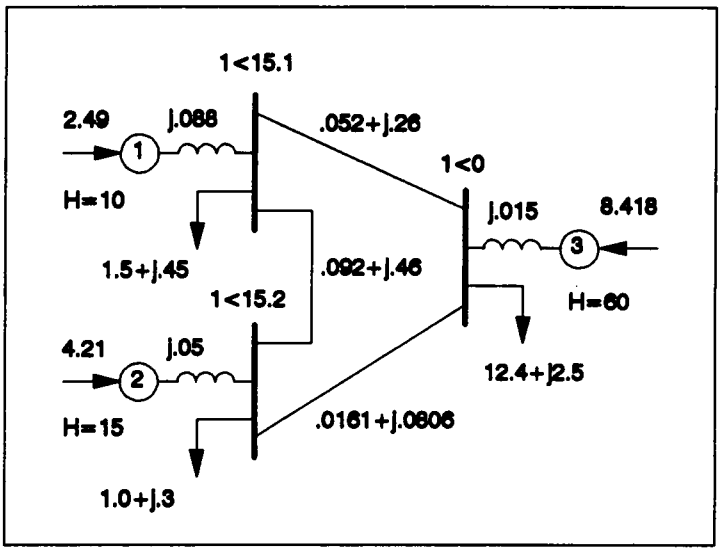

Figure 3-11: R/X=.2 for 3 - Machine System

A three-phase fault near bus 2 occurs at $t = 0.$ with a fault impedance of $Z_f = 1.e-5+j1.e-5$, the fault clears itself at 0.2 seconds. Fig. 3-12a) shows the angle subspace versus time. We can see that although the swing in machine two is decreasing with time, the swing in machine one is increasing, i.e. the transient energy remains constant as shown in Fig. 3-12c). Fig. 3-12b) shows the angular velocity subspace in COA, $\tilde{\omega}$, versus time.The power of the center of angle equals the input mechanical power minus the power generated in the system, $P_{coa} = P_m - P_{gen} = P_{gen}(t=0) - P_{gen}$. This is illustrated in Fig. 3-12e) and Fig. 3-12f). This figure shows that the losses in the lines have increased drastically due to the angle oscillations. P_{coa}, however, averages more than zero due to the reduction in the power at the loads.

In this example we have seen that *due to the angle oscillations, the power dissipated in the lines increases. This will affect the dynamics of the center of angle, but this increase in the losses will not dampen the oscillations of individual machines with respect to the center of angle.*

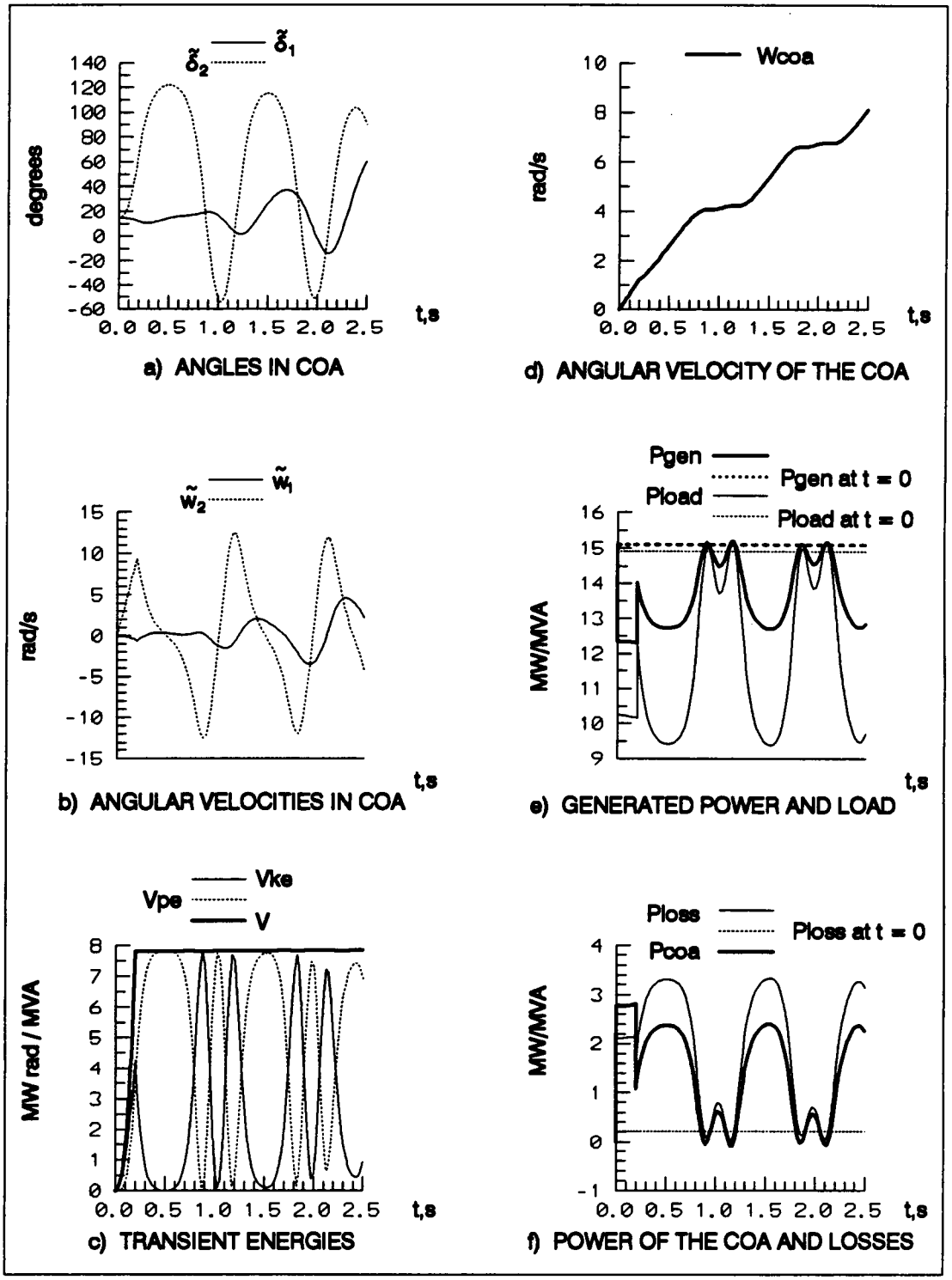

Figure 3-12: Self Clearing Fault on bus 2, tcl=.2s

Chapter 4

Fundamentals of Direct Methods

4.1 Uniform damping

So far damping has been neglected. It will be included now because it plays an indispensable roll in the characterization of the region of attraction. In order to characterize the region of attraction, the equilibrium points must be hyperbolic, and this requires damping. In Appendix C a detailed model and a classical model are presented along with their linearized versions. Using the data of two large machines, three procedures to obtain the damping coefficient are illustrated. For these two machines damping is 10 percent on their own base and the ratio $\frac{D}{M}$ is

$$\frac{D_{hydro}}{M_{hydro}} \approx 2.5$$

$$\frac{D_{steam}}{M_{steam}} \approx 3.3661$$

Although the ratio $\frac{D}{M}$ is not the same for all the machines in a power system, it will be assumed that this ratio is the same because the number of state variables is the same as with zero damping.

$$n_{state} = 2(n-1)$$

where

n is the number of buses with generation.

Uniform damping is mathematically stated as

$$\frac{D_1}{M_1} = \frac{D_2}{M_2} = \cdots = \frac{D_n}{M_n} = \lambda_D$$

A useful result is presented now:

If

$$D_t = \sum_{j=1}^{n} D_j$$
$$M_t = \sum_{j=1}^{n} M_j$$

then

$$\frac{D_t}{M_t} = \lambda_D \tag{4.1}$$

The following equations show that this result is true.

$$\frac{D_t}{M_t} = \frac{D_1 + D_2 + \cdots + D_n}{M_1 + M_2 + \cdots + M_n}$$

$$D_i = \frac{M_i}{M_1} D_1$$

After substituting the last equation in the previous one we get the following equation:

$$\frac{D_t}{M_t} = \frac{D_1 \left(1 + \frac{M_2}{M_1} + \cdots + \frac{M_n}{M_1}\right)}{M_1 \left(1 + \frac{M_2}{M_1} + \cdots + \frac{M_n}{M_1}\right)}$$

or

$$\frac{D_t}{M_t} = \lambda_D$$

4.1.1 State equation in the one-machine reference frame formulation

The differential equations for machine i and n are the following:

$$\begin{bmatrix} \dot{\delta}_i = \omega_i \\ \dot{\omega}_i = \frac{P_i - P_{ei} - D_i \omega_i}{M_i} \end{bmatrix}$$

$$\begin{bmatrix} \dot{\delta}_n = \omega_n \\ \dot{\omega}_n = \frac{P_n - P_{en} - D_n \omega_n}{M_n} \end{bmatrix}$$

By subtracting the equation corresponding to machine n from the one corresponding to machine i, the state equation with machine n as reference results.

$$\begin{bmatrix} \dot{\delta}_{in} = \omega_{in} \\ \dot{\omega}_{in} = \frac{P_i - P_{ei}}{M_i} - \frac{P_n - P_{en}}{M_n} - \lambda_D \omega_{in} \end{bmatrix} \quad i = 1, 2, \ldots, n-1$$

4.1.2 State equation in center of angle formulation

The swing equation for machine i is

$$M_i \ddot{\delta}_i = P_i - P_{ei} - D_i \omega_i \tag{4.2}$$

The COA center of angle is defined as

$$\delta_0 = \frac{1}{M_t} \sum_{j=1}^{n} M_j \delta_j; \; M_t = \sum_{j=1}^{n} M_j \tag{4.3}$$

Taking the first derivative, the center of angular velocity is obtained.

$$\omega_0 = \frac{1}{M_t} \sum_{j=1}^{n} M_j \omega_j$$

The angle and the angular velocity of machine i in COA are

$$\tilde{\delta}_i = \delta_i - \delta_0$$
$$\tilde{\omega}_i = \omega_i - \omega_0$$

The summation from $i = 1$ to n of the product $M_i \tilde{\delta}_i$ is zero, as shown in the following:

$$\begin{aligned} \textstyle\sum_{i=1}^{n} M_i \tilde{\delta}_i &= \textstyle\sum_{i=1}^{n} M_i \delta_i - \sum_{i=1}^{n} M_i \delta_0 \\ &= \textstyle\sum_{i=1}^{n} M_i \delta_i - M_t \delta_0 \end{aligned}$$

From Eq. 4.3

$$\textstyle\sum_{i=1}^{n} M_i \tilde{\delta}_i = \sum_{i=1}^{n} M_i \delta_i - \sum_{j=1}^{n} M_j \delta_j$$

$$\sum_{i=1}^{n} M_i \tilde{\delta}_i = 0 \tag{4.4}$$

By taking the first derivative of Eq. 4.4 the following is obtained.

$$\sum_{i=1}^{n} M_i \tilde{\omega}_i = 0 \tag{4.5}$$

To obtain the differential equation of the COA, let us multiply Eq. 4.3 by M_t and take the second derivative.

$$M_t \ddot{\delta}_0 = \sum_{i=1}^{n} M_i \ddot{\delta}_i$$

From Eq. 4.2 we get the following:

$$M_t \ddot{\delta}_0 = \sum_{i=1}^{n} P_i - 2 \sum_{i=1}^{n-1} \sum_{j=i+1}^{n} D_{ij} \cos \delta_{ij} - \sum_{i=1}^{n} D_i \omega_i$$

where

$\sum_{i=1}^{n} D_i \omega_i = \sum_{i=1}^{n} D_i (\tilde{\omega}_i + \omega_0)$

The following equation results.

$$M_t \ddot{\delta}_0 = \sum_{i=1}^{n} P_i - 2 \sum_{i=1}^{n-1} \sum_{j=i+1}^{n} D_{ij} \cos \delta_{ij} - D_t \omega_0 - \sum_{i=1}^{n} D_i \tilde{\omega}_i$$

Now we will show that for uniform damping, the last term in the above equation is zero.

$$\sum_{i=1}^{n} D_i \tilde{\omega}_i = \sum_{i=1}^{n} \lambda_D M_i \tilde{\omega}_i$$

From Eq. 4.5 we get the following equation.

$$\sum_{i=1}^{n} D_i \tilde{\omega}_i = 0$$

The power of the COA is defined as

$$P_{COA} = \sum_{i=1}^{n} P_i - 2 \sum_{i=1}^{n-1} \sum_{j=i+1}^{n} D_{ij} \cos \delta_{ij}$$

The differential equation of the COA for uniform damping then results.

$$M_t\ddot{\tilde{\delta}}_0 = P_{COA} - D_t\omega_0$$

If the last equation is multiplied by $\frac{M_i}{M_t}$, the following results

$$M_i\ddot{\tilde{\delta}}_0 = \frac{M_i}{M_t}P_{COA} - \frac{M_i}{M_t}D_t\omega_0$$

or

$$M_i\ddot{\tilde{\delta}}_0 = \frac{M_i}{M_t}P_{COA} - D_i\omega_0$$

Subtracting the above equation from Eq. 4.2 we get

$$M_i\frac{d^2\tilde{\delta}_i}{dt^2} = P_i - P_{ei} - \frac{M_i}{M_t}P_{COA} + D_i\omega_0 - D_i\omega_i$$

or

$$M_i\frac{d^2\tilde{\delta}_i}{dt^2} = P_i - P_{ei} - \frac{M_i}{M_t}P_{COA} - D_i\tilde{\omega}_i \text{ for } i = 1, 2, \ldots, n$$

As indicated by Eq. 4.5 and Eq. 4.4, any of the n equations above may be expressed as a linear combination of the rest. The last equation is chosen; the state equation using COA results.

$$\begin{aligned} \frac{d\tilde{\delta}_i}{dt} &= \tilde{\omega}_i \\ \frac{d\tilde{\omega}_i}{dt} &= \frac{P_i - P_{ei}}{M_i} - \frac{P_{COA}}{M_t} - \lambda_D\tilde{\omega}_i \\ & i = 1, 2, \ldots n-1 \end{aligned}$$

4.2 Characterization of the region of attraction

4.2.1 Definitions, theorems and procedures

The definitions and theorems in this section are adapted from [20] and [95]. Several background definitions should be understood when trying to determine whether or not a multi-machine power system is transiently stable. These definitions include the following:

- equilibrium points (e.p.'s)

- Jacobian matrix

- hyperbolic equilibrium points and sources

- type-k equilibrium points

- stability region or region of attraction or domain of attraction

- stability boundary

- stable and unstable manifolds

The state equation in both COA formulation and machine-n-as-reference formulation was found in the previous section. This state equation may be expressed in this more general form:

$$\dot{\underline{x}} = \underline{f}(\underline{x})$$

This equation describes a *non-linear autonomous dynamical system.* The *equilibrium points,* the set of which is denoted by E, are defined as the points satisfying the equation

$$\underline{0} = \underline{f}(\underline{x})$$

From the second chapter we obtain the following result for a multi-machine system in the COA formulation:

$$0 = \tilde{\omega}_i, \text{ rad/s};$$
$$0 = \frac{P_i - P_{ei}}{M_i} - \frac{P_{coa}}{M_t}, \text{ rad/s}^2 \text{ (for } i = 1, 2, \cdots, n-1)$$

The derivative of $\underline{f}$ with respect to $\underline{x}$ is called the *Jacobian* matrix.

$$\underline{J} = \frac{\partial \underline{f}}{\partial \underline{x}}$$

An e.p. is said to be *hyperbolic* if the Jacobian evaluated there has no eigenvalues on the imaginary axis.

For a *stable e.p. (s.e.p.),* the Jacobian matrix has no eigenvalues in the positive real plane; an s.e.p. is denoted by $\underline{x}_s$.

For an *unstable e.p. (u.e.p.)*, the Jacobian matrix has at least one eigenvalue in the positive real plane; a u.e.p. is denoted by $\underline{x}_u$.

An e.p. is called a *source* if all eigenvalues of the Jacobian matrix at the e.p. are in the positive real plane. The *type* of the e.p is defined by the number of Jacobian matrix eigenvalues in the real plane. For instance, a *type-one* e.p. has exactly one unstable eigenvalue.

The solution curve of $\dot{\underline{x}} = \underline{f}(\underline{x})$ starting at $\underline{x}$ is called a *trajectory* and it is denoted by $\Phi(\underline{x}, \cdot) : R \rightarrow R^{nstate}$, $nstate = 2(n-1)$.

The *stability region* or *region of attraction* of an s.e.p. is denoted by $A(\underline{x}_s)$. This region is the set of all state points such that the trajectory of the system starting at these points tends towards the s.e.p. as time tends toward infinity.

$$A(\underline{x}_s) \doteq \{\underline{x} \mid \lim_{t \rightarrow \infty} \Phi(\underline{x}, t) = \underline{x}_s\}$$

The *stability boundary* is denoted by $\partial A(\underline{x}_s)$.

In order to characterize the region of attraction, the notions of stable and unstable manifolds and the stability boundary should be understood. If $\underline{x}_i$ is a hyperbolic e.p., its stable and unstable manifolds are defined by the following:

$$W^s(\underline{x}_i) = \{\underline{x} \mid \Phi(\underline{x}, t) \rightarrow \underline{x}_i \text{ as } t \rightarrow \infty$$
$$W^u(\underline{x}_i) = \{\underline{x} \mid \Phi(\underline{x}, t) \rightarrow \underline{x}_i \text{ as } t \rightarrow -\infty$$

The unstable manifold $W^u(\underline{x}_i)$ of a type-k equilibrium point $\underline{x}_i$ is a k-dimensional smooth manifold. The stable manifold $W^s(\underline{x}_i)$ of a type-k equilibrium point $\underline{x}_i$ is a $nstate - k$-dimensional smooth manifold.

Using these definitions and the following assumptions, we may describe the region of attraction mathematically.

Assumptions:

A1. All e.p.'s on the stability boundary of the system are hyperbolic.

A2. The intersection of $W^s(\underline{x}_i)$ and $W^u(\underline{x}_j)$ satisfies the transversality condition, for all e.p.'s $\underline{x}_i$, $\underline{x}_j$ on the stability boundary. (The stable and unstable manifolds of u.e.p.'s on the stability boundary satisfy the transversality condition [17]). The

transversality condition is satisfied if a) the tangent lines of each manifold at the intersection point span the state space or b) the manifolds do not intersect at all.

A3. There exists a C^1 function $V : R^{nstate} \rightarrow R$ for the system such that

i $\dot{V}(\Phi(\underline{x}, t)) \leq 0$ at $\underline{x} \notin E$

ii If $\underline{x}$ is not an e.p., the set $\{t \in R : \dot{V}(\Phi(\underline{x}, t)) = 0\}$ has measure 0 in R

iii $V(\Phi(\underline{x}, t))$ is bounded implies $\Phi(\underline{x}, t)$ is bounded. We will refer to this function as the energy function of the system.

After these assumptions are met, two theorems describe the region of attraction.

Theorem 1 (Necessary and sufficient condition for a u.e.p. to lie on the stability boundary) [20] For the dynamical system satisfying the previous assumptions, x_i is a u.e.p. on the stability boundary $\partial A(\underline{x}_s)$ of an s.e.p. x_s if and only if $W^u(x_i) \cap A(\underline{x}_s) \neq \phi$.

Theorem 2 (Characterization of the stability boundary) [20] For the dynamical system satisfying the previous assumptions, let $\underline{x}_i, i = 1, 2, ...$be the u.e.p.'s on the stability boundary $\partial A(\underline{x}_s)$ of an s.e.p. This theorem results in the following union:

$$\partial A(\underline{x}_s) = \bigcup_{\underline{x}_k^1 \in E \cap \partial A} W^s(\underline{x}_i)$$

Theorem 2 states that the boundary is defined by the union of the stable manifolds of the u.e.p.'s that lie on that boundary. In order to characterize the stability boundary, the u.e.p.'s on this stability boundary must be found.

Procedure 1 The unstable manifold of the type-1 e.p. $\hat{\underline{x}}$ may be found using the following procedure (as mentioned above, the unstable manifold of a type-1 u.e.p. is a one-dimensional smooth manifold):

(a) Find the Jacobian at $\hat{\underline{x}}$.

(b) Find the normalized unstable eigenvector of the Jacobian ($\underline{y}_u$). (Note that the Jacobian has only one unstable eigenvector for a type-1 e.p.)

(c) Find the starting points $\hat{\underline{x}}+0.01\underline{y}_u$ and $\hat{\underline{x}}-0.01\underline{y}_u$.

(d) Numerically integrate the state equation starting from these points.

(e) Since the unstable manifold integrating in forward time tends either to infinity or to an s.e.p., stop the integration when the absolute value of any of the elements of the angle subspace exceeds some large value, (270°) or after detecting that the trajectory approaches an s.e.p.

Procedure 2 To determine if a u.e.p. lies on the stability boundary. This procedure is a direct application of Theorem 1, i.e. if the unstable manifold of an u.e.p. intersects with the region of attraction of an s.e.p., the u.e.p. lies on the stability boundary of the region of attraction. .

(a) Go through Procedure 1.

(b) If any of these trajectories approach $\underline{x}_s$, then $\hat{\underline{x}}$ is on the stability boundary.

Procedure 3 A *one-dimensional stable manifold* of $\hat{\underline{x}}$ may be found using the following procedure:

(a) Evaluate the Jacobian at $\hat{\underline{x}}$.

(b) Find the normalized stable eigenvector of the Jacobian. and designate it by

$$\underline{y}_s$$

1. Find the starting points $\hat{\underline{x}} + 0.01\underline{y}_s$ and $\hat{\underline{x}} - 0.01\underline{y}_s$

(a) Using the above starting points, integrate the state equation in *reverse time.* This integration is equivalent to integrating the following state equation in forward time.

$$\dot{\underline{x}} = -\underline{f}(\underline{x})$$

(b) The region of attraction of a classical power system is unbounded. Therefore, stop the numerical integration when any of the absolute values of the angles exceed 270°.

Procedure 3 can be applied to find the stability boundary of power systems with at most two machines. It can also be used to find the region of attraction of the associated-reduced

order systems of power systems with at most three machines. Associated reduced order systems are introduced in the next chapter.

In order to explain the reason for this limitation, let us consider a system with three machines. The Jacobian matrix at a type-1 u.e.p. will have one positive real eigenvalue, one negative real eigenvalue and a complex conjugate pair of eigenvalues with negative real part. Using the positive real eigenvalue and its corresponding eigenvector in Procedure 1 the unstable manifold is found. The rest of the eigenvalues and their corresponding eigenvectors define the stable manifold, a 3-dimensional smooth manifold. Unfortunately, we do not know of a procedure to find such a manifold. This is a subject which requires further research.

4.2.2 OMIB example

For a one-machine infinite-bus system, the state equation is the following:

$$\begin{bmatrix} \dot{\delta} \\ \dot{\omega} \end{bmatrix} = \begin{bmatrix} \omega \\ \frac{P_m - P_{max}\sin\delta - D\omega}{M} \end{bmatrix}$$

The s.e.p is given by

$$\underline{x}_s = \begin{bmatrix} \delta_s \\ 0 \end{bmatrix} = \begin{bmatrix} \arcsin\left(\frac{P_m}{P_{max}}\right) \\ 0 \end{bmatrix}$$

There are two u.e.p.'s surrounding the s.e.p., $\hat{\underline{x}}_{u1}$ and $\hat{\underline{x}}_{u2}$:

$$\hat{\underline{x}}_{u1} = \begin{bmatrix} \pi - \delta_s \\ 0 \end{bmatrix}$$

$$\hat{\underline{x}}_{u2} = \begin{bmatrix} -\pi - \delta_s \\ 0 \end{bmatrix}$$

The Jacobian results in the following matrix:

$$\underline{J} = \begin{bmatrix} 0 & 1 \\ -\frac{P_{max}\cos\delta}{M} & -\frac{D}{M} \end{bmatrix}$$

The eigenvalues of the Jacobian are given by

$$\lambda_1 = -\frac{D}{2M} + \sqrt{\left(\frac{D}{2M}\right)^2 - \frac{P_{\max}}{M}\cos\delta}$$

$$\lambda_2 = -\frac{D}{2M} - \sqrt{\left(\frac{D}{2M}\right)^2 - \frac{P_{\max}}{M}\cos\delta}$$

The corresponding normalized eigenvectors are

$$\underline{y}_1 = \begin{bmatrix} \sqrt{\frac{1}{1+\lambda_1^2}} \\ \lambda_1\left(\sqrt{\frac{1}{1+\lambda_1^2}}\right) \end{bmatrix}$$

$$\underline{y}_2 = \begin{bmatrix} \sqrt{\frac{1}{1+\lambda_2^2}} \\ \lambda_2\left(\sqrt{\frac{1}{1+\lambda_2^2}}\right) \end{bmatrix}$$

To illustrate stable and unstable e.p.'s, eigenvalues, eigenvectors and manifolds, let us assign values to the following parameters:

$P_{\max} = 1.5$ pu

$P_m = 1.0$ pu

$M = 0.025 \ \frac{\text{MW s}^2}{\text{MVA rad}}$

$D = 0.01 \ \frac{\text{MW s}}{\text{MVA rad}}$

The following values are obtained:

	$\underline{x}_s$	$\hat{\underline{x}}_{u1}$	$\hat{\underline{x}}_{u2}$
e.p.	$\begin{pmatrix} 41.81° \\ 0 \end{pmatrix}$	$\begin{pmatrix} 138.2° \\ 0 \end{pmatrix}$	$\begin{pmatrix} -221.81° \\ 0 \end{pmatrix}$
$\underline{J}$	$\begin{bmatrix} 0 & 1 \\ -44.72 & -0.4 \end{bmatrix}$	$\begin{bmatrix} 0 & 1 \\ 44.72 & -0.4 \end{bmatrix}$	$\begin{bmatrix} 0 & 1 \\ 44.72 & -0.4 \end{bmatrix}$
λ_1	$-0.2 + j6.684$	6.4904	6.4904
$\underline{y}_1$	$\begin{pmatrix} .148 - j.0044 \\ j0.989 \end{pmatrix}$	$\begin{pmatrix} 0.1523 \\ 0.9883 \end{pmatrix}$	$\begin{pmatrix} 0.1523 \\ 0.9883 \end{pmatrix}$
λ_2	$-0.2 - j6.684$	-6.8904	-6.8904
$\underline{y}_2$	$\begin{pmatrix} .148 + j.0044 \\ -j0.989 \end{pmatrix}$	$\begin{pmatrix} -0.1436 \\ 0.9896 \end{pmatrix}$	$\begin{pmatrix} -0.1436 \\ 0.9896 \end{pmatrix}$

The Jacobian evaluated at $\underline{x}_s$ has no unstable eigenvalues (eigenvalues with positive real parts). The u.e.p.'s are *type-1*. Now, we will follow Procedure 1 above to find the unstable manifolds of $\hat{\underline{x}}_{u1}$ and $\hat{\underline{x}}_{u2}$. Once these unstable manifolds are found we will determine which of these u.e.p.'s are on stability boundary of $\underline{x}_s$.

For $\hat{\underline{x}}_{u1}$, the two starting points are the following:

$$\begin{bmatrix} 2.411865 \\ 0.0 \end{bmatrix} + \frac{1}{100} \begin{bmatrix} 0.1523 \\ 0.9883 \end{bmatrix} = \begin{bmatrix} 2.413388 \\ 0.009883 \end{bmatrix}$$

As shown in Fig. 4-1, the trajectory corresponding to this starting point tends to infinity as time increases.

$$\begin{bmatrix} 2.411865 \\ 0.0 \end{bmatrix} - \frac{1}{100} \begin{bmatrix} 0.1523 \\ 0.9883 \end{bmatrix} = \begin{bmatrix} 2.410342 \\ -0.009883 \end{bmatrix}$$

The trajectory corresponding to this starting point tends towards $\underline{x}_s$; *therefore,* $\hat{\underline{x}}_{u1}$ *is on the stability boundary of* $\underline{x}_s$.

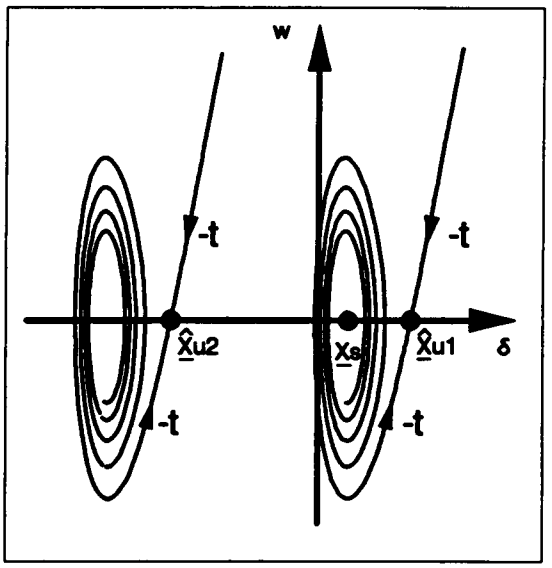

Figure 4-1: Unstable Manifolds

For $\hat{\underline{x}}_{u2}$ the two starting points are the following:

$$\begin{bmatrix} -3.871320 \\ 0.0 \end{bmatrix} + \frac{1}{100}\begin{bmatrix} 0.1523 \\ 0.9883 \end{bmatrix} = \begin{bmatrix} -3.869797 \\ 0.009883 \end{bmatrix}$$

$$\begin{bmatrix} -3.871320 \\ 0.0 \end{bmatrix} - \frac{1}{100}\begin{bmatrix} 0.1523 \\ 0.9883 \end{bmatrix} = \begin{bmatrix} -3.872843 \\ -0.009883 \end{bmatrix}$$

As shown in Fig. 4-1, the unstable manifold of $\hat{\underline{x}}_{u2}$ does not intersect with the region of attraction of $\underline{x}_s$; *therefore,* $\hat{\underline{x}}_{u2}$ *does not belong to the stability boundary of* $\underline{x}_s$.

We have determined that the u.e.p. in the accelerating direction, $\hat{\underline{x}}_{u1}$, is on $\partial A(\underline{x}_s)$; whereas, the u.e.p. in the decelerating direction, $\hat{\underline{x}}_{u2}$, does not belong to $\partial A(\underline{x}_s)$. This result is true for the values of the parameters used, but $\hat{\underline{x}}_{u2}$ may also be on $\partial A(\underline{x}_s)$.

According to Theorem 2, the stability boundary $\partial A(\underline{x}_s)$ is the union of the stable manifolds of the u.e.p.'s on $\partial A(\underline{x}_s)$. For the OMIB system, the only u.e.p. belonging to $\partial A(\underline{x}_s)$ is $\hat{\underline{x}}_{u1}$; therefore, $\partial A(\underline{x}_s) = W^s(\hat{\underline{x}}_{u1})$. The stable manifold of $\hat{\underline{x}}_{u1}$ is shown in Fig. 4-2. The starting

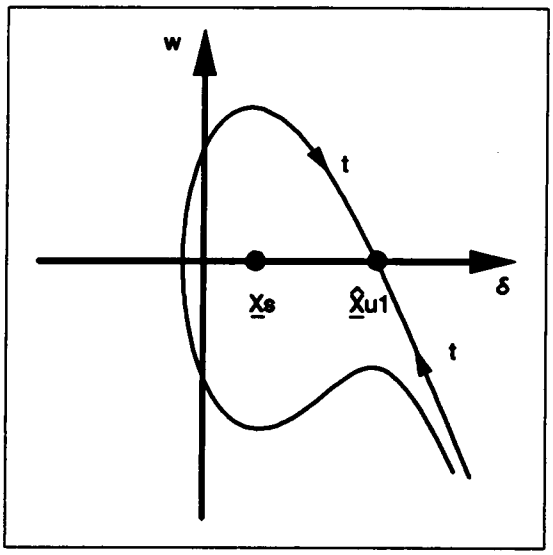

Figure 4-2: Stabilty Boundary of the s.e.p. or stable manifold of u.e.p. 1

points are the following:

$$\begin{bmatrix} 2.411865 \\ 0.0 \end{bmatrix} + \frac{1}{100} \begin{bmatrix} -0.1436 \\ 0.9896 \end{bmatrix} = \begin{bmatrix} 2.410429 \\ 0.009896 \end{bmatrix}$$

$$\begin{bmatrix} 2.411865 \\ 0.0 \end{bmatrix} - \frac{1}{100} \begin{bmatrix} -0.1436 \\ 0.9896 \end{bmatrix} = \begin{bmatrix} 2.413301 \\ -0.009896 \end{bmatrix}$$

4.3 Exit point method

4.3.1 Definitions and procedures

The *exit point*, $\underline{x}_e$, is the point where the fault-on trajectory intersects the stability boundary [20]. The transient energy evaluated at this point is the *true critical energy*, the corresponding clearing time is the *true critical clearing time.*

$$V_{true}^{cr} = V(\underline{x}_e) = V_k(\underline{\omega}_e) + V_p(\underline{\delta}_e)$$

$$\underline{x}_e = \begin{bmatrix} \underline{\delta}_e \\ \underline{\omega}_e \end{bmatrix}$$

$$t_{cl} = t_{cr}$$

For a fault cleared when the energy is less than the critical energy, the system is stable; otherwise, it is unstable. Notice that according to its definition the true critical energy is fault-dependent.

The exit-point must then be found. We will first define the *controlling u.e.p* as the u.e.p. whose stable manifold intersects with the fault-on trajectory [20], i.e. it is the u.e.p. whose stable manifold contains the exit point [10].

The *exit-point method* is as follows:

1. Obtain the controlling u.e.p. from the fault-on trajectory and designate it as $\underline{x}_{co}$. This procedure will be discussed in detail later.

2. Follow Procedure 3 above to find $W^s(\underline{x}_{co})$.

3. Find the first intersection of the fault-on trajectory with $W^s(\underline{x}_{co})$. This is the exit point. The corresponding time is the critical clearing time, c.c.t., and the corresponding energy is the true critical energy.

As explained before, the stability boundary of a 2-machine system can be found easily by locating the two u.e.p.'s and applying Procedures 1 to 3 and Theorems 1 and 2 above. Unfortunately, we can not find the stable manifold of a type-1 u.e.p. for a power system with more than two generator buses. Therefore, for more than two machines this method is a *conceptual one.*

4.3.2 Two-machine example, exit-point method

The two-machine system shown in Fig. 4-3 is used to describe the exit-point method.

The disturbance consists of a self-clearing, 3-phase fault, $R_f = 0.25$ pu, $X_f = 0.0$ pu. The fault-on parameters of the system reduced to internal nodes are

$$P_1^f = -1.2254,\ P_2^f = -0.5679,\ C_{12}^f = 1.5076,\ \textit{and}\ D_{12}^f = 0.8773$$

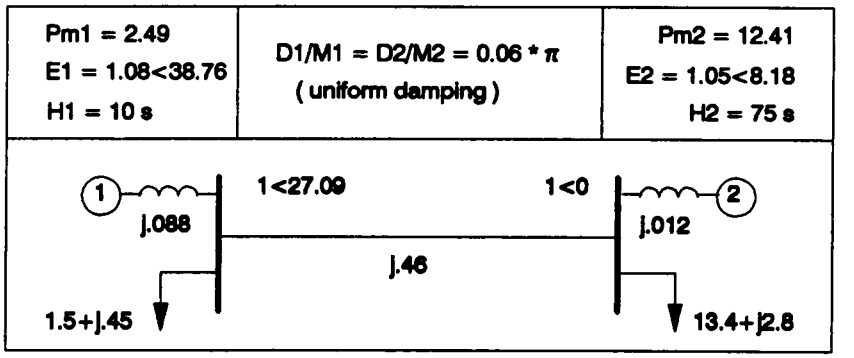

Figure 4-3: Two-machine system with uniform damping

The corresponding post-fault parameters are

$$P_1 = 1.3275,\ P_2 = -0.5072,\ C_{12} = 1.8028,\ and\ D_{12} = 0.4765$$

The stable manifold of $\underline{x}_{co}$ is shown in Fig. 4-4. The Jacobian evaluated at $\underline{x}_{co}$, the stable eigenvalue and the corresponding eigenvector are

$$\underline{J}(\underline{x}_{co}) = \begin{matrix} 0 & 1 \\ 29.1933 & -0.1885 \end{matrix},\ \lambda_s = -5.4981,\ \underline{y}_s = \begin{bmatrix} -0.1789 \\ 0.9839 \end{bmatrix}$$

The two starting points are

$$\underline{x}_{co} + 0.01\ \underline{y}_s = \begin{bmatrix} 2.2071 \\ 0.0098 \end{bmatrix}$$

$$\underline{x}_{co} - 0.01\ \underline{y}_s = \begin{bmatrix} 2.2107 \\ -0.0098 \end{bmatrix}$$

The critical clearing time is 0.1158 s. It is worthwhile to notice that this particular fault caused machine 1 to decelerate.

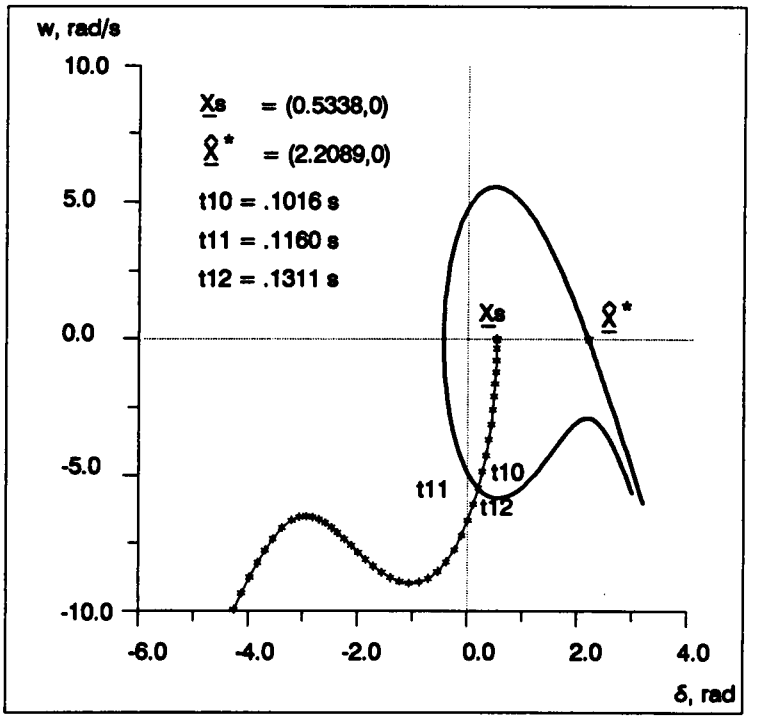

Figure 4-4: Exit-point method

4.4 Closest or nearest unstable equilibrium point method

4.4.1 Definitions

This section is adapted from [20]. In this method the region of attraction is approximated by $\{\underline{x} \mid V(\underline{x}) < V_{closest}^{cr}\}$, where

$$V_{closest}^{cr} = \min\left[V(\underline{x}_1), V(\underline{x}_2), \cdots, V\left(\underline{x}_{nuep}\right)\right]$$

$\underline{x}_1, \underline{x}_2, \cdots, \underline{x}_{nuep}$ is the set of u.e.p.'s on the stability boundary $\partial A(\underline{x}_s)$

The *nuep* is the number of u.e.p.'s on the stability boundary $\partial A(\underline{x}_s)$. Notice that $V_{closest}^{cr}$ is not fault dependent and its use may yield conservative results.

Procedure 4 Determination of $V_{closest}^{cr}$.

1. Find all the type-1 u.e.p.'s. (For an excellent algorithm to find the possible u.e.p.'s on $\partial A(\underline{x}_s)$ see chapter V of [56])
2. Order these type-1 e.p.'s according to the values of their energy function.
3. Starting from the u.e.p. with the lowest value of transient energy, follow Procedure 2 to determine if it lies on $\partial A(\underline{x}_s)$. The first u.e.p. belonging to $\partial A(\underline{x}_s)$ is the closest u.e.p.

1. The critical energy is

$$V_{closest}^{cr} = V(\underline{x}_{closest}) = V_p(\underline{\delta}_{closest})$$

$$\underline{x}_{closest} = \begin{matrix} \underline{\delta}_{closest} \\ \underline{\omega}_{closest} = 0 \end{matrix}$$

4.4.2 Two-machine example, closest u.e.p. method

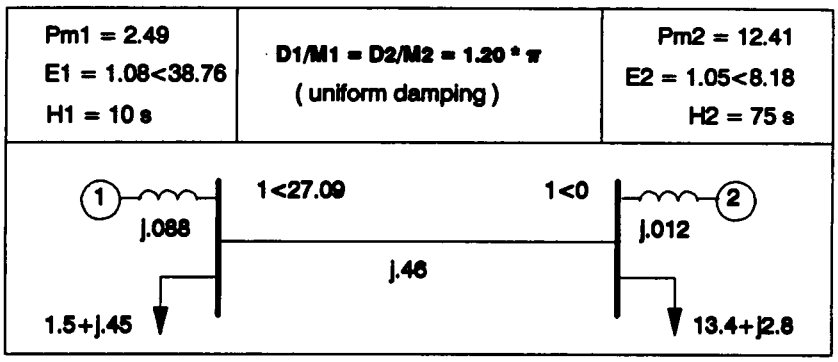

Figure 4-5: Two-machine system with increased uniform damping

Let us consider the two-machine system shown in Fig. 4-5. This system is the same as the one shown in Fig. 4-3 but in order to get $\hat{\underline{x}}_{u2}$ to belong to $\partial A(\underline{x}_s)$, the damping has been increased from $D = 0.01$ to $D = 0.2 \frac{\text{MW s}}{\text{MVA rad}}$. As shown in Fig. 4-6, the equilibrium points are the same as before

$$\underline{x}_s = \begin{bmatrix} 0.5339 \\ 0 \end{bmatrix}, \hat{\underline{x}}_{u1} = \begin{bmatrix} 2.2089 \\ 0 \end{bmatrix}, \hat{\underline{x}}_{u2} = \begin{bmatrix} -4.074286 \\ 0 \end{bmatrix}$$

Notice that the left branch of $W^u(\hat{\underline{x}}_{u2})$ (the unstable manifold of $\hat{\underline{x}}_{u2}$) converges to $\underline{x}_{s2}$ and

its right branch converges to $\underline{x}_s$. Since $\hat{\underline{x}}_{u2}$ and $\hat{\underline{x}}_{u1}$ belong to $\partial A(\underline{x}_s)$, $\partial A(\underline{x}_s) = W^s(\hat{\underline{x}}_{u2}) \cup W^s(\hat{\underline{x}}_{u1})$, as illustrated in Fig. 4-6.

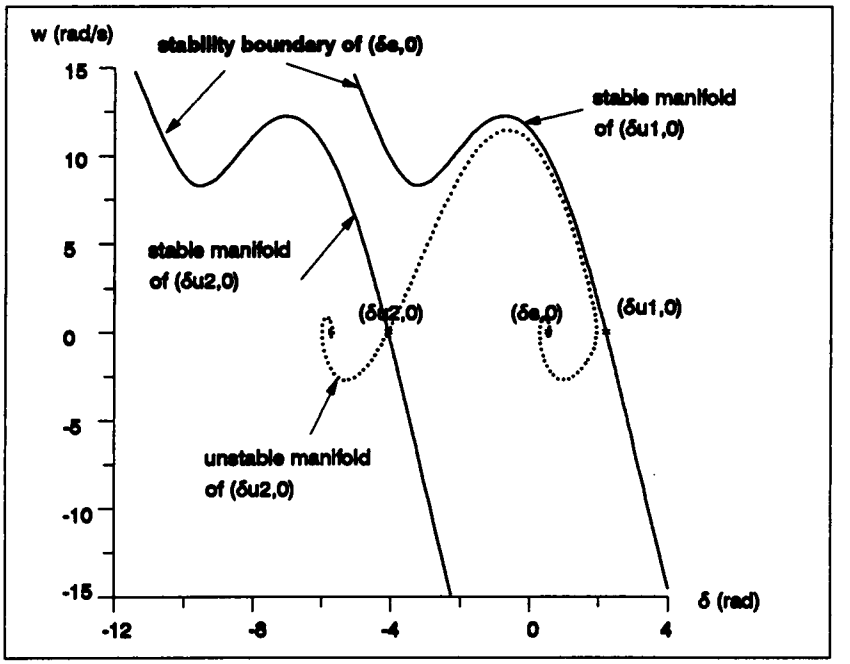

Figure 4-6: Two u.e.p.'s on the stability boundary

The post-fault parameters of the system reduced to internal nodes are

$$P_1 = 1.3275,\ P_2 = -0.5072,\ C_{12} = 1.8028,\ and\ D_{12} = 0.4747$$

The Jacobian evaluated at the u.e.p.'s and the stable eigenvalue and stable eigenvector are

$$\underline{J}(\hat{\underline{x}}_{u1}) = \begin{bmatrix} 0 & 1 \\ 29.1936 & -3.7699 \end{bmatrix},\ \lambda_s = -7.6074,\ \underline{y}_s = \begin{bmatrix} -0.1303 \\ 0.9915 \end{bmatrix}$$

$$\underline{J}(\hat{\underline{x}}_{u2}) = \underline{J}(\hat{\underline{x}}_{u1})$$

As shown in Fig. 4-7, $V^{cr}_{closest} = V_p(\delta_{closest}) = V_p(\delta_{u1}) = 0.6711\ \frac{\text{MW rad}}{\text{MVA}}$. Two values of fault impedance are considered (both faults are self-clearing on bus 1).

1. $\mathbf{Z}_f = 0.0 + j\ 0.00001$, which accelerates machine 1. The fault-on parameters of the system

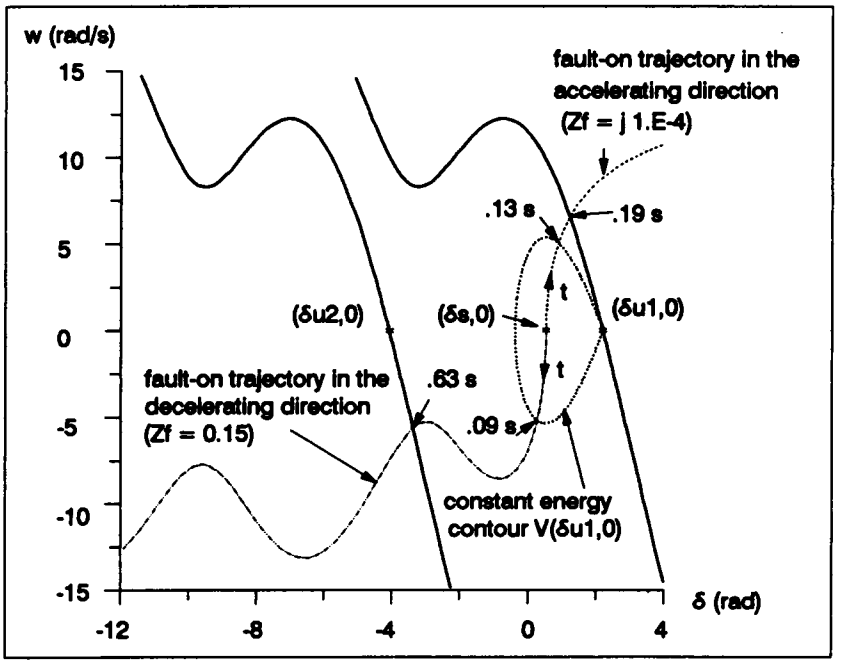

Figure 4-7: Closest unstable equilibrium point method

reduced to internal nodes are

$$P_1^f = 2.4900,\ P_2^f = -0.3792,\ C_{12}^f = 2.5837 \times 10^{-4},\ and\ D_{12}^f = 3.9210 \times 10^{-5}$$

The critical clearing time obtained by using the closest u.e.p. method is 0.13 s; using the exit-point method, it is 0.19 s.

2. $Z_f = 0.15 + j\ 0.0$, which decelerates machine 1. The fault-on parameters of the system reduced to internal nodes are

$$P_1^f = -2.2533,\ P_2^f = -0.5856,\ C_{12}^f = 1.2568,\ and\ D_{12}^f = 1.0186$$

The critical clearing time obtained by using closest u.e.p. method is 0.09 s; using the exit-point method it is 0.63 s.

From these results, we can see that when the exit-point is contained by the manifold of the closest u.e.p. (the closest u.e.p. is the controlling u.e.p.), the closest u.e.p. method yields

a good approximation for the critical clearing time. These results also show that the contour of constant energy evaluated at the closest u.e.p. gives a good approximation of the stability boundary. However, the closest u.e.p. method may be extremely conservative when the exit-point does not intersect with the stable manifold of the closest u.e.p. (the controlling u.e.p. is not the closest u.e.p.).

We can also learn from this example that the fault-on trajectory depends on the value of the fault impedance. It also depends on the fault location, the type of the fault, and the clearing time [56].

4.5 Controlling unstable equilibrium point method

Let us list the advantages and the disadvantages of the methods described so far.

Exit-point method

- Advantages:

  1. It yields true critical clearing time.
  2. It yields true critical energy (fault dependent).
  3. It is not based on an approximation of the region of attraction.

- Disadvantages:

  1. Once the controlling u.e.p. has been found, its stable manifold must be determined. This method is only practical for a small number of machines.

Closest u.e.p. method

- Advantages:

  1. It can be applied to a multi-machine system.
  2. The closest critical energy must be found only once, since it is not fault dependent. The closest critical energy is used for different fault configurations, but not for different post-fault configurations.

- Disadvantages:

  1. It may yield very conservative results.
  2. For a large number of machines it is very difficult to determine all of the u.e.p.'s on the stability boundary. If the closest u.e.p. is missed, a very optimistic result may be obtained by using a wrong u.e.p.

It is clear that a method yielding less conservative results and a method feasible for a large number of machines is required. The controlling u.e.p. method is this method, since it is not required to find the stable manifold of any u.e.p. and the critical energy is fault dependent.

4.5.1 Definitions and procedures

The *controlling u.e.p.* was defined as the u.e.p. whose stable manifold intersects with the fault-on trajectory [20]. This definition means that the controlling u.e.p. is the u.e.p. whose stable manifold contains the exit point [10].

In this method, the region of attraction is approximated by

$$\{\underline{x} \mid V(\underline{x}) < V_{co}^{cr}\}$$

where

$$V_{co}^{cr} = V(\underline{x}_{co})$$

$\underline{x}_{co}$ is the controlling u.e.p., also known as the relevant u.e.p.

The *controlling u.e.p. method* is the following procedure:

1. Obtain the controlling u.e.p. from the fault-on trajectory and designate it as $\underline{x}_{co}$. This procedure will be discussed in detail later.
2. Evaluate the energy function at $\underline{x}_{co}$, $V_{co}^{cr} = V(\underline{x}_{co}) = V_p(\underline{\delta}_{co})$, where $\underline{\delta}_{co}$ is the angle subspace of $\underline{x}_{co}$.

$$\underline{x}_{co} = \begin{bmatrix} \underline{\delta}_{co} \\ \underline{\omega}_{co} = \underline{0} \end{bmatrix}$$

3. Find the first intersection of the fault-on trajectory with the boundary of the region defined by

$$\{\underline{x} \mid V(\underline{x}) < V_{co}^{cr}\}$$

In other words, evaluate the transient energy along the fault-on trajectory, the time at which the transient energy reaches V_{co}^{cr} is the critical clearing time, c.c.t.. It is important to emphasize that the parameters of this system, reduced to internal nodes, used in calculating the fault-on trajectory are not the same as those used in evaluating the transient energy. The fault-on trajectory is obtained by the numerical integration of $\dot{\underline{x}} = \underline{f}(\underline{x})$ using $P_i^f, C_{ij}^f, D_{ij}^f$ for $i = 1, 2, \cdots, n;\ j \neq i$. The energy function, as well as the s.e.p., are evaluated using the post-fault parameters, P_i, C_{ij}, D_{ij} for $i = 1, 2, \cdots, n;\ j \neq i$.

4.5.2 Two-machine system example, controlling u. e. p. method

The two-machine system shown in Fig. 4-5 will be used again.

As shown in Fig. 4-8, two values of the fault impedance are considered (both faults are self-clearing on bus 1).

1. $\mathbf{Z}_f = 0.0 + j\ 0.00001$, which accelerates machine 1. The controlling u.e.p. for this particular fault is $\underline{x}_{co} = (\delta_{u1}, 0)$. The critical energy is $V(\delta_{u1}, 0) = V_p(\delta_{u1}) = 0.6711$ $\frac{\text{MW rad}}{\text{MVA s}}$. The region of attraction is approximated by the segment of this contour level as shown in Fig. 4-8.The critical clearing time obtained by using the controlling u.e.p. method is 0.13 s; using the exit-point method it is 0.19 s. This result is the same as the one obtained by closest u.e.p. method because $\underline{x}_{co} = \underline{x}_{closest}$.

2. $Z_f = 0.15 + j\ 0.0$, which decelerates machine 1. The controlling u.e.p. for this particular fault is $\underline{x}_{co} = (\delta_{u2}, 0)$. The critical energy is $V(\delta_{u2}, 0) = V_p(\delta_{u2}) = 8.4057$. The region of attraction is approximated by the segment of this contour level as shown in Fig. 4-8.The critical clearing time obtained by using controlling u.e.p. method is 0.59 s; using the exit-point method it is 0.63 s.

The thick, dotted lines in Fig. 4-8 are the approximation of the stability boundary using the controlling u.e.p. method. Notice the following:

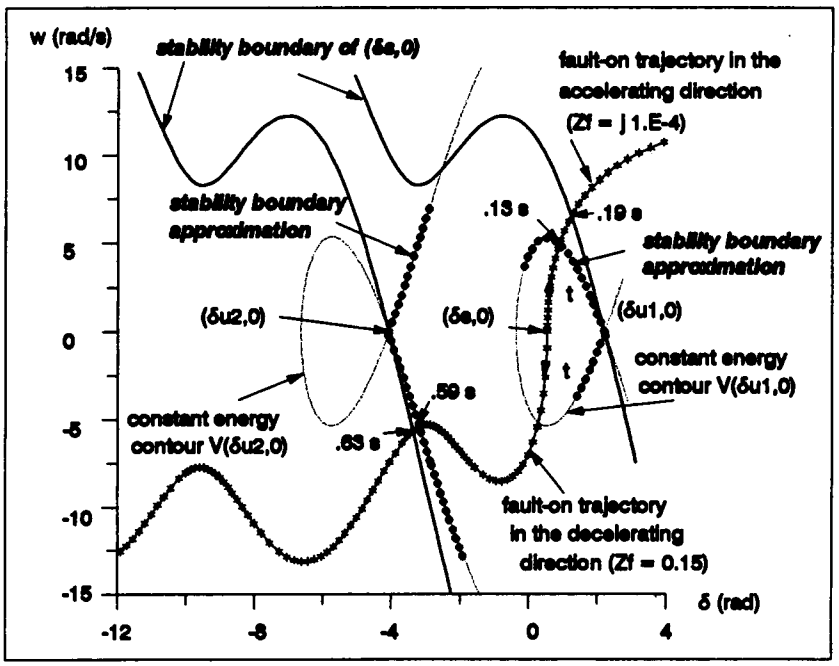

Figure 4-8: Controlling unstable equilibrium point method

1. the closer the exit-point gets to the controlling u.e.p., the more accurate the approximation is.

2. the controlling u.e.p. method always yields a conservative result. Theorem 6-4 in [17].

Chapter 5

PEBS and BCU Methods

5.1 Associated reduced-order systems

Associated reduced-order systems have been presented in [1], [83], [76], [17], [55] , [10] and [77]. In this section we will obtain these associated reduced-order systems.

1. Reduced system in center of angle formulation. This reduced system is presented in reference [77]
2. Reduced system in machine-n-as-reference formulation. This reduced system is presented in [10] and [9].
3. Associated gradient system in center of angle formulation.

We will show that the reduced system and the gradient system are the same only if the reference machine is an infinite bus.

5.1.1 Reduced system using center of angle

To obtain the reduced system we will start with the state equation of the original system.

$$\begin{aligned} \frac{d\tilde{\delta}_i}{dt} &= \tilde{\omega}_i \\ \frac{d\tilde{\omega}_i}{dt} &= \frac{P_i - P_{ei}}{M_i} - \frac{P_{COA}}{M_t} - \lambda_D \tilde{\omega}_i \\ & i = 1, 2, \ldots n-1 \end{aligned} \tag{5.1}$$

Let us consider the following equation of angular acceleration:

$$\frac{d\tilde{\omega}_i}{dt} = \frac{P_i - P_{ei}}{M_i} - \frac{P_{COA}}{M_t} - \lambda_D \tilde{\omega}_i$$

or

$$M_i \frac{d\tilde{\omega}_i}{dt} + D_i \tilde{\omega}_i = P_i - P_{ei} - \frac{M_i}{M_t} P_{COA}$$

Notice that the right-hand side of the above equation is a function of the angle subspace, i.e.

$$f_i^{red}\left(\tilde{\underline{\delta}}\right) = P_i - P_{ei} - \frac{M_i}{M_t} P_{COA}$$

The reduced system is then defined by the following state equation:

$$\frac{d\tilde{\delta}_i}{dt} = P_i - P_{ei} - \frac{M_i}{M_t} P_{COA}, \quad i = 1, 2, \ldots, n-1 \tag{5.2}$$

Notice that the original system is a second-order dynamic system and the reduced system is a first-order dynamic system. Therefore, they have different dynamics. However, there is a one-to-one correspondence between the equilibrium points of the original system (Eq. 5.1) and the equilibrium points of the reduced system (Eq. 5.2).

The equilibrium points of the original system must satisfy the following equations.

$$\begin{aligned} 0 &= \tilde{\omega}_i \\ 0 &= \frac{P_i - P_{ei}}{M_i} - \frac{P_{COA}}{M_t} - \lambda_D \tilde{\omega}_i \\ & i = 1, 2, \ldots, n-1 \end{aligned}$$

$$\underline{0} = \tilde{\underline{\omega}}$$

$$\underline{0} = \underline{f}^{red}\left(\tilde{\underline{\delta}}\right) - \lambda_D \cdot \underline{0} = \underline{f}^{red}\left(\tilde{\underline{\delta}}\right)$$

The equilibrium points of the reduced system must satisfy the following equation.

$$\begin{aligned} 0 &= P_i - P_{ei} - \frac{M_i}{M_t} P_{COA} \\ & i = 1, 2, \ldots, n-1 \end{aligned}$$

$$0 = \underline{f}^{red}\left(\underline{\tilde{\delta}}\right)$$

Therefore, if an e.p. of the original system is $\left(\underline{\tilde{\delta}}, \underline{0}\right)$, the corresponding e.p. of the reduced system is $\left(\underline{\tilde{\delta}}\right)$.

Notice that in Eq. 5.2 i goes from 1 to $n-1$. We will show that $\frac{d\tilde{\delta}_n}{dt}$ may be expressed as a linear combination of the rest, i.e. there are only $n-1$ state variables.

$$\sum_{i=1}^{n} \frac{d\tilde{\delta}_i}{dt} = \sum_{1=1}^{n} (P_i - P_{ei}) - \frac{P_{COA}}{M_t} \sum_{i=1}^{n} M_i$$

or

$$\sum_{i=1}^{n} \frac{d\tilde{\delta}_i}{dt} = 0$$

The following equation results.

$$\frac{d\tilde{\delta}_n}{dt} = -\sum_{i=1}^{n-1} \frac{d\tilde{\delta}_i}{dt}$$

5.1.2 Reduced system using machine n as reference

The starting point will be the state equation of the original system.

$$\left[\begin{array}{c} \dot{\delta}_{in} = \omega_{in} \\ \dot{\omega}_{in} = \frac{P_i - P_{ei}}{M_i} - \frac{P_n - P_{en}}{M_n} - \lambda_D \omega_{in} \end{array}\right] \qquad i = 1, 2, \ldots, n-1 \tag{5.3}$$

Let us consider the following equation corresponding to angular acceleration:

$$\dot{\omega}_{in} = \frac{P_i - P_{ei}}{M_i} - \frac{P_n - P_{en}}{M_n} - \lambda_D \omega_{in}$$

or

$$\dot{\omega}_{in} + \frac{D_i}{M_i}\omega_{in} = \frac{P_i - P_{ei}}{M_i} - \frac{P_n - P_{en}}{M_n} \tag{5.4}$$

If we multiply Eq. 5.4 by M_i the result is

$$M_i\dot{\omega}_{in} + D_i\omega_{in} = P_i - P_{ei} - \frac{M_i}{M_n}(P_n - P_{en})$$

The reduced system is the following equation:

$$\begin{aligned}\dot{\delta}_{in} &= P_i - P_{ei} - \frac{M_i}{M_n}(P_n - P_{en}) \\ &= f_i^{red}(\underline{\delta})\end{aligned} \tag{5.5}$$

The equilibrium points of the original system must satisfy the following:

$$\begin{gathered}0 = \omega_{in} \\ 0 = \frac{P_i - P_{ei}}{M_i} - \frac{P_n - P_{en}}{M_n} - \lambda_D \omega_{in} \\ i = 1, 2, \ldots, n-1\end{gathered}$$

$$\begin{gathered}\underline{0} = \underline{\omega} \\ \underline{0} = \underline{f}^{red}(\underline{\delta}) - \lambda_D \cdot \underline{0} = \underline{f}^{red}(\underline{\delta})\end{gathered}$$

The equilibrium points of the reduced system must satisfy the following:

$$\begin{aligned}0 &= P_i - P_{ei} - \frac{M_i}{M_n}(P_n - P_{en}) \\ &\quad i = 1, 2, \ldots, n-1\end{aligned}$$

$$\underline{0} = \underline{f}^{red}(\underline{\delta})$$

Therefore, if an e.p. of the original system is $(\underline{\delta}, \underline{0})$ the corresponding e.p. of the reduced system is $(\underline{\delta})$.

5.1.3 The associated gradient system using center of angle

The gradient system is a reduced-order system whose state equation is defined by the following equation:

$$\dot{\delta}_j = -\frac{\partial V_{pe}}{\partial \delta_j}, \quad j = 1, 2, \ldots, n-1$$

V_{pe} is the potential energy.

According to Eq. 3.17 and Eq. 3.18 the potential energy is given by Eq. 5.6.

$$V_{pe}\left(\tilde{\underline{\delta}}\right) = \int_{t_o}^{t} \left\{ \sum_{i=1}^{n} \left[-P_i + P_{ei}\left(\tilde{\underline{\delta}}\right) + \frac{M_i}{M_t} P_{COA}\left(\tilde{\underline{\delta}}\right) \right] \frac{d\tilde{\delta}_i}{dt} \right\} dt \tag{5.6}$$

Since $V_{pe}\left(\tilde{\underline{\delta}}\right) = \int_{t_o}^{t} \sum_{i=1}^{n} \left[-P_i + P_{ei}\left(\tilde{\underline{\delta}}\right)\right] \frac{d\tilde{\delta}_i}{dt} dt + \int_{t_o}^{t} \frac{P_{COA}(\tilde{\underline{\delta}})}{M_t} \left[\sum_{i=1}^{n} M_i \frac{d\tilde{\delta}_i}{dt}\right] dt$, the following results.

$$\sum_{i=1}^{n} M_i \frac{d\tilde{\delta}_i}{dt} = 0$$

$$V_{pe}\left(\tilde{\underline{\delta}}\right) = \int_{t_o}^{t} \sum_{i=1}^{n} \left[-P_i + P_{ei}\left(\tilde{\underline{\delta}}\right)\right] \frac{d\tilde{\delta}_i}{dt} dt$$

By taking the summation out of the integral, canceling dt and changing the limits of integration the following potential energy function results.

$$V_{pe}\left(\tilde{\underline{\delta}}\right) = \sum_{i=1}^{n} \int_{\tilde{\delta}_i^o}^{\tilde{\delta}_i} \left[-P_i + P_{ei}\left(\tilde{\underline{\delta}}\right)\right] d\tilde{\delta}_i$$

The last angle, $\tilde{\delta}_n$ is a function of the angle subspace.

$$\tilde{\delta}_n = -\frac{1}{M_n} \sum_{i=1}^{n-1} M_i \tilde{\delta}_i$$

$$\frac{d\tilde{\delta}_n}{d\tilde{\delta}_i} = -\frac{M_i}{M_n}$$

$$V_{pe}\left(\tilde{\underline{\delta}}\right) = \sum_{i=1}^{n-1} \int_{\tilde{\delta}_i^o}^{\tilde{\delta}_i} \left[-P_i + P_{ei}\left(\tilde{\underline{\delta}}\right)\right] d\tilde{\delta}_i + \int_{\tilde{\delta}_n^o}^{\tilde{\delta}_n(\tilde{\underline{\delta}})} \left[-P_n + P_{en}\left(\tilde{\underline{\delta}}\right)\right] d\tilde{\delta}_n$$

To obtain $\frac{\partial V_{pe}(\tilde{\underline{\delta}})}{\partial \tilde{\delta}_i}$ we will make use of the chain rule as indicated in Eq. 5.7

$$\frac{\partial V_{pe}\left(\tilde{\underline{\delta}}\right)}{\partial \tilde{\delta}_i} = \frac{\partial}{\partial \tilde{\delta}_i} \left\{ \int_{\tilde{\delta}_i^o}^{\tilde{\delta}_i} \left[-P_i + P_{ei}\left(\tilde{\underline{\delta}}\right)\right] d\tilde{\delta}_i \right\} + \frac{\partial}{\partial \tilde{\delta}_n} \left\{ \int_{\tilde{\delta}_n^o}^{\tilde{\delta}_n(\tilde{\underline{\delta}})} \left[-P_n + P_{en}\left(\tilde{\underline{\delta}}\right)\right] d\tilde{\delta}_n \right\} \frac{d\tilde{\delta}_n}{d\tilde{\delta}_i} \quad (5.7)$$

Therefore, the potential energy gradient in COA formulation is the following:

$$\frac{\partial V_{pe}\left(\tilde{\underline{\delta}}\right)}{\partial \tilde{\delta}_i} = -P_i + P_{ei}\left(\tilde{\underline{\delta}}\right) - \frac{M_i}{M_n}\left[-P_n + P_{en}\left(\tilde{\underline{\delta}}\right)\right] \quad (5.8)$$

$$i = 1, 2, \cdots, n-1$$

This result can be verified by using $n = 2$ in Eq. 3.24 and taking the derivative of the

potential energy with respect to $\tilde{\delta}_1$. This yields

$$\frac{\partial V_{pe}\left(\tilde{\underline{\delta}}\right)}{\partial \tilde{\delta}_1} = -P_1 + P_{e1}\left(\tilde{\underline{\delta}}\right) - \frac{M_1}{M_2}\left[-P_2 + P_{e2}\left(\tilde{\underline{\delta}}\right)\right]$$

This result agrees with Eq. 5.8.

Except for a two-machine system, the potential energy can be found only if the transfer conductances are neglected . In the presence of loads, which in the classical model are modeled as constant impedances, the transfer conductances are not negligible. The ray approximation of the potential energy is used to overcome this problem. The potential energy gradient does not make use of the ray approximation, i.e. the potential energy gradient as given by Eq. 5.8 is not an approximation.

The state equation of the gradient system using COA formulation is

$$\frac{d\tilde{\delta}_i}{dt} = (P_i - P_{e1}) - \frac{M_i}{M_n}(P_n - P_{en}) \tag{5.9}$$

$$i = 1, 2, \cdots, n-1$$

From the fact that the gradient system and the reduced system in machine-n-as-reference formulation are given by the same equation, it follows that there is a one-to-one correspondence between the e.p.'s of the gradient system and the e.p.'s of the original system.

If the reference machine is an infinite bus then the reduced system of Eq. 5.2 and the gradient system of Eq. 5.9 are given respectively by Eq. 5.10 and Eq. 5.11.

$$\begin{aligned} \frac{d\tilde{\delta}_i}{dt} &= P_i - P_{ei} - \frac{M_i}{M_t} P_{COA} \\ &= P_i - P_{ei} \\ & i = 1, 2, \ldots, n-1 \end{aligned} \tag{5.10}$$

$$\begin{aligned} \frac{d\tilde{\delta}_i}{dt} &= (P_i - P_{e1}) - \frac{M_i}{M_n}(P_n - P_{en}) \\ &= P_i - P_{ei} \\ & i = 1, 2, \ldots, n-1 \end{aligned} \tag{5.11}$$

We can see that these lower dimensional systems are the same if the reference machine is an infinite bus.

5.1.4 A conservative system and the potential energy gradient

An interesting situation to verify the potential energy gradient as given by Eq. 5.8 is to consider a conservative system, i.e. a system with no damping (regardless of transfer conductances). In this case the total transient energy after the disturbance is constant.

$$\dot{V}\left(\tilde{\underline{\delta}},\tilde{\underline{\omega}}\right) = 0$$

$$\frac{d}{dt}V_k\left(\tilde{\underline{\omega}}\right) = -\frac{d}{dt}V_{pe}\left(\tilde{\underline{\delta}}\right)$$

To simplify matters we will assume $n = 3$. The angle subspace, the angular velocity of machine 3, its angular acceleration, the vector of accelerating powers, and the transient kinetic energy are respectively given by the following equations:

$$\tilde{\underline{\omega}} = \begin{bmatrix} \tilde{\omega}_1 \\ \tilde{\omega}_2 \end{bmatrix}$$

$$\tilde{\omega}_3 = -\frac{M_1}{M_3}\tilde{\omega}_1 - \frac{M_2}{M_3}\tilde{\omega}_2 \tag{5.12}$$

$$\frac{d}{dt}\tilde{\omega}_3 = -\frac{M_1}{M_3}\frac{d}{dt}\tilde{\omega}_1 - \frac{M_2}{M_3}\frac{d}{dt}\tilde{\omega}_2 \tag{5.13}$$

$$\begin{bmatrix} M_1\frac{d}{dt}\tilde{\omega}_1 \\ M_2\frac{d}{dt}\tilde{\omega}_2 \\ M_3\frac{d}{dt}\tilde{\omega}_3 \end{bmatrix} = \begin{bmatrix} P_1 - P_{e1}\left(\tilde{\underline{\delta}}\right) - \frac{M_1}{M_t}P_{COA}\left(\tilde{\underline{\delta}}\right) \\ P_2 - P_{e2}\left(\tilde{\underline{\delta}}\right) - \frac{M_2}{M_t}P_{COA}\left(\tilde{\underline{\delta}}\right) \\ P_3 - P_{e3}\left(\tilde{\underline{\delta}}\right) - \frac{M_3}{M_t}P_{COA}\left(\tilde{\underline{\delta}}\right) \end{bmatrix} \tag{5.14}$$

$$V_k\left(\tilde{\underline{\omega}}\right) = \frac{1}{2}M_1\tilde{\omega}_1^2 + \frac{1}{2}M_2\tilde{\omega}_2^2 + \frac{1}{2}M_3\tilde{\omega}_3^2 \tag{5.15}$$

Substituting Eq. 5.12 into Eq. 5.15 results in the following equation:

$$V_k\left(\tilde{\underline{\omega}}\right) = \frac{1}{2}M_1\tilde{\omega}_1^2 + \frac{1}{2}M_2\tilde{\omega}_2^2 + \frac{M_1^2}{2M_3}\tilde{\omega}_1^2 + \frac{M_2^2}{2M_3}\tilde{\omega}_2^2 + \frac{M_1M_2}{M_3}\tilde{\omega}_1\tilde{\omega}_2$$

The rate of change of the transient kinetic energy is obtained from this equation.

$$\dot{V}_k(\tilde{\underline{\omega}}) = \left[M_1\frac{d\tilde{\omega}_1}{dt} + M_1\left(\frac{M_1}{M_3}\frac{d\tilde{\omega}_1}{dt} + \frac{M_2}{M_3}\frac{d\tilde{\omega}_2}{dt}\right)\right]\tilde{\omega}_1 + \left[M_2\frac{d\tilde{\omega}_2}{dt} + M_2\left(\frac{M_1}{M_3}\frac{d\tilde{\omega}_1}{dt} + M_2\frac{d\tilde{\omega}_2}{dt}\right)\right]\tilde{\omega}_2$$

Notice that the expression enclosed by parenthesis, i.e. $\left(\frac{M_1}{M_3}\frac{d\tilde{\omega}_1}{dt} + \frac{M_2}{M_3}\frac{d\tilde{\omega}_2}{dt}\right)$, is the negative of the angular acceleration of unit 3, Eq. 5.13. Therefore, a more convenient expression for rate of change of the transient kinetic energy is obtained.

$$\dot{V}_k(\tilde{\underline{\omega}}) = M_1\left[\frac{d\tilde{\omega}_1}{dt} - \frac{d\tilde{\omega}_3}{dt}\right]\tilde{\omega}_1 + M_2\left[\frac{d\tilde{\omega}_2}{dt} - \frac{d\tilde{\omega}_3}{dt}\right]\tilde{\omega}_2$$

Substituting Eq. 5.14 into the last result yields Eq. 5.16.

$$\dot{V}_k(\tilde{\underline{\omega}}) = \left[P_1 - P_{e1} - \frac{M_1}{M_3}(P_3 - P_{e3})\right]\frac{d\tilde{\delta}_1}{dt} + \left[P_2 - P_{e2} - \frac{M_2}{M_3}(P_3 - P_{e3})\right]\frac{d\tilde{\delta}_2}{dt} \tag{5.16}$$

Now, we have to get the negative of the rate of change of transient potential energy.

$$-\frac{d}{dt}V_{pe}\left(\tilde{\underline{\delta}}\right) = -\frac{\partial V_{pe}\left(\tilde{\underline{\delta}}\right)}{\partial\tilde{\delta}_1}\frac{d\tilde{\delta}_1}{dt} - \frac{\partial V_{pe}\left(\tilde{\underline{\delta}}\right)}{\partial\tilde{\delta}2}\frac{d\tilde{\delta}_2}{dt}$$

Replacing the gradient of the transient potential energy as given by Eq. 5.8 results in the following equation. The right-hand side is identical to Eq. 5.16.

$$-\dot{V}_{pe}\left(\tilde{\underline{\delta}}\right) = \left[P_1 - P_{e1} - \frac{M_1}{M_3}(P_3 - P_{e3})\right]\frac{d\tilde{\delta}_1}{dt} + \left[P_2 - P_{e2} - \frac{M_2}{M_3}(P_3 - P_{e3})\right]\frac{d\tilde{\delta}_2}{dt}$$

This proves Eq. 5.8 to be correct.

5.1.5 Three-Machine system example

Since the potential energy gradient is not an approximation it is possible to illustrate, with an example, the error introduced due to the ray approximation in the path dependent component of potential energy.

Two cases are considered. In the first case, the power system reduced to internal nodes has transfer conductances hence, the ray approximation has to be used. The second case consists of a power system with no loads, therefore the system reduced to internal nodes has no transfer

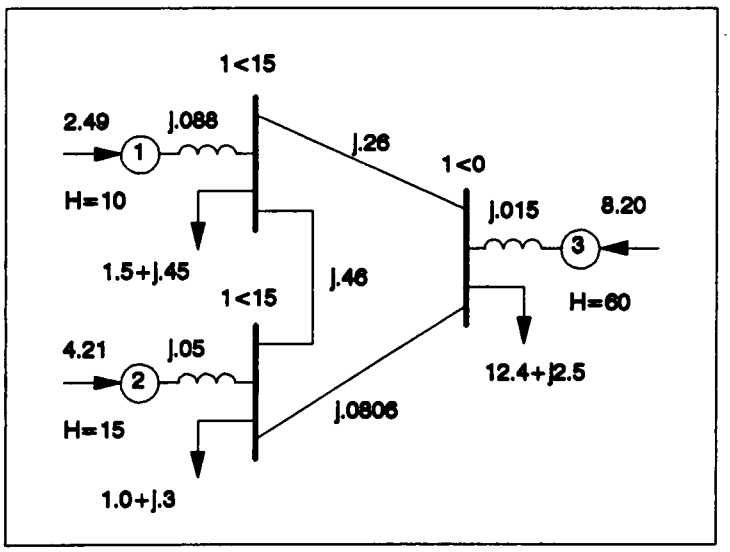

Figure 5-1: 3 - machine system of reference [1]

conductances, hence there is no need for ray approximation.

Power system with transfer conductances

Let us consider the three-machine system of reference [1] shown in Fig. 5-1. The contour map of $V_{pe}^{ray}\left(\tilde{\underline{\delta}}\right)$ is shown in Fig. 5-2. Also shown are the 0-level contours of $\frac{\partial}{\partial\tilde{\delta}_1}V_{pe}\left(\tilde{\underline{\delta}}\right)$ and $\frac{\partial}{\partial\tilde{\delta}_2}V_{pe}\left(\tilde{\underline{\delta}}\right)$. The intersections of these 0-level contours are the equilibrium points of the gradient system, i.e. the equilibrium points must satisfy the following equation:

$$\begin{bmatrix} 0 \\ 0 \end{bmatrix} = \begin{bmatrix} P_1 - P_{e1} - \frac{M_1}{M_3}(P_3 - P_{e3}) \\ P_2 - P_{e2} - \frac{M_2}{M_3}(P_3 - P_{e3}) \end{bmatrix}$$

Notice that the ray approximation of the potential energy does not reflect all of the equilibrium points. A source and a saddle are missing in the lower right-hand corner of the contour map near 26-level contour. The tangent of the contour level of V_{pe} at the intersection with 0-level contour of $\frac{\partial}{\partial\tilde{\delta}_1}V_{pe}\left(\tilde{\underline{\delta}}\right)$ is not always parallel to $\tilde{\delta}_1$-axis. Similarly, the tangent of the contour level of V_{pe} at the intersection with 0-level contour of $\frac{\partial}{\partial\tilde{\delta}_2}V_{pe}\left(\tilde{\underline{\delta}}\right)$ is not always parallel to $\tilde{\delta}_2$-axis.

Power system without transfer conductances

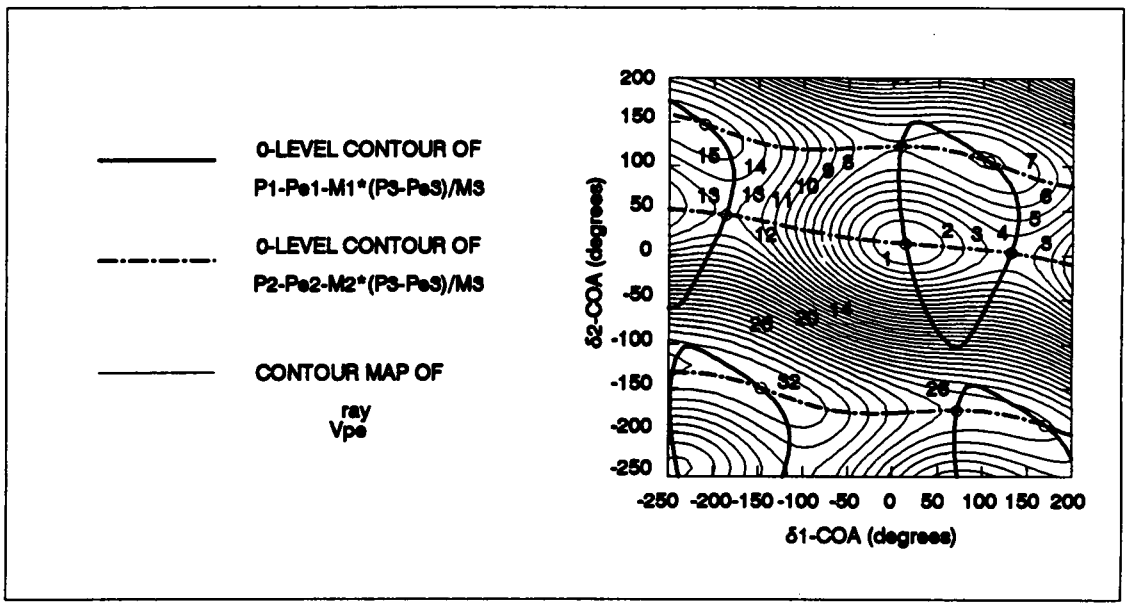

Figure 5-2: Contour map of potential energy approximation for the 3-machine system of reference [1]

The power system shown in Fig. 5-3 is based on the three-machine system of reference [1]. The loads have been eliminated. The mechanical input power of each machine has been modified to include the loads as indicated by the following equation:

$$P_{mi}^{new} = P_{mi}^{old} - P_i^{load}$$

Since this system has no load, the system reduced to internal nodes has no transfer conductances, hence the contour map of the energy function shows all of the saddles and sources, see Fig. 5-4. For comparison with the previous case, notice the presence of a saddle point with energy level slightly above 26 MW rad / MVA. Another interesting comparison between the two cases is that the tangent of the contour level of V_{pe} at the intersection with 0-level contour of $\frac{\partial}{\partial \tilde{\delta}_1} V_{pe}\left(\tilde{\underline{\delta}}\right)$ is always parallel to $\tilde{\delta}_1$-axis. Similarly, the tangent of the contour level of V_{pe} at the intersection with 0-level contour of $\frac{\partial}{\partial \tilde{\delta}_2} V_{pe}\left(\tilde{\underline{\delta}}\right)$ is always parallel to $\tilde{\delta}_2$-axis.

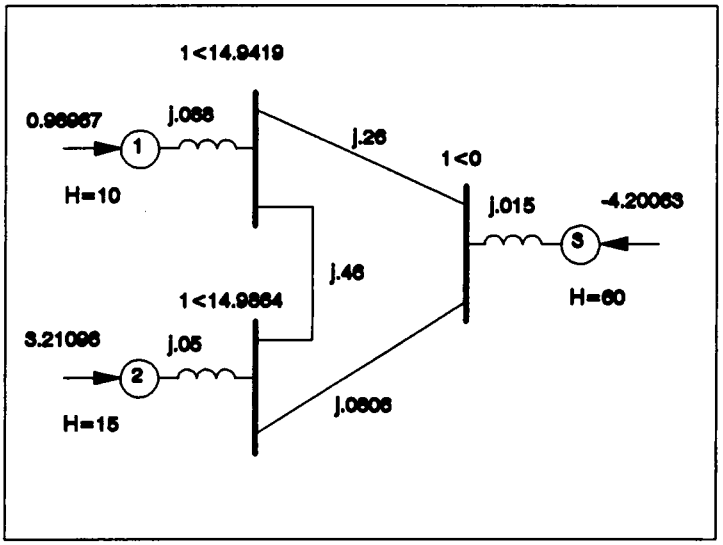

Figure 5-3: 3 - machine system with no loads

5.2 The Potential Energy Boundary Surface

The Potential Energy Boundary Surface, PEBS, method was proposed in 1978 by Kakimoto et. al. [46], and in 1979 by Athay et. al. [1]. It is also described in [56], in [44], and in [25]. As defined in [1], [56] and [25], the Potential Energy Boundary Surface, PEBS, is *obtained by setting the directional derivative of the potential energy (along a ray emanating from the s.e.p.) equal to zero.* In 1985 Varaiya et. al. [83] defined the PEBS as *the stability boundary of the gradient system.* In the following subsections, these two definitions are analyzed and presented.

5.2.1 PEBS setting the directional derivative of the potential energy equal to zero

The PEBS is obtained by setting the directional derivative of the potential energy along a ray emanating from the s.e.p. equal to zero. The directional derivative is the dot product of the gradient and the normalized vector along . Therefore, before getting the directional derivative of the potential energy we need to obtain its gradient. Neglecting damping, the swing equation

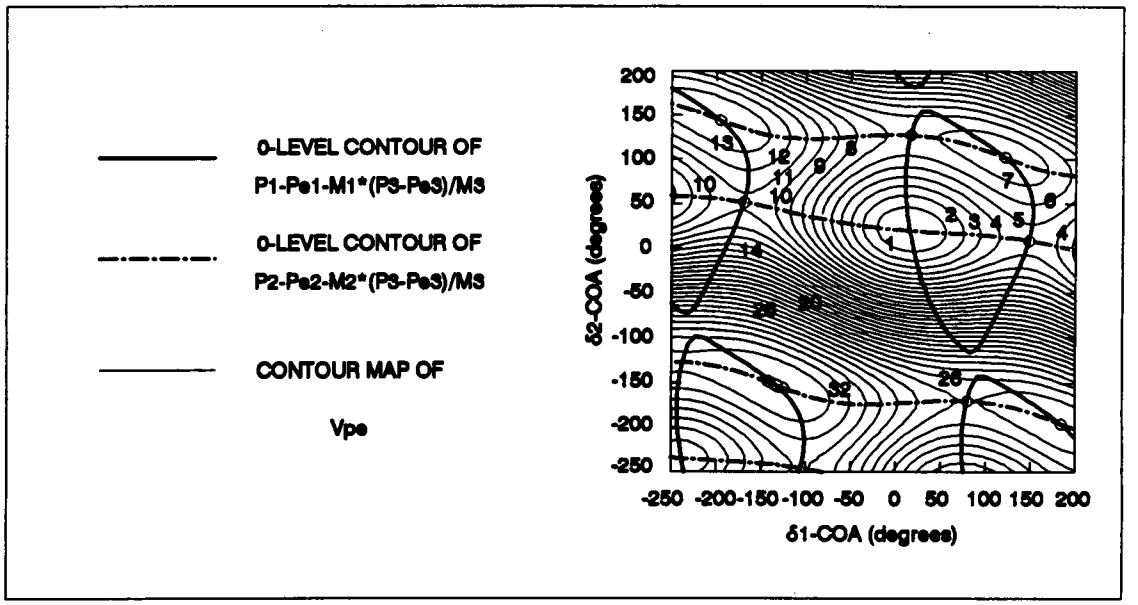

Figure 5-4: Contour map of potential energy for a 3-machine system with no loads

of machine i is given by the following equation:

$$M_i \frac{d\tilde{\omega}_i}{dt} = P_i - P_{ei}\left(\tilde{\underline{\delta}}\right) - \frac{M_i}{M_t} P_{COA}\left(\tilde{\underline{\delta}}\right)$$

$$i = 1, 2, \cdots, n$$

The right-hand side are the accelerating powers, and the vector of accelerating powers is

$$\underline{f_i}\left(\tilde{\underline{\delta}}\right) = \begin{matrix} P_1 - P_{e1}\left(\tilde{\underline{\delta}}\right) - \frac{M_1}{M_t} P_{COA}\left(\tilde{\underline{\delta}}\right) \\ P_2 - P_{e2}\left(\tilde{\underline{\delta}}\right) - \frac{M_2}{M_t} P_{COA}\left(\tilde{\underline{\delta}}\right) \\ \vdots \\ P_n - P_{en}\left(\tilde{\underline{\delta}}\right) - \frac{M_n}{M_t} P_{COA}\left(\tilde{\underline{\delta}}\right) \end{matrix} \tag{5.17}$$

The potential energy gradient is the negative of the vector of accelerating powers [2].

$$\underline{\nabla V_{pe}} = -\left[\underline{f_i}\left(\tilde{\underline{\delta}}\right)\right]^T$$

The normalized ray emanating from the s.e.p. is

$$\underline{u} = \begin{bmatrix} \tilde{\delta}_1 - \tilde{\delta}_1^s \\ \tilde{\delta}_2 - \tilde{\delta}_2^s \\ \vdots \\ \tilde{\delta}_n - \tilde{\delta}_n^s \end{bmatrix} \frac{1}{\sqrt{\left(\tilde{\delta}_1 - \tilde{\delta}_1^s\right)^2 + \left(\tilde{\delta}_2 - \tilde{\delta}_2^s\right)^2 + \cdots + \left(\tilde{\delta}_n - \tilde{\delta}_n^s\right)^2}}$$

The dot product of this two vectors is the directional derivative.

$$\underline{\nabla V_{pe}} \cdot \underline{u} = -\sum_{i=1}^{n} \frac{\underline{f_i}\left(\tilde{\underline{\delta}}\right) \times \left(\tilde{\delta}_i - \tilde{\delta}_i^s\right)}{\sqrt{\left(\tilde{\delta}_1 - \tilde{\delta}_1^s\right)^2 + \left(\tilde{\delta}_2 - \tilde{\delta}_2^s\right)^2 + \cdots + \left(\tilde{\delta}_n - \tilde{\delta}_n^s\right)^2}}$$

As mentioned before the PEBS is obtained by setting this directional derivative equal to zero. Therefore, the PEBS is the angle subspace which satisfies

$$\sum_{i=1}^{n} \underline{f_i}\left(\tilde{\underline{\delta}}\right) \cdot \left(\tilde{\delta}_i - \tilde{\delta}_i^s\right) = 0$$

$$\sum_{i=1}^{n} \left[P_i - P_{ei}\left(\tilde{\underline{\delta}}\right) - \frac{M_i}{M_t} P_{COA}\left(\tilde{\underline{\delta}}\right)\right] \cdot \left(\tilde{\delta}_i - \tilde{\delta}_i^s\right) = 0 \tag{5.18}$$

This result, although obtained in a different way, can be found in [1], [56], [55], and [25].

The potential energy gradient is not given by the vector of accelerating powers as in [2], i.e.

$$\frac{\partial V_{pe}\left(\tilde{\underline{\delta}}\right)}{\partial \tilde{\delta}_i} = -\left[P_i - P_{ei}\left(\tilde{\underline{\delta}}\right) - \frac{M_i}{M_t} P_{COA}\left(\tilde{\underline{\delta}}\right)\right]$$

$$i = 1, 2, \cdots, n$$

The following is the potential energy gradient as given in Eq. 5.8.

$$\frac{\partial V_{pe}\left(\tilde{\underline{\delta}}\right)}{\partial \tilde{\delta}_i} = -\left[P_i - P_{ei}\left(\tilde{\underline{\delta}}\right) - \frac{M_i}{M_n}\left[P_n - P_{en}\left(\tilde{\underline{\delta}}\right)\right]\right]$$

$$i = 1, 2, \cdots, n-1$$

However, the PEBS as stated in Eq. 5.18 is correct. To prove it, let us find the PEBS using

the above equation of the potential energy gradient.

$$\underline{\nabla V_{pe}} = - \begin{matrix} P_1 - P_{e1}\left(\tilde{\underline{\delta}}\right) - \frac{M_1}{M_n}\left[P_n - P_{en}\left(\tilde{\underline{\delta}}\right)\right] \\ P_2 - P_{e2}\left(\tilde{\underline{\delta}}\right) - \frac{M_2}{M_n}\left[P_n - P_{en}\left(\tilde{\underline{\delta}}\right)\right] \\ \vdots \\ P_{n-1} - P_{en-1}\left(\tilde{\underline{\delta}}\right) - \frac{M_{n-1}}{M_n}\left[P_n - P_{en}\left(\tilde{\underline{\delta}}\right)\right] \end{matrix}$$

The normalized ray emanating from the s.e.p. is

$$\underline{u} = \begin{bmatrix} \tilde{\delta}_1 - \tilde{\delta}_1^s \\ \tilde{\delta}_2 - \tilde{\delta}_2^s \\ \vdots \\ \tilde{\delta}_{n-1} - \tilde{\delta}_{n-1}^s \end{bmatrix} \frac{1}{\sqrt{\left(\tilde{\delta}_1 - \tilde{\delta}_1^s\right)^2 + \left(\tilde{\delta}_2 - \tilde{\delta}_2^s\right)^2 + \cdots + \left(\tilde{\delta}_{n-1} - \tilde{\delta}_{n-1}^s\right)^2}}$$

The dot product of this two vectors is the directional derivative.

$$\underline{\nabla V_{pe}} \cdot \underline{u} = -\sum_{i=1}^{n-1} \frac{\left\{P_i - P_{ei}\left(\tilde{\underline{\delta}}\right) - \frac{M_i}{M_n}\left[P_n - P_{en}\left(\tilde{\underline{\delta}}\right)\right]\right\} \times \left(\tilde{\delta}_1 - \tilde{\delta}_1^s\right)}{\sqrt{\left(\tilde{\delta}_1 - \tilde{\delta}_1^s\right)^2 + \left(\tilde{\delta}_2 - \tilde{\delta}_2^s\right)^2 + \cdots + \left(\tilde{\delta}_{n-1} - \tilde{\delta}_{n-1}^s\right)^2}}$$

Setting this directional derivative equal to zero, the PEBS is the angle subspace which satisfies Eq. 5.19.

$$\sum_{i=1}^{n-1} \left\{P_i - P_{ei}\left(\tilde{\underline{\delta}}\right) - \frac{M_i}{M_n}\left[P_n - P_{en}\left(\tilde{\underline{\delta}}\right)\right]\right\} \cdot \left(\tilde{\delta}_i - \tilde{\delta}_i^s\right) = 0 \tag{5.19}$$

Now, it will be shown that Eq. 5.18 is the same as Eq. 5.19.

Since $\sum_{i=1}^{n} \frac{M_i}{M_t} P_{COA}\left(\tilde{\underline{\delta}}\right) \cdot \left(\tilde{\delta}_i - \tilde{\delta}_i^s\right) = 0$, the following holds:

$$\sum_{i=1}^{n} \left[P_i - P_{ei}\left(\tilde{\underline{\delta}}\right) - \frac{M_i}{M_t} P_{COA}\left(\tilde{\underline{\delta}}\right)\right] \cdot \left(\tilde{\delta}_i - \tilde{\delta}_i^s\right) = \sum_{i=1}^{n} \left[P_i - P_{ei}\left(\tilde{\underline{\delta}}\right)\right] \cdot \left(\tilde{\delta}_i - \tilde{\delta}_i^s\right)$$

or

$$\sum_{i=1}^{n} \left[P_i - P_{ei}\left(\tilde{\underline{\delta}}\right) - \frac{M_i}{M_t} P_{COA}\left(\tilde{\underline{\delta}}\right)\right] \cdot \left(\tilde{\delta}_i - \tilde{\delta}_i^s\right) =$$

$$\sum_{i=1}^{n-1}\left[P_i - P_{ei}\left(\tilde{\underline{\delta}}\right)\right]\cdot\left(\tilde{\delta}_i - \tilde{\delta}_i^s\right) + \left[P_n - P_{en}\left(\tilde{\underline{\delta}}\right)\right]\cdot\left(\tilde{\delta}_n - \tilde{\delta}_n^s\right)$$

The angle of the last unit is a function of the angle subspace. The following results.

$$\sum_{i=1}^{n}\left[P_i - P_{ei}\left(\tilde{\underline{\delta}}\right) - \frac{M_i}{M_t}P_{COA}\left(\tilde{\underline{\delta}}\right)\right]\cdot\left(\tilde{\delta}_i - \tilde{\delta}_i^s\right) =$$

$$\sum_{i=1}^{n-1}\left[P_i - P_{ei}\left(\tilde{\underline{\delta}}\right)\right]\cdot\left(\tilde{\delta}_i - \tilde{\delta}_i^s\right) + \left[P_n - P_{en}\left(\tilde{\underline{\delta}}\right)\right]\cdot\sum_{i=1}^{n-1}\frac{-M_i}{M_n}\left(\tilde{\delta}_i - \tilde{\delta}_i^s\right)$$

or

$$\sum_{i=1}^{n}\left[P_i - P_{ei}\left(\tilde{\underline{\delta}}\right) - \frac{M_i}{M_t}P_{COA}\left(\tilde{\underline{\delta}}\right)\right]\cdot\left(\tilde{\delta}_i - \tilde{\delta}_i^s\right) =$$

$$\sum_{i=1}^{n-1}\left[P_i - P_{ei}\left(\tilde{\underline{\delta}}\right) - \frac{M_i}{M_n}\left[P_n - P_{en}\left(\tilde{\underline{\delta}}\right)\right]\right]\cdot\left(\tilde{\delta}_i - \tilde{\delta}_i^s\right)$$

Therefore, the left-hand side of Eq. 5.18 is the same as the left-hand side of Eq. 5.19. This implies that either equation can be used to obtain the PEBS.

5.2.2 Three-machine system example

Let us consider the three-machine system of Fig. 5-3. As mentioned before, due to the absence of loads, the ray approximation of the potential energy is not required. To illustrate that the negative of the vector of accelerating powers is not the potential energy gradient we will refer to Fig. 5-5(a), in which the contour map of the potential energy along with the 0-level contour of $P_1 - P_{e1} - \frac{M_1}{M_t}P_{COA}$ and the 0-level contour of $P_2 - P_{e2} - \frac{M_2}{M_t}P_{COA}$ are shown. Notice that the tangent of the contour level of V_{pe} at its intersection with the 0-level contour of $P_1 - P_{e1} - \frac{M_1}{M_t}P_{COA}$ is not always parallel to $\tilde{\delta}_1$-axis. Similarly, the tangent of the contour level of V_{pe} at its intersection with the 0-level contour of $P_2 - P_{e2} - \frac{M_2}{M_t}P_{COA}$ is not always parallel to $\tilde{\delta}_2$-axis. For comparison, see in Fig. 5-5(b) that the tangent at the intersections is always parallel to the corresponding axis.

Fig. 5-6 shows the contour map of the potential energy and the PEBS. It was verified that both Eq. 5.18 and Eq. 5.19 yield the same PEBS.

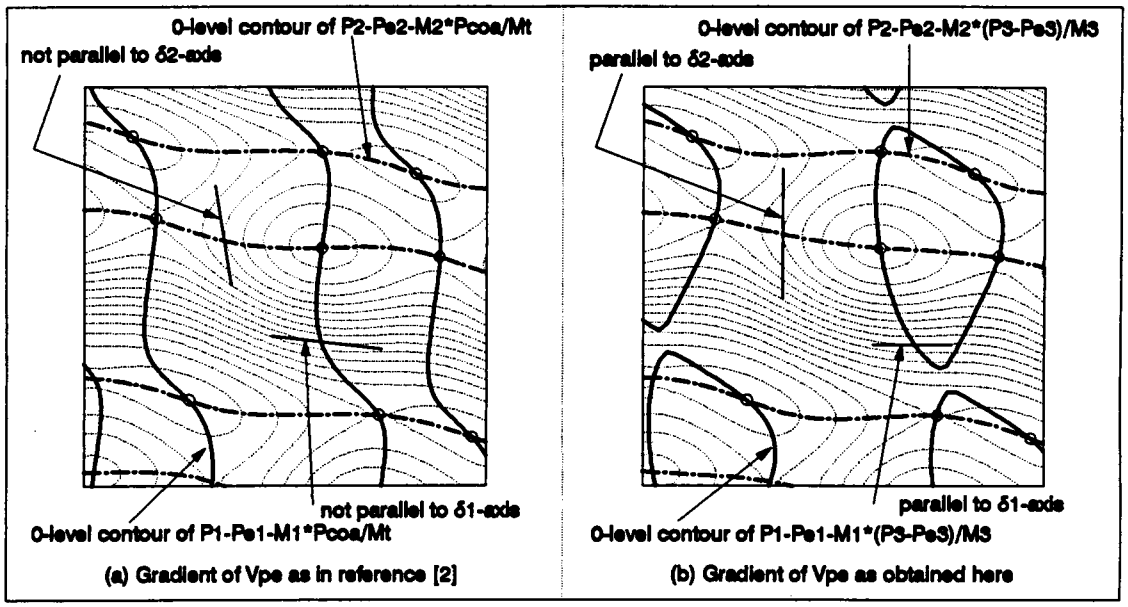

Figure 5-5: Potential energy gradient as in reference [2] compared to potential energy gradient as obtained here

5.2.3 PEBS redefined as the stability boundary of the gradient system

In 1985 Varaiya et. al. [83] defined the PEBS as *the stability boundary of the gradient system.* The formulation used in [83] includes an infinite bus. This allows us to rewrite the state equation to include the potential energy gradient. This is shown as follows.

The negative of the potential energy gradient is

$$-\frac{\partial V_{pe}\left(\tilde{\underline{\delta}}\right)}{\partial \tilde{\delta}_i} = P_i - P_{ei}\left(\tilde{\underline{\delta}}\right) - \frac{M_i}{M_n}\left[P_n - P_{en}\left(\tilde{\underline{\delta}}\right)\right]$$

If the reference machine is an infinite bus, then

$$-\frac{\partial V_{pe}\left(\tilde{\underline{\delta}}\right)}{\partial \tilde{\delta}_i} = P_i - P_{ei}\left(\tilde{\underline{\delta}}\right) \tag{5.20}$$

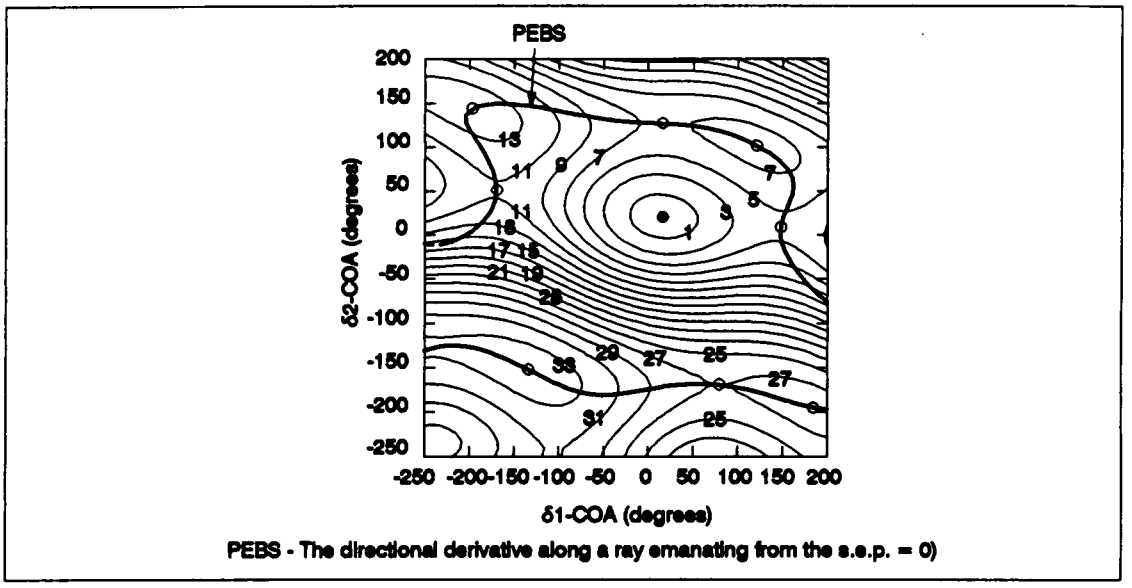

Figure 5-6: PEBS as defined in reference [1]

The state equation is

$$\begin{aligned} \frac{d\tilde{\delta}_i}{dt} &= \tilde{\omega}_i \\ \frac{d\tilde{\omega}_i}{dt} &= \frac{1}{M_i}\left[P_i - P_{ei}\left(\tilde{\underline{\delta}}\right)\right] - \frac{1}{M_t}P_{coa}\left(\tilde{\underline{\delta}}\right) - \frac{D_i}{M_i}\tilde{\omega}_i \end{aligned}$$

If the reference machine is an infinite bus, then

$$\begin{aligned} \frac{d\tilde{\delta}_i}{dt} &= \tilde{\omega}_i \\ \frac{d\tilde{\omega}_i}{dt} &= \frac{1}{M_i}\left[P_i - P_{ei}\left(\tilde{\underline{\delta}}\right)\right] - \frac{D_i}{M_i}\tilde{\omega}_i \end{aligned} \tag{5.21}$$

From Eq. 5.20, Eq. 5.21 can be written as

$$\begin{aligned} \frac{d\tilde{\delta}_i}{dt} &= \tilde{\omega}_i \\ \frac{d\tilde{\omega}_i}{dt} &= \frac{1}{M_i}\left[-\frac{\partial V_{pe}(\tilde{\underline{\delta}})}{\partial \tilde{\delta}_i}\right] - \frac{D_i}{M_i}\tilde{\omega}_i \end{aligned} \tag{5.22}$$

Comment 1 It is possible to write the state equation as in Eq. 5.22 only when the reference machine is an infinite bus.

Comment 2 The PEBS is the stability boundary of the gradient system.

$$\frac{d\tilde{\delta}_i}{dt} = (P_i - P_{ei}) - \frac{M_i}{M_n}(P_n - P_{en})$$

$$i = 1, 2, \cdots, n-1$$

It is not the stability boundary of the reduced system

$$\frac{d\tilde{\delta}_i}{dt} = P_i - P_{ei} - \frac{M_i}{M_t} P_{COA}$$

$$i = 1, 2, \cdots, n-1$$

5.2.4 Three-machine system example

Let us consider the three-machine system of Fig. 5-3. As mentioned before due to the absence of loads, the ray approximation of the potential energy is not required. Fig. 5-7 shows the contour map of the potential energy, the region of attraction of the reduced system as given by Eq. 5.2 and the region of attraction of the gradient system as given by Eq. 5.9. It can be seen from this figure that the region of attraction of the gradient system is orthogonal to the equipotential curves, whereas the region of attraction of the reduced system is not.

Concluding, in this example we have seen that the region of attraction of the gradient system is orthogonal to the equipotential lines. The PEBS intersects the level surface $\{\delta : V_p(\delta) = c\}$ orthogonally [17].

5.3 The Potential Energy Boundary Surface method

This method may be summarized by the following steps.

1. Integrate the fault-on trajectory. The parameters used in this step-by-step integration are the fault-on parameters.

2. Project the fault-on trajectory onto the angle subspace, i.e. drop $\tilde{\omega}$.

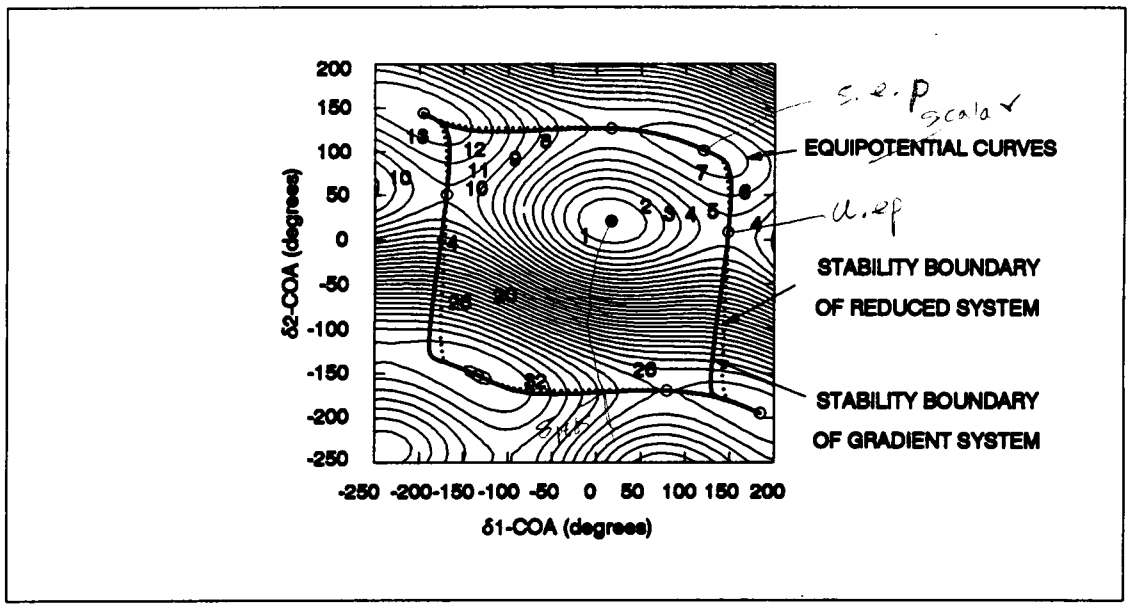

Figure 5-7: PEBS - Region of attraction of gradient system

3. *Determine when this projection crosses the PEBS*, let us designate this point on the angle subspace $\tilde{\underline{\delta}}_{PEBS}$. The potential energy at this point is the critical energy.

$$V_{cr} = V_{pe}\left(\tilde{\underline{\delta}}_{PEBS}\right)$$

It is worthwhile to emphasize that the transient energy is calculated using the post-fault parameters.

4. Use the surface $\left\{\left(\tilde{\underline{\delta}}, \tilde{\underline{\omega}}\right) : V\left(\tilde{\underline{\delta}}, \tilde{\underline{\omega}}\right) = V_{cr}\right\}$ as a local approximation of $\partial A\left(\tilde{\underline{\delta}}_s, \underline{0}\right)$. In other words, determine when the total energy on fault-on trajectory equals V_{cr}. This is the critical clearing time.

The question now is: How to determine the intersection of the projection of the fault-on trajectory with the PEBS.

There are two approaches, one proposed by Kakimoto et. al [44], and one proposed by Athay et. al [1].

Let us present the method of Kakimoto first. Fig. 5-8 corresponds to a three-machine system with no loads. The thick arrows represent the projection of fault-on trajectories onto the angle sub-space. It has been assumed that these projections intersect orthogonally with the PEBS. From this figure it is clear that at the intersection, $V_{pe}\left(\tilde{\underline{\delta}}\right)$ is a maximum. Therefore, to determine the intersection of the projection of the fault-on trajectory with the PEBS, Kakimoto et. al proposed to monitor the rate of change of potential energy, and the intersection occurs when the sign of $\frac{d}{dt}V_{pe}\left(\tilde{\underline{\delta}}\right)$ changes from positive to maximum. The intersection occurs when $V_{pe}\left(\tilde{\underline{\delta}}\right)$ reaches a maximum [17].

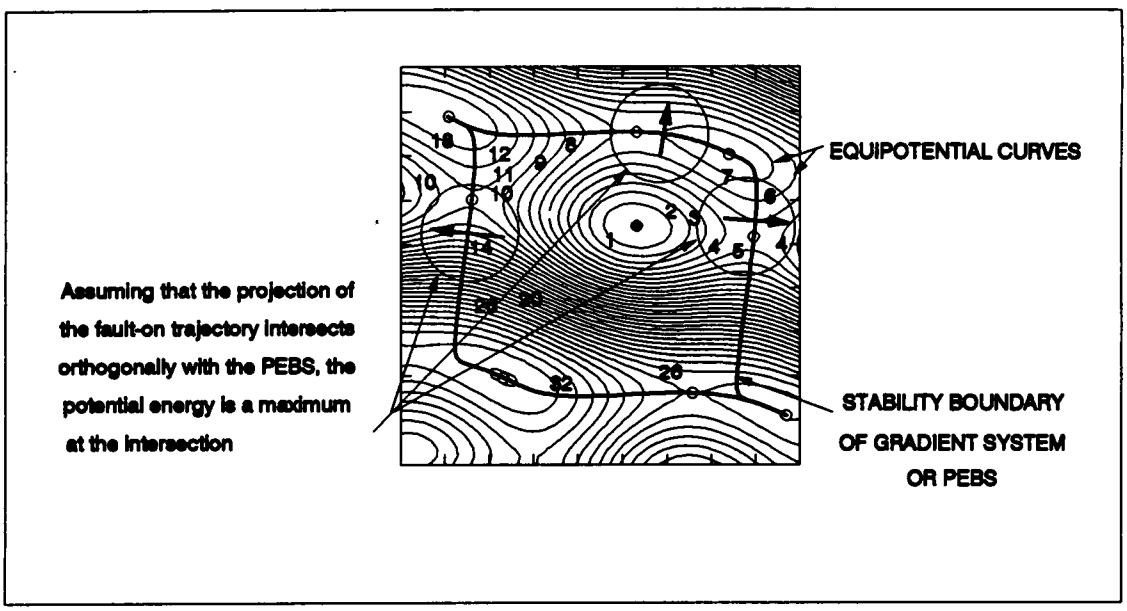

Figure 5-8: Assuming that the projection of the fault-on trajectory intersects orthogonally with the PEBS, Vpe at the intersection is a maximum

The method proposed by Athay et. al [1] is based on their definition of the PEBS.

$$\sum_{i=1}^{n}\left[P_i - P_{ei}\left(\tilde{\underline{\delta}}\right) - \frac{M_i}{M_t}P_{COA}\left(\tilde{\underline{\delta}}\right)\right]\cdot\left(\tilde{\delta}_i - \tilde{\delta}_i^s\right) = 0$$

The idea is to monitor this quantity along the fault-on trajectory. The intersection with the PEBS occurs when the sign of this quantity changes from negative to positive. It must be kept in mind that the fault on trajectory uses the fault-on parameters, whereas the parameters in

the equation defining the PEBS are post-fault parameters.

Fig. 5-9 shows the PEBS as defined by Varaiya et. al (stability boundary of the gradient system) and the PEBS as defined by Athay et. al (curve obtained by setting the directional derivative along a ray emanating from the s.e.p. equal to zero). Notice that they match in the following situations:

(a) When the PEBS - stability boundary of the reduced system is orthogonal to the ray emanating from the s.e.p. as indicated by the dotted lines

(b) At the e.p.'s

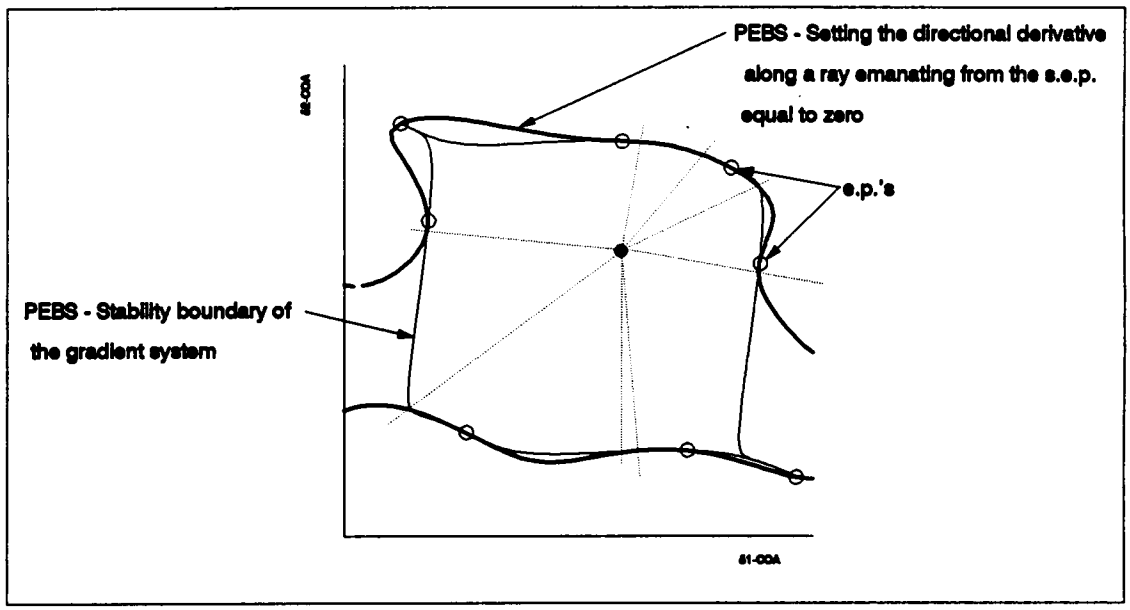

Figure 5-9: Comparing PEBS

The region of attraction of the gradient system is orthogonal to the equipotential lines. This corresponds to the original definition by Kakimoto et. al in [46], "O_1, O_2 and O_3 are the curves which are orthogonal to the equipotential curves and go through the points u_1, u_2 and u_3 respectively". The points u_1, u_2 and u_3 are e. p.'s of the gradient system. The curves O_1, O_2 and O_3 are the PEBS. We can see From Fig. 5-9 that the PEBS defined by Athay et. al differs considerably from the stability boundary of the gradient system. Therefore, from now on we will refer to the stability boundary of the gradient system as PEBS.

There are two methods for assessing when the projection of the fault-on trajectory onto the angle subspace exits the PEBS, these are the following:

(a) The potential energy, V_{pe} reaches a maximum along the fault-on trajectory.

(b) The directional derivative of V_{pe} along a ray emanating from the s.e.p. is zero, i.e.

$$\sum_{i=1}^{n}\left[P_i - P_{ei}\left(\tilde{\underline{\delta}}\right) - \frac{M_i}{M_t}P_{COA}\left(\tilde{\underline{\delta}}\right)\right]\cdot\left(\tilde{\delta}_i - \tilde{\delta}_i^s\right) = 0$$

In the first method, it is assumed that the projection of the fault-on trajectory crosses the PEBS orthogonally. If this is not the case, the assessment is in error. The second method is equivalent to assume that the projection of the fault-on trajectory onto the angular subspace is a ray emanating from the s.e.p., and if the projection of the fault-on trajectory onto the angle subspace exits the PEBS near an u.e.p. it yields a good assessment even if the crossing is not orthogonal. None of these methods is error free; however they are our only choices.

5.3.1 Conditions for the PEBS method to yield a conservative result

This subsection has been adapted from [17]. The PEBS may yield an *optimistic* result, i.e. a *critical clearing time which exceeds the true critical clearing time.* It is desirable to obtain a *conservative* result, i.e. a *critical clearing time which is less than the true critical clearing time.* Two conditions must be satisfied for the PEBS to yield a conservative result. Before describing these two conditions, let us make the following designations:

1. $\tilde{\underline{\delta}}_{PEBS}$ denotes the intersection of the projection of the fault-on trajectory onto the angular subspace with the PEBS, or gradient system exit point.

2. $\tilde{\underline{\delta}}_{uep}$ denotes the u.e.p. whose stable manifold contains the gradient system exit point, $\tilde{\underline{\delta}}_{PEBS}$.

3. $\left(\tilde{\underline{\delta}}_e, \tilde{\underline{\omega}}_e\right)$ denotes the exit point, i.e. the intersection of the fault-on trajectory with the stability boundary of the post-fault system.

4. $W^s\left(\tilde{\underline{\delta}}_{co}, \underline{0}\right)$ denotes the stable manifold containing $\left(\tilde{\underline{\delta}}_e, \tilde{\underline{\omega}}_e\right)$.

5. $\left(\tilde{\underline{\delta}}_{co}, \underline{0}\right)$ is the controlling u.e.p.

6. $\partial V\left(\tilde{\underline{\delta}}_{PEBS}, \underline{0}\right)$ denotes the constant energy surface used to approximate the local stability boundary, i.e.

$$\partial V\left(\tilde{\underline{\delta}}^{PEBS}, 0\right) = \left\{\left(\tilde{\underline{\delta}}, \tilde{\underline{\omega}}\right) : V\left(\tilde{\underline{\delta}}, \tilde{\underline{\omega}}\right) = V_{pe}\left(\tilde{\underline{\delta}}^{PEBS}\right)\right\}$$

7. $\left(\tilde{\underline{\delta}}^{f}(t), \tilde{\underline{\omega}}^{f}(t)\right)$ denotes the fault-on trajectory.

The two conditions which must be satisfied for the PEBS method to yield a conservative result are the following:

(a) $\tilde{\underline{\delta}}_{PEBS}$ is on the stable manifold of $\tilde{\underline{\delta}}_{uep}$ implies $\left(\tilde{\underline{\delta}}_{e}, \tilde{\underline{\omega}}_{e}\right)$ is on $W^{s}\left(\tilde{\underline{\delta}}_{co}, \underline{0}\right)$.

(b) The fault-on trajectory $\left(\tilde{\underline{\delta}}^{f}(t), \tilde{\underline{\omega}}^{f}(t)\right)$ passes through the constant energy surface $\partial V\left(\tilde{\underline{\delta}}_{PEBS}, 0\right)$ before it passes through the stable manifold $W^{s}\left(\tilde{\underline{\delta}}_{co}, \underline{0}\right)$.

Condition 0a implies that the equilibrium point $\tilde{\underline{\delta}}_{uep}$ is on the PEBS if and only if the equilibrium point $\left(\tilde{\underline{\delta}}_{uep}, \underline{0}\right)$ is on the stability boundary of the original system ($\tilde{\delta}_{uep} = \tilde{\underline{\delta}}_{co}$, we will see that this is not always the case). Condition 0a requires the following:

i. The *one parameter transversality condition* is satisfied.

ii. The number of equilibrium points on the stability boundary is finite.

Condition 0b is difficult to check. If we can find the stable manifold $W^{s}\left(\tilde{\underline{\delta}}_{co}, \underline{0}\right)$ of the controlling u.e.p. $\left(\tilde{\underline{\delta}}_{co}, \underline{0}\right)$ and the exit point $\left(\tilde{\underline{\delta}}_{e}, \tilde{\underline{\omega}}_{e}\right)$, then we do not need the PEBS!

The limitation of the PEBS yielding optimistic results may be overcome if the stability boundary is locally approximated by the following surface:

$$\partial V\left(\tilde{\underline{\delta}}_{uep}, \underline{0}\right) = \left\{\left(\tilde{\underline{\delta}}, \tilde{\underline{\omega}}\right) : V\left(\tilde{\underline{\delta}}, \tilde{\underline{\omega}}\right) = V_{pe}\left(\tilde{\underline{\delta}}_{uep}\right)\right\}$$

This secures condition 0b. Notice that if $\tilde{\underline{\delta}}_{uep} = \tilde{\underline{\delta}}_{co}$, this method is the same as the controlling u.e.p. method. Theorem 6-4 in [17] asserts that the controlling u.e.p. method always yields conservative results. The main issue now is to determine the controlling u.e.p., this problem is solved by the Boundary of stability region based Controlling Unstable equilibrium point, BCU, method.

5.4 The BCU method

The Boundary of stability region based Controlling Unstable equilibrium point, BCU, method is a very ingenious combination of the PEBS method and the controlling u.e.p. method. It has received many names:

1. Modified PEBS method [17], [55].
2. Algorithm to find the controlling u.e.p. method [11].
3. Hybrid method using the gradient system [55].
4. Exit point method [25].
5. Modified exit point [25].
6. BCU method [10], [9], [77].

For convenience in reading the following paragraphs, some equations obtained in previous sections are shown now.

- The state equation of the original system in COA is given by Eq. 5.23.

$$\begin{aligned} \frac{d\tilde{\delta}_i}{dt} &= \tilde{\omega}_i \\ \frac{d\tilde{\omega}_i}{dt} &= \frac{P_i - P_{ei}(\tilde{\underline{\delta}})}{M_i} - \frac{P_{COA}(\tilde{\underline{\delta}})}{M_t} - \lambda_D \tilde{\omega}_i \\ & i = 1, 2, \ldots n-1. \end{aligned} \tag{5.23}$$

- The state equation of the gradient system is given by Eq. 5.24.

$$\begin{aligned} \frac{d\tilde{\delta}_i}{dt} &= P_i - P_{ei}\left(\tilde{\underline{\delta}}\right) - \frac{M_i}{M_n}\left[P_n - P_{en}\left(\tilde{\underline{\delta}}\right)\right] \\ & i = 1, 2, \cdots, n-1 \end{aligned} \tag{5.24}$$

- The state equation of the reduced system is given by Eq. 5.25

$$\begin{aligned} \frac{d\tilde{\delta}_i}{dt} &= P_i - P_{ei}\left(\tilde{\underline{\delta}}\right) - \frac{M_i}{M_t} P_{COA}\left(\tilde{\underline{\delta}}\right) \\ & i = 1, 2, \ldots, n-1. \end{aligned} \tag{5.25}$$

The rest of this section has been adapted from [10], [9], [11] and [77]. The BCU method presented here differs from the one in the above references because the formulation of the state equations does not include an infinite bus. The state equation of the original system cannot include the gradient system. We have shown that the PEBS is the stability boundary of the gradient system, Eq. 5.24. The PEBS is not the stability boundary of the reduced system, Eq. 5.25. It has also been shown that in the presence of an infinite bus these two lower dimensional systems are the same. The previous references refer to reduced system which corresponds to the gradient system used here.

Let us present the following results which are the foundation of the BCU method:

(R1) $\left(\tilde{\underline{\delta}}_s\right)$ is a s.e.p. of the gradient system if and only if $\left(\tilde{\underline{\delta}}_s, \underline{0}\right)$ is a s.e.p. of the original system.

(R2) $\left(\tilde{\underline{\delta}}_k\right)$ is a type-k e.p. of the gradient system if and only if $\left(\tilde{\underline{\delta}}_k, \underline{0}\right)$ is a type-k equilibrium of the original system.

(R3) If the one-parameter transversality condition is satisfied, then $\left(\tilde{\underline{\delta}}_{uep}\right)$ is on the stability boundary $\partial A\left(\tilde{\underline{\delta}}_s\right)$ of the gradient system if and only if $\left(\tilde{\underline{\delta}}_{uep}, \underline{0}\right)$ is on the stability boundary $\partial A\left(\tilde{\underline{\delta}}_s, \underline{0}\right)$ of the original system.

As result (R1) asserts, it has been shown that there is a one-to-one correspondence between the e.p.'s of the original system and the e.p.'s of the gradient system, i.e.

$$\left(\tilde{\underline{\delta}}_{ep}\right) \longleftrightarrow \left(\tilde{\underline{\delta}}_{ep}, \underline{0}\right)$$

Result (R2) follows from Theorem 5-1 in [17], which asserts that the Jacobian matrix of both systems has no eigenvalues with zero real part. It also asserts that the number of Jacobian matrix eigenvalues with positive real part is the same for both systems.

Result (R3) establishes that when the *one-parameter transversality condition* is satisfied, a u.e.p. is on the PEBS if and only the corresponding original system u.e.p. is also on the original system stability boundary. In a later section, we will show examples of simple power systems where this may be true or not depending on the damping.

The BCU method is the following:

1. From the fault-on trajectory $\left(\tilde{\underline{\delta}}^f(t), \tilde{\underline{\omega}}^f(t)\right)$, detect the point $\tilde{\underline{\delta}}_{PEBS}$ at which the projected trajectory $\tilde{\underline{\delta}}^f(t)$ reaches the first local maximum of potential energy. Also compute the point $\tilde{\underline{\delta}}^-_{PEBS}$ that is one step behind of $\tilde{\underline{\delta}}_{PEBS}$ along $\tilde{\underline{\delta}}^f(t)$, and the point $\tilde{\underline{\delta}}^+_{PEBS}$ that is one step after $\tilde{\underline{\delta}}_{PEBS}$.

2. Use $\tilde{\underline{\delta}}_{PEBS}$ as initial condition and integrate the post-fault gradient system to find the first local minimum, at $\tilde{\underline{\delta}}_0$, of

$$\sqrt{\sum_{i=1}^{n-1}\left\{P_i - P_{ei}\left(\tilde{\underline{\delta}}\right) - \frac{M_i}{M_n}\left[P_n - P_{en}\left(\tilde{\underline{\delta}}\right)\right]\right\}^2} \tag{5.26}$$

3. Repeat the previous step with $\tilde{\underline{\delta}}^-_{PEBS}$ and $\tilde{\underline{\delta}}^+_{PEBS}$ as initial condition to find $\tilde{\underline{\delta}}^-_0$ and $\tilde{\underline{\delta}}^+_0$ respectively.

4. Compare the values of the Euclidean norm, Eq. 5.26, at $\tilde{\underline{\delta}}^-_0$, $\tilde{\underline{\delta}}_0$ and $\tilde{\underline{\delta}}^+_0$. The one with the smallest value is used to find the e.p. of the gradient system, i.e. the one with the smallest value is used to solve the following equation:

$$0 = P_i - P_{ei}\left(\tilde{\underline{\delta}}\right) - \frac{M_i}{M_n}\left[P_n - P_{en}\left(\tilde{\underline{\delta}}\right)\right]$$
$$i = 1, 2, \cdots, n-1$$

   Let us call this point $\tilde{\underline{\delta}}_{co-grad}$. This is the controlling u.e.p. of the gradient system.

5. The controlling u.e.p. of the original system with respect to the fault-on trajectory is $\left(\tilde{\underline{\delta}}_{co-grad}, \underline{0}\right)$,i.e.

$$\left(\tilde{\underline{\delta}}_{co}, \underline{0}\right) = \left(\tilde{\underline{\delta}}_{co-grad}, \underline{0}\right) \tag{5.27}$$

- In step 1 an approximation of the PEBS crossing is found. This approximation is good if the projected fault-on trajectory is orthogonal to the PEBS and the time step is small. Because there is no control on the way the projected fault-on trajectory intersects with the PEBS and because the time step can not be reduced without limit, three points are considered as "candidates".

- In steps 2 and 3, three post-fault gradient system trajectories are found. Each trajectory has one of the above "candidates" as an initial condition. Of these candidates, the one with a trajectory which gets closer to the controlling u.e.p. of the gradient system is PEBS crossing point. A measure of how close the post-fault trajectory of the gradient system is to its controlling u.e.p. is the Euclidean norm, Eq. 5.26. Notice that, exactly at the controlling u.e.p. (at any e.p. as a matter of fact), this norm is zero. Therefore, the candidate with the lowest value of the Euclidean norm along this trajectory is the PEBS crossing point. The point with the lowest norm (out of the three minimums found) is used as an initial guess in solving the set of non-linear equations of the gradient system.

$$0 = P_i - P_{ei}\left(\tilde{\underline{\delta}}\right) - \frac{M_i}{M_n}\left[P_n - P_{en}\left(\tilde{\underline{\delta}}\right)\right]$$
$$i = 1, 2, \cdots n-1.$$

  Notice that the reduced system can also be solved, since they have the same equilibrium points.

- In step 4 the controlling u.e.p. of the gradient system is found.

- In step 5 the controlling u.e.p. of the gradient system is related to the controlling u.e.p. of the original system. It has to be remembered that this is correct if *the one-parameter transversality condition holds.* Furthermore, if the one-parameter transversality does not hold, then $\left(\tilde{\underline{\delta}}_{co-grad}, \underline{0}\right)$ may not be the controlling u.e.p. of the original system. It may be only a u.e.p. not belonging to the stability boundary of the original system.

5.4.1 Three-machine system example

A three-machine system without loads (no transfer conductances) is considered now. However, the application of BCU method is not restricted to any number of generator buses nor to systems with negligible transfer conductances. The reason for using a three machine system is to be able to show its PEBS. The reason for using a system with zero transfer conductances is that, in this case, the potential energy is not path dependent, and we need no approximation for it. As shown in a previous example, if transfer conductances are negligible, the potential energy will show the equilibrium points accurately.

Let us consider the three-machine system of Fig. 5-3. As mentioned before due to the absence of loads, the ray approximation of the potential energy is not required. For convenience, this three-machine system is also shown in Fig. 5-10.

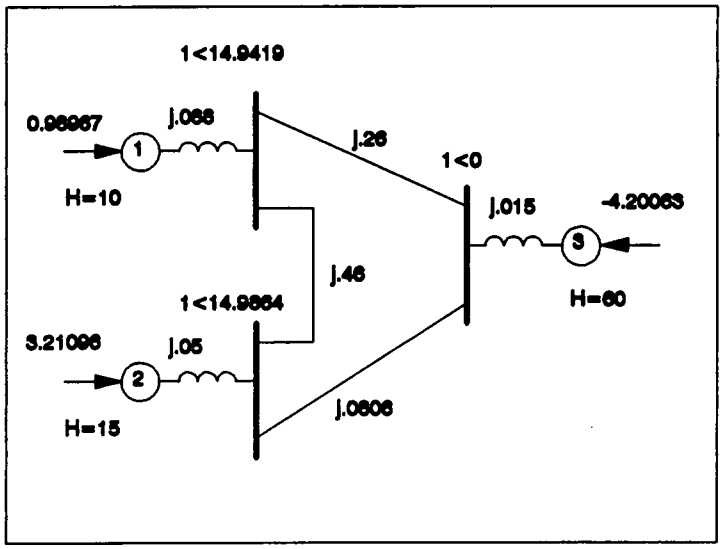

Figure 5-10: 3 - machine system with no loads

A uniform damping of $\lambda_d = 2.5 \frac{\text{MW s}}{\text{MVA rad}}$ is used. The disturbance is a self-clearing fault on bus 1, $\mathbf{Z}_f = (1 + j\,1) \times 10^{-5}$ pu.

- STEP 1.
  - The fault-on parameters are the following:

$$
\begin{aligned}
P_1^f &= 0.9887 \\
P_2^f &= 3.2100 \\
P_3^f &= -4.2002
\end{aligned}
$$

$$
\begin{aligned}
C_{12}^f &= 2.0037 \times 10^{-4} \\
C_{13}^f &= 4.5806 \times 10^{-4} \\
C_{23}^f &= 6.3661
\end{aligned}
$$

$$
\begin{aligned}
D_{12}^f &= 2.0030 \times 10^{-4} \\
D_{13}^f &= 4.5790 \times 10^{-4} \\
D_{23}^f &= 6.8940 \times 10^{-5}
\end{aligned}
$$

- These fault-on parameters are used in a step-by-step simulation where the state equation is the following:

$$
\frac{d}{dt}\begin{bmatrix} \tilde{\delta}_1 \\ \tilde{\delta}_2 \\ \tilde{\omega}_1 \\ \tilde{\omega}_2 \end{bmatrix} = \begin{bmatrix} \tilde{\omega}_1 \\ \tilde{\omega}_2 \\ \frac{P_1^f - P_{e1}^f}{M_1} - \frac{P_{coa}^f}{M_t} - \lambda_D \tilde{\omega}_1 \\ \frac{P_2^f - P_{e2}^f}{M_2} - \frac{P_{coa}^f}{M_t} - \lambda_D \tilde{\omega}_2 \end{bmatrix}
$$

- The potential energy is calculated along the fault-on trajectory. The post-fault parameters, which are used in calculating the potential energy, are the following:

$$
\begin{aligned}
P_1 &= 0.9900 \\
P_2 &= 3.2100 \\
P_3 &= -4.2000
\end{aligned}
$$

$$
\begin{aligned}
C_{12} &= 1.1804 \\
C_{13} &= 2.6985 \\
C_{23} &= 6.7723
\end{aligned}
$$

This power system has no constant impedance loads. Therefore,

$$
D_{12} = D_{13} = D_{23} = 0
$$

i.e. the transfer conductances are zero.

- The potential energy is monitored and three points are chosen as candidates for the

PEBS crossing point: $\tilde{\underline{\delta}}^{-}_{PEBS}$, $\tilde{\underline{\delta}}_{PEBS}$ and $\tilde{\underline{\delta}}^{+}_{PEBS}$.

$$
\begin{array}{lll}
t & \begin{bmatrix} \tilde{\delta}_1 \\ \tilde{\delta}_2 \end{bmatrix} & V_{pe}\left(\tilde{\delta}_1, \tilde{\delta}_2\right) \\
\text{(s)} & \text{(deg)} & \left(\frac{\text{MW s}}{\text{MVA rad}}\right) \\
0.6250 \quad \tilde{\underline{\delta}}^{-}_{PEBS} = & \begin{bmatrix} 147.676 \\ 4.85594 \end{bmatrix} & 4.68669 \\
0.6275 \quad \tilde{\underline{\delta}}_{PEBS} = & \begin{bmatrix} 148.521 \\ 4.72041 \end{bmatrix} & 4.68689 \\
0.6300 \quad \tilde{\underline{\delta}}^{+}_{PEBS} = & \begin{bmatrix} 149.367 \\ 4.58555 \end{bmatrix} & 4.68606
\end{array}
$$

Notice that $\Delta t = 0.0025$ s. Steps 1 to 4 are illustrated in Fig. 5-11

- STEPS 2 and 3.
  - The point $\tilde{\underline{\delta}}^{-}_{PEBS}$, $\tilde{\underline{\delta}}_{PEBS}$ and $\tilde{\underline{\delta}}^{+}_{PEBS}$ are three initial conditions for the gradient system. The step-by-step integrations ends when a local minimum of the Euclidean norm is found. The local minimum of the norm and the corresponding points are the following:

$$
\begin{array}{lll}
 & 0.08795 & \\
\tilde{\underline{\delta}}^{-}_{0} = & \begin{bmatrix} 147.42 \\ 8.7082 \end{bmatrix} & \\
 & 0.16824 & \\
\tilde{\underline{\delta}}_{0} = & \begin{bmatrix} 149.93 \\ 8.0809 \end{bmatrix} & \\
 & 0.29758 & \\
\tilde{\underline{\delta}}^{+}_{0} = & \begin{bmatrix} 151.15 \\ 7.3646 \end{bmatrix} &
\end{array}
$$

- STEP 4.
  - Since $\tilde{\underline{\delta}}^{-}_{0} = \begin{bmatrix} 147.42 \\ 8.7082 \end{bmatrix}$ has the lowest Euclidean norm, it is used as an initial guess to find the controlling u.e.p. of the gradient system.

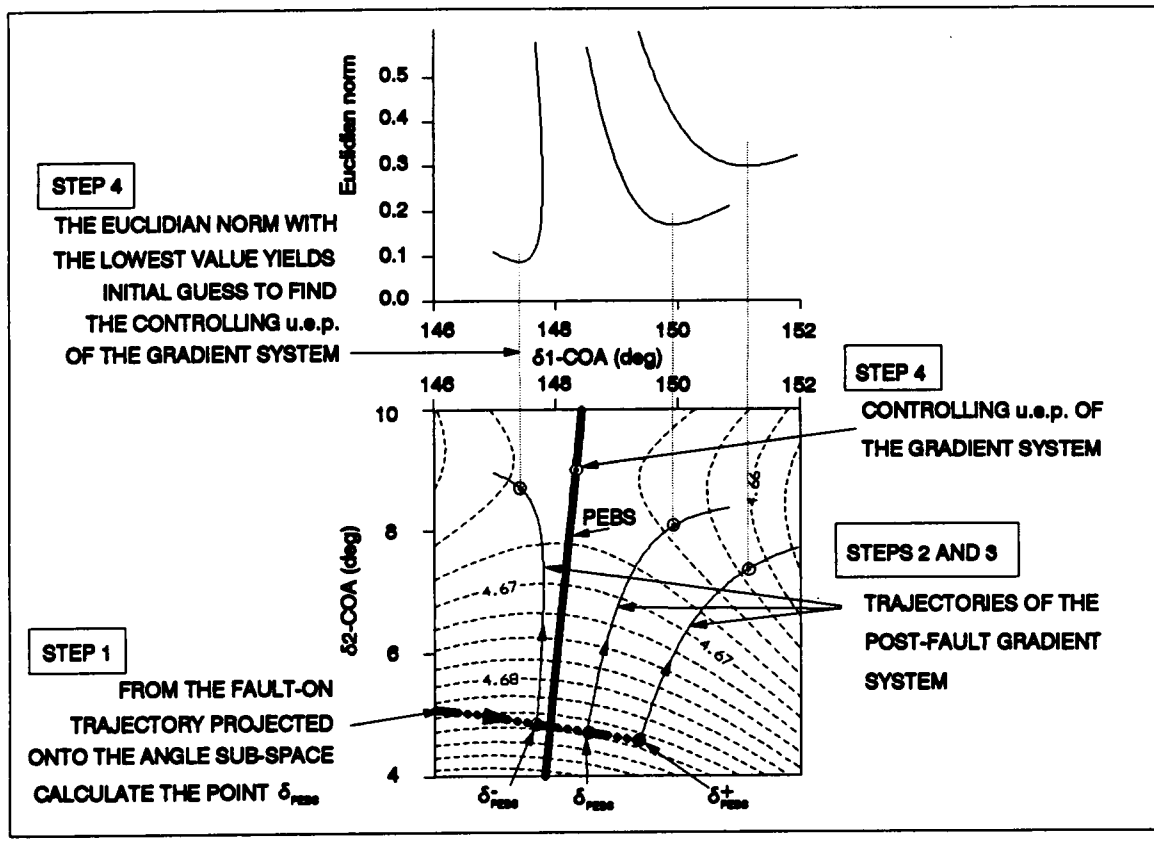

Figure 5-11: BCU method applied to a 3 - machine system with no loads

– The controlling u.e.p. of the gradient system is

$$\tilde{\delta}_{co-grad} = \begin{bmatrix} 148.33 \\ 9.0112 \end{bmatrix}$$

- STEP 5.

– Assuming that the one-parameter transversality condition is satisfied, the controlling

u.e.p. of the original system is

$$\left(\tilde{\delta}_{co-grad}, \underline{0}\right) = \begin{bmatrix} 148.33° \\ 9.0112° \\ 0\ \frac{\text{rad}}{\text{s}} \\ 0\ \frac{\text{rad}}{\text{s}} \end{bmatrix}$$

- Once the controlling u.e.p. has been found, the controlling u.e.p. method can be applied.
  - * The transient energy at the controlling u.e.p. is

$$V\left(\tilde{\delta}_{co-grad}, \underline{0}\right) = V_{pe}\left(\tilde{\delta}_{co-grad}\right) = 4.666\ \frac{\text{MW rad}}{\text{MVA}}$$

  - * The point along the fault-on trajectory when this value of transient energy is reached is some point between the following two points:

t (s)	$\tilde{\delta}_1 T$ (deg)	$\tilde{\delta}_2$ (deg)	$\tilde{\omega}_1$ (rad/s)	$\tilde{\omega}_2$ (rad/s)
0.5100	110.501	11.5975	5.3689	−1.05126
0.5125	111.271	11.4469	5.3819	−1.05242

    The corresponding energies are

t (s)	$V_k\ \frac{\text{MW rad}}{\text{MVA}}$	$V_p\ \frac{\text{MW rad}}{\text{MVA}}$	$V_d\ \frac{\text{MW rad}}{\text{MVA}}$	$V\ \frac{\text{MW rad}}{\text{MVA}}$
0.5100	0.87215	3.7812	0	4.6533
0.5125	0.87633	3.8145	0	4.6909

  - * The critical clearing time is 0.5100 s. This is not the true critical clearing time, but a conservative assessment of it.

5.5 BCU method and the one-parameter transversality condition

Of all the methods explained in the last two chapters, the best is the BCU method. It was explained in Chapter 3 that the controlling u.e.p. method has advantages over the closest u.e.p. and the exit-point method. However, the controlling u.e.p. method of Chapter 3 is a *conceptual* u.e.p. method, whereas the BCU method is a *practical* controlling u.e.p. method. There is at least a problem with it and in this section we will discuss it.

When Kakimoto et. al [46] proposed the PEBS, they addressed the so called first-swing stability problem. As we have seen, Chiang et. al [17] gave the foundations of the PEBS method and addressed the multi-swing stability problem. Later, they proposed the BCU method in which the controlling u.e.p. of the original system is determined by finding first the controlling u.e.p. of the gradient system. Then, assuming that the *one-parameter transversality condition* is satisfied, the controlling u.e.p. of the original system $\left(\tilde{\underline{\delta}}_{co}, \underline{0}\right)$ is related to the controlling u.e.p. of the gradient system $\left(\tilde{\underline{\delta}}_{co-grad}\right)$ (controlling u.e.p. on the PEBS) as follows.

$$\left(\tilde{\underline{\delta}}_{co}, \underline{0}\right) = \left(\tilde{\underline{\delta}}_{co-grad}, \underline{0}\right) \tag{5.28}$$

5.5.1 The one-parameter transversality condition

This subsection is adapted from [17]. Before establishing the one-parameter transversality condition, we will introduce some of the notations used in [17]. To simplify matters, we will also use an infinite bus in our formulation. Let us remember that this allows us to write the dynamical equation of the original system as Eq. 5.29.

$$\begin{gathered} \dot{\delta}_i = \omega_i \\ M_i\dot{\omega}_i = \left[-\frac{\partial V_{pe}(\underline{\delta})}{\partial \delta_i}\right] - D_i\omega_i \\ i = 1, 2, \cdots, n-1 \\ n \text{ is the infinite bus} \end{gathered} \tag{5.29}$$

- $d_p\left(\underline{M}, \underline{D}\right)$ denotes the dynamical equation Eq. 5.29. Matrix $\underline{M}$ is the inertia diagonal matrix, $M_i > 0$. Matrix $\underline{D}$ is the damping diagonal matrix, $D_i > 0$.

- $\partial A_p(\underline{M}, \underline{D})$ denotes the stability boundary of the s.e.p. of the system given by Eq. 5.29
- $d_p\left(\underline{D}^{-1}\right)$ denotes the following system (generalized gradient system):

$$\dot{\underline{\delta}} = -\underline{D}^{-1}\frac{\partial V_{pe}(\underline{\delta})}{\partial \underline{\delta}}$$

- $d_p(\underline{I})$ denotes the gradient system:

$$\dot{\underline{\delta}} = -\frac{\partial V_{pe}(\underline{\delta})}{\partial \underline{\delta}}$$

Now the *one-parameter transversality* condition can be established.

One-parameter transversality condition

- Let us consider the dynamical system $d_p(\underline{M}_\lambda, \underline{D})$, with $\underline{M}_\lambda = \lambda \underline{M} + (1-\lambda)\epsilon \underline{I}$, where ϵ is a small positive number, and $\lambda \in [0,1]$.
- Let us consider the dynamical system $d_p\left(\left[\underline{D}^{-1}\right]_\lambda\right)$, with $\left[\underline{D}^{-1}\right]_\lambda = \lambda \underline{D}^{-1} + (1-\lambda)\underline{I}$, and $\lambda \in [0,1]$.
- The *one-parameter transversality condition* is satisfied if the dynamical systems $d_p(\underline{M}_\lambda, \underline{D})$ and $d_p\left(\left[\underline{D}^{-1}\right]_\lambda\right)$ satisfy the following assumptions:
  - *(Transverse intersection)* The intersections of the stable and unstable manifolds of the equilibrium points on the stability boundary satisfy the transversality condition.
  - *(Finite number of points on the stability boundary)* The number of equilibrium points on the stability boundary is finite.

Theorem 6-3 in [17]

If the one-parameter transversality condition is satisfied then the following is true.

1. The equilibrium points $(\underline{\delta}_i)$ on the PEBS correspond to the equilibrium points $(\underline{\delta}_i, \underline{0})$ on the stability boundary of the original system Eq. 5.29, $\partial A_p(\underline{M}, \underline{D})$.
2. The stability boundary of the original system $\partial A_p(\underline{M}, \underline{D})$ is the union of the stable manifolds of the equilibrium points on the stability boundary $\partial A_p(\underline{M}, \underline{D})$.

5.5.2 One-parameter transversality condition on a OMIB system

To simplify matters, a one-machine infinite-bus power system is considered now. The dynamical equation of the *original system* from Eq. 5.29 is the following:

$$d_p(M,D): \left[\begin{array}{c} \dot{\delta} = \omega \\ M\dot{\omega} = [P_m - P_{\max}\sin\delta] - D_i\omega_i \end{array}\right] \tag{5.30}$$

The s.e.p. is $[\delta_s, 0]$, $\delta_s = \arcsin\frac{P_m}{P_{\max}}$ and its stability boundary is $\partial A_p(M,D)$.

The *generalized gradient system* $d_p\left(D^{-1}\right)$ is given by the following:

$$d_p\left(D^{-1}\right): \quad \dot{\underline{\delta}} = \frac{1}{D}[P_m - P_{\max}\sin\delta]$$

This system becomes the *gradient system* when $D^{-1} = 1$.

$$\dot{\delta} = [P_m - P_{\max}\sin\delta] \tag{5.31}$$

Let us consider the dynamical system $d_p(M_\lambda, D)$. If we choose $\epsilon = \frac{M}{10}$, then the inertia constant M_λ is given by the following:

$$M_\lambda = (0.9\lambda + 0.1)M$$

This result is a linear relation, $M_{\lambda=0} = 0.1M$, $M_{\lambda=1} = M$.

$$d_p(M_\lambda, D): \left[\begin{array}{c} \dot{\delta} = \omega \\ M_\lambda\dot{\omega} = [P_m - P_{\max}\sin\delta] - D_i\omega_i \end{array}\right]$$

The previous dynamical system, therefore, differs from the original system Eq. 5.30 only because it has an inertia M_λ, which changes from $0.1M$ to M. Notice that they are the same when $\lambda = 1$.

Let us consider the dynamical system $d_p\left(\left[D^{-1}\right]_\lambda\right)$. The parameter $\left[D^{-1}\right]_\lambda$ is given by the following:

$$\left[D^{-1}\right]_\lambda = \lambda\left(\frac{1}{D} - 1\right) + 1$$

This is a linear relation, $[D^{-1}]_{\lambda=0} = 1$, $[D^{-1}]_{\lambda=0} = \frac{1}{D}$.

$$d_p\left(\left[D^{-1}\right]_\lambda\right): \quad \dot{\underline{\delta}} = \left[D^{-1}\right]_\lambda [P_m - P_{\max} \sin \delta]$$

Therefore, the previous dynamical system differs from the gradient system Eq. 5.31 only because of $[D^{-1}]_\lambda$, which changes from 1 to $\frac{1}{D}$. Notice that they are the same when $\lambda = 0$.

The original system Eq. 5.30 satisfies the one-parameter transversality condition if its associated systems (one with a changing inertia the other with a changing inverse of damping) satisfy the transverse intersection and have a finite number of equilibrium points on the stability boundary.

Now we will present two cases of OMIB (one-machine infinite bus) systems. One system will have some damping, and the one-parameter transversality condition will fail. The second example has increased damping and satisfies the one-parameter transversality condition.

5.5.3 Normal Damping

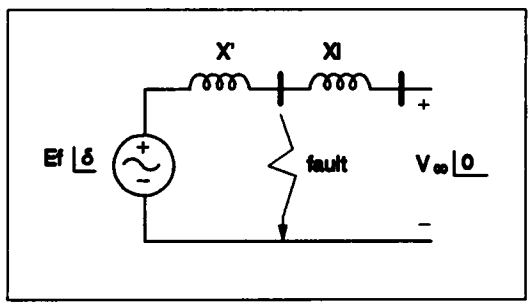

Figure 5-12: OMIB System

We will use the system shown in Fig. 5-12 as the example system in both cases. The damping is $D = 0.15 \frac{\text{MW s}}{\text{MVA rad}}$ in this case; the rest of the parameters are the following:

$E_f = 1.05$ pu

$V_\infty = 1.00$ pu

$X' = 0.10$ pu

$X_l = 0.25$ pu

$M = 0.05 \frac{\text{MW s}^2}{\text{MVA rad}}$

$P_m = 2.00 \frac{\text{MW}}{\text{MVA}}$

$P_{\max} = \frac{E_t V_\infty}{X'+X_t} = 3.0$

Since the value $\frac{D}{M} = 3$, we decided to call this case *Normal Damping.*

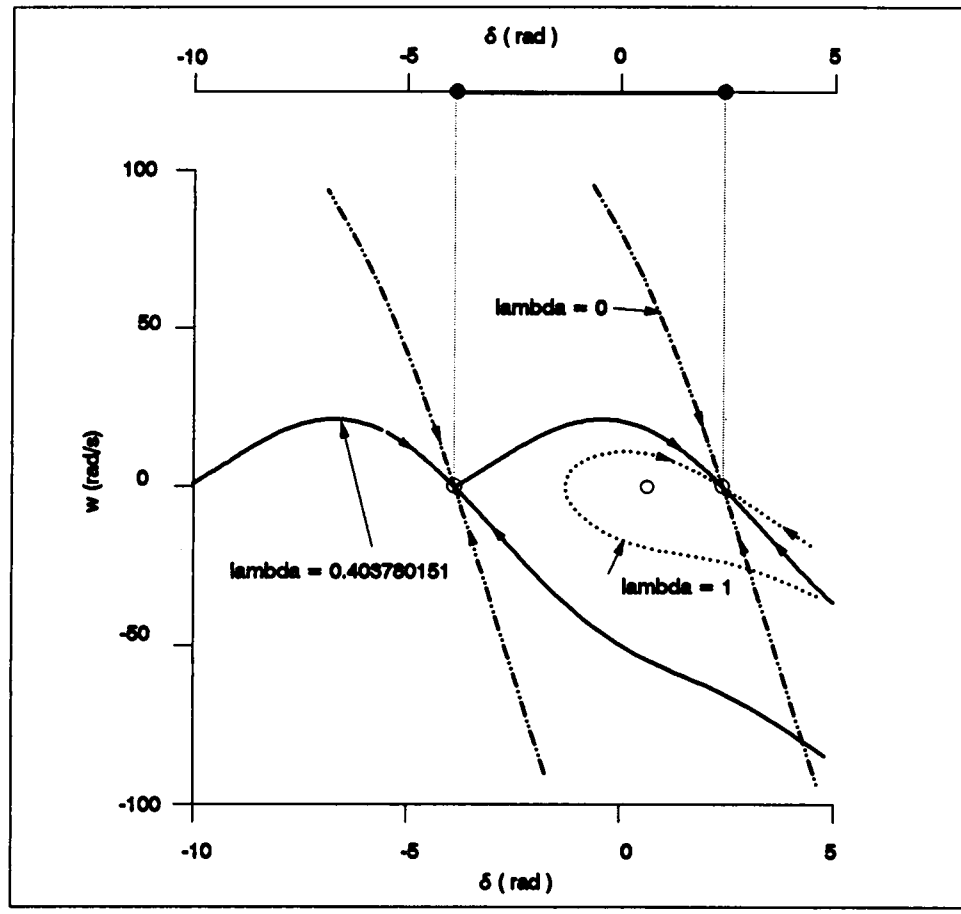

Figure 5-13: Region of attraction-Normal Damping

Let us consider the lower dimensional order system first. The dynamical system $d_p\left(\left[D^{-1}\right]_\lambda\right)$ is given by the following:

$$d_p\left(\left[D^{-1}\right]_\lambda\right): \quad \dot{\underline{\delta}} = \left[D^{-1}\right]_\lambda [2 - 3.0 \sin\delta]$$

$$\left[D^{-1}\right]_\lambda = \left\{ \begin{array}{c} 1 \text{ if } \lambda = 0 \\ \frac{1}{0.15} \text{ if } \lambda = 1 \end{array} \right\}$$

The s.e.p. for this dynamical system is

$$\delta_s = \arcsin\frac{2}{3.0} = 0.72973 \text{ rad} = 41.81°$$

The two u.e.p.'s surrounding it are

$$\delta_{u1} = \pi - \delta_s = 2.4119 \text{ rad}$$

$$\delta_{u2} = \delta_{u1} - 2\pi = -3.8713 \text{ rad}$$

The region of attraction of δ_s is the part of the $\delta - axis$ bounded by δ_{u2} and δ_{u1}. This is shown in Fig. 5-13. Notice that the stability boundary is $\delta_{u2} \cup \delta_{u1}$. And also notice that the stability boundary does not change with lambda. The following questions must be answered now:

(a) Does this lower dimensional satisfy the transverse intersection? The answer is yes.

(b) Does this lower dimensional system have a finite number of equilibrium points on the stability boundary? The answer is yes.

Let us consider the dynamical system $d_p(M_\lambda, D)$. If we choose $\epsilon = \frac{M}{10}$, then the inertia constant M_λ is given by the following:

$$M_\lambda = (0.9\lambda + 0.1)M = \left\{ \begin{array}{c} 0.05 \text{ if } \lambda = 1 \\ 0.005 \text{ if } \lambda = 0 \end{array} \right\}$$

The s.e.p. for this dynamical system is

$$\left[\begin{array}{c} \delta_s \\ \omega_s \end{array} \right] = \left[\begin{array}{c} 0.72973 \text{ rad} \\ 0 \text{ rad/s} \end{array} \right]$$

The two u.e.p.'s surrounding it are

$$\left[\begin{array}{c} \delta_{u1} \\ \omega_{u1} \end{array} \right] = \begin{array}{c} 2.4119 \text{ rad} \\ 0 \text{ rad/s} \end{array}$$

$$\begin{bmatrix} \delta_{u2} \\ \omega_{u2} \end{bmatrix} = \begin{bmatrix} -3.8713 \text{ rad} \\ 0 \text{ rad/s} \end{bmatrix}$$

The region of attraction of this system changes with lambda as shown in Fig. 5-13. Notice that the stability boundary changes with lambda and there is a value of lambda which yields a non-transverse intersection. The following questions must be answered now:

(a) Does this lower dimensional system have a finite number of equilibrium points on the stability boundary? The answer is yes.

(b) Does the dynamical system $d_p(M_\lambda, D)$ satisfy the transverse intersection? The answer is no. When $\lambda = 0.403780151$ there is a saddle connection. In this situation part of the unstable manifold of $(\delta_{u2}, 0)$ is also part of the stable manifold of $(\delta_{u1}, 0)$. The tangent space at this intersection is of dimension 1. Notice that for this non-transverse intersection the stability boundary $\partial A_p(M_\lambda, D) \in W^s(\delta_{u2}, 0) \cup W^s(\delta_{u1}, 0)$. When the transversality condition holds, i.e. for any other value of λ, $\partial A_p(M_\lambda, D) = W^s(\delta_{u2}, 0) \cup W^s(\delta_{u1}, 0.)$.

This case does not satisfy the one-parameter transversality condition.

5.5.4 High Damping

The damping in this example is changed to $D = 0.25 \frac{\text{MW s}}{\text{MVA rad}}$. Since the value $\frac{D}{M} = 5$, we decided to call this case *High Damping*. Fig. 5-14 shows that the region of attraction of the lower dimensional system $d_p([D^{-1}]_\lambda)$ is identical in both cases. It has two equilibrium points on the stability boundary. Furthermore, they constitute the stability boundary. As in the previous case, we answer yes the above questions.

Fig. 5-14 also shows the region of attraction of the full-dimensional system. It also shows that there is no value of λ between 0 and 1 for which a non-transverse intersection occurs.

This case satisfies the one-parameter transversality condition.

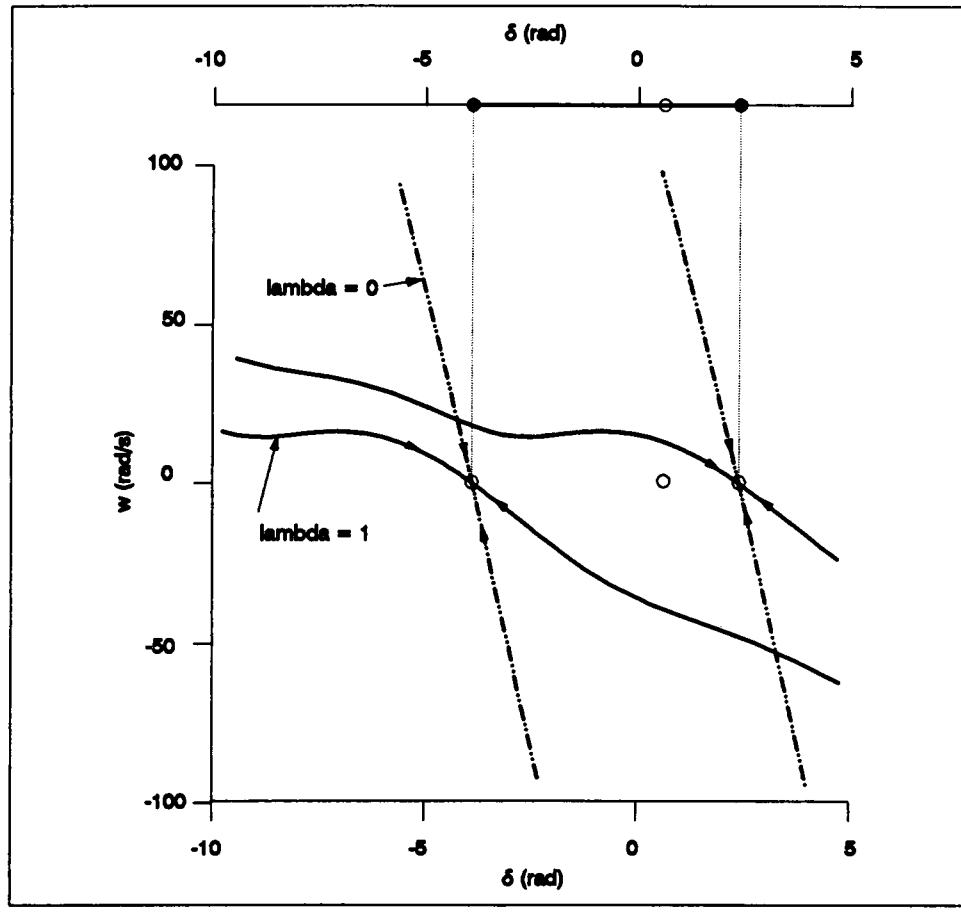

Figure 5-14: Region of attraction-Highl Damping

5.5.5 Effect of uniform damping on the one-parameter transversality condition

Two cases of OMIB systems are presented in this section. First, it is shown that a system with a typical uniform damping of three does not satisfy the one-parameter transversality condition and that the BCU method may fail under this condition. This is in contrast to the second case in which increased damping ensures the satisfaction of the one-parameter transversality condition, allowing the BCU method to work correctly.

Normal damping

As mentioned before, the ratio of $\frac{D}{M}$ is 3, and the one-parameter transversality condition is not satisfied. The fault impedance is $\mathbf{Z}_f = 0.075 + j0$ self clearing. The rest of the parameters

are as follows,

$E_f = 1.05$ pu

$V_\infty = 1.00$ pu

$X' = 0.10$ pu

$X_l = 0.25$ pu

$M = 0.05 \frac{\text{MW s}^2}{\text{MVA rad}}$

$P_m = 2.00 \frac{\text{MW}}{\text{MVA}}$

$P_{\max} = \frac{E_f V_\infty}{X'+X_l} = 3.0$

Fig. 5-15(a) shows the stability boundary for both the gradient system and the original system. These systems are one-dimensional and two-dimensional respectively. The region of stability of the original system is the shaded area. It can be seen that δ_{u2}, when projected from the gradient system onto the original system, does not even lie on the stability boundary of the full system. This figure also illustrates that, when a *decelerating* fault occurs, and the system is insufficiently damped, the critical energy contour, $V(\delta,\omega) = V_{cr}$, is a very inaccurate approximation of the stability boundary of the original system. In the next section, only the damping changes, the gradient system remains the same.

High damping

The ratio of $\frac{D}{M}$ is 5 in this case. The one-parameter transversality condition is therefore satisfied. Fig. 5-15(b) shows that the region of attraction of the gradient system is identical in both cases. When a fault, represented by the *decelerating* fault-on trajectory in the figure, occurs in the system, the contour representing the critical energy, $V(\delta,\omega) = V_{cr}$, is a good approximation of the stability boundary of the original system. With this approximation, the critical clearing time is accurate. It may also be seen here that $(\delta_{u2}, 0)$ lies on the stability boundary of the original system and (δ_{u2}) lies on the PEBS. This result occurs because the one-parameter transversality condition is met.

It is evident that the amount of system damping can have a major effect on the ability of the BCU method to correctly determine the controlling u.e.p.. The previous example shows that a power system may satisfy the one-parameter transversality condition at one value of damping (the high damping case), but may fail to do so at a lower value (the normal damping case).

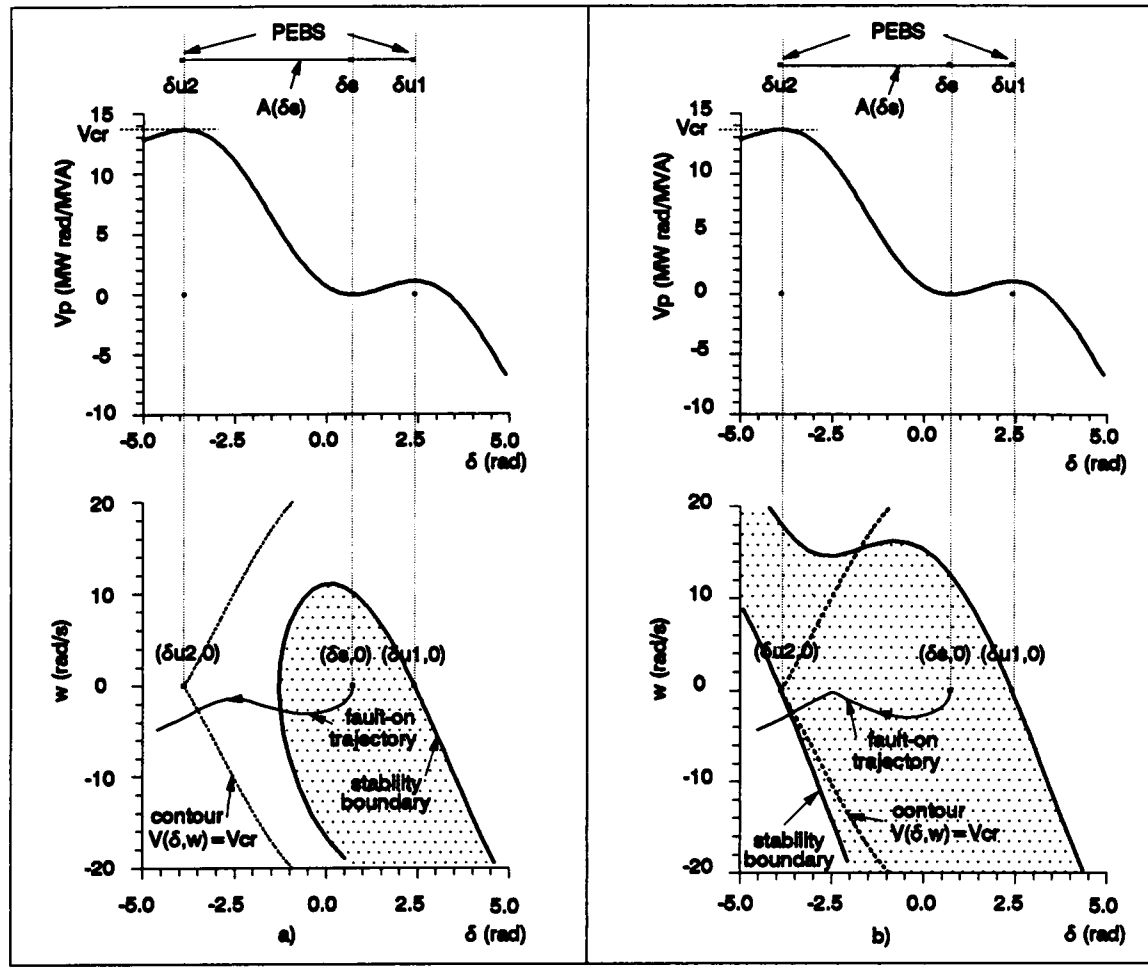

Figure 5-15: Stability regions of the original system and the gradient system with a) normal damping and b) high damping

5.5.6 Effect of system loading on the one-parameter transversality condition

Two cases of OMIB systems are presented in this section. First, it is shown that a system with a high loading does not satisfy the one-parameter transversality condition and that the BCU method may fail under this condition. This is in contrast to the second case in which decreased loading ensures the satisfaction of the one-parameter transversality condition, allowing the BCU method to work correctly. A uniform damping of three is considered in both cases, $\lambda_d = 3$. The rest of the parameters are as follows,

$E_f = 1.05$ pu

$V_\infty = 1.00$ pu

$X' = 0.10$ pu

$X_l = 0.25$ pu

$M = 0.05 \frac{\text{MW s}^2}{\text{MVA rad}}$

$P_m = 2.00 \frac{\text{MW}}{\text{MVA}}$

$P_{\max} = \frac{E_f V_\infty}{X'+X_l} = 3.0$

We may use the following norm as a measure of system loading :

$$\text{loading} = \frac{\|\underline{\delta}_s\|}{n-1}$$

High loading

The input mechanical power to machine one is two, $P_{m1} = 2.0$. Fig. 5-16 (a) shows the stability boundary and the potential energy function for this case. Also shown are the e.p.'s, these are the following:

$$(\delta_s, 0) = (0.72973 \text{ rad}, 0 \text{ rad/s})$$
$$(\delta_{u1}, 0) = (2.4119 \text{ rad}, 0 \text{ rad/s})$$
$$(\delta_{u2}, 0) = (-3.8713 \text{ rad}, 0 \text{ rad/s})$$

Notice that $V_{pe}(\delta_{u2}) = 14 \frac{\text{MW rad}}{\text{MVA}}$ and $V_{pe}(\delta_{u1}) = 1.5 \frac{\text{MW rad}}{\text{MVA}}$. The back-wall of potential energy is very tall and the front-wall is very shallow.

Light loading

The input mechanical power to machine one is $P_{m1} = 0.5$. Fig. 5-16 (b) shows the stability boundary and the potential energy function for this case. Also shown are the e.p.'s, these are the following:

$$(\delta_s, 0) = (0.16745 \text{ rad}, 0 \text{ rad/s})$$
$$(\delta_{u1}, 0) = (2.9741 \text{ rad}, 0 \text{ rad/s})$$
$$(\delta_{u2}, 0) = (-3.3090 \text{ rad}, 0 \text{ rad/s})$$

Notice that $V_{pe}(\delta_{u2}) = 7.5 \frac{\text{MW rad}}{\text{MVA}}$ and $V_{pe}(\delta_{u1}) = 4.0 \frac{\text{MW rad}}{\text{MVA}}$. The back-wall of potential energy is not as tall as the previous case and the front-wall is not so shallow.

It is evident that the degree of system loading can also have a major effect on the ability

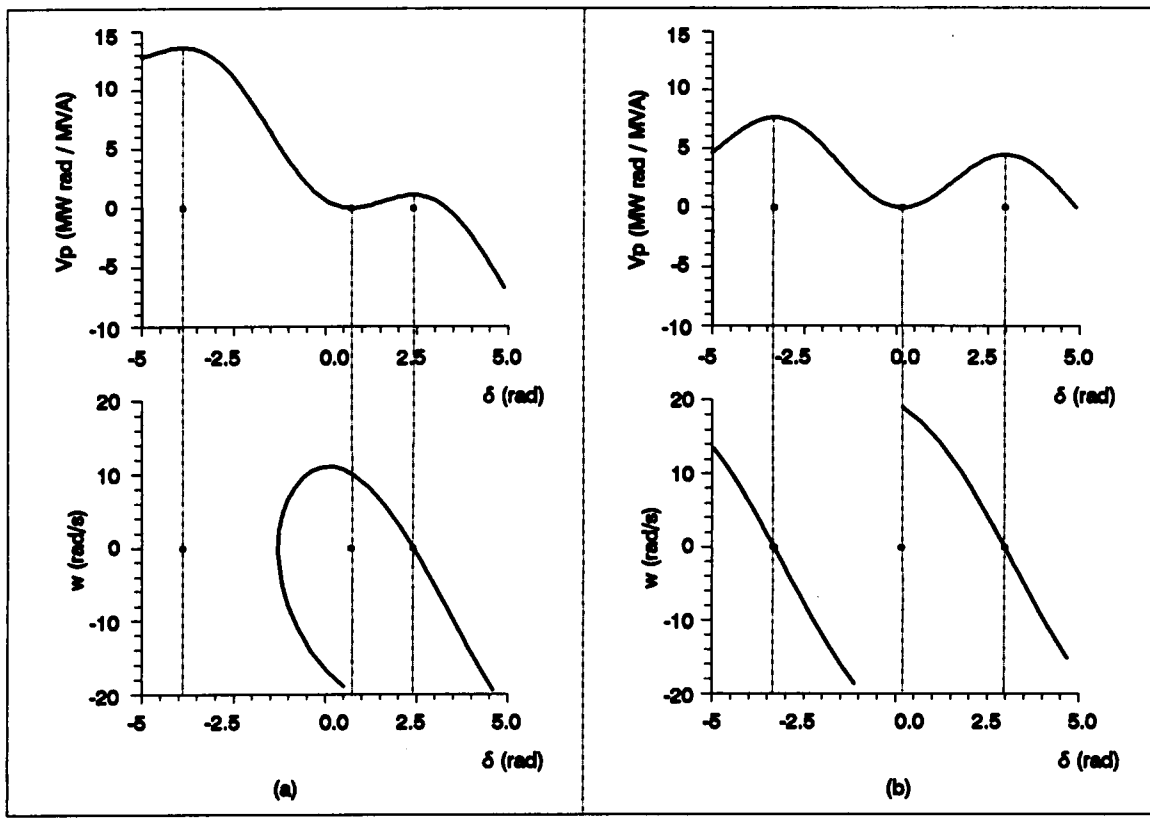

Figure 5-16: Effect of system loading on the one-parameter transversality condition. (a) high loading and (b) light loading

of the BCU method to correctly determine the controlling u.e.p.. The previous example shows that a power system may satisfy the one-parameter transversality condition at one loading condition (the light loading case), but may fail to do so at a higher value (the high loading case).

5.6 Verification of BCU u.e.p.(s)

A discrepancy results in the BCU method when insufficient damping or excessive loading is present in the system. The third result of [10] is stated as follows,

- If the one-parameter transversality condition is satisfied, then $\underline{\delta}$ is on the stability boundary $\partial A(\underline{\delta}_s)$, of the gradient system if and only if $(\underline{\delta},\underline{0})$ is on the stability boundary,

$\partial A(\underline{\delta}_s, \underline{0})$, of the original system.

This result always applies, regardless of damping. The difficulty in this result is finding when the one-parameter transversality condition is satisfied in a multi-machine system. In the previous two cases, the one with insufficient damping did not satisfy this condition.If the one-parameter transversality condition is not satisfied, the result obtained by the BCU method may not be correct for multi-swing stability. In order to find if the u.e.p. obtained lies on the stability boundary of the original system, the following method is proposed:

1. Define the normalized vector $\underline{z}$ as the following:

$$\underline{z} = \frac{\underline{\delta}_s - \underline{\delta}_{co-grad}}{\left\| \underline{\delta}_s - \underline{\delta}_{co-grad} \right\|}$$

2. Find the starting point as the following point:

$$(\underline{\delta}_{co-grad} + 0.01\underline{z}, \underline{0})$$

3. Integrate the state equation of the original system using the previous starting point.

   (a) If the trajectory tends toward $(\underline{\delta}_s, \underline{0})$ then the point $\left(\underline{\delta}_{co-grad}, \underline{0}\right)$ lies on the stability boundary of the original system. The stability boundary may be locally approximated by the following surface:

$$\partial V\left(\underline{\delta}_{co-grad}, \underline{0}\right) = \left\{ \left(\tilde{\delta}, \tilde{\omega}\right) : V\left(\tilde{\delta}, \tilde{\omega}\right) = V_{pe}\left(\underline{\delta}_{co-grad}\right) \right\}$$

   The critical clearing time may be approximated by the time at which the fault-on trajectory intersects with this surface. This results in a multi-swing assessment of stability.

   (b) If the trajectory tends towards infinity then the point $\left(\underline{\delta}_{co-grad}, \underline{0}\right)$ does not lie on the stability boundary of the original system. The intersection of the fault-on trajectory with the above surface will only yield an upper bound for the critical clearing time and conventional methods will be required to determine the critical clearing time.

The idea of using direct methods and conventional methods is not new, see page 1 of [1]. There is a method which combines direct and conventional methods, it is called as Hybrid method of power system transient stability [53].

5.6.1 Three-machine system example

The three-machine system of reference [1] shown in Fig. 5-17 is used to illustrate the suggested procedure. A small uniform damping $\lambda_d = 0.02$ is used.

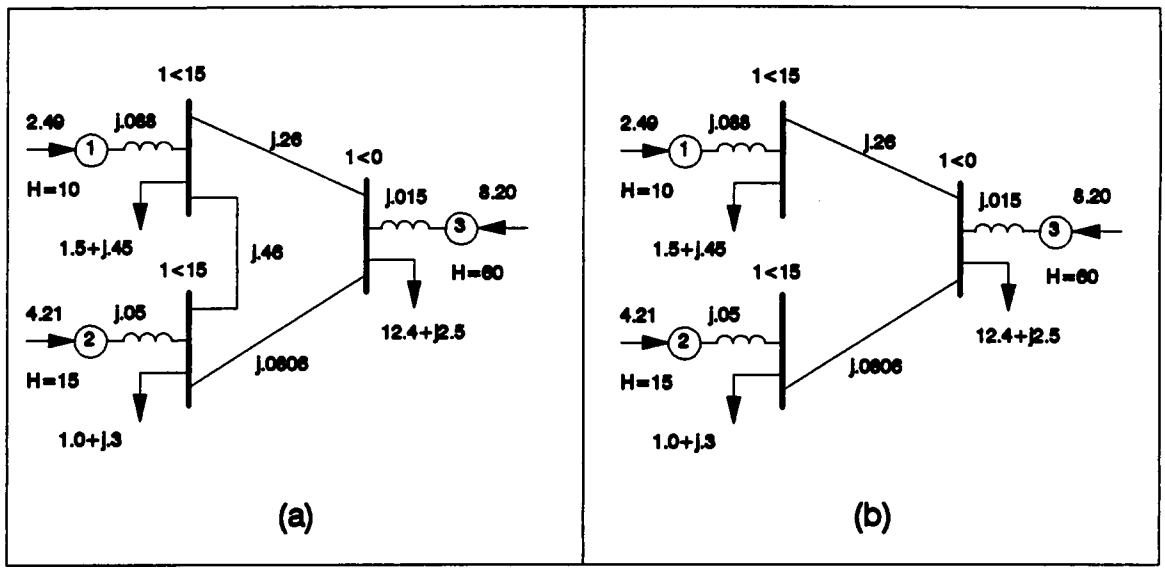

Figure 5-17: (a) 3 - machine system of reference [1], (b) Post-fault system with line 1-2 open

Four faults on line 1-2 are considered (2 faults near bus 1 and 2 faults near bus 2), *in all cases line 1-2 opens to isolate the fault.* Fault location, fault impedances, gradient system controlling u.e.p.s, corresponding energy level and critical clearing times as found by the BCU method are as follows,

1. Near bus 1, $Z_f = j5 \times 10^{-6}$, $\underline{\delta}_1 = (121.32°, -.89302°)$, $V_{pe}(\underline{\delta}_1) = 2.0062 \frac{\text{MW rad}}{\text{MVA}}$, c.c.t. = 0.17 s

2. Near bus 1, $Z_f = 0.06$, $\underline{\delta}_2 = (-196.32°, 41.460°)$, $V_{pe}(\underline{\delta}_2) = 10.729 \frac{\text{MW rad}}{\text{MVA}}$, c.c.t. = 0.325 s

3. Near bus 2, $Z_f = j5 \times 10^{-6}$, $\underline{\delta}_3 = (-13.512°, 119.612°)$, $V_{pe}(\underline{\delta}_3) = 5.8383\ \frac{\text{MW rad}}{\text{MVA}}$, c.c.t. = 0.1955 s

4. Near bus 2, $Z_f = 0.03$, $\underline{\delta}_4 = (50.017° - 176.86°)$, $V_{pe}(\underline{\delta}_4) = 25.713\ \frac{\text{MW rad}}{\text{MVA}}$, c.c.t. = 0.455 s

The PEBS, the u.e.p.'s on the PEBS, and the equipotential curves are shown in Fig. 5-18, $\underline{\delta}_1$ to $\underline{\delta}_4$ are type-one e.p.'s, $\underline{\delta}_5$ to $\underline{\delta}_8$ are type-two e.p.'s.

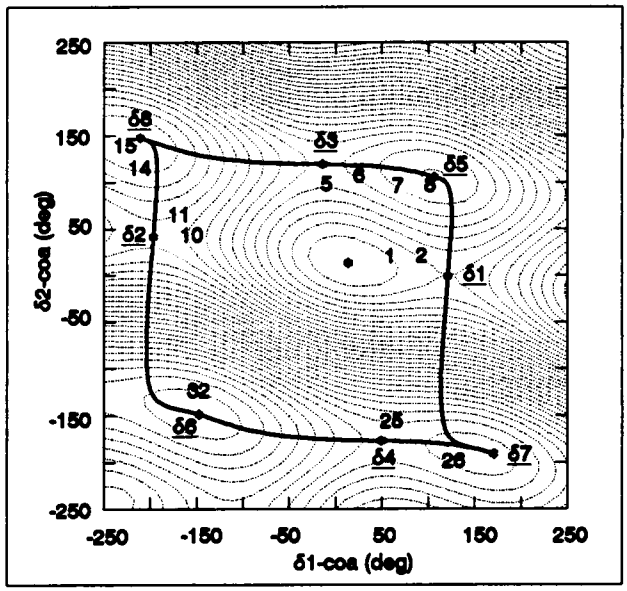

Figure 5-18: Contour map of potential energy using ray approximation and PEBS for three-machine system of reference [1] with line 1-2 open

The post-fault trajectories of the above procedure projected onto the angle subspace are shown in Fig. 5-19. We can see that $(\underline{\delta}_1, \underline{0})$ lies on the stability boundary of the original system, but the rest of the type-one e.p.'s - $(\underline{\delta}_2, \underline{0})$, $(\underline{\delta}_3, \underline{0})$ and $(\underline{\delta}_4, \underline{0})$ - do not. We can conclude that this power system does not satisfy the one-parameter transversality condition since there are three type-one e.p.'s on the PEBS, $\partial A(\underline{\delta}_s)$, for which their corresponding e.p.'s of the original

system do not belong to the stability boundary of the original system, $\partial A(\underline{\delta}_s, \underline{0})$.

$$
\begin{aligned}
(\underline{\delta}_1) \in \partial A(\underline{\delta}_s) \quad & (\underline{\delta}_1, \underline{0}) \in \partial A(\underline{\delta}_s, \underline{0}) \\
(\underline{\delta}_2) \in \partial A(\underline{\delta}_s) \quad & (\underline{\delta}_2, \underline{0}) \notin \partial A(\underline{\delta}_s, \underline{0}) \\
(\underline{\delta}_3) \in \partial A(\underline{\delta}_s) \quad & (\underline{\delta}_3, \underline{0}) \notin \partial A(\underline{\delta}_s, \underline{0}) \\
(\underline{\delta}_4) \in \partial A(\underline{\delta}_s) \quad & (\underline{\delta}_4, \underline{0}) \notin \partial A(\underline{\delta}_s, \underline{0})
\end{aligned}
$$

An interesting result is that when the one-parameter transversality condition is not satisfied, the number of e.p.'s on the PEBS is greater than the number of e.p.'s on the stability boundary of the original system. When it is satisfied the number of e.p.'s on the PEBS is the same as the number of e.p.'s on the stability boundary of the original system.

This particular example shows failure of the one-parameter transversality condition on both accelerating (fault 3) and decelerating faults (faults 2 and 4). This is not a common situation. It is easier to find cases which do not satisfy this condition for decelerating faults only.

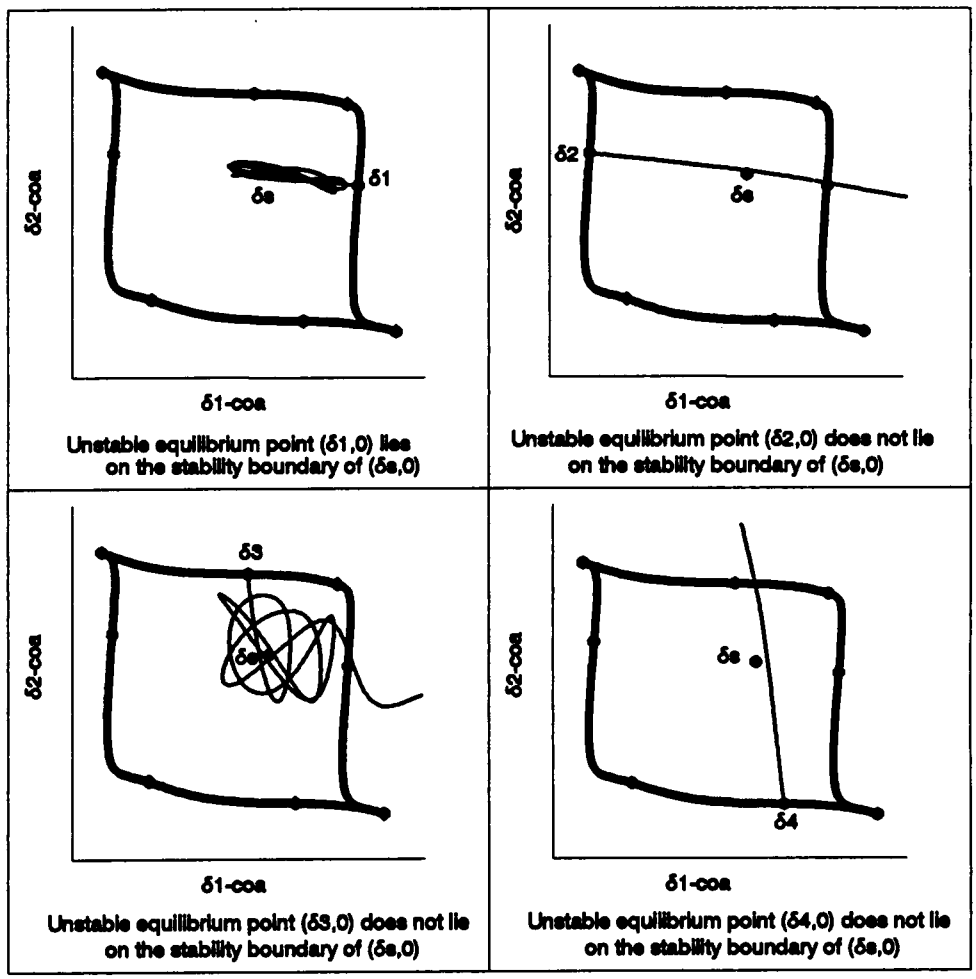

Figure 5-19: Post-fault trajectories projected onto the angle subspace

Chapter 6

Conclusions

Both system damping and loading can have major effects on the ability of the BCU method to correctly determine the controlling u.e.p.. A power system may satisfy the one-parameter transversality condition at one value of uniform damping or loading, but may fail to do so at a lower damping value or higher loading condition. Power systems not satisfying the assumption of one-parameter transversality condition are not uncommon, especially for power systems with high loading and/or low uniform damping.under decelerating faults. However, power systems exposing the failure of this assumption under accelerating faults are rare indeed.

When the one-parameter transversality condition is satisfied, the number of e.p.'s on the PEBS is the same as the number of e.p.'s on the stability boundary of the original system. When it is *not* satisfied the number of e.p.'s on the PEBS is greater than the number of e.p.'s on the stability boundary of the original system.

Failure to satisfy the one-parameter transversality condition may result in the PEBS and BCU methods giving incorrect results for multi-swing stability. A procedure to determine if the u.e.p. found by the BCU method lies on the stability boundary of the original system is given. This procedure is appropriate for off-line applications when there is sufficient time for a hybrid approach (combination of direct and conventional methods). Its use for on-line applications is limited due to the following: a) it is time consuming and b) if it finds that the u.e.p. does not belong to the stability boundary it provides no information concerning the stability/instability of the system, it only provides an upper bound for the critical clearing time.

The BCU and PEBS methods as presented here are appropriate methods for off-line appli-

cations. For on-line applications they must be combined with very fast conventional methods or they must be improved to avoid their failure when the one-parameter transversality condition is not met.

Appendix A

Finding the Transient Energy in the One Machine Reference Frame

In this formulation, machine n will be the reference [85].

1. The starting point is the swing equation of machine i (Eq. 3.4).

$$M_i \frac{d^2\delta_i}{dt^2} - P_i + P_{ei} = 0, i = 1, 2, \cdots, n$$

2. The set of $n(n-1)/2$ equations of relative acceleration must be obtained. We will begin with a 4-machine system and then generalize to an n-machine system.

$$\begin{aligned} M_1 \tfrac{d^2\delta_1}{dt^2} - P_1 + P_{e1} &= 0 \\ M_2 \tfrac{d^2\delta_2}{dt^2} - P_2 + P_{e2} &= 0 \\ M_3 \tfrac{d^2\delta_3}{dt^2} - P_3 + P_{e3} &= 0 \\ M_4 \tfrac{d^2\delta_4}{dt^2} - P_4 + P_{e4} &= 0 \end{aligned} \tag{A.1}$$

Multiply the first row of Eq. A.1 by M_2, the second row by M_1, and subtract the resulting equations.

$$+M_1 M_2 \frac{d^2\delta_1}{dt^2} - M_2 P_1 + M_2 P_{e1} = 0$$

$$\underline{-M_1 M_2 \frac{d^2\delta_2}{dt^2} + M_1 P_2 - M_1 P_{e2} = 0}$$

$$M_1 M_2 \frac{d^2\delta_{12}}{dt^2} - (M_2 P_1 - M_1 P_2) + (M_2 P_{e1} - M_1 P_{e2}) = 0$$

We just got the first of the $n(n-1)/2$ equations of relative acceleration. By repeating the above procedure using the corresponding Ms we will get:

$$\begin{aligned}
M_1\ M_2 \tfrac{d^2\delta_{12}}{dt^2} - (M_2\ P_1 - M_1\ P_2) + (M_2\ P_{e1} - M_1\ P_{e2}) &= 0 \\
M_1\ M_3 \tfrac{d^2\delta_{13}}{dt^2} - (M_3\ P_1 - M_1\ P_3) + (M_3\ P_{e1} - M_1\ P_{e3}) &= 0 \\
M_1\ M_4 \tfrac{d^2\delta_{14}}{dt^2} - (M_4\ P_1 - M_1\ P_4) + (M_4\ P_{e1} - M_1\ P_{e4}) &= 0 \\
M_2\ M_3 \tfrac{d^2\delta_{23}}{dt^2} - (M_3\ P_2 - M_2\ P_3) + (M_3\ P_{e2} - M_2\ P_{e3}) &= 0 \\
M_2\ M_4 \tfrac{d^2\delta_{24}}{dt^2} - (M_4\ P_2 - M_2\ P_4) + (M_4\ P_{e2} - M_2\ P_{e4}) &= 0 \\
M_3\ M_4 \tfrac{d^2\delta_{34}}{dt^2} - (M_4\ P_3 - M_3\ P_4) + (M_4\ P_{e3} - M_3\ P_{e4}) &= 0
\end{aligned}$$

We can see from the above equations that, in general,

$$M_i M_j \frac{d^2\delta_{ij}}{dt^2} - (M_j P_i - M_i P_j) + (M_j P_{ei} - M_i P_{ej}) = 0$$
$$\text{for } i = 1, \cdots, n-1;\ j = i+1, \cdots, n$$

3. We then multiply the above generalized equation of relative acceleration by the corresponding relative speed $\dot{\delta}_{ij}$.

$$M_i M_j \dot{\delta}_{ij} \frac{d\dot{\delta}_{ij}}{dt} - (M_j P_i - M_i P_j) \frac{d\delta_{ij}}{dt} + (M_j P_{ei} - M_i P_{ej}) \frac{d\delta_{ij}}{dt} = 0$$
$$\text{for } i = 1, \cdots, n-1;\ j = i+1, \cdots, n$$

4. We will add these $n(n-1)/2$ equations in the following manner:

$$\sum_{i=1}^{n-1} \sum_{j=i+1}^{n} \left[M_i M_j \dot{\delta}_{ij} \frac{d\dot{\delta}_{ij}}{dt} - (M_j P_i - M_i P_j) \frac{d\delta_{ij}}{dt} + (M_j P_{ei} - M_i P_{ej}) \frac{d\delta_{ij}}{dt} \right] = 0$$

This equation is $-M_t \frac{dV}{dt} = 0$, and, to get $V(\underline{\delta}, \underline{\omega})$, we must integrate the following equation:

$$V(\underline{\delta}, \underline{\omega}) = \int_t^{ts} \left(\frac{dV}{dt} \right) dt$$

or

$$V(\underline{\delta},\underline{\omega}) = \int_{t_s}^{t} -\left(\frac{dV}{dt}\right) dt$$

Since $-\frac{dV}{dt} = 0$, we know that $V(\underline{\delta},\underline{\omega}) = constant$.

At t_s the *s.e.p.* is reached, *i.e.* $\omega_i(t_s) = 0$, $\delta_i(t_s) = \delta_i^s$.

$$-M_t\frac{dV}{dt} = \sum_{i=1}^{n-1}\sum_{j=i+1}^{n}\left[M_iM_j\dot{\delta}_{ij}\frac{d\dot{\delta}_{ij}}{dt} - (M_jP_i - M_iP_j)\frac{d\delta_{ij}}{dt} + \underline{(M_jP_{ei} - M_iP_{ej})}\frac{d\delta_{ij}}{dt}\right] \tag{A.2}$$

5. Before integrating Eq. A.2, we must find a convenient expression for the underlined term, since P_{ei} and P_{ej} are functions of the relative angles δ_{ij}.

$$\sum_{i=1}^{n-1}\sum_{j=i+1}^{n}(M_jP_{ei} - M_iP_{ej}) =$$

$$\sum_{i=1}^{n-1}\sum_{j=i+1}^{n}\left[M_j\sum_{k=1}^{n}(C_{ik}\sin\delta_{ik} + D_{ik}\cos\delta_{ik}) - M_i\sum_{k=1}^{n}(C_{jk}\sin\delta_{jk} + D_{jk}\cos\delta_{jk})\right]$$

or

$$\sum_{i=1}^{n-1}\sum_{j=i+1}^{n}(M_jP_{ei} - M_iP_{ej}) =$$

$$\sum_{i=1}^{n-1}\sum_{j=i+1}^{n}\left[M_j\sum_{k=1,\neq i}^{n}(C_{ik}\sin\delta_{ik}) - M_i\sum_{k=1,\neq j}^{n}(C_{jk}\sin\delta_{jk})\right]$$

$$+\sum_{i=1}^{n-1}\sum_{j=i+1}^{n}\left[M_j\sum_{k=1,\neq i}^{n}(D_{ik}\cos\delta_{ik}) - M_i\sum_{k=1,\neq j}^{n}(D_{jk}\cos\delta_{jk})\right]$$

Notice that in the right hand side of the above equation, the first summation of i from 1 to $n-1$ corresponds to the transfer susceptances of the postfault reduced admittance matrix. The second corresponds to the transfer conductances.

- Corresponding to *transfer susceptances* for $n = 4$

$$+M_2\,(+C_{12}\sin\delta_{12} + C_{13}\sin\delta_{13} + C_{14}\sin\delta_{14})\,\dot{\delta}_{12}$$

$$-M_1\,(-C_{12}\sin\delta_{12} + C_{23}\sin\delta_{23} + C_{24}\sin\delta_{24})\,\dot{\delta}_{12}$$

$$+M_3\,(+C_{12}\sin\delta_{12}+C_{13}\sin\delta_{13}+C_{14}\sin\delta_{14})\,\dot{\delta}_{13}$$

$$-M_1\,(-C_{13}\sin\delta_{13}-C_{23}\sin\delta_{23}+C_{34}\sin\delta_{34})\,\dot{\delta}_{13}$$

$$+M_4\,(+C_{12}\sin\delta_{12}+C_{13}\sin\delta_{13}+C_{14}\sin\delta_{14})\,\dot{\delta}_{14}$$

$$-M_1\,(-C_{14}\sin\delta_{14}-C_{24}\sin\delta_{24}-C_{34}\sin\delta_{34})\,\dot{\delta}_{14}$$

$$+M_3\,(-C_{12}\sin\delta_{12}+C_{23}\sin\delta_{23}+C_{24}\sin\delta_{24})\,\dot{\delta}_{23}$$

$$-M_2\,(-C_{13}\sin\delta_{13}-C_{23}\sin\delta_{23}+C_{34}\sin\delta_{34})\,\dot{\delta}_{23}$$

$$+M_4\,(-C_{12}\sin\delta_{12}+C_{23}\sin\delta_{23}+C_{24}\sin\delta_{24})\,\dot{\delta}_{24}$$

$$-M_2\,(-C_{14}\sin\delta_{14}-C_{24}\sin\delta_{24}-C_{34}\sin\delta_{34})\,\dot{\delta}_{24}$$

$$+M_4\,(-C_{13}\sin\delta_{13}-C_{23}\sin\delta_{23}+C_{34}\sin\delta_{34})\,\dot{\delta}_{24}$$

$$-M_3\,(-C_{14}\sin\delta_{14}-C_{24}\sin\delta_{24}-C_{34}\sin\delta_{34})\,\dot{\delta}_{24}$$

The coefficient of $C_{12}\sin\delta_{12}$ is

$$\begin{aligned}
& \dot{\delta}_{12}(M_1+M_2)+\dot{\delta}_{13}M_3+\dot{\delta}_{14}M_4-\dot{\delta}_{23}M_3-\dot{\delta}_{24}M_4 \\
= \quad & \dot{\delta}_{12}(M_1+M_2)+M_3(\dot{\delta}_{13}+\dot{\delta}_{32})+M_4(\dot{\delta}_{14}+\dot{\delta}_{42}) \\
= \quad & \dot{\delta}_{12}(M_1+M_2+M_3+M_4) \\
= \quad & \dot{\delta}_{12}M_t
\end{aligned}$$

Similarly, the coefficients of $C_{13}\ \sin\delta_{13}$, $C_{14}\ \sin\delta_{14}$, $C_{23}\ \sin\delta_{23}$, $C_{24}\ \sin\delta_{24}$ and $C_{34}\ \sin\delta_{34}$ are $\dot{\delta}_{13}M_t$, $\dot{\delta}_{14}M_t$, $\dot{\delta}_{23}M_t$, $\dot{\delta}_{24}M_t$, $\dot{\delta}_{34}M_t$, respectively, resulting in the following equation:

$$\sum_{i=1}^{4-1}\sum_{j=i+1}^{4}\left[M_j\sum_{k=1,\neq i}^{4}(C_{ik}\sin\delta_{ik})-M_i\sum_{k=1,\neq j}^{4}(C_{jk}\sin\delta_{jk})\right]\dot{\delta}_{ij}=$$

$$M_t\sum_{i=1}^{4-1}\sum_{j=i+1}^{4}C_{ij}\sin\delta_{ij}\dot{\delta}_{ij}$$

The general form of this equation is Eq. A.3.

$$\sum_{i=1}^{n-1}\sum_{j=i+1}^{n}\left[M_j\sum_{k=1,\neq i}^{n}(C_{ik}\sin\delta_{ik})-M_i\sum_{k=1,\neq j}^{n}(C_{jk}\sin\delta_{jk})\right]\dot{\delta}_{ij}= M_t\sum_{i=1}^{n-1}\sum_{j=i+1}^{n}C_{ij}\sin\delta_{ij}\dot{\delta}_{ij} \tag{A.3}$$

– Corresponding to *transfer conductances* for $n = 4$

$$+M_2(D_{12}\cos\delta_{12}+D_{13}\cos\delta_{13}+D_{14}\cos\delta_{14})\dot{\delta}_{12}$$

$$-M_1(D_{12}\cos\delta_{12}+D_{23}\cos\delta_{23}+D_{24}\cos\delta_{24})\dot{\delta}_{12}$$

$$+M_3(D_{12}\cos\delta_{12}+D_{13}\cos\delta_{13}+D_{14}\cos\delta_{14})\dot{\delta}_{13}$$

$$-M_1(D_{13}\cos\delta_{13}+D_{23}\cos\delta_{23}+D_{34}\cos\delta_{34})\dot{\delta}_{13}$$

$$+M_4(D_{12}\cos\delta_{12}+D_{13}\cos\delta_{13}+D_{14}\cos\delta_{14})\dot{\delta}_{14}$$

$$-M_1(D_{14}\cos\delta_{14}+D_{24}\cos\delta_{24}+D_{34}\cos\delta_{34})\dot{\delta}_{14}$$

$$+M_3(D_{12}\cos\delta_{12}+D_{23}\cos\delta_{23}+D_{24}\cos\delta_{24})\dot{\delta}_{23}$$

$$-M_2(D_{13}\cos\delta_{13}+D_{23}\cos\delta_{23}+D_{34}\cos\delta_{34})\dot{\delta}_{23}$$

$$+M_4(D_{12}\cos\delta_{12}+D_{23}\cos\delta_{23}+D_{24}\cos\delta_{24})\dot{\delta}_{24}$$

$$-M_2(D_{14}\cos\delta_{14}+D_{24}\cos\delta_{24}+D_{34}\cos\delta_{34})\dot{\delta}_{24}$$

$$+M_4(D_{13}\cos\delta_{13}+D_{23}\cos\delta_{23}+D_{34}\cos\delta_{34})\dot{\delta}_{24}$$

$$-M_3(D_{14}\cos\delta_{14}+D_{24}\cos\delta_{24}+D_{34}\cos\delta_{34})\dot{\delta}_{24}$$

The coefficient of $D_{12}\ \cos\delta_{12}$ is

$$\begin{aligned}
&(M_2-M_1)\dot{\delta}_{12}+M_3\dot{\delta}_{13}+M_4\dot{\delta}_{14}+M_3\dot{\delta}_{23}+M_4\dot{\delta}_{24}\\
=\ &(-M_1+M_2+M_3+M_4)\dot{\delta}_1+(M_1-M_2+M_3+M_4)\dot{\delta}_2-2\,M_3\dot{\delta}_3-2\,M_4\dot{\delta}_4\\
=\ &M_t\dot{\delta}_1+M_t\dot{\delta}_2-2(M_1\dot{\delta}_1+M_2\dot{\delta}_2+M_3\dot{\delta}_3+M_4\dot{\delta}_4)\\
=\ &M_t(\dot{\delta}_1+\dot{\delta}_2-2\,\dot{\delta}_0)
\end{aligned}$$

Similarly, the coefficients of $D_{13}\cos\delta_{13}$, $D_{14}\cos\delta_{14}$, $D_{23}\cos\delta_{23}$, $D_{24}\cos\delta_{24}$ and $D_{34}\cos\delta_{34}$ are $M_t(\dot{\delta}_1+\dot{\delta}_3-2\dot{\delta}_0)$, $M_t(\dot{\delta}_1+\dot{\delta}_4-2\dot{\delta}_0)$, $M_t(\dot{\delta}_2+\dot{\delta}_3-2\dot{\delta}_0)$, $M_t(\dot{\delta}_2+\dot{\delta}_4-2\dot{\delta}_0)$, and $M_t(\dot{\delta}_3+\dot{\delta}_4-2\dot{\delta}_0)$, respectively, resulting in the following equation:

$$\sum_{i=1}^{4-1}\sum_{j=i+1}^{4}\left[M_j\sum_{k=1,\neq i}^{4}(D_{ik}\cos\delta_{ik})-M_i\sum_{k=1,\neq j}^{4}(D_{jk}\cos\delta_{jk})\right]\dot{\delta}_{ij}=$$

$$M_t\sum_{i=1}^{4-1}\sum_{j=i+1}^{4}D_{ij}\cos\delta_{ij}\cdot(\dot{\delta}_i+\dot{\delta}_j-2\dot{\delta}_0)$$

The general form of this equation is Eq. A.4

$$\begin{aligned}\textstyle\sum_{i=1}^{n-1}\sum_{j=i+1}^{n}\left[M_j\sum_{k=1,i}^{n}(D_{ik}\cos\delta_{ik})-M_i\sum_{k=1,\neq j}^{n}(D_{jk}\cos\delta_{jk})\right]\dot{\delta}_{ij}=\\ M_t\textstyle\sum_{i=1}^{n-1}\sum_{j=i+1}^{n}D_{ij}\cos\delta_{ij}\cdot(\dot{\delta}_i+\dot{\delta}_j-2\dot{\delta}_o)\end{aligned}\qquad\text{(A.4)}$$

Substituting Eq. A.3 and Eq. A.4 into Eq. A.2 we get

$$-M_t\frac{dV}{dt}=$$

$$+\sum_{i=1}^{n-1}\sum_{j=i+1}^{n}\left[M_iM_j\dot{\delta}_{ij}\frac{d\dot{\delta}_{ij}}{dt}\right]$$

$$+\sum_{i=1}^{n-1}\sum_{j=i+1}^{n}\left[-(M_jP_i-M_iP_j)\frac{d\delta_{ij}}{dt}+M_tC_{ij}\sin\delta_{ij}\frac{d\delta_{ij}}{dt}\right]$$

$$+\sum_{i=1}^{n-1}\sum_{j=i+1}^{n}\left[M_tD_{ij}\cos\delta_{ij}\frac{d}{dt}(\delta_i+\delta_j-2\delta_0)\right]$$

By multiplying both sides of the above equation by $\frac{1}{M_t}$ we get

$$-\frac{dV}{dt}=$$

$$+\sum_{i=1}^{n-1}\sum_{j=i+1}^{n}\left[\frac{M_iM_j}{M_t}\dot{\delta}_{ij}\frac{d\dot{\delta}_{ij}}{dt}\right]$$

$$+\sum_{i=1}^{n-1}\sum_{j=i+1}^{n}\left[-\frac{M_jP_i-M_iP_j}{M_t}\frac{d\delta_{ij}}{dt}+C_{ij}\sin\delta_{ij}\frac{d\delta_{ij}}{dt}\right]$$

$$+\sum_{i=1}^{n-1}\sum_{j=i+1}^{n}\left[D_{ij}\cos\delta_{ij}\frac{d}{dt}\left(\delta_i+\delta_j-2\delta_0\right)\right]$$

6. We then integrate the above equation from t to t_s (post-fault).

$$V\left(\underline{\delta},\underline{\omega}\right)=\int_t^{t_s}\left(\frac{dV}{dt}\right)dt$$

$$V\left(\underline{\delta},\underline{\omega}\right)=\int_{t_s}^{t}\left(-\frac{dV}{dt}\right)dt$$

$$V\left(\underline{\delta},\underline{\omega}\right)=$$

$$+\sum_{i=1}^{n-1}\sum_{j=i+1}^{n}\int_{t_s}^{t}\left[\frac{M_iM_j}{M_t}\dot{\delta}_{ij}\frac{d\dot{\delta}_{ij}}{dt}\right]dt$$

$$+\sum_{i=1}^{n-1}\sum_{j=i+1}^{n}\int_{t_s}^{t}\left[-\frac{M_jP_i-M_iP_j}{M_t}\frac{d\delta_{ij}}{dt}+C_{ij}\sin\delta_{ij}\frac{d\delta_{ij}}{dt}\right]dt$$

$$+\sum_{i=1}^{n-1}\sum_{j=i+1}^{n}\int_{t_s}^{t}\left[D_{ij}\cos\delta_{ij}\frac{d}{dt}\left(\delta_i+\delta_j-2\delta_0\right)\right]dt$$

or

$$V\left(\underline{\delta},\underline{\omega}\right)=$$

$$+\sum_{i=1}^{n-1}\sum_{j=i+1}^{n}\frac{M_iM_j}{M_t}\int_0^{\omega_{ij}}\omega_{ij}d\omega_{ij}$$

$$-\sum_{i=1}^{n-1}\sum_{j=i+1}^{n}\frac{M_jP_i-M_iP_j}{M_t}\int_{\delta_{ij}^s}^{\delta_{ij}}d\delta_{ij}$$

$$+\sum_{i=1}^{n-1}\sum_{j=i+1}^{n}C_{ij}\int_{\delta_{ij}^s}^{\delta_{ij}}\sin\delta_{ij}d\delta_{ij}$$

$$+\sum_{i=1}^{n-1}\sum_{j=i+1}^{n}D_{ij}\int_{\delta_i^s+\delta_j^s-2\delta_0^s}^{\delta_i+\delta_j-2\delta_0}\cos\left(\delta_i-\delta_j\right)d\left(\delta_i+\delta_j-2\delta_0\right)$$

The transient energy in *relative angle formulation* results in the following equation:

$$\sum_{i=1}^{n-1}\sum_{j=i+1}^{n}\frac{1}{2}\frac{M_iM_j}{M_t}\omega_{ij}^2-\frac{M_jP_i-M_iP_j}{M_t}\left(\delta_{ij}-\delta_{ij}^s\right)-C_{ij}\left(\cos\delta_{ij}-\cos\delta_{ij}^s\right)+D_{ij}I_{ij}$$

where $I_{ij}=\int_{\delta_i^s+\delta_j^s-2\delta_0^s}^{\delta_i+\delta_j-2\delta_0}\cos\left(\delta_i-\delta_j\right)d\left(\delta_i+\delta_j-2\delta_0\right).$

7. Notice that the transient energy function given by the previous equation is formulated in *relative angle.* To get the formulation with *one machine as reference,* we must use the following equations:

$$\delta_{ij} = \delta_{in} - \delta_{jn},$$

$$\omega_{ij} = \omega_{in} - \omega_{jn}$$

$$\delta_i + \delta_j - 2\delta_o = \delta_{in} + \delta_{jn} + 2\tilde{\delta}_n$$

Now we must find an expression for $\tilde{\delta}_n$ as a function of the angle subspace

$$\underline{\delta} = \{\delta_{in}, i = 1, \cdots, n-1\}$$

$$\delta_o = \frac{1}{M_t} \sum_{i=1}^{n} M_i \, \delta_i$$

According to Eq. 3.7,

$$\begin{aligned}
\delta_n - \delta_o &= \delta_n - \tfrac{1}{M_t} \textstyle\sum_{i=1}^{n} M_i \delta_i \\
&= \delta_n - \tfrac{M_n}{M_t} \delta_n - \tfrac{1}{M_t} \textstyle\sum_{i=1}^{n-1} M_i \delta_i \\
&= \tfrac{(\sum_{1=1}^{n} M_i)\delta_n - M_n \delta_n}{M_t} - \tfrac{1}{M_t} \textstyle\sum_{i=1}^{n-1} [M_i \, (\delta_{in} + \delta_n)] \\
&= \tfrac{1}{M_t} \textstyle\sum_{i=1}^{n-1} M_i \delta_n - \tfrac{1}{M_t} \textstyle\sum_{i=1}^{n-1} M_i \delta_{in} - \tfrac{1}{M_t} \textstyle\sum_{i=1}^{n-1} M_i \delta_n
\end{aligned}$$

or

$$\tilde{\delta}_n \, (\underline{\delta}) = -\frac{1}{M_t} \sum_{i=1}^{n-1} M_i \delta_{in} \tag{A.5}$$

Appendix B

The Equality of the COA and One Machine Reference Frames

To obtain the relationship between $V(\tilde{\delta},\tilde{\omega})$ and $V(\delta,\omega)$, we will begin with the kinetic energy.

- Kinetic energy.

$$V_k(\underline{\omega}) = \sum_{i=1}^{n-2}\sum_{j=i+1}^{n-1}\frac{M_iM_j}{2M_t}(\omega_{in}-\omega_{jn})^2 + \sum_{i=1}^{n-1}\frac{M_iM_n}{2M_t}\omega_{in}^2$$

$$V_k(\underline{\tilde{\omega}}) = \frac{1}{2}\sum_{i=1}^{n} M_i\tilde{\omega}_1^2$$

$$V_k(\underline{\tilde{\omega}}) = \frac{1}{2}\sum_{i=1}^{n} M_i(\omega_i-\omega_o)^2$$

$$= \frac{1}{2}\sum_{i=1}^{n} M_i\left(\omega_i^2 - 2\omega_i\omega_0 + \omega_0^2\right)$$

$$= \frac{1}{2}\sum_{i=1}^{n} M_i\omega_i^2 - \omega_0\sum_{i=1}^{n} M_i\omega_i + \frac{\omega_0^2}{2}\sum_{i=1}^{n} M_i$$

$$= \frac{1}{2}\sum_{i=1}^{n} M_i\omega_i^2 - M_t\omega_0^2 + \frac{1}{2}M_t\omega_0^2$$

$$= \frac{1}{2}\sum_{i=1}^{n} M_i\omega_i^2 - \frac{M_t}{2}\omega_0^2$$

$$= \frac{1}{2}\sum_{i=1}^{n} M_i\omega_i^2 - \frac{M_t}{2}\left(\frac{1}{M_t}\sum_{i=1}^{n} M_i\omega_i\right)^2$$

$$= \frac{1}{2}\sum_{i=1}^{n} M_i\omega_i^2 - \frac{1}{2M_t}\left(\sum_{i=1}^{n} M_i\omega_i\right)^2$$

$$= \frac{1}{2M_t}\left(\sum_{k=1}^{n} M_k\right)\left(\sum_{i=1}^{n} M_i\omega_i^2\right) - \frac{1}{2M_t}\left(\sum_{i=1}^{n} M_i^2\omega_i^2 + 2\sum_{i=1}^{n-1}\sum_{j=i+1}^{n} M_i\omega_i M_j\omega_j\right)$$

$$= \frac{1}{2M_t}\left[\sum_{i=1}^{n}\left(M_i\omega_i^2\sum_{k=1}^{n} M_k\right) - \sum_{i=1}^{n} M_i^2\omega_i^2 - \sum_{i=1}^{n-1}\sum_{j=i+1}^{n} 2M_i\omega_i M_j\omega_j\right]$$

$$= \frac{1}{2M_t}\left[\sum_{i=1}^{n}\left(M_i\omega_i^2\sum_{k=1,\neq i}^{n} M_k\right) + \sum_{i=1}^{n} M_i^2\omega_i^2 - \sum_{i=1}^{n} M_i^2\omega_i^2 - \sum_{i=1}^{n-1}\sum_{j=i+1}^{n} 2M_i\omega_i M_j\omega_j\right]$$

$$= \frac{1}{2M_t}\left[\sum_{i=1}^{n-1}\sum_{j=i+1}^{n}\left(M_iM_j\omega_i^2 + M_iM_j\omega_j^2\right) - \sum_{i=1}^{n-1}\sum_{j=i+1}^{n} 2M_i\omega_i M_j\omega_j\right]$$

$$= \frac{1}{2M_t}\sum_{i=1}^{n-1}\sum_{j=i+1}^{n}\left[M_i\ M_j\left(\omega_i^2 - 2\omega_i\omega_j + \omega_j^2\right)\right] = \frac{1}{2M_t}\sum_{i=1}^{n-1}\sum_{j=i+1}^{n} M_iM_j\left(\omega_i - \omega_j\right)^2$$

$$= \sum_{i=1}^{n-2}\sum_{j=i+1}^{n-1}\frac{M_iM_j}{2M_t}\left(\omega_{in} - \omega_{jn}\right)^2 + \sum_{i=1}^{n-1}\frac{M_iM_n}{2M_t}\omega_{in}^2$$

$$\boxed{\mathrm{V}_k(\underline{\tilde{\omega}}) = \mathrm{V}_k(\underline{\omega})}$$

- Path-independent potential energy.

$$\boxed{\textbf{COA:}}\ V_p\left(\underline{\tilde{\delta}}\right) = V_{p1}\left(\underline{\tilde{\delta}}\right) + V_{p2}\left(\underline{\tilde{\delta}}\right)$$

where

$$V_{p1}\left(\underline{\tilde{\delta}}\right) = -\sum_{i=1}^{n-1}\left[P_i\left(\tilde{\delta}_i - \tilde{\delta}_i^s\right)\right] - P_n\left(\tilde{\delta}_n - \tilde{\delta}_n^s\right)$$

$$V_{p2}\left(\underline{\tilde{\delta}}\right) =$$

$$-\sum_{i=1}^{n-2}\sum_{j=i+1}^{n-1}\left[C_{ij}\left(\cos\tilde{\delta}_{ij} - \cos\tilde{\delta}_{ij}^s\right)\right] - \sum_{i=1}^{n-1} C_{in}\left[\cos\left(\tilde{\delta}_i - \tilde{\delta}_n\right) - \cos\left(\tilde{\delta}_i^s - \tilde{\delta}_n^s\right)\right]$$

$$\boxed{\textbf{Machine n as reference:}}\ V_p\left(\underline{\delta}\right) = V_{p1}\left(\underline{\delta}\right) + V_{p2}\left(\underline{\delta}\right)$$

where

$$V_{p1}(\underline{\delta}) = -\sum_{i=1}^{n-2}\sum_{j=i+1}^{n-1}\frac{M_jP_i - M_iP_j}{M_t}\left(\delta_{in} - \delta_{jn} - \delta_{in}^s + \delta_{jn}^s\right)$$

$$-\sum_{i=1}^{n-1}\frac{M_nP_i - M_iP_n}{M_t}\left(\delta_{in} - \delta_{in}^s\right)$$

$$V_{p2}(\underline{\delta}) =$$

$$-\sum_{i=1}^{n-2}\sum_{j=i+1}^{n-1}C_{ij}\left[\cos\left(\delta_{in} - \delta_{jn}\right) - \cos\left(\delta_{in}^s - \delta_{jn}^s\right)\right] - \sum_{i=1}^{n-1}C_{in}\left[cos\delta_{in} - cos\delta_{in}^s\right]$$

* Let us consider V_{p2}.

$$V_{p2}(\underline{\delta}) = -\sum_{i=1}^{n-1}\sum_{j=i+1}^{n}C_{ij}\left(cos\delta_{ij} - cos\delta_{ij}^s\right)$$

$$= -\sum_{i=1}^{n-1}\sum_{j=i+1}^{n}C_{ij}\left(\cos\tilde{\delta}_{ij} - \cos\tilde{\delta}_{ij}\right)$$

$$= -\sum_{i=1}^{n-2}\sum_{j=i+1}^{n-1}\left[C_{ij}\left(\cos\tilde{\delta}_{ij} - \cos\tilde{\delta}_{ij}^s\right)\right] - \sum_{i=1}^{n-1}C_{in}\left[\cos\left(\tilde{\delta}_i - \tilde{\delta}_n\right) - \cos\left(\tilde{\delta}_i^s - \tilde{\delta}_n^s\right)\right]$$

This equation is also equal to $V_{p2}\left(\tilde{\underline{\delta}}\right)$.

* Now, let us consider V_{p1}.

$$V_{p1}(\underline{\delta})$$

$$= -\textstyle\sum_{i=1}^{n-2}\sum_{j=i+1}^{n-1}\frac{M_jP_i - M_iP_j}{M_t}\left(\delta_{in} - \delta_{jn} - \delta_{in}^s + \delta_{jn}^s\right)$$
$$-\textstyle\sum_{i=1}^{n-1}\frac{M_nP_i - M_iP_n}{M_t}\left(\delta_{in} - \delta_{in}^s\right)$$

$$= -\textstyle\sum_{i=1}^{n-1}\sum_{j=i+1}^{n}\frac{M_jP_i - M_iP_j}{M_t}\left(\delta_{ij} - \delta_{ij}^s\right)$$

$$= -\tfrac{1}{M_t}\textstyle\sum_{i=1}^{n-1}\sum_{j=i+1}^{n}\left(M_jP_i\delta_i + M_iP_j\delta_j - P_iM_j\delta_j - P_jM_i\delta_i\right)$$
$$+\tfrac{1}{M_t}\textstyle\sum_{i=1}^{n-1}\sum_{j=i+1}^{n}\left(M_jP_i\delta_i^s + M_iP_j\delta_j^s - P_iM_j\delta_j^s - P_jM_i\delta_i^s\right)$$

$$= -\tfrac{1}{M_t}\textstyle\sum_{i=1}^{n}\left(P_i\delta_i\sum_{k=1,\neq i}^{n}M_k - P_i\sum_{k=1,\neq i}^{n}M_k\delta_k\right)$$
$$+\tfrac{1}{M_t}\textstyle\sum_{i=1}^{n}\left(P_i\delta_i^s\sum_{k=1,\neq i}^{n}M_k - P_i\sum_{k=1,\neq i}^{n}M_k\delta_k^s\right)$$

$$= -\sum_{i=1}^{n}\left(\frac{P_i}{M_t}\delta_i M_t - \frac{P_i}{M_t}\delta_i M_i - \frac{P_i}{M_t}\sum_{k=1,\neq i}^{n} M_k\delta_k\right)$$
$$+\sum_{i=1}^{n}\left(\frac{P_i}{M_t}\delta_i^s M_t - \frac{P_i}{M_t}\delta_i^s M_i - \frac{P_i}{M_t}\sum_{k=1,\neq i}^{n} M_k\delta_k^s\right)$$

$$= -\frac{1}{M_t}\sum_{i=1}^{n}\left(P_i\delta_i M_t - P_i\sum_{k=1}^{n} M_k\delta_k\right)$$
$$+\frac{1}{M_t}\sum_{i=1}^{n}\left(P_i\delta_i^s M_t - P_i\sum_{k=1}^{n} M_k\delta_k^s\right)$$

$$= -\frac{1}{M_t}\sum_{i=1}^{n}\left[\left(P_i\delta_i M_t - P_i M_t\delta_0\right) - \left(P_i\delta_i^s M_t - P_i M_t\delta_0^s\right)\right]$$

$$= -\sum_{i=1}^{n}\left\{P_i\left[\left(\delta_i - \delta_0\right) - \left(\delta_i^s - \delta_0^s\right)\right]\right\}$$

$$= -\sum_{i=1}^{n} P_i\left(\tilde{\delta}_i - \tilde{\delta}_i^s\right)$$

This equation is also equal to $V_{p1}\left(\tilde{\underline{\delta}}\right)$. In conclusion, we get the following result:

$$\boxed{V_p\left(\underline{\delta}\right) = V_p\left(\tilde{\underline{\delta}}\right)}$$

- Path-dependent potential energy.

$$\boxed{\text{COA:}}\ V_d\left(\tilde{\underline{\delta}}\right) = \sum_{i=1}^{n-1}\sum_{j=i+1}^{n} D_{ij}\int_{\tilde{\delta}_i^s+\tilde{\delta}_j^s}^{\tilde{\delta}_i+\tilde{\delta}_j}\cos\left(\tilde{\delta}_i - \tilde{\delta}_j\right)\, d\left(\tilde{\delta}_i + \tilde{\delta}_j\right)$$

$$\boxed{\text{Machine n as reference:}}\ V_d\left(\underline{\delta}\right) =$$

$$+\sum_{i=1}^{n-2}\sum_{j=i+1}^{n-1} D_{ij}\int_{\delta_{in}^s+\delta_{jn}^s+2\tilde{\delta}_n^s}^{\delta_{in}+\delta_{jn}+2\tilde{\delta}_n}\cos\left(\delta_{in} - \delta_{jn}\right)\, d\left(\delta_{in} + \delta_{jn} + 2\tilde{\delta}_n\right)$$

$$+\sum_{i=1}^{n-1} D_{in}\int_{\delta_{in}^s+2\tilde{\delta}_n^s}^{\delta_{in}+2\tilde{\delta}_n}\cos\delta_{in}\, d\left(\delta_{in} + 2\tilde{\delta}_n\right)$$

$V_d\left(\underline{\delta}\right) = \sum_{i=1}^{n-1}\sum_{j=i+1}^{n} D_{ij}\int_{\delta_i^s+\delta_j^s-2\delta_0^s}^{\delta_i+\delta_j-2\delta_0}\cos\left(\delta_i - \delta_j\right)\, d\left(\delta_i + \delta_j - 2\delta o\right)$, since $\delta_i - \delta_j = \tilde{\delta}_i - \tilde{\delta}_j$ and $\delta_i + \delta_j - 2\,\delta_0 = \tilde{\delta}_i + \tilde{\delta}_j$. We can then conclude that the following equation holds.

$$\boxed{\mathrm{V}_d\left(\underline{\delta}\right)=\mathrm{V}_d\left(\tilde{\underline{\delta}}\right)}$$

The transient energy is the same in the COA and one-machine-as-reference formulations, i.e.

$$\boxed{V\left(\tilde{\underline{\delta}}, \tilde{\underline{\omega}}\right) = V(\underline{\delta}, \underline{\omega})}$$

Appendix C

The Synchronous Machine

C.0.2 State equation, detailed model.

This section has been adapted from [47]. Usually, the following parameters are given:

1. rating S_{base}
2. line to line voltage V_{LL}
3. number of poles P
4. combined inertia of generator and turbine J
5. stator resistance per phase r_s
6. stator leakage reactance per phase X_{ls}
7. q-axis reactance X_q
8. resistance and leakage reactance per phase of the q-axis damper winding-1 referred to the stator, r_{kq1}, X_{lkq1}
9. resistance and leakage reactance per phase of the q-axis damper winding-2 referred to the stator r_{kq2}, X_{lkq2}
10. d-axis reactance X_d
11. resistance and leakage reactance of the field winding referred to the stator r_{fd}, X_{lfd}

12. resistance and leakage reactance per phase of the d-axis damper winding referred to the stator r_{kd}, X_{lkd}

Let us assume that the machine is connected to an infinite bus with voltage V_t pu, then

$$\begin{bmatrix} v_{as} \\ v_{bs} \\ v_{cs} \end{bmatrix} = V_t \begin{bmatrix} \cos(\omega_s t) \\ \cos\left(\omega_s t - \frac{2\pi}{3}\right) \\ \cos\left(\omega_s t + \frac{2\pi}{3}\right) \end{bmatrix} \text{ pu}$$

After taking Park's transformation, the following applies:

$$\begin{aligned} v_{qs} &= V_t \cos(\delta) \\ v_{ds} &= V_t \cos(\delta) \text{ pu} \\ v_{0s} &= 0. \end{aligned}$$

Let us define the following variables before obtaining the state equation.

$$Z_{base} = \frac{V_{LL}^2}{S_{base}} \Omega$$

$$\omega_s = 120\,\pi \frac{\text{rad}}{\text{s}}$$

$$\left[\begin{array}{lcl} L_{ls} & = & \frac{X_{ls}}{\omega_s} \\ L_q & = & \frac{X_q}{\omega_s} \\ L_{mq} & = & L_q - L_{ls} \\ L_d & = & \frac{X_d}{\omega_s} \\ L_{md} & = & L_d - L_{ls} \\ L_{lfd} & = & \frac{X_{lfd}}{\omega_s} \\ L_{fd} & = & L_{lfd} + L_{md} \\ L_{lkq1} & = & \frac{X_{lkq1}}{\omega_s} \\ L_{kq1} & = & L_{lkq1} + L_{mq} \\ L_{lkq2} & = & \frac{X_{lkq2}}{\omega_s} \\ L_{kq2} & = & L_{lkq2} + L_{mq} \\ L_{lkd} & = & \frac{X_{lkd}}{\omega_s} \\ L_{kd} & = & L_{lkd} + L_{md} \end{array}\right], \text{ reactances in pu, } \omega_s \text{ in } \frac{\text{rad}}{\text{s}}$$

$$\left.\begin{array}{l} X_{md} = \omega_s L_{md} \\ X_{mq} = \omega_s L_{mq} \end{array}\right\}, \text{ pu}$$

$$H = \frac{\frac{1}{2} J \left(\frac{2}{p} \omega_s\right)^2}{S_{base}}, \text{ s}$$

$$[E] = \left[\begin{array}{cccccccc} -L_q & 0 & L_{mq} & L_{mq} & 0 & 0 & 0 & 0 \\ 0 & -L_d & 0 & 0 & L_{md} & L_{md} & 0 & 0 \\ -L_{mq} & 0 & L_{kq1} & L_{mq} & 0 & 0 & 0 & 0 \\ -L_{mq} & 0 & L_{mq} & L_{kq2} & 0 & 0 & 0 & 0 \\ 0 & -L_{md}\frac{X_{md}}{r_{fd}} & 0 & 0 & L_{fd}\frac{X_{md}}{r_{fd}} & L_{md}\frac{X_{md}}{r_{fd}} & 0 & 0 \\ 0 & -L_{md} & 0 & 0 & L_{md} & L_{kd} & 0 & 0 \\ 0 & 0 & 0 & 0 & 0 & 0 & \frac{2H}{\omega_s} & 0 \\ 0 & 0 & 0 & 0 & 0 & 0 & 0 & 1 \end{array}\right] \tag{C.1}$$

$$\underline{x} = \left[\begin{array}{cccccccc} i_{qs} & i_{ds} & i_{kq1} & i_{kq2} & i_{fd} & i_{kd} & \omega & \delta \end{array}\right]^T$$

$$\underline{F}(\underline{x}) = \begin{bmatrix} V_t \cos(\delta) + r_s i_{qs} + (\omega + \omega_s) L_d i_{ds} - (\omega + \omega_s) L_{md} (i_{fd} + i_{kd}) \\ V_t \sin(\delta) - (\omega + \omega_s) L_q i_{qs} + r_s i_{ds} + (\omega + \omega_s) L_{mq} (i_{kq1} + i_{kq2}) \\ -r_{kq1} i_{kq1} \\ -r_{kq2} i_{kq2} \\ -X_{md} i_{fd} \\ -r_{kd} i_{kd} \\ -X_{md} (i_{fd} + i_{kd} - i_{ds}) i_{qs} - X_{mq} (i_{qs} - i_{kq1} - i_{kq2}) i_{ds} \\ \omega \end{bmatrix}$$

$$\underline{u} = \begin{bmatrix} 0 & 0 & 0 & 0 & V_{oc} & 0 & T_l & 0 \end{bmatrix}^T$$

The state equation results.

$$\dot{\underline{x}} = [E]^{-1} \{[F(\underline{x})] + \underline{u}\} \tag{C.2}$$

The input torque, T_l, and the voltage of the field supply referred to the stator, V_{oc}, are the only forcing functions in this particular case.

C.0.3 State equation, classical model

For comparison, the state equation of the classical model is

$$\begin{aligned} \dot{\omega} &= \tfrac{P - P_e}{M} - \tfrac{D}{M} \omega \\ \dot{\delta} &= \omega \end{aligned} \tag{C.3}$$

where

$$P_e(\delta) = \frac{V_t E}{X'_d} \sin(\delta), \ \frac{\text{MW}}{\text{MVA}}$$

$$M = \frac{2H}{\omega_s}$$

According to [47], the transient reactance X'_d relates to the reactances of the detailed model by

$$X'_d = X_d - \frac{(X_d - X_{ls})^2}{X_{lfd} + X_d - X_{ls}}$$

Now the only parameter to determine is the damping factor D. The damping power P_d is

proportional to the angular velocity deviation ω, i.e.

$$P_d = D\omega$$

Friction and windage losses also contribute to the damping power [6], but this contribution is negligible. The damping is mainly due to asynchronous torque and, since the angular velocity deviation is small, it will be assumed that the damping power is proportional to the angular velocity deviation $\omega = \omega_r - \omega_s$ rad/s.

C.1 Linearized state equations

C.1.1 Detailed model

Given a state equation of the form $\dot{\underline{x}} = \underline{f}(\underline{x}) + \underline{u}$ the linearized state equation around the operating point $\underline{x}_0$ is

$$\Delta\dot{\underline{x}} = \left[\frac{\partial \underline{f}(\underline{x})}{\partial \underline{x}}\right]_{\underline{x}_0} \Delta\underline{x} + \Delta\underline{u}$$

The corresponding homogeneous system is the following:

$$\Delta\dot{\underline{x}} = \left[\frac{\partial \underline{f}(\underline{x})}{\partial \underline{x}}\right]_{\underline{x}_0} \Delta\underline{x}$$

Now, this result is used to obtain the homogeneous linearized equation. Matrix E in Eq. C.2 remains constant. All then that is needed is $\left[\frac{\partial \underline{F}(\underline{x})}{\partial \underline{x}}\right]_{\underline{x}_0}$.

$$\left[\frac{\partial \underline{F}(\underline{x})}{\partial \underline{x}}\right]_{\underline{x}_0} =$$

$$\begin{bmatrix} r_s & X_d & 0 & 0 & -X_{md} & -X_{md} & \begin{pmatrix} +L_d I_{ds} \\ -L_{md} I_{fd} \end{pmatrix} & -\sin\delta_0 \\ -X_q & r_s & X_{mq} & X_{mq} & 0 & 0 & -L_q I_{qs} & \cos\delta_0 \\ 0 & 0 & -r_{kq1} & 0 & 0 & 0 & 0 & 0 \\ 0 & 0 & 0 & -r_{kq2} & 0 & 0 & 0 & 0 \\ 0 & 0 & 0 & 0 & -X_{md} & 0 & 0 & 0 \\ 0 & 0 & 0 & 0 & 0 & -r_{kd} & 0 & 0 \\ \begin{pmatrix} X_{dq} I_{ds} \\ -V_{oc} \end{pmatrix} & X_{dq} I_{qs} & X_{mq} I_{ds} & X_{mq} I_{ds} & -X_{md} I_{qs} & -X_{md} I_{qs} & 0 & 0 \\ 0 & 0 & 0 & 0 & 0 & 0 & 1 & 0 \end{bmatrix}$$

The stable equilibrium point is

$$\underline{x_0} = \begin{bmatrix} I_{qs} & I_{ds} & 0 & 0 & I_{fd} & 0 & 0 & \delta_0 \end{bmatrix}^T$$

Given the line current phasor $\mathbf{I_a} = I_{ar} + j\, I_{ai} = I_a \underline{|\, -\theta}$, the voltage phasor at the infinite bus $V_t = V_t \underline{|\, 0}$, the operating point is obtained by the following:

$$\delta_0 = \arctan\left[\frac{-r_s I_{ai} + X_q I_{ar}}{V_t + r_s I_{ar} - X_q I_{ai}}\right]$$

$$I_{qs} = I_a \cos(\delta_0 + \theta)\,;\ \mathbf{I_{qs}} = I_{qs} \underline{|\, \delta_0}$$

$$I_{ds} = \sqrt{I_a^2 - I_{qs}^2};\ \mathbf{I_{ds}} = I_{ds} \underline{|\, \delta_0 - \pi/2}$$

$$V_{oc} = \mathbf{V_t} + r_s\, \mathbf{I_a} + j\, X_d\, \mathbf{I_{ds}} + j\, X_q\, \mathbf{I_{qs}}$$

Note: These equations correspond to $\delta_0 + \theta > 0$; in this case $\mathbf{I_{ds}}$ *lags* $\mathbf{I_{qs}}$ by 90°. These equations do not apply if $\mathbf{I_{ds}}$ *leads* $\mathbf{I_{qs}}$ by 90°. To conclude, the linearized homogeneous equation is

$$\underline{\Delta \dot{x}} = [A]\, \Delta x \tag{C.4}$$

where

$$[A] = [E]^{-1} \left[\frac{\partial \underline{F}(\underline{x})}{\partial \underline{x}}\right]_{\underline{x}_0}$$

$$\underline{\Delta x} = \left[\begin{array}{cccccccc} \Delta i_{qs} & \Delta i_{ds} & \Delta i_{kq1} & \Delta i_{kq2} & \Delta i_{fd} & \Delta i_{kd} & \Delta\omega & \Delta\delta \end{array} \right]^T$$

$[E]$ is given by Eq. $C.1$.

C.1.2 Classical model

The linearized homogeneous equation is

$$\left[\begin{array}{c} \Delta\dot{\delta} \\ \Delta\dot{\omega} \end{array} \right] = \left[\begin{array}{cc} 0 & 1 \\ -\frac{1}{M} P_{\max} \cos(\delta_0) & -\frac{D}{M} \end{array} \right] \left[\begin{array}{c} \Delta\delta \\ \Delta\omega \end{array} \right] \tag{C.5}$$

The Jacobian is

$$\left[\begin{array}{cc} 0 & 1 \\ -\frac{1}{M} P_{\max} \cos(\delta_0) & -\frac{D}{M} \end{array} \right]$$

The Jacobian's eigenvalues are

$$\lambda = -\frac{D}{2M} \pm \sqrt{\left(\frac{D}{2M}\right)^2 - \frac{P_{\max} \cos(\delta_0)}{M}}$$

C.2 Machine data

Data taken from [47].

The data corresponding to a large *hydro turbine generator* is the following

$$S_{base} = 325 \text{ MVA}$$

$$power\ factor = 0.85$$

$$V_{LL} = 20 \text{ kV}$$

$$P = 64$$

$$J = 35.1x10^6 \text{ J s}^2$$

$$\begin{aligned} H &= 7.5 \text{ s on its own base} \\ &= 24.375 \text{ s on a 100 MVAbase} \end{aligned}$$

$$r_s = 0.00234\ \Omega$$

$$X_{ls} = 0.1478\ \Omega$$

$$X_q = 0.5911\ \Omega \qquad X_d = 1.0467\ \Omega$$

$$r_{fd} = 0.00050\ \Omega$$

$$X_{lfd} = 0.2523\ \Omega$$

$$r_{kq2} = 0.01675\ \Omega \qquad r_{kd} = 0.01736\ \Omega$$

$$X_{lkq2} = 0.1267\ \Omega \qquad X_{lkd} = 0.1970\ \Omega.$$

The data corresponding to a large *steam turbine generator* is the following:

$$S_{base} = 835\ \text{MVA}$$

$$power\ factor = 0.85$$

$$V_{LL} = 26\ \text{kV}$$

$$P = 2\ \text{poles}$$

$$J = 0.0658x10^6\ \text{J s}^2$$

$$H = 5.6\ \text{s on its own base}$$

$$= 46.76\ \text{s on a 100 MVAbase}$$

$$r_s = 0.00243\ \Omega$$

$$X_{ls} = 0.1538\ \Omega$$

$$X_q = 1.4570\ \Omega \qquad X_d = 1.4570\ \Omega$$

$$r_{kq1} = 0.00144\ \Omega \qquad r_{fd} = 0.00075\ \Omega$$

$$X_{lkq1} = 0.6578\ \Omega \qquad X_{lfd} = 0.1145\ \Omega$$

$$r_{kq2} = 0.00681\ \Omega \qquad r_{kd} = 0.01080\ \Omega$$

$$X_{lkq2} = 0.0762\ \Omega \qquad X_{lkd} = 0.06577\ \Omega.$$

C.3 Damping calculation - Free acceleration

To illustrate the effect of the damper windings, a simulation called free acceleration is realized using Eq. C.2 with $V_{oc} = 0$ and $T_l = 0$ and the following initial conditions:

$$\underline{x}_0 = \begin{bmatrix} i_{qs} \\ i_{ds} \\ i_{kqq1} \\ i_{kq2} \\ i_{fd} \\ i_{kd} \\ \omega \\ \delta \end{bmatrix}_0 = \begin{bmatrix} 0 \\ 0 \\ 0 \\ 0 \\ 0 \\ 0 \\ -\omega_s \\ 0 \end{bmatrix}$$

Notice that in this simulation, the applied voltage to the field winding is zero. The results of these simulations are shown in Fig. C-1. The base torque is the following:

$$T_{base} = \frac{S_{base}}{\frac{2}{p}\omega_s} \text{ N m}$$

The torque shown is the asynchronous torque and the simulations can be used to determine the damping factor D. This factor is given by

$$D = \frac{P_d}{\omega} \frac{\text{MW s}}{\text{MVA rad}}$$

where

$$P_d = T_e \frac{\omega + \omega_s}{\omega_s}$$

Both P_d and T_e are in pu. Therefore, if we plot the damping power P_d versus the angular velocity ω, an estimate of D may be obtained graphically. This result is illustrated in Fig. C-2. These plots start with an angular velocity of $-30 \frac{\text{rad}}{\text{s}}$ because the region of interest is for small angular velocity deviations. The average damping power is drawn, and the slope after the knee

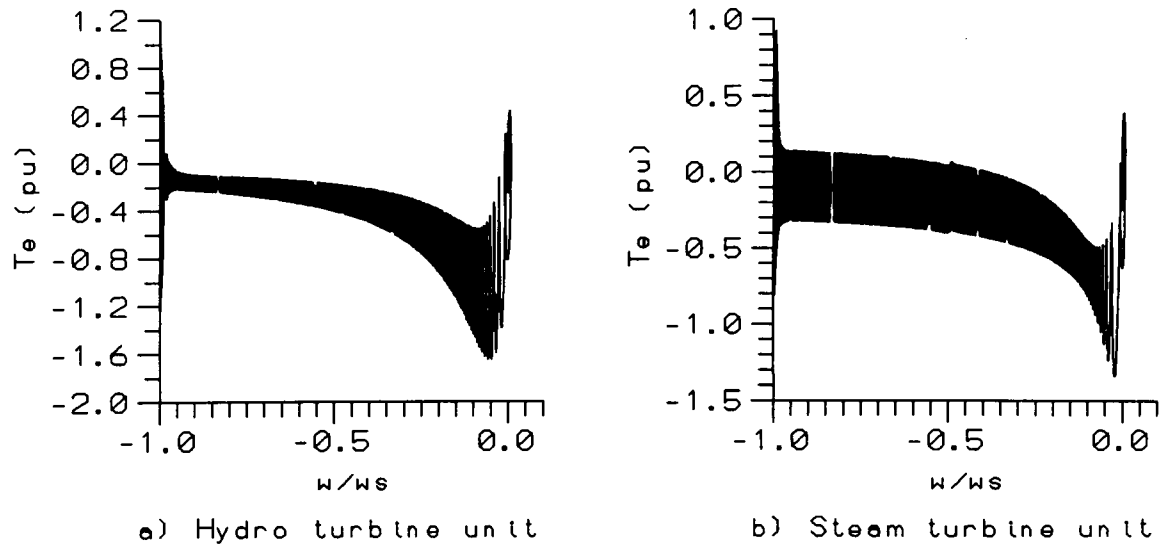

Figure C-1: Asynchronous torque versus angular velocity deviation in pu

is D. The damping coefficient for the hydro turbine unit is the following:

$$D = \frac{1.6}{15.5} = 0.103 \frac{\text{MW s}}{\text{MVA rad}}, S_{base} = 325 \text{ MVA}$$

For the steam turbine unit the damping is

$$D = \frac{1.4}{13.2} = 0.106 \frac{\text{MW s}}{\text{MVA rad}}, S_{base} = 835 \text{ MVA}$$

C.4 Damping calculation - Step increase in input torque

A second procedure to determine the damping consists on simulating a sudden change in input torque, the asynchronous torque is obtained from subtracting the steady state synchronous torque T_{ss} from the electro-magnetic torque T_e, i.e. $T_d = T_e - T_{ss}$. The steady state torque is given by the following equation:

$$T_{ss} = \frac{V_t V_{oc}}{X_d} \sin(\delta) + \frac{V_t^2}{2} \left(\frac{1}{X_q} - \frac{1}{X_d} \right) \sin(2\delta)$$

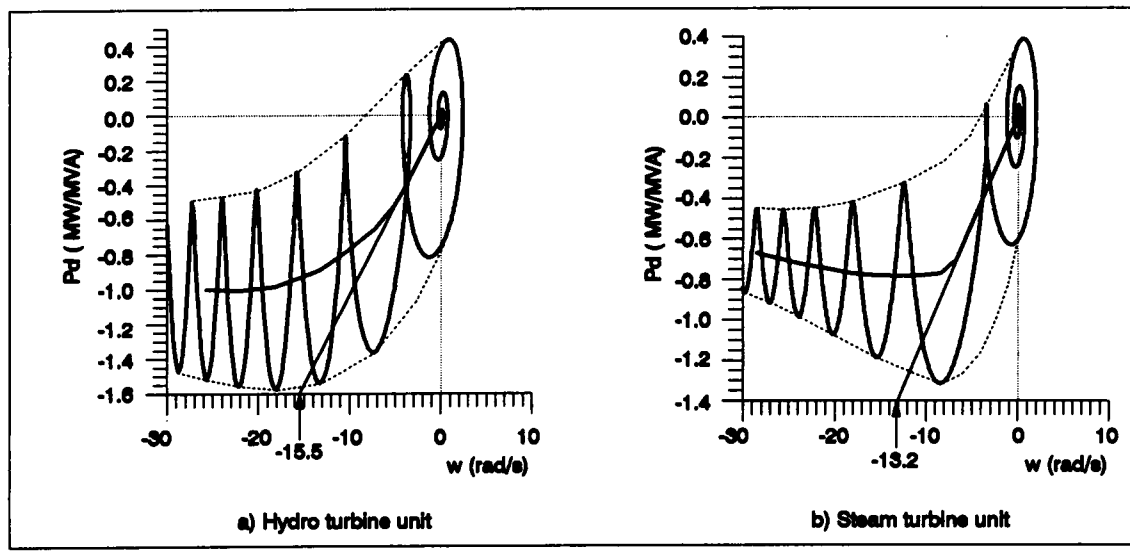

Figure C-2: Damping power versus angular velocity deviation-Free acceleration

We will define the internal power as

$$P_e = T_e \frac{\omega + \omega_s}{\omega_s}$$

The steady state power is defined as the following equation:

$$P_{ss} = T_{ss} \frac{\omega + \omega_s}{\omega_s}$$

The damping power results in the following:

$$P_d = P_e - P_{ss} = T_d \frac{\omega + \omega_s}{\omega_s}$$

It will be assumed that the input torque was zero before time zero, and in order to avoid non-linearities, the input step will be 0.1 pu. It will also be assumed that the open circuit voltage is 1.0 pu. Therefore, with $T_l = 0.1$ pu, $V_{oc} = 1.0$ pu, the initial conditions are the

following:

$$\underline{x}_0 = \begin{bmatrix} i_{qs} \\ i_{ds} \\ i_{kqq1} \\ i_{kq2} \\ i_{fd} \\ i_{kd} \\ \omega \\ \delta \end{bmatrix}_0 = \begin{bmatrix} 0 \\ 0 \\ 0 \\ 0 \\ X_{md} \\ 0 \\ 0 \\ 0 \end{bmatrix}$$

The results of these simulations are shown in Fig. C-3. Notice that for the hydro turbine unit the new stable equilibrium point is reached promptly, however for the steam turbine unit the oscillations disappear promptly but it takes considerably longer to achieve the new stable equilibrium point.

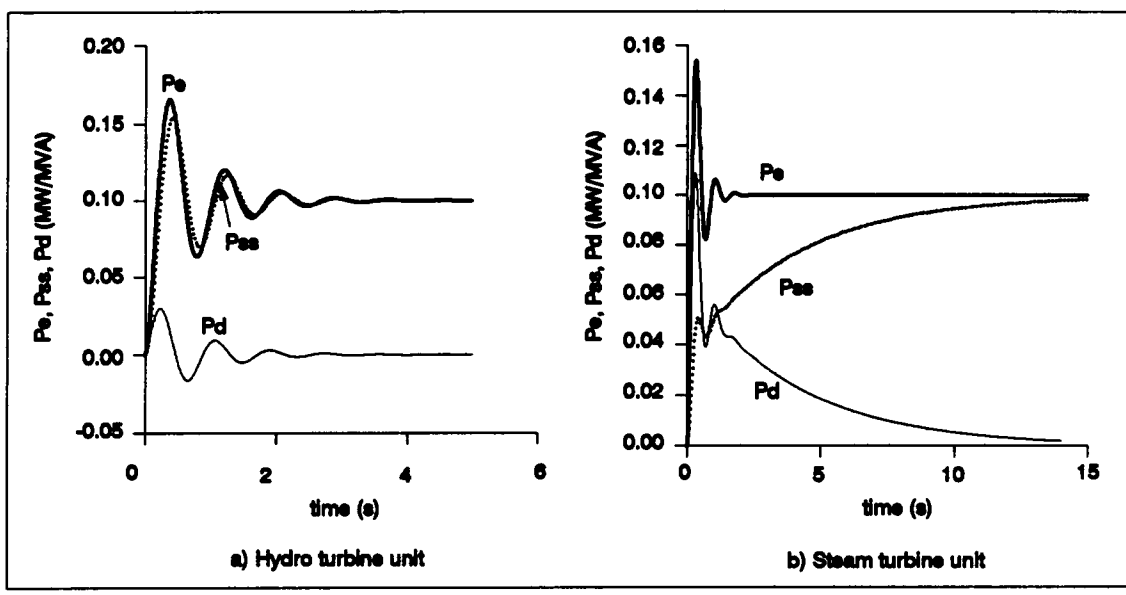

Figure C-3: Power versus time for a step input torque of 0.1 pu

The damping power is plotted versus the angular velocity deviation. After drawing the average damping power, the corresponding slope is D. Notice that due to the slow dynamics involved in the steam turbine unit, this method of finding D can not be applied for this unit.

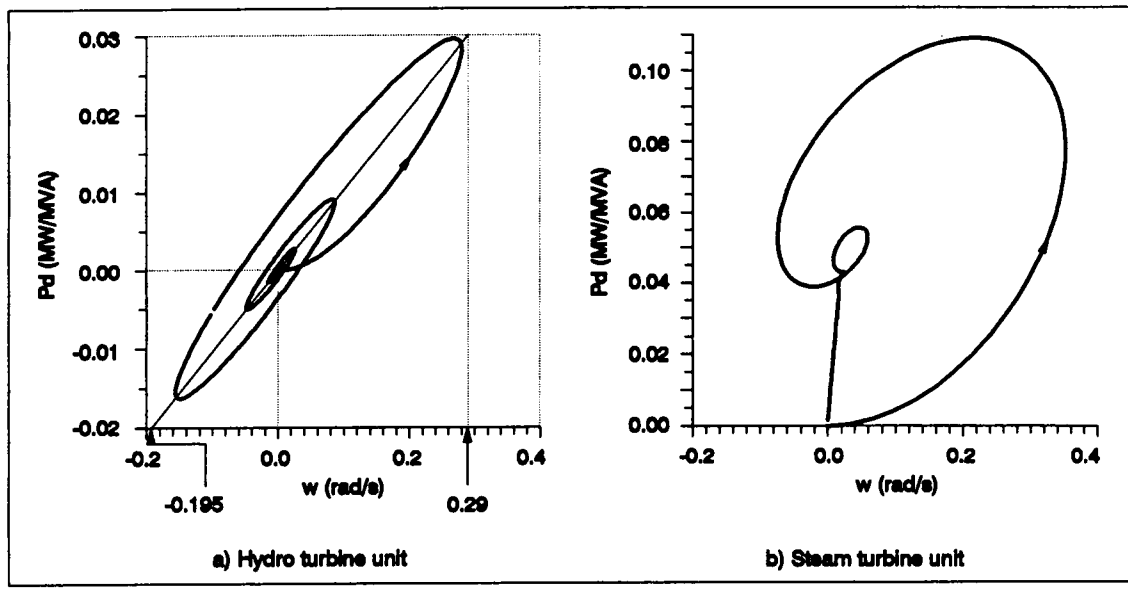

Figure C-4: Damping power versus angular velocity deviation-Step input torque

According to Fig. C-4, the damping for the hydro turbine unit is

$$D = \frac{0.05}{0.485} = 0.103 \frac{\text{MW s}}{\text{MVA rad}}$$

C.5 Damping calculation - Eigenanalyisis

A third method of finding the damping factor consists of the following:

1. Calculate the eigenvalues of the homogeneous dynamic equation of the detailed model, Eq. C.4, and identify the swing mode eigenvalue, λ_{swing}.

2. Find the eigenvalues of the homogeneous dynamic equation of the classical model, Eq. C.5. As mentioned before, these eigenvalues are

$$\lambda_{classical} = -\frac{D}{2M} \pm \sqrt{\left(\frac{D}{2M}\right)^2 - \frac{P_{\max} \cos(\delta_0)}{M}}$$

3. Set the real part of the classical model eigenvalues equal to the real part of the swing mode eigenvalue, i.e.

$$-\frac{D}{2M} = (real\ part\ of\ \lambda_{swing})$$

or

$$D = -2\frac{2H}{\omega_s}(\textit{real part of } \lambda_{swing})$$

Rated operating conditions for the *hydro turbine unit* are the following:

$$\mathbf{V_t} = 1 + j0$$

$$\mathbf{I_a} = 0.8500 + j\,0.52678$$

$$V_{oc} = 1.602$$

$$T_l = 0.8519$$

The stable equilibrium point is

$$\begin{bmatrix} I_{qs} \\ I_{ds} \\ I_{kq2} \\ I_{fd} \\ I_{kd} \\ \omega_0 \\ \delta_0 \end{bmatrix} = \begin{bmatrix} 0.64474 \\ 0.76440 \\ 0 \\ 2.1935 \\ 0 \\ 0 \\ 0.3153 \end{bmatrix}$$

The eigenvalues at the rated operating condition are

$$\begin{bmatrix} -3.5769 \pm j376.89 \\ -1.3270 \pm j8.6843 \\ -24.401 \\ -22.910 \\ -0.45282 \end{bmatrix}$$

The swing mode eigenvalue must be complex conjugate, and its natural frequency must be low.

$$\lambda_{swing} = -1.3270 \pm j8.6843$$

Therefore

$$D = 2\frac{2 \times 7.5}{120\pi}1.327 = 0.106\ \frac{\text{MW s}}{\text{MVA rad}}$$

Rated operating conditions for the *steam turbine unit* are the following:

$$\mathbf{V_t} = 1 + j0$$

$$\mathbf{I_a} = 0.8500 + j\ 0.52678$$

$$V_{oc} = 2.4779$$

$$T_l = 0.8530$$

The stable equilibrium point is

$$\begin{bmatrix} I_{qs} \\ I_{ds} \\ I_{kq1} \\ I_{kq2} \\ I_{fd} \\ I_{kd} \\ \omega_0 \\ \delta_0 \end{bmatrix} = \begin{bmatrix} 0.34330 \\ 0.93923 \\ 0 \\ 0 \\ 1.5394 \\ 0 \\ 0 \\ 0.66456 \end{bmatrix}$$

The eigenvalues at the rated operating condition are

$$\begin{bmatrix} -4.4514 \pm 376.89 \\ -1.7042 \pm 10.476 \\ -11.105 \\ -32.103 \\ -0.34959 \\ -0.85578 \end{bmatrix}$$

Again, the swing mode eigenvalue must be a complex conjugate, and its natural frequency must be low.

$$\lambda_{swing} = -1.7042 \pm 10.476$$

Therefore

$$D = 2\frac{2 \times 5.6}{120\pi}1.7042 = 0.101 \ \frac{\text{MW s}}{\text{MVA rad}}$$

C.6 Comparison of results

The damping coefficient has been obtained for two large machines, using three different methods. Let us compare these results.

Hydro turbine unit	
Free acceleration	0.103
Step input torque	0.103
Eigenvalue	0.106

Steam turbine unit	
Free acceleration	0.106
Step input torque	0.10
Eigenvalue	0.101

As shown in [47], the swing eigenvalue does not change drastically with the operating conditions. It seems from the results obtained, that a typical value of damping for a large synchronous machine is 0.1 $\frac{\text{MW s}}{\text{MVA rad}}$ *on its own base.*

C.6.1 Uniform damping

In direct methods for transient stability, uniform damping is usually assumed. Uniform damping means that the ratio $\frac{D}{M}$ is the same for all the machines in the system.

$$\frac{D_{hydro}}{M_{hydro}} = \frac{0.1}{0.039761} \approx 2.5$$

$$\frac{D_{steam}}{M_{steam}} = \frac{0.1}{0.029708} \approx 3.3661$$

Although the ratio $\frac{D}{M}$ is not the same for both machines we see that it does not change drastically.

Bibliography

[1] T. Athay, V.R. Sherkart, R. Podmore, S. Virmani, C. Puech, "Transient Energy Stability Analysis", *Final Report of U.S. Department of Energy Contract Number EX-76-C-01-2076*, June 5, 1979.

[2] T. Athay, R. Podmore, S. Virmani, "A practical method for the direct analysis of transient stability", *IEEE Transactions on Power Apparatus and Systems*, Vol. PAS-98, No. 2 March/April 1979.

[3] T. Athay, D.T. Sun, "An improved energy function for transient stability analysis", *IEEE Internacional Symposium on Circuits and Systems*, CH1635-2/81/0000-0930, Chicago, April 1981.

[4] T.L. Baldwin, L. Mili, A. G. Phadke, "Ward-Type Equivalents for Transient Stability Analysis", *IFAC Symposium on Control of Power Plants and Power Systems*, March 9-11, 1992, Munich, Germany

[5] P.D. Aylett, "The energy-integral criterion of transient stability limits of power systems," *IEE Proceeedings*, Vol. 105-C, 1958.

[6] Arthur R. Bergen, *Power Systems Analysis* (Book), Prentice Hall, 1986.

[7] A.R. Bergen and D.J. Hill, "A structure preserving model for power system stability analysis", *IEEE Transactions on Power Apparatus and Systems*, Vol PAS-100, No. 1, January, 1981.

[8] H.D. Chiang, C. W. Liu, P. P. Varaiya, F. F. Wu and M. G. Lauby, "Chaos in a Simple Power System", *presented at the* IEEE/PES 1992 *Winter Meeting*, Paper 92 WM 151-1 PWRS, January 1992.

[9] H.D. Chiang, "Analitical Results on Direct Methods for Power System Transient Stability Analysis, *Control and Dynamic Systems,* Vol 43, Academic Press, Inc, 1991.

[10] H.D. Chiang, F.F. Wu, P.P. Varaiya, "A BCU method for direct analysis of power system transient stability", presented at the IEEE/PES Summer Meeting, San Diego California, July 28 — August 1, 1991. 91 SM 423-4 PWRS.

[11] H.D. Chiang, "A theory-based controlling u.e.p. method for direct analysis of power system transient stability", *IEEE Proceedings of the Internacional Symposium on Circuits and Systems*, 1989. Vol. 3, CH2692-2/89/0000-1980, TK 4504.2 I2 1989 V.3.

[12] H.D. Chiang and L.Fekih-Ahmed, "A constructive methodology for estimating the stability regions of interconnected Nonlinear Systems" *IEEE, Transactions on Circuits and Systems,* Vol. 37, No. 5, May 1990.

[13] H.D. Chiang and J. S. Thorp, "The closest unstable equilibriun point method for power dynamic security assessment", *IEEE, Transactions on Circuits and Systems*, Vol. 36, No. 9, September 1989.

[14] H.D. Chiang, "Study of the existence of energy functions for power sistems with losses", *IEEE Transactions on Circuits and Systems*, Vol. 36, No. 11 November 1989.

[15] H.D. Chiang and J.S. Thorp, "Stability regions of nonlinear dynamical systems: A constructive methodology, *IEEE Transactions on Automatic Control*, Vol-34, No. 12, December 1989.

[16] H.D. Chiang and F.F. Wu, "Stability of nonlinear systems described by a second-order vector differential equation", *IEEE Transactions on Circuits and Systems*, Vol. 35, No. 6, pp. 703-711, June 1988.

[17] H.D. Chiang, F.F. Wu. and P.P. Varaiya, "Foundations of the potential energy boundary surface method for power systems transient stability analisis", *IEEE Transactions on Circuits and Systems*, Vol. 35, No. 6, pp. 712-728, June 1988.

[18] H.D. Chiang, B.Y. Ku and J. S. Thorp, "A constructive method for direct analisis of transient stability", *Proceeding of the 27th Conference on Decision and Control*, Austin, Texas, Dec. 1988.

[19] H.D. Chiang, M. W. Hirsch, F. F. Wu, "Stability regions of nonlinear autonomous dynamical Systems", *IEEE Transactions on Automatic Control*, Vol. 33, No. 1, January 1988.

[20] H.D. Chiang, F.F. Wu, and P.P. Varaiya, "Foundations of direct methods for power system transient stability analysis," *IEEE Transactions on Circuits and Systems*, Vol. CAS-34, No. 2, February 1987.

[21] F. Dobraca, MA. Pai and P W Sauer," Relay margins as a tool for dynamical security analysis", *Electrical Power and Energy Systems*, Vol. 12 No. 4, October 1990.

[22] H.W. Dommel, N. Sato, "Fast Transiente stability solutions," *IEEE Transactions on Power Apparatus and Systems*," Vol. PAS-91, No. 4, July/August 1972.

[23] A.H. El-Abiad and K. Nagappan, "Transient stability regions of multimachine power systems" *IEEE Transactions on Power Apparatus and Systems*," Vol. PAS-85, No. 2, February 1966.

[24] L. Fekih-Ahmed and H. D. Chiang, "A new aproach to estimate stability regions of interconnected nonlinear systems via the nonlinear comparison principle", *IEEE Internacional Symposium on Circuits and Systems*, ISCAS'90.

[25] A. A. Fouad, V. Vittal, *Power System Transient Stability Analysis Using the Transient Energy Function Method* (Book), Prentice Hall, 1992.

[26] A. A. Fouad, V. Vittal, Y-X. Ni, H. R. Pota, K. Nodehi, H. M. Zein-Eldin, E. Vaahedi, J. Kim, "Direct transient stability assessment with excitation control," *IEEE Transactions on Power Systems*, Vol. 4, No.1, February 1989.

[27] A. A. Fouad, V. Vittal, S. Rajagopal, V.F. Carvalho, M. A. El-Kady, C. K. Tang, J. V. Mitsche, M. V. Pereira, "Direct transient stability analysis using energy functions application to large power networks," *IEEE Transactions on Power Systems*, Vol. PWRS-2, No.1, February 1987.

[28] A.A. Fouad, K.C. Kruempel, V. Vittal, A. Ghafurian, K. Nodehi, and J.V. Mitsche, "Transient stability program output analysis," *IEEE Transactions on Power Systems*, Vol. PWRS-1, No.1, February 1986.

[29] A.A. Fouad, V. Vittal, T.K. Oh, "Critical energy for direct transient stability assessment of a multimachine power system," *IEEE Transactions on Power Apparatus and Systems*, Vol. PAS-103, No. 8, August 1984.

[30] A. A. Fouad, V. Vittal, "Power system response to a large disturbance: Energy associated with system separation," *PICA 83 116-122,* also *IEEE Transactions on Power Apparatus and Systems*, Vol. PAS-102, No. 11, 3534-3540, November 1983.

[31] A.A. Fouad and S.E. Stanton, "Transient stability of a multi-machine power system. Part. I: Investigation of system trajectories", *IEEE Transactions on Power Apparatus and Systems*, Vol. PAS-100, No. 7, July 1981.

[32] A.A. Fouad and S.E. Stanton, "Transient stability of a multi-machine power system. Part. II: Critical Transient Energy", *IEEE Transactions on Power Apparatus and Systems*, Vol. PAS-100, No. 7, July 1981.

[33] A. A. Fouad, "Stability theory-criteria for transient stability," Proceedings Engineering Foundation Conference on *System Engineering for Power,* Henniker, New Hampshire, 1975, pp. 421-450.

[34] G.E. Gless, "Direct Method of Liapunov Applied to transiente power system stability," *IEEE Transactions on Power Apparatus and Systems*, Vol. PAS-85, No. 2, February 1966, pp. 159-168.

[35] C.L. Gupta and A.H. El-Abiad, "Determination of the closest unstable equilibrium state for Liapunov methods in transient stability analysis," *IEEE Transactions on Power Apparatus and Systems*, Vol. PAS-95, No. 5, September/October 1976, pp. 1699-1712.

[36] M.H. Haque and A.H.M.A. Rahim, "Determination of first swing stability limit of multimachine power systems through Taylor series expansions", *IEE Proceedings*, Vol. 136, Pt. C, No. 6, November 1989.

[37] D.J. Hill and C. N. Chong, "Lyapunov functions of Lure'- Postnikov form for structure preserving models of power systems", *Automatica, Vol, 25, No. 3, pp 453- 460, 1989.*

[38] D.J. Hill and A.R. Bergen, "Stability Analysis of Multimachine Power Networks with Linear Frequency Dependent Loads," *IEEE Transactions on Circuits and Systems*, Vol. CAS-29, No. 12, 1982.

[39] Ian. A. Hiskens, David J. Hill, "Energy functions, transient stability and voltage behaviour in power systems with nonlinear loads," *IEEE Transactions on Power Systems*, Vol. 4, No.4, October 1989.

[40] IEEE Commitee Report, "Transient stability test systems for direct stability methods," *IEEE Transactions on Power Systems*, Vol. 7, No. 1, February 1992.

[41] IEEE Commitee Report, "Application of direct methods to transient stability analysis of power systems," *IEEE Transactions on Power Apparatus and System*, Vol. PAS-103, July, 1984.

[42] IEEE Comitee Report, "Proposed terms & definitions for power systems stability," *IEEE Transactions on Power Apparatus and Systems*, Vol PAS-101 , No. 7 July 1982.

[43] N. Kakimoto, Y. Ohnogi, H. Matsuda and H. Shibuya, "Transient stability analysis of large-scale power system by lyapunov's direct method", *IEEE Transactions on Power Apparatus and Systems*, Vol. PAS-103, No. 1 January 1984.

[44] N. Kakimoto and M. Hayashi, "Transient stability analysis of multimachine power system by Lyapunov's direct method," *IEEE Proceedings of 20th Conference on Decision and Control*, 1981.

[45] N. Kakimoto, Y. Ohsawa and M. Hayashi, " Transient stability analysis of multimachine power systems with field flux decays via Lyapunov's direct method", *IEEE Transactions on Power Apparatus and Systems*, Vol. PAS-99, No. 5, Sep/Oct 1980.

[46] N. Kakimoto, Y. Ohawa and M. Hayashi, "Transient stability analysis of electric power system via Lur'e type Lyapunov function", *Trans IEE of Japan*, Vol.98, No. 5/6, May/June, 1978.

[47] Paul C. Krause, *Analysis of Electric Machinery* (Book), McGraw-Hill, 1986.

[48] B. Y. Ku, J. Lu, R. J. Thomas, J. S. Thorp, "Prediction of power system transient stability in real-time using on-line phasor measurements", School of Electrical Engineering, Cornell University, Ithaca, NY, 14853, (607)-255-3586.

[49] Jin Lu, James S. Thorp, "A method for fast stability prediction of one-machine infinite-bus power system using real-time phasor measurements," School of Electrical Engineering, Cornell University, Ithaca, NY 14853.

[50] G. A. Luders, "Transient stability of multimachine power systems via the direct method of Lyapunov", *IEEE Transactions on Power Apparatus and Systems*, Vol PAS 90, No. 1, Jan/Feb 1971.

[51] W. Ma, J. S. Thorp, "An efficient algorithm to locate all the load-flow solutions", School of Electrical Engineering, Cornell University, Ithaca, NY, 14853, (607)-255-3586, August 29, 1991, revised January 20, 1992.

[52] P.C. Magnusson, "The Transient-Energy Method of Calculating Stability," AIEE Transactions, Vol. 66, 1947.

[53] G. A. Maria, C. Tang, J. Kim, "Hybrid transient stability analysis," *IEEE Transactions on Power Systems*, Vol. 5, No. 2, May 1990.

[54] A. N. Michel, A.A. Fouad and V. Vittal, "Power system transient stability using individual machine energy functions", *IEEE Transactions on Circuits and Systems*, Vol. CAS 30, No. 5, May 1983.

[55] M.A. Pai, *Energy Function Analysis for Power System Stability* (Book), Kluwer Academic Publishers, 1989.

[56] M.A. Pai, *Power System Stability — Analysis by the Direct Method of Lyapunov* (Book), New York, NY, North Holland, 1981.

[57] R. Podmore, S. Virmani, T. Athay, Transient Energy Stability Analysis," *Engineering Foundation Conference, Systems Engineering for Power: Emergency Operating State Control,* Henniker, New Hampshire, August 24, 1977.

[58] F. S. Prabhakara, A. H. El-Abiad, "A simplified determination of transient stability regions for Lyapunov methods," *IEEE Transactions on Power Apparatus and Systems*, Vol PAS 94, No. 2, March/April 1975.

[59] C. Rajagopalan, B. Lesieutre, P. W. Sauer, M. A. Pai, "Dynamic Aspects of Voltage/Power Characteristics", *presented at the IEEE/PES 1991 Summer Meeting*, Paper 91 SM 419-2 PWRS, July 28 - August 1, 1991.

[60] A.H.M.A. Rahim and M.H.Haque, "A simple method of computing critical clearing time of a multimachine power system through evaluation of system rate of chance of kinetic energy", *Electric Machines and Power Systems*, Vol. 17, No. 6, 1989.

[61] F. A. Rahimi, M. G. Lauby, J. N. Wrubel and K. L. Lee, "Evaluation of the transient energy function method for on-line dynamic security analysis", *presented at the IEEE/PES 1992 Winter Meeting*, Paper 92 WM 148-7 PWRS, January 1992.

[62] N. D. Rao, "A new approach to the transient stability problem", *AIEE* , June 1962.

[63] P. Rastgoufgard, R.A. Schlueter, " Application of critical machine energy function in power system transient stability analysis," *Electric Machines and Power Systems*, Vol. 16, No. 5, 1989.

[64] M. Ribbens -Pavella and F.J. Evans, "Direct methods for studying dynamics of large-scale electric power systems — A Survey," *Automatica*, Vol-21, January 1985, pp. 1-21.

[65] M. Ribbens-Pavella, "Coments on Direct methods for transient stability studies in power system analysis", *IEEE Transactions on Automatic Control, AC-17.*

[66] W. D. Stevenson, Jr., *Elements of power system analysis* (Book), McGraw-Hill, Fourth Edition, 1982.

[67] B.Stott, "Power system dynamic response calculations", *Proceedings of the IEEE*, Vol. 67, No. 2, February 1979.

[68] P. W. Sauer, A. K. Behera, M. A. Pai, J. R. Winkelman, J. H. Chow, "Trajectory approximations for direct energy methods that use sustained faults with detailed power system models," *IEEE Transactions on Power Systems*, Vol. 4, No. 2, May 1989.

[69] P.W. Sauer, A.K. Behera, M.A. Pai, J. R. Winkelman and J. H. Chow, "A direct method for transient stability analysis of power systems with detailed models", *Electric Machines and Power Systems*, Vol. 15, No. 1, pp. 1-15, 1988.

[70] Stewart E. Stanton, "Transient stability monitoring for electric power systems using a partial energy function," *IEEE Transactions on Power Systems*, Vol. 4, No. 4, October 1989.

[71] S. E. Stanton, "Partial Energy Function Analysis Applied to Transient Control of Power Systems", *Interim report on a project sponsored by Bonneville Power Administration.*

[72] C.J. Távora, O. J. M. Smith, "Stability analysis of power systems", *IEEE Transactions on Power Apparatus and Systems*, Vol. PAS-91, May/June, pp. 1138-1145, 1972.

[73] Carlos Tavora and O.J.M. Smith, "Stability Analysis of Power Systems," *Electronics Research Laboratory, College of Engineering University of California, Berkeley,* August 2, 1970.

[74] J.S. Thorp and S.A. Naqavi "Load Flow Fractals", *Proceedings of the 28 IEEE Conference on Decision and Control*, Tampa, FL, December 1989, pp. 1822-1827.

[75] J.S. Thorp, "Determination of Power System Stability in Real Time", Visual Aid Material on a Conference at Virginia Tech.

[76] R.J.Thomas and J. S. Thorp, "Towards a direct test for large scale electric power system instabilities", *IEEE Procceedings of 24th Conference on Decision and Control*, December 1985.

[77] J. Tong, H. D. Chiang and T. P. Coneen, "A Sensitivity-Based BCU Method for Fast Derivation of Stability Limits in Electric Power Systems", *presented at the IEEE/PES 1992 Winter Meeting*, Paper 92 WM 149-5 PWRS, January 1992.

[78] B. Toumi, R. Dhifaoui, Th. Van Cutsem, M. Ribbens-Pavella, "Fast transient stability assessment revisited", *presented at PICA, San Francisco, May 6-10, 1985.* (*IEEE Transactions on Power Systems*, Vol. 1, 1986).

[79] N. A. Tsolas, A. Arapostathis, P. P. Varaiya, "A Structure Preserving Energy Function for Power System Transient Stability Analysis", *IEEE Transactions on Circuits and Systems*, Vol. CAS-32, No. 10, October 1985.

[80] Approximation of an energy function in transient stability analysis of power systems, *"Electrical Engineering in Japan,"* Vol. 92 No. 6, pp. 96-100, 1972.

[81] A computational algorithm for evaluating unstable equilibrium states in power systems, *"Electrical Engineering in Japan,"* Vol. 92, No. 4, pp. 41-47, 1972.

[82] Th. V. Cutsem, B. Toumi, Y. Xue, M. Ribbens-Pavella,"Direct Criteria for structure preserving models of electric power systems, *IFAC Symposium on Power Systems and Power Plant Control*, August 12-15, 1986, Beijing, China.

[83] P.P. Varaiya, F.F. Wu and R-L Chen, "Direct methods for transient stability analysis of power systems: Recent results," *Proceedings of the IEEE*, December 1985, pp. 1703-1715.

[84] P.P. Varaiya, F.F. Wu and R-L Chen, "Direct methods for transient stability analysis of power systems: Recent results," Memorandum No. UCB/ERL M84/72, Electronics Research Laboratory College of Engineering, University of California Berkeley. September 10, 1984.

[85] S. Virmani, R. Podmore, "Anlysis of systems with transfer conductances and calculation of equilibrium points," *Transient energy stability analyisis, technical memorandum #2, Systems Control Incorporated,* July 20, 1978.

[86] V. Vittal, N. Bhatia, A. A. Fouad, G. A. Maria, H. M. Zein El-Din, "Incorporation of nonlinear load models in the transient energy function", *IEEE Transactions on Power Systems*, Vol. 4, No.3, August 1989.

[87] V. Vittal, "A generalized procedure to obtain first integrals for non-conservative dynamical systems: application to power systems", *IEEE Proceedings of the International Symposium on Circuits and Systems 1989.*

[88] V. Vittal, T. Oh, A. A. Fouad, "Apparent impedance correlation of transient energy margin and time simulation," *IEEE Transactions on Power Systems*, Vol. 3, No.2, May 1988.

[89] V. Vittal, S. Rajagopal, A. A. Fouad, M. A. El-Kady, E. Vaahedi, V. F. Carvalho, "Transient stability analysis of stressed power systems using the energy function method," *IEEE Transactions on Power Systems*, Vol. 3, No.1, February 1988.

[90] J. L. Willems, "Direct Methods for transient stability studies in power system analysis", *IEEE Transactions on Automatic Control, Vol, Ac-16, No. 4, August 1971.*

[91] Y. Xue, L. Wehenkel, R. Belhomme, P. Rousseaux, M. Pavella, E. Euxibie, B. Heilbronn, J.F. Lesigne, "Extended equal area criterion revisited", *IEEE Transactions on Power Systems*, Vol. 7, No.3, August 1992.

[92] Y. Xue, Th. Van Cutsem, M. Ribbens-Pavella,"Extended equal criterion justifications, generalizations, applications", *IEEE Transactions on Power Systems*, Vol. 4, No. 1, February 1989.

[93] Y. Xue, Th. Van Cutsem, M. Ribbens-Pavella, "A simple direct method for fast transient stability assesment of large power systems", *IEEE Transactions on Power Systems*, Vol, 3, No. 2, May 1988.

[94] Y.Xue, Th. Van Cutsem, M. Ribbens-Pavella, "A new decomposition method and direct criterion for transient stability assessment of large scale electric power systems", *IMACS-IFAC Symposium on modelling and simulation for control of lumped and distributed parameter systems, Villeneuve d'Ascq, France, June 3-6, 1986.*

[95] J. Zaborszky, G. Huang, B. Zheng, T. C. Leung, "On the Phase Portrait of a Class of Large Nonlinear Dynamic Systems Such as the Power System", *IEEE Transactions on Automatic Control*, Vol. 33, No. 1, January 1988.

The vita has been removed from the scanned document